Parameterisation of Microprotozooplankton Grazing and Growth:

From data analysis to simulations in ecosystem model coupled to general circulation-biogeochemical model.

Dissertation
Zur Erlangung des Akademischen Grades eines
Doktors der Naturwissenschaften
- Dr. rer. Nat. –

Im Fachbereich 2 (Biologie/Chemie)
Der Universität Bremen

vorgelegt von
Sévrine Sailley

Institutes:
Alfred Wegener Institut for Polar and Marine Research (AWI), Bremerhaven, Germany
University of East Anglia (UEA), Norwich, UK
British Antarctic Survey (BAS), Cambridge, UK
University Bremen, Germany

This work was funded by Euroceans program, project number WP3.2-SYS-1092.

Erster Gutachter: Prof. Dr. Dieter Wolf-Gladrow
Zweiter Gutachter: Prof. Dr. Corinne Le Quéré

Tag des öffentlichen Kolloquims: Universität Bremen, 23 November 2009

Eidesstattliche Erklärung

Hiermit erkläre ich nach § 6 Abs. 5 der Promotionsordnung der Uni Bremen (vom 14 März 2007), dass ich die Vorliegende Dissertation

(1) ohne unerlaubte Hilfe angefertigt habe,
(2) keine anderen als die von mir angegebenen Quellen und Hilfsmittel benutzt habe
und
(3) die den benutzen Werken wörtlich oder inhaltlich entnommen Stellen als solche kenntlich gemacht habe

_____

Sévrine Sailley

Acknowledgments

Here, I would like to thank people who helped me in different ways through this thesis. There are quite a lot of people who should figure here, so if I've forgotten somebody, I'm sorry it wasn't on purpose.

Thanks to Christine and Dieter for welcoming me at AWI and in Bremerhaven and helping not just with the thesis but also simply life in Germany, thanks for being more than just supervisors.
Thanks to Clare Enright for helping me arrange my stay at BAS, but also with going through all the bugs that happened in PlankTOM, or simply little problems with the cluster.
Thank you Roisin for the discussions, shared complaints and exchange of idea about everything and nothing while I was at BAS and after.
Thanks Corinne for the brainstorming on different occasions, integrating me in the Green Ocean Project, and making me feel welcome in the UK. I think I need to find this book you mentioned once about how people think and how to best communicate with them.
Thanks Erik for helping me with every problem I had with the model, I'm not sure I'd have made it to the end otherwise.
Thanks to all the friends I've made in Germany; Delphine for sharing her office with me at the beginning and helping me adjust to Germany; Joao, Fabi, Gustavo for great parties and fun time (I won't forget the little Portuguese I learned); Sven, well I don't know what to say, there's a lot of thanks in here for you. And the friend in the UK, Marie-Pierre, Roisin, Meike sorry but I'm running out of words.
Special thanks to Lys who had to deal with me in the last year of the thesis, not the best one I daresay. So even though you broke the deal you'll have your blue footed booby.
Thanks to Reza who supported me through the whole thing without any complaints, without you I think I would have simply given up.
Et aussi merci à ma famille pour m'avoir soutenue dans cette experience.

Table of content

ABSTRACT *11*

ZUSAMMENFASSUNG *13*

CHAPTER 1: INTRODUCTION *17*

1- MARINE BIOGEOCHEMISTRY AND CLIMATE **17**
2- THE PELAGIC COMMUNITIES AND THE BIOLOGICAL PUMP **19**
3- MICROZOOPLANKTON **21**
4- BIOGEOCHEMICAL OCEAN GENERAL CIRCULATION MODELS (BOGCMS) **24**
5- AIM OF THE THESIS **25**
6- THESIS OUTLINE **25**
7- CONTRIBUTIONS **27**
8- REFERENCES **28**
CHISHOLM, SW (2000) OCEANOGRAPHY: STIRRING TIMES IN THE SOUTHERN OCEAN. *NATURE,* 407:685-687 **29**

CHAPTER 2: PELAGIC CILIATE FEEDING BEHAVIOUR AND GROWTH RATE. AN ANALYSIS BASED ON LABORATORY EXPERIMENTS *33*

1-INTRODUCTION **33**
2- DATA AND METHOD **35**
2.1- Data selection and acquisition *35*
2.2- Modelling the functional response *38*
2.3- Correction for temperature effects and estimation of Q_{10} *41*
3- RESULTS **42**
3.1- Q_{10} estimate for grazing and growth *42*
3.2- Functional response *45*
3.3- Gross Growth Efficiency (GGE) *53*
4-DISCUSSION **57**
4.1- Temperature effects *57*
4.2- Functional response and GGE. *57*
5- CONCLUSION **59**
6-REFERENCES **61**

CHAPTER 3: HETEROTROPHIC DINOFLAGELLATE FEEDING BEHAVIOUR AND GROWTH RATES. AN ANALYSIS BASED ON LABORATORY RESULTS. *67*

1- INTRODUCTION **67**
2- DATA AND METHOD **68**
2.1- Data selection and acquisition *68*
2.2- Modelling the functional response *71*
2.3- Correction for temperature effects and estimation of Q_{10} *73*
3-RESULTS **74**
3.1- Temperature *74*
3.2- Size and prey PFT impact *75*
3.3- Gross Growth Efficiency (GGE) *84*
3.4- Comparison with ciliates *85*
4- DISCUSSION **90**
4.1- Functional response *90*
4.2- Prey selection *91*
4.3- Comparison to ciliates *92*
4.4- Impact on food web representation and models *93*
5- CONCLUSION **93**
6-REFERENCES **94**

CHAPTER 4: MICROZOOPLANKTON REPRESENTATION IN MODEL: COMPARISON OF PELAGIC CILIATES AND HETEROTROPHIC DINOFLAGELLATES. *99*

1-INTRODUCTION **99**
2- MODEL DESCRIPTION **101**
2.1-PlankTOM5 biogeochemical model *101*
2.2- Grazing *102*
2.3- Partitioning of grazing *102*
2.4- Basal respiration *103*
3- PHYSICAL MODEL AND MODEL FORCING **105**
4- PARAMETERISATION **105**
5- DESIGN OF THE MODEL EXPERIMENTS **106**
6- RESULTS **107**
6.1- Parameterization. *107*
6.2- Model simulation. *108*
7- DISCUSSION **121**
7.1- Sensibility to grazing parameterisation *121*
7.2- Sensibility to food preferences *123*
7.3- Other features *126*
8- CONCLUSION **127**
9- REFERENCES **129**
10- SUPPLEMENTARY FIGURES **132**

CHAPTER 5: GENERAL CONCLUSION AND OUTLOOK *145*

1- CONCLUSIONS **145**
1.1- Main steps. *145*
1.2- Relationship between grazing and growth *146*
1.3- Feeding behaviours *148*
1.4- Temperature *150*
1.5- Modelling of microzooplankton *150*
2- OUTLOOK **151**
3- REFERENCES **153**

ANNEXES *155*

ANNEXE A: BIOGEOCHEMICAL FLUXES THROUGH MICROZOOPLANKTON **157**
ABSTRACT **157**
1. INTRODUCTION **158**
2. MODEL DESCRIPTION **159**
2.1 PlankTOM5 biogeochemical model *159*
2.2 Physical model *161*
2.3 Model forcing *162*
3. DATA SYNTHESIS OF MICROZOOPLANKTON FLUX RATES AND BIOMASSES **162**
3.1 Parameterisation of the biogeochemical model *163*
3.2 Evaluation data *166*
4 RESULTS **167**
5 DISCUSSION **170**
CONCLUSION **173**
LITERATURE **175**

ANNEXE B: BAYESIAN PARAMETER ESTIMATION **191**
B.1- Theory *191*
B.2- Example *195*

ANNEXE C: MATLAB CODES USED FOR PARAMETER ESTIMATION. **201**
C.1- Main code. *201*
C.2- Parallel code (MMtrchsq.m). *205*

ABSTRACT

In the context of global warming and climate change Biogeochemical Ocean General Circulation Models (BOGCM) are hard pressed to provide clear and realistic answers as to how ecosystems and the carbon cycle are affected. Ecosystem models have developed from the NPZ type (Nutrient-Plankton-Zooplankton) towards the use of several plankton functional types (PFTs) to enhance the prediction of ecosystem feedback on climate change. PFTs are selected on their impact on biogeochemical cycles. Zooplankton PFTs, for example, are mostly defined by size. Microzooplankton, one of these size classes, is a group of interest due to a high biomass and growth rates which allow these organisms to follow fluctuations in prey concentration. Furthermore, they are known to graze ~40-75% of particulate primary production in the surface ocean, against ~10-15% for the mesozooplankton. As a size class, microzooplankton includes several organisms – pelagic ciliates, heterotrophic dinoflagellates, foraminifera, metazoans larva and copepods nauplii – with different feeding modes, food preferences, grazing and growth rates. Ciliates and heterotrophic dinoflagellates are the main microzooplankton organisms. Although they are both protozoans, their feeding behaviour and preferred prey size have a substantial difference. In order to assess their differences, results from laboratory experiments were compiled from the literature – a total of 342 for ciliates and 161 for dinoflagellates. It emerged that both organisms have a growth and a grazing threshold, also both grazing and growth rates depends on organism size and the size ratio with their prey (size expressed as diameter, volume or carbon content). Ciliates exhibit an increase of their maximal grazing rate past the optimal prey:ciliate ratio of 1:10. Dinoflagellates have a maximal grazing rate which increases to a prey:dinoflagellate ratio of 2:1, then continues to increase past this value, with a marked preference for diatoms over other possible prey types. As both ciliates and heterotrophic dinoflagellates have different size ratios with their prey, they will target different prey types. Moreover, both have different functional responses to fluctuations in prey concentration. Ciliates, with a higher threshold concentration and lower half-saturation concentration, will commence grazing later than dinoflagellates, but reach their maximal rates faster. They differ further from dinoflagellates with a higher maximal grazing rate and a lower metabolism. Parameterisation for a microzooplankton, ciliates and heterotrophic dinoflagellates PFTs were obtained from the data and used in a BOGCM. The

PFTs have a different impact on the ecosystem and biogeochemical cycles. The dinoflagellate PFT reduces the export and alters the distribution area of high primary production. The ciliate PFT has a similar impact to that of microzooplankton. It is doubtful that the microzooplankton PFT in itself correctly represents ciliates and heterotrophic dinoflagellates. Consequently a separation of both organisms in future models is recommanded to provide a better representation of the ecosystem and its response to climate change.

ZUSAMMENFASSUNG

Im Kontext von globaler Erwärmung und Klimawandel werden allgemeine biogeochemische Ozeanzirkulationsmodelle (BOGCM) gedrängt, klare und realistische Antworten zu liefern, wie Ökosysteme und der Kohlenstoffkreislauf beeinflusst werden. Ökosystemmodelle wurden ausgehend vom NPZ-Typ (Nährstoff-Phytoplanktonlankton-Zooplankton) zu Modellen mit verschiedenen Plankton-Funktionstypen (PFT) weiterentwickelt, um die Vorhersage der Antwort des Ökosystems auf den Klimawandel zu verbessern. PFTs wurden mit Hinblick auf ihren Einfluss auf biogeochemische Kreisläufe, Biomasse und Größenklassen ausgewählt. Zooplankton PFTs werden z. B. meistens durch die Größe definiert. Mikrozooplankton ist von Interesse aufgrund der großen Biomasse und hohen Wachstumsraten, die es diesen Organismen erlauben, Schwankungen in der Beutekonzentration zu folgen. Außerdem ist es bekannt dafür, dass es ca. 60 – 77% der partikulären Primärproduktion im Oberflächenwasser abweidet, gegenüber ca. 10 – 15% durch Mesozooplankton.

Als eine Größenklasse schließt Mikrozooplankton mehrere Organismengruppen mit Unterschieden bei Fressverhalten, Futterpräferenz, Fraß- und Wachstumsraten ein: pelagische Ciliaten, heterotrophe Dinoflagellaten, Foraminiferen, Metazoenlarven und Nauplien von Ruderfußkrebsen. Ciliaten und heterotrophe Dinoflagellaten sind die Hauptgruppen im Mikrozooplankton. Obwohl beide Protozoen sind, unterscheiden sie sich beträchtlich im Fressverhalten und der bevorzugten Beutegröße. Um diese Unterschiede zu bewerten wurden Ergebnisse aus Laborexperimenten aus der Literatur zusammengetragen, insgesamt 342 für Ciliaten und 161 für Dinoflagellaten. Es zeichnete sich ab, dass beide Organismen eine Wachstums- und Freß-Schwelle haben. Sowohl die Freß- als auch die Wachstumsrate hängen von der Organismengröße ab und das Größenverhältnis zu ihrer Beute (Größe ausgedrückt als Durchmesser, Volumen oder Kohlenstoffgehalt). Ciliaten weisen einen Ansteig ihrer maximalen Freßrate jenseits des Beute:Ciliat Verhältnisses von 1:10 auf. Dinoflagellaten haben eine maximale Freßrate, die bis zu einem Verhältnis Beute: Dinoflagellat von 2:1 ansteigt und weiter über diesen Wert hinaus ansteigt, mit einer merklichen Präferenz für Diatomeen gegenüber anderen möglichen Beutetypen. Da beide, Ciliaten und Heterotrophe Dinoflagellaten verschiedene Größenverhältnisse bei ihrer Beute haben, werden sie auf

verschiedene Beutetypen zielen. Zudem reagieren beide verschieden auf Schwankungen in der Beutekonzentration. Ciliaten mit einer höheren Schwellenkonzentration und niedrigerer Halbsättigungskonzentration werden später als Dinoflagellaten mit dem Fraß beginnen, aber sie erreichen schneller Maximalraten. Außerdem unterscheiden sie sich von Dinoflagellaten durch eine höhere maximale Freßrate und einen niedrigeren Stoffwechsel. Die Parametrisierung für Mikrozooplankton, Ciliaten und heterotrophen Dinoflagellaten wurde aus den Daten gewonnen und in ein BOGCM implementiert. Die PFTs haben einen unterschiedlichen Einfluss auf das Ökosystem und biogeochemische Kreisläufe. Dinoflagellaten reduzieren den Export und ändern die Verteilung der Bereiche mit hoher Primärproduktion. Ciliaten haben einen ähnlichen Einfluss wie das Mikrozooplankton wie es bisher in BOGCMs repräsentiert ist. In zukünftigen Modellen ist eine Trennung der Ciliaten und heterotrophen Dinoflagellaten erforderlich, um eine bessere Repräsentation des Ökosystems und seiner Antwort auf den Klimawandel zu liefern.

CHAPTER 1:

Introduction

1- Marine biogeochemistry and climate

The oceans contain about 38000 Gt C in dissolved form (DIC) that can be exchanged with the atmosphere on time scales ranging between months to thousand of years for the surface and deep ocean, respectively. The ocean biological activity contributes to creating a gradient in DIC from the surface to the deep ocean through the process commonly called the "biological carbon pump": using sunlight for energy and dissolved inorganic nutrients, phytoplankton converts CO_2 to particulate organic carbon (POC), which forms the base of the marine food web. Roughly 80% of the organic carbon is transferred by consumers through the marine food web and finally converted back to CO_2. The remaining POC is exported to the deep ocean where it is remineralized back to CO_2 with approximately 0.5% remaining to be buried in deep-sea sediments. The effect of the biological pump is a net transport of CO_2 from the atmosphere to the deep ocean, with residence times varying from years to thousands of years depending on the depth at which POC is remineralized. At steady state, the strength of the biological pump is determined by the rate of upwelling of macronutrients (nitrate, phosphate) and micronutrients (iron) into the photic layer where light levels can support phytoplankton growth. With a changing climate, however, the steady-state will be disturbed due to modifications of the composition of phytoplankton assemblages and foodweb structures, changing the strength of the biological carbon pump, and possible affecting the amount of CO_2 sequestrated by the ocean (Fig. 1 and 2).

Human activities have caused an increase in the release of greenhouse gases (primarily CO_2) causing an increase in global surface temperatures by 0.45°C (Trenberth et al., 2007) as well as a decrease in ocean pH by 0.02 pH units per decades in the last 20 years (Bindoff et al., 2007). The IPCC report 2007 states that "continued greenhouse gas emissions at or above current rates will cause further warming and induce many changes in the global climate

system during the 21st century that would *very likely* be larger than those observed during the 20th century", temperature would increase by 0.66°C in the next 20 years and pH would go through an additional decrease between 0.14 and 0.35 units by 2100 (Meehl et al., 2007). These climatic changes will affect marine biota directly (e.g. increased temperature and decreased pH will have effects on the physiology of marine organisms), or indirectly (e.g. changes in the ocean circulation patterns that result in changes in environmental conditions that will affect in distribution or functioning of marine communities).

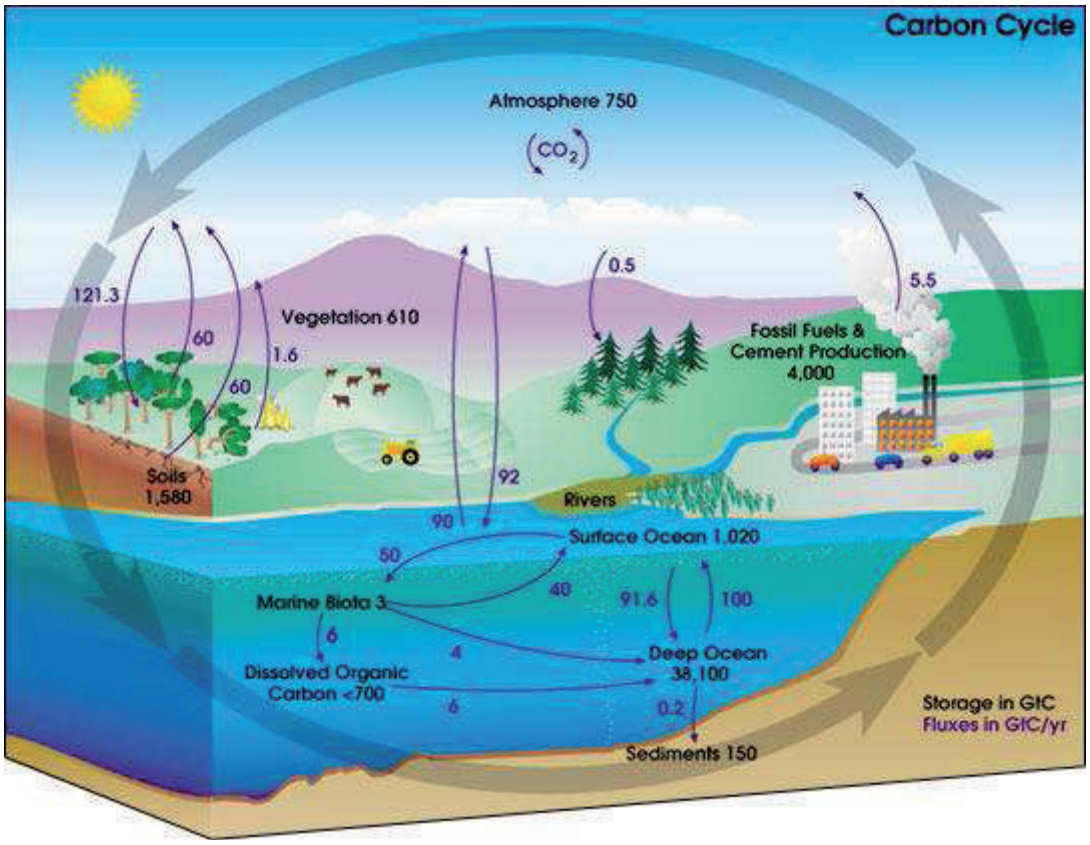

Figure 1: The Global Carbon Cycle. Picture from http://www.uwsp.edu/geO/faculty/ritter/geog101/textbook/earth_system/carbon_cycle_NASA.jpg

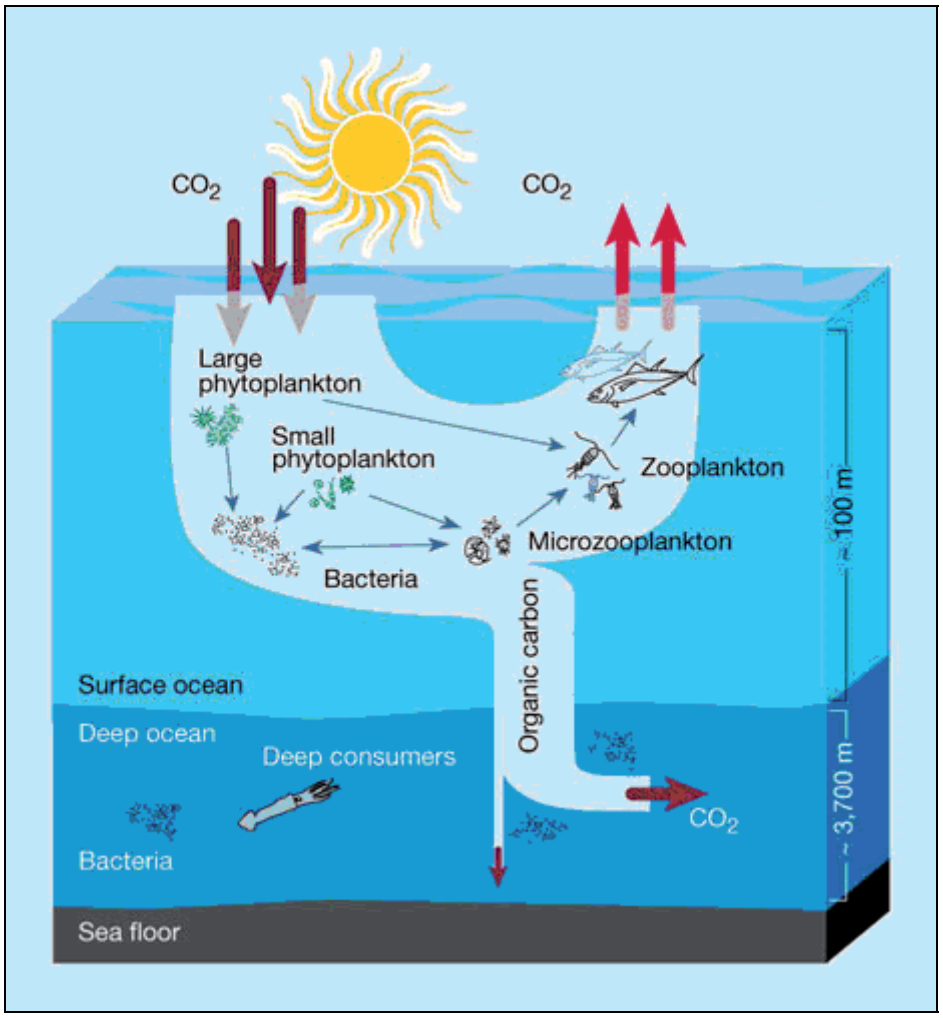

Figure 2: The biological carbon pump. Adapted from Chisholm (2000).

2- The pelagic communities and the biological pump

Pelagic ecosystems are thought to function in two modes (Barber and Hiscock., 2006; Fig. 3):

(i) The "classical" food chain where large phytoplankton (primarily large diatoms) is grazed by metazoans in turn preyed upon by larger organisms (i.e. squids, fish, birds and mammals). This type of food chain tends to occur in areas with high nutrient supply (spring bloom in temperate and coastal areas) and is associated with high vertical fluxes mediated trough large fast sinking phytoplankton aggregates - once nutrients are exhausted - and large predator faecal pellets. This export system is the main driver of the biological pump.

(ii) The “microbial loop” (Pomeroy 1974; Azam et al., 1983), powered by dissolved organic matter (DOM) produced by phytoplankton and heterotrophs. DOM is taken up by bacteria as a source of elements and energy. Bacteria are consumed by nanoflagellates in turn consumed by microzooplankton. At each trophic level respiration and excretion produce DOM and CO_2, and release nutrients that can then be used either by bacteria or phytoplankton. This regenerating system is characteristic for oligotrophic regimes and summer communities in productive system, it tends to be dominated by small phytoplankton (nanoflagellates).

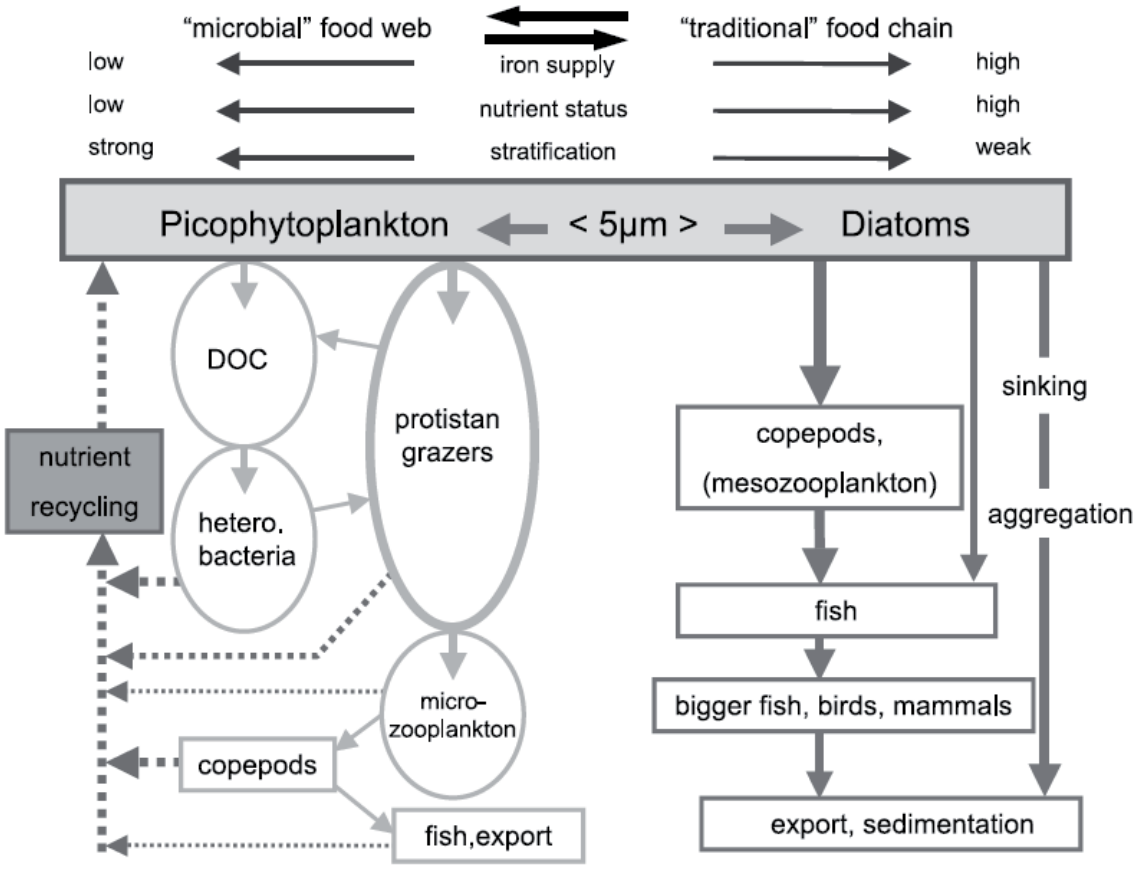

Figure 3: Pelagic ecosystem pathways. Figure from Barber and Hiscock (2006).

Therefore, the biological pump efficiency depends also on the plankton community composition. However, because the temporal and spatial evolution of phytoplankton depends on the balance between growth and mortality, a correct understanding of grazer-mediated mortality is also key to obtain realistic spatial and temporal dynamics of plankton communities. More importantly, if we are to assess the feedbacks between climate and

plankton communities a comprehensive representation of marine ecosystem is needed from primary producers to grazers. Recent estimates of herbivores grazing show that mesozooplankton directly consumes ~10-15% of particulate primary production in the surface ocean (Calbet 2001; Behrenfeld and Falkowski 1997), while microzooplankton consumes ~59-75% (Calbet 2008). Microzooplankton growth rates are close to those of phytoplankton enabling them to closely follow fluctuation in phytoplankton concentration (Banse 1982). As such they are a key component of pelagic ecosystems.

3- Microzooplankton

According to the classification of Sieburth et al. (1978), microzooplankton is a group of heterotrophic and mixotrophic organisms 20-200 µm in size. This size class include many protists such as pelagic ciliates, heterotrophic dinoflagellates and foraminifera, as well as small metazoans such as copepod nauplii, some copepodites, and some meroplanktonic larvae. Ciliates and heterotrophic dinoflagellates tend to dominate the microzooplankton numerically and in term of biomass in the open ocean. Ciliates prey on organisms – including small diatoms – that are on average eight times smaller than their own size (Verity and Villareal 1986; Hansen et al., 1994). Field observations suggest that ciliates can also prey diatoms and diatom chains as large as themselves. However, no quantitative data is available to estimate their grazing impact on diatoms populations. Dinoflagellates eat a broad range of prey sizes, including prey significantly larger than themselves, and have a marked preference for diatom, even the chain forming species (Buck et al., 2005). Considering (i) the size range of microzooplankton organisms, (ii) the relative size to that of their prey and (iii) the ability of both ciliates and dinoflagellates to prey on diatoms, it appears that the microzooplankton could also act as a link between primary producers and higher trophic levels in productive systems. This aspect of microzooplankton ecology has however been poorly investigated.

Pelagic ciliate species range in size from about 10 µm to 200 µm and belong almost exclusively to the order Oligotrichida and Choreotrichida characterised by a conspicuous circular or semi-circular anterior row of ciliate organelles used to create feeding currents (Jonsson 1986). Ciliates filter the surrounding water through a crown of cilia (Fig. 4). This sieving system and the mouth apparatus set the size limit for the prey.

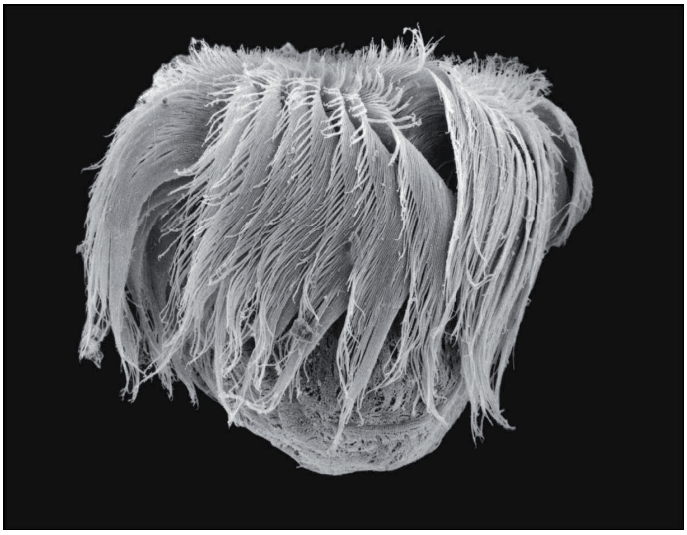

Figure 4: A ciliate (*Strobilidium neptuni*) photographed in Scanning Electron Microscopy (SEM). Picture from The user-friendly key to coastal planktonic ciliates, http://www.liv.ac.uk/ciliate/

Pelagic heterotrophic dinoflagellates are raptorial feeders with three main modes of prey capture and consumption: (i) extra-thecal digestion with a pallium in many heterotrophic thecate dinoflagellates (Fig. 5a), (ii) sucking the prey cell content with a peduncle, a mode also common in thecate dinoflagellates (Fig. 5b) or (iii) engulfment of prey cell primarily found in naked dinoflagellates (Fig. 5c).

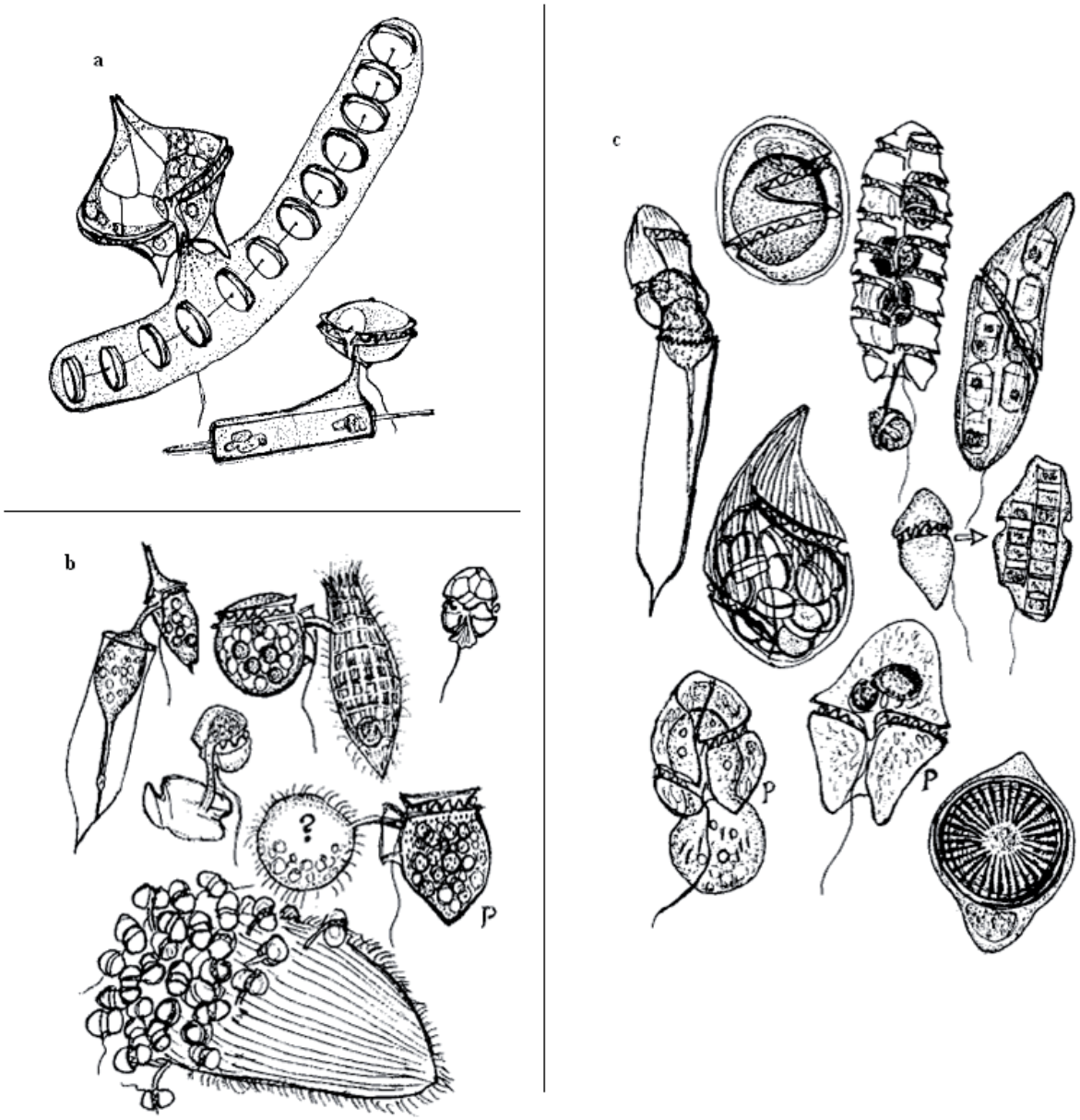

Figure 5: Dinoflagellates feeding modes. Drawings from Jacobson (1999). 'P' design species that are photosynthetic. a: thecate dinoflagellates with pallium feeding; b: dinoflagellates with peduncle feeding; c: dinoflagellates feeding by engulfing the prey cell.

These differences in feeding modes result in a difference in prey size spectrum: ciliates tend to feed on prey one tenth of their size and dinoflagellates feed on prey up to ten times larger than their own size. Differences in feeding mode are also reflected in metabolic differences with maximal grazing and growth rates of ciliates being higher than those of dinoflagellates (Strom and Morello 1998).

4- Biogeochemical Ocean General Circulation Models (BOGCMs)

In order to study the effect of, among others, biology on cycle of elements as well as sensitivity and feedbacks using climate change scenarios, coupled Biogeochemical - Ocean General Circulation Models have been developed starting in the 1980 (see, for example Fasham et al., 1990). Such models encompass ecosystem model of various complexity (Aumont et al., 2003; Moore et al., 2002; Gregg et al., 2003; Le Quéré et al., 2005). Overall ecosystem models within BOGCM are usually in the form of so-called NPZD models consisting of a small number of highly aggregated compartments (Nutrients, Phytoplankton, Zooplankton, Detritus), where the diversity of individual organisms and species are replaced with generic variables such as "phytoplankton" and "microzooplankton". The main goal of these biogeochemical models is to simulate the cycles of C, N and/or P in order to describe the role of oceanic ecosystem in export from the surface to the deep-sea (Najjar et al., 1992; Maier-Reimer 1993). With the current global warming and climate change issue, the question of how the ocean's biota will respond (Denman et al., 1996) and its impact on carbon cycling, has become urgent. A major challenge is to determine the level of biological complexity required to accurately capture climate change impacts and biologically driven feedbacks on biogeochemical cycles (Anderson 2005; Doney 1999). Also, although there is a general agreement on the need for a more detailed representation of biology in BOGCMs the level of complexity and formulation of biological processes is still hotly debated (Le Quéré et al., 2005; Anderson 2005; Le Quéré 2006; Flynn 2006; Anderson 2006). Based on the current conceptual understanding of the relations between ocean ecosystems and biogeochemical cycles, several groups have expanded the classical NPZD models in BOGCMs, by incorporating or expanding the number of planktonic compartments using Plankton Functional Types (PFTs; Le Quéré et al., 2005; Moore et al., 2002). The definition of a PFT is based on a combination of criteria such as size (as determinant for physiological rates), biogeochemical function (opal and $CaCO_3$ production, nitrogen fixation) and broad taxonomic affiliation (diatoms, coccolithophores, bacteria). Because autotrophs dominate the production of biominerals (Opal, $CaCO_3$), nitrogen fixation and are thought to be the primary mediators for vertical fluxes in the ocean, PFTs have been defined primarily for the phytoplankton. In contrast, little to no effort has been allocated to developing representations of the phytoplankton grazers: the zooplankton. In state of the art ecosystem models coupled to BOGCMs, the zooplankton is represented as a single group of organisms (occasionally two groups) whose primary function is to represent the loss terms influencing phytoplankton

dynamics. Hence, parameterization of zooplankton grazing is generally adapted to the model configurations to result in the best representation of phytoplankton dynamics (Aumont et al., 2003; Gregg et al., 2003; Lima and Doney 2004; Moore et al., 2004; Le Quéré et al., 2005).

5- Aim of the thesis

The temporal and spatial evolution of a given phytoplankton functional group depends on the balance between growth and mortality. A correct representation of grazer-mediated mortality in models is key to obtaining realistic spatial and temporal dynamics of phytoplankton functional groups. More importantly, if ecosystem models coupled to BOGCMs are to give robust assessments of the feedbacks between climate and plankton communities, a comprehensive representation of PFTs is needed. This also applies to the representation of grazers. In particular, the size classes commonly used for the phytoplankton in state of the art ecosystem models coupled to BOGCMs (pico: < 2 μm, nano: 2-20 μm, micro: 20-200 μm and meso: ≥ 200 μm) can be directly applied to the zooplankton and represent different metabolic capacities, but also, broad taxonomic and trophic groups (Sieburth et al., 1978; Fenchel 1987). The purpose of this study is to derive ground-trusted parameterizations of microzooplankton grazing behavior and growth characteristics, from information available in the literature. The derived parameterizations are implemented in a state of the art BOGCM, the Dynamic Green Ocean Model PlankTOM (DGOM, Le Quéré et al., 2005) and evaluated on the basis of model simulations to compare microzooplankton, ciliates and dinoflagellates as well as their impact on model ecosystem.

6- Thesis outline

The thesis is constructed around the following questions: (i) What are the feeding behaviours and the growth rates of ciliates and dinoflagellates? (ii) Is there a difference between their feeding behaviours and rates for grazing and growth? (iii) What impact do they have on a model ecosystem? (iv) Is a separation of ciliates and dinoflagellates in future ecosystem model necessary?

To answer these questions, data on the functional response, *i.e.* grazing and growth as a function of prey concentration, was collected from the literature for ciliates and heterotrophic dinoflagellates species when offered a single prey species. To see the influence of external factors such as temperature, relative size and the type of the prey, parameters of

the functional response (maximal growth and grazing rate, half-saturation concentration and threshold concentration) were obtained by fitting the collected data to a Michaelis-Menten equation modified to include a threshold. The variation of the functional response parameters as a function of size of the predator, size ratio with the prey and prey species was analyzed. The data and analysis results were used to improve the representation of microzooplankton in BOGCMs. Improving the representation and the separation was done using the ecosystem model PlankTOM5 coupled to the OGCM NEMO. PlankTOM5 only posses two zooplankton PFTs: the mesozooplankton and the microzooplankton. The mesozooplankton had to be kept as it is in order to have a closure term in the model. The microzooplankton grazing parameters (maximal grazing rate, half-saturation concentration, temperature dependence and feeding respiration) for a mixed-microzooplankton group, were changed according to values obtained for ciliates only or dinoflagellates only. For these three types of microzooplankton representations specific food preferences for the phytoplankton PFTs where assigned. Model runs using these different parameterisations were carried-out and compared to each other.

The thesis is articulated in three steps. (Chapter 1) Factors affecting ciliate feeding behaviour and growth rates are analysed quantitatively and discussed. (Chapter 2) Factor affecting dinoflagellates feeding behaviour and growth rates are analysed quantitatively, discussed and compared to those of ciliates. (Chapter 3) Parameterization of microzooplankton and impact of ciliates and dinoflagellates on global biogeochemical cycles are compared in model experiments using PlankTOM5 coupled to the OGCM NEMO. Finally the conclusion gives a summary and an outlook on this work.

7- Contributions

Chapters I to III describe research performed in cooperation with colleagues from England and Germany. Submission of manuscripts for publication in international peer-reviewed journals is planned for each chapter, respectively, with myself (Sévrine Sailley) as first author. A fourth manuscript where I am co-author has been submitted already to Global Biogeochemical Cycles; it is included in the appendix. In the following I describe my contribution to the research and writing of the chapters.

Chapter I to III have been drafted by myself. They have been discussed and modified by the potential co-authors of future publications, namely, Christine Klaas and Dieter Wolf-Gladrow for Chapter I and II, Erik Buitenhuis, Christine Klaas, and Corinne Le Quéré for Chapter III.

The research presented in Chapters I and II were carried-out by myself. This included data compilation, data analysis, estimation of model parameters and their uncertainties, interpretation of results. Christine Klaas and Dieter Wolf-Gladrow provided critical discussion and comments for both chapters. The procedure (including MATLAB code) for the estimation of model parameters and their uncertainties was developed in cooperation with Dieter Wolf-Gladrow.

The research described in Chapter III was carried out by myself while working at the British Antarctic Survey (England) for one year. Work included design of numerical experiments, handling and analysis of large data sets. Erik Buitenhuis, Clare Enright and Roisin Moriarty assisted in model runs. Erik Buitenhuis and Christine Klaas provided critical comments on this chapter.

The submitted manuscript by Erik Buitenhuis, Richard Rivkin, Sévrine Sailley, and Corinne Le Quéré (Appendix C) has been drafted by the first author with contributions by co-authors. I provided the parameterization for microzooplankton and was involved in the analysis of model results.

8- References

Anderson (2005) Plankton functional type modelling: running before we can walk? *Journal of Plankton Research,* 27 (11) 1073-1081

Anderson (2006) Confronting complexity: Reply to Le Quéré and Flynn. *Journal of Plankton research*, 28(9): 877-878

Aumont, O, Maier-Reimer, E, Blain, S and Monfray, P (2003) An ecosystem model of the global ocean including Fe, Si, P co-limitation. *Global Biogeochemical Cycles,* 17. doi:10.1029/2001GB0011745

Azam F, Fenchel T, Field JG, Gray JS, Meyer-Reil LA and Thingstad F (1983) The ecological role of water-column microbes in the sea. *Mar. Ecol. Prog. Ser.,* 10:257-263

Barber, RT andHiscock MR (2006) A rising tide lifts all phytoplankton: Growth response of other phytoplankton taxa in diatom-dominated blooms. *Global Biogeochemical Cycles,* 20. doi:10.1029/2006GB002726

Banse K (1982) Cell volumes, maximal growth rates of unicellular algae and ciliates, and the role of ciliates in the marine pelagial. *Limnol. Oceanogr.,* 27(6):1059-1071

Behrenfeld, MJ, and Falkowski PG (1997), Photosynthetic rates derived from satellite-based chlorophyll concentration, *Limnol. Oceanogr.,* 42(1), 1-20.

Bindoff, N.L., J. Willebrand, V. Artale, A, Cazenave, J. Gregory, S. Gulev, K. Hanawa, C. Le Quéré, S. Levitus, Y. Nojiri, C.K. Shum, L.D. Talley and A. Unnikrishnan, (2007) Observations: Oceanic Climate Change and Sea Level. In: Climate Change 2007: The Physical Science Basis. Contribution of Working Group I to the Fourth Assessment Report of the Intergovernmental Panel on Climate Change [Solomon, S., D. Qin, M. Manning, Z. Chen, M. Marquis, K.B. Averyt, M. Tignor and H.L. Miller (eds.)]. Cambridge University Press, Cambridge, United Kingdom and New York, NY, USA.

Buck, KR, Marin III, R, Chavez, FP (2005) Heterotrophic dinoflagellate fecal pellet production: grazing of large, chain-forming diatoms during upwelling events in Monterey Bay, California. *Aquat. Microb. Ecol.,* 40: 293-298

Calbet, A (2001) Mesozooplankton grazing effect on primary production: A global comparative analysis in marine ecosystems. *Limnol. Oceanogr.*, 46, 1824-1830.

Calbet, A, (2008) The trophic roles of microzooplankton in marine systems. *ICES Journal of Marine Science,* 65:325-331

Chisholm, SW (2000) Oceanography: Stirring times in the Southern Ocean. *Nature,* 407:685-687

Denman, K, Hoffmann, E, Marchant H (1996) Marine biotic responses to environmental change and feedbacks to climate, in Climate Change 1995, IPCC, edited by JT Houghton et al, pp. 487-516, Cambridge Univ. Press, New York, 1996.

Doney, SC (1999) Major challenges confronting marine biogeochemical modelling, *Global Biogeochem. Cycles*, 13, 705– 714.

Falkowski, P et al (2000) The global carbon cycle: A test of our knowledge of earth as a system, *Science*, 290, 291– 296.

Fasham, MJR, Ducklow, HW, McKelvie (1990) A nitrogen-based model of plankton dynamics in the oceanic mixed layer, *J. Mar. Res.,* 48:591-639

Fenchel, T (1987) Ecology of protozoa: the biology of free-living phagotrophic protists, Science Tech Publishers, Madison Wisconsin / Springer Verlag, Berlin, Heidelberg, New York, London, Paris, Tokyo, 1-193.

Flynn, KJ (2006) Reply to Horizons article: "Plankton Functional Type modelling: Running before we can walk" (Anderson 2005) II. Putting trophic functionality into plankton functional types. *Journal of Plankton research*, 28(9): 873-875

Gregg, WW, Ginoux, P, Schopf, PS, Casey, NW (2003) Phytoplankton and iron: validation of a global three-dimensional ocean biogeochemical model. *Deep-Sea Res. II*, 50: 3143-3169.

Hansen B, Bjoernsen PK, Hansen PJ (1994) The size ratio between planktonic predators and their prey. *Limnol. Oceanogr.,* 39(2):395-403

Jacobson, DM (1999) A brief history of dinoflagellates feeding research. *J. Eukaryot. Microbiol.*, 46(4): 376-381

Jonsson R (1986) Particle size selection, feeding rates and growth dynamics of marine planktonic oligotrichous ciliates (Ciliophoa: Oligotrichina) *Mar Ecol Prog Ser,* 33:265-277

Landry, MR, Hassett, RP (1982) Estimating the grazing impact of marine micro-zooplankton. *Mar. Biol.,* 67: 283-288

Lima, I.D. and Doney, S.C., (2004) A three-dimensional, multinutrient, and size-structured ecosystem model for the North Atlantic. *Global Biogeoche.l Cycles*, 18, GB3019, doi:10.1029/2003GB002146.

Le Quéré, C, Harrison, SP, Prentice, IC, Buitenhuis, ET, Aumont, O, et al (2005) Ecosystem dynamics based on plankton functional types for global ocean biogeochemistry models. *Global Change Biol.*, 11: 1-25

Le Quéré, C (2006) Reply to Horizons article: "Plankton Functional Type modelling: Running before we can walk" (Anderson 2005) I. Abrupt changes in marine ecosystems? *Journal of Plankton research*, 28(9): 871-872

Maier-Reimer, E (1993) Geochemical cycles in an ocean general circulation model. Preindustrial tracer distributions. *Global Biogeochem. Cycles*, 7:645-677

Meehl, G.A., T.F. Stocker, W.D. Collins, P. Friedlingstein, A.T. Gaye, J.M. Gregory, A. Kitoh, R. Knutti, J.M. Murphy, A. Noda, S.C.B. Raper, I.G. Watterson, A.J. Weaver and Z.-C. Zhao, 2007: Global Climate Projections. In: Climate Change 2007: The Physical Science Basis. Contribution of Working Group I to the Fourth Assessment Report of the Intergovernmental Panel on Climate Change [Solomon, S., D. Qin, M. Manning, Z. Chen, M. Marquis, K.B. Averyt, M. Tignor and H.L. Miller (eds.)]. Cambridge University Press, Cambridge, United Kingdom and New York, NY, USA.

Moore, J.K., Doney, S.C., Kleypas, J.A., Glover, D.M. and Fung I.Y (2002) An intermediate complexity marine ecosystem model for the global domain. *Deep-sea Res.*, 10:463-507

Moore, J.K, Doney, S.C. and Lindsay, K. (2004) Upper ocean ecosystem dynamicsand iron cycling in a global three-dimensional model. *Global Biogeochem. Cycles*, 18, GB4028, doi:10.1029/2004GB002220

Najjar R, Sarmiento JL and Toggweiler JR (1992) Downward transport and fate of organic matter in the ocean: Simulations with a general circulation model, *Global Biogeochem. Cycles,* 6: 45-76

Pomeroy LR (1974) The Ocean's food web, a changing paradigm. *Bioscience,* 24:499-504

Sieburth, J. McN., V. Smetacek, and J. Lenz, Pelagic ecosystem structure: Heterotrophic compartments of the plankton and their relationship to plankton size fractions, *Limnology and Oceanography*, 23, 1256-1263, 1978

Strom, SL, Morello, TA (1998) Comparative growth rates and yields of ciliates and heterotrophic dinoflagellates. *Journal of Plankton Research,* 20(3):571-584

Trenberth, K.E., P.D. Jones, P. Ambenje, R. Bojariu, D. Easterling, A. Klein Tank, D. Parker, F. Rahimzadeh, J.A. Renwick, M. Rusticucci, B. Soden and P. Zhai, (2007) Observations: Surface and Atmospheric Climate Change. In: Climate Change 2007: The Physical Science Basis. Contribution of Working Group I to the Fourth

Assessment Report of the Intergovernmental Panel on Climate Change [Solomon, S., D. Qin, M. Manning, Z. Chen, M. Marquis, K.B. Averyt, M. Tignor and H.L. Miller (eds.)]. Cambridge University Press, Cambridge, United Kingdom and New York, NY, USA.

Verity PG and Villareal TA (1986) The relative food value of diatoms, dinoflagellates, flagellates, and cyanobacteria for tintinnid ciliates. *Arch Protistenkd,* 131:71-84

CHAPTER 2:

Pelagic ciliate feeding behaviour and growth rate. An analysis based on laboratory experiments

---

1-Introduction

Pelagic ciliates are an important component of the microzooplankton in terms of biomass and grazing impact (Sherr and Sherr 2002; Calbet and Landry 2004). Furthermore their high growth rates enable them to follow change of phytoplankton concentration (Banse 1982; Johansson et al., 2004) more closely than mesozooplankton organisms. Pelagic ciliates species range in size from about 10 μm to 200 μm and belong almost exclusively to the order Oligotrichida and Choreotrichida characterised by a conspicuous circular or semi-circular anterior row of ciliates organelles used to create feeding currents (Jonsson 1986). Feeding and growth rates in pelagic ciliates are primarily affected by changes in food availability. The feeding and growth response of a heterotrophic ciliate species feeding on a single prey types at a different prey concentration (so-called functional response) can be described by semi-empirical functions with characteristic parameters, such as maximum growth, grazing and clearance rates, that vary depending on ciliate and prey species. To date, an important number of field and laboratory experiments have been carried out to determine the functional response as a function of prey concentration. However, field measurements encompass the whole microzooplankton and phytoplankton communities, whereas experiments using single ciliate species feeding on a single prey species are needed to determine species-specific and size effect on the functional response. Our knowledge of ciliates feeding, in particular prey-size selection is primarily derived from a few laboratory experiments using artificial food particles of standardized size and shape (Heinbokel 1978; Jonsson 1986). Results from these studies indicate that the relative range and optimal prey size is similar for most pelagic ciliates (Fig. 1, Jonsson 1986; Hansen et al., 1994). Optimum prey size is thought to be around 10% of oral

diameter and maximum prey size up to 48% of oral diameter, corresponding to a prey:predator diameter ratio of approximately 1:8 (Hansen et al., 1994). In field observations, however, pelagic ciliates were often observed with ingested food particles as large as or larger than themselves in field samples. Results from earlier laboratory experiments also suggest differences in ciliate feeding behaviour when fed natural or artificial prey items (Fig. 1).

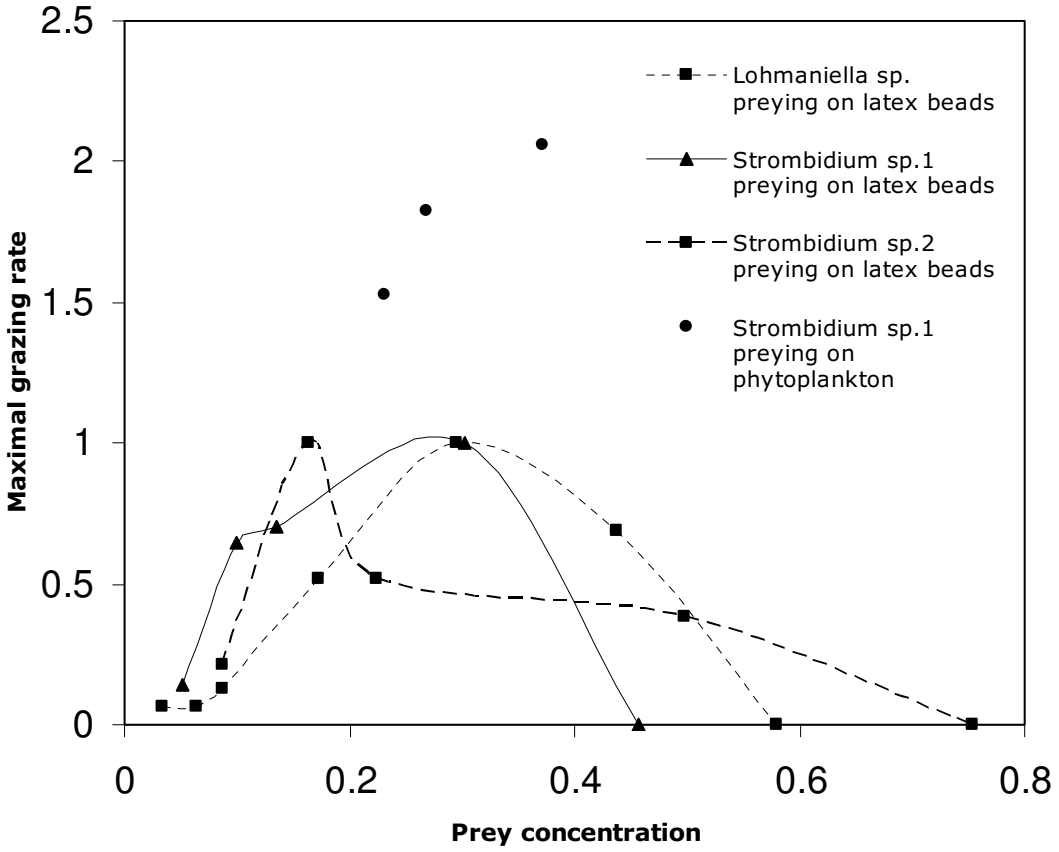

Figure 1: Grazing difference between real prey and latex beads. Maximal grazing rate in (d^{-1}), prey concentration in μm^3 mL^{-1}. Data from Jonsson 1986.

The aim of this study is to determine the effect of ciliate size, prey size and prey quality (as reflected by the taxonomic affiliation of the prey) on feeding and growth response of pelagic ciliates. In this study, available data from laboratory experiments are used in order to determine of the functional response for different ciliate-prey combinations. Further the effect of ciliate and prey characteristic on estimates of parameters of the functional response and gross growth efficiency are analysed. Finally we develop a quantitative description of rates and food preferences that can be used to improve parameterization of ciliates as a community in ecosystem model and within the framework of coupled global ocean biogeochemical-general circulation models (Le Quéré et al., 2005).

2- Data and method

2.1- Data selection and acquisition

Individual data points on growth and grazing rates (or alternatively clearance rate) and corresponding prey concentration were collected from experiment results available in the literature. No article had been intentionally omitted, but some could have been overlooked. A total of 31 articles were selected with results from 342 laboratory experiments (Table 1). If data was available as graphics only the value were extracted using the ImageJ software of the National Health Institute (http://rsb.info.nih.gov/ij/download.html). In addition, for each experiment, ancillary information was collected encompassing experimental conditions, prey and predator information (i.e. species name, strain information, cell size, volume, carbon content) together with corresponding method when available (database is available at: PANGAEA, http://www.pangaea.de). When not available, size, carbon content (C in pg C $cell^{-1}$) and volume (V in μm^3 $cell^{-1}$) of prey and predators were estimated from available ancillary information using appropriate geometrical shapes for conversion of size to volume or volume to size, respectively and volume – carbon conversion equations ($C = a * V^b$; with a and b being group specific) of Menden-Deuer and Lessard (1995). Food concentration can be expressed in number of prey cell, biovolume of prey or prey carbon. Ciliates are known to feed on a certain size class of organisms (Hansen et al., 1994). However it is unknown if inside of this prey size class there is active selection of one prey based on something else then mechanical size selection. Verity (1991) showed that ciliates are not randomly selecting their prey, so there is some other criteria of selection. One of these possible criteria is the suitability of the prey to sustain ciliates growth, which is the nutritional value of the prey. Carbon is a measure of the nutritional value of a prey organism (Lee 1980) and can be derived from its volume, is unknown. For these reasons and considering a non-random acquisition of the prey (Verity 1991) size of the organisms as well as grazing and clearance rate are expressed in carbon units.

Table 1: List of the articles used to collect data, ciliate species used and rates provided.

Author	Ciliate species	Information provided	Number of data (maximal rate)
Aelion and Chisholm 1985	Favella sp.	maximal grazing and growth rates, at different temperature	5
Bernard and Rassoulzadegan 1990	Strombidium sulcatum	grazing as a function of prey concentration	5
Buskey and Stoecker 1988	Favella sp	grazing as a function of prey concentration	1
Cristaki et al., 1998	Strombidium sulcatum	maximal grazing and clearance rate	11
	Uronema sp.	maximal grazing and clearance rate	12
Fenchel 1980	Cyclidium sp.	grazing as a function of prey concentration	2
	Glaucoma scintillans	grazing as a function of prey concentration	1
Fenchel and Jonsson 1988	Strombidium sulcatum	grazing and growth as a function of prey concentration	1
Gismervik 2005	Lohmaniella oviformis	grazing and growth as a function of prey concentration	1
	Strombidium spiralis	grazing and growth as a function of prey concentration	1
	Strombidium spiralis	grazing and growth as a function of prey concentration	1
	Strombidium acutum	grazing and growth as a function of prey concentration	1
	Strombidium conicum	grazing and growth as a function of prey concentration	1
	Strombidium sp	grazing and growth as a function of prey concentration	1
	Strombidium vestitum	grazing and growth as a function of prey concentration	1
Graneli and Johansson 2003	Euplotes affinis	grazing as a function of prey concentration	1
Hansen et al., 1991	Favella ehrenbergii	grazing and growth as a function of prey concentration	1
Heinbokel 1978	Eutintinnus pectinis	grazing and growth as a function of prey concentration	1
	Helicostomella subulata	grazing and growth as a function of prey concentration	1
	Helicostomella subulata	grazing and growth as a function of prey concentration	1
	Tintinnopsis cf. Acuminata	grazing and growth as a function of prey concentration	1
Jeong et al., 1999	Strombidinopsis sp.	grazing and growth as a function of prey concentration	5
Jeong et al., 2002	Tiarina fusus	grazing and growth as a function of prey concentration	6

Table 1: Continued

Jeong et al., 2004	Strombidinopsis jeokjo	grazing and growth as a function of prey concentration	2
Jonsson 1986	Lohmaniella spiralis	grazing as a function of prey concentration	12
	Strombidium reticulatum	grazing as a function of prey concentration	14
Kamiyama et al., 2001	Favella ehrenbergii	maximal grazing rate	10
	Favella taraikensis	maximal grazing rate	10
Montagnes et al., 1996	Strobilidium neptuni	maximal growth rate	1
	Strobilidium veniliae	maximal growth rate	1
	Strombidium siculum	maximal growth rate	1
		maximal growth rate	1
Montagnes et al., 1999	Strombidinopsis subclone 1	maximal growth rate	1
	Strombidinopsis subclone 2	maximal growth rate	1
	Strombidinopsis subclone 4	maximal growth rate	1
	Strombidinopsis subclone 5	maximal growth rate	1
	Strombidinopsis subclone 7	maximal growth rate	1
Montagnes and Lessard 1999	Strombidinopsis multiauris	grazing and growth as a function of prey concentration	12
Rassoulzadegan 1982	Lohmanniella spiralis	maximal grazing, clearance and growth rate at different temperature and prey size	60
Rivier et al., 1985	Strombidium sulcatum	growth as a function of prey concentration	4
Scott 1985	Strombidium sp	maximal grazing and growth rate	11
Setala et al., 2005	Strombidium sp	grazing as a function of prey concentration	1
Stoecker et al., 1981	Favella sp	maximal growth rate	7
Stoecker 1988	Favella sp	grazing as a function of prey concentration	1
	Balanion sp	grazing as a function of prey concentration	1
Stoecker and Evans 1985	Favella sp	maximal growth rate and gross growth efficiency	5
	Balanion sp	maximal growth rate and gross growth efficiency	8
Stoecker et al., 2000	Favella sp.	maximal grazing and clearance rate	1
	Strombidium sp. A	maximal grazing and clearance rate	1
	Strombidium sp. A	maximal grazing and clearance rate	1
	Strombidium sp. C	maximal grazing and clearance rate	1
	Strombidium sp.B	maximal grazing and clearance rate	1
	Tintinnopsis cf. Baltica	maximal grazing and clearance rate	1
	Tintinnopsis cf. Baltica	maximal grazing and clearance rate	1

Table 1 : Continued

	Tintinnopsis cf. Baltica	maximal grazing and clearance rate	1
	Tintinnopsis cf. Dadayi	maximal grazing and clearance rate	1
	Tintinnopsis cf. tubulosides	maximal grazing and clearance rate	1
	Tintinnopsis sp. A	maximal grazing and clearance rate	1
	Tintinnopsis sp. A	maximal grazing and clearance rate	1
	Tintinnopsis sp. B	maximal grazing and clearance rate	1
Verity 1985	Tintinnopsis acuminata	grazing as a function of prey concentration	3
	Tintinnopsis vasculum	grazing as a function of prey concentration	3
Verity 1991	Strobilidium cf. Spiralis	grazing and growth as a function of prey concentration	11
	Tintinnopsis cf. Dadayi	grazing and growth as a function of prey concentration	11
Verity and Villareal 1986	Tintinnopsis vasculum	maximal growth rate	34
	Tintinnopsis acuminata	maximal growth rate	34

2.2- Modelling the functional response

Ingestion of food items depend on several factors: detecting, capturing, handling and digesting the prey. Although prey encounter rate increases in proportion to prey density, the functional response of ingestion typically saturates at high prey densities. Based on the work of Holling (1959) one can distinguish three types of functional responses: a linear increase (Holling I), a decelerating increase (Holling II), and a S-shape increase (Holling III) of ingestion rate with prey concentration (each functional response type is characterised by a different variation of the clearance rate). Ingestion but also growth rates of ciliates usually follows a Holling type II response (Fenchel 1980a; Fenchel 1980b; Verity 1991).

Several mathematical expressions exist to represent the Holling II response (e.g. Michaelis-Menten, Ivlev, and Rectilinear). However, on a statistical basis they usually give equally good fits (Mullin et al., 1975; Gentleman et al., 2003). The Michaelis-Menten function was chosen for fitting the data since this choice allows comparison with previous studies (since all use this equation). Further, present mechanistic understanding of the grazing

process as well as observational evidence supports the use of the Michaelis-Menten model (Fenchel 1980a; Fenchel 1980b; Kiørboe 2008).

Grazing and growth response to food concentration in ciliates might, however, present threshold concentration betond which no grazing or growth occurs. Therefore, when fitting the data we include a threshold concentration (P_t) by modifying the Michaelis-Menten as follows:

$$r = r_{\max} \times \left(\frac{P - P_t}{K + (P - P_t)} \right) \quad (1)$$

with: r corresponding to the rate of grazing or growth at a given prey concentration P, r_{max} the maximal rate, K the half-saturation concentration and P_t the threshold concentration. Grazing and growth follow the same function but with different value for K, P_t and r_{max}, depending on the conversion efficiency of food ingestion into ciliate biomass.

2.2.a- Grazing

$$g(P) = g_{\max} \times \left(\frac{P - P_t g}{Kg + (P - P_t g)} \right) \quad (2)$$

In the case of the grazing response g_{max} is also equivalent to the inverse of the handling time for one prey ($\tau = 1/ g_{max}$): corresponding to the time needed to ingest and digest a prey at saturating concentration. The half-saturation concentration is the concentration at which the grazing or growth rates are half the maximum rate. The half saturation constant for grazing, g_{max} and the maximal clearance rate (F_{max}) are related through Equation 2. F_{max} is the maximum amount of suspension volume that individual grazers (in this case ciliates) can clear of prey items.

$$K = \frac{g_{\max}}{F_{\max}} \quad (3)$$

F_{max} is equivalent to the encounter rate kernel (β) for a given grazer and prey system when the grazer capture all prey encountered (Kiørboe, 2008). If a grazer is not 100% efficient at catching its prey, F_{max} is equivalent to the encounter kernel times the capture

efficiency (α). Encounter and capture efficiency are the limiting process at low prey concentration, while handling time is the limiting process at saturating food.

2.2.b- Growth

Growth rates (μ) in protozoa follows the similar response to food concentration as grazing rate (g) whereby :

$$\mu = g \times GGE \tag{4}$$

with GGE (Gross Growth Efficiency) representing the efficiency of conversion of ingested food into biomass of grazer. GGE will depend on the energetic demands of the grazer and food quality but can also vary with food concentration depending on the feeding strategy of grazers (Jakobsen and Hansen, 1997).

$$\mu(P) = \mu_{\max} \times \left(\frac{P - P_t\mu}{K\mu + (P - P_t\mu)} \right) \tag{5}$$

Note that the earlier definitions are for the grazing parameters, their meaning is different for growth parameters. Considering the threshold, to the detection level of prey is added the metabolism cost thus growth threshold ($P_t\mu$) is expected to be higher than the grazing threshold (P_tg). The growth half saturation concentration ($K\mu$) will be a measure of the assimilation efficiency of a prey carbon and other component, a low value meaning that the prey is assimilated faster and allow better growth.

The data collected were fitted to the modified Michaelis-Menten (Equation 1), parameter estimates μ_{max}, g_{max}, as well as respective threshold concentration and half-saturation constant, and their uncertainties were estimated using a Bayesian approach (Sivia and Skilling 2006) assuming flat priors and additive Gaussian noise. A detailed explanation is to be found in the Annex B. The estimated parameters (r_{max}, K and P_t) where then used to determine how size and prey type affect the functional response.

2.3- Correction for temperature effects and estimation of Q_{10}

In order to correct for temperature effects, Q_{10} of growth and grazing was also estimated based on compilation of data found in the literature on growth and grazing rates of pelagic ciliates as a function of temperature. The temperature dependence of metabolic rates in protozoa usually follows an exponential decay with decreasing temperature within the range best tolerated by the organisms (Montagnes et al., 2003). Here we use this relationship for our estimate of Q_{10}. Data on the temperature dependence of growth and grazing rates for the each set of experiment was plotted on a log scale and visually examined, data points on the lower or upper temperature range that did not follow the linear relationship were flagged and not included in the following analysis. For the remaining data points and for each individual set of experiment, temperatures were adjusted by subtraction of the lowest temperature value ($T_{\min}$) resulting in temperatures ranging from 0 to the maximum temperature range investigated ($T_{\min}$- $T_{\max}$). Similarly the growth or grazing rates were normalised by dividing by the grazing, respectively, growth rates (r) obtained at the lowest temperature studied for each dataset ($r_{\min}$) resulting in rates ranging from 1 to the maximum relative rates (r_{max}/r_{min}) for each set of experiments. This procedure has the advantage of giving a Q_{10} estimate for growth and grazing, respectively, by combining data on different species and experimental set-up in one single analysis that contains the variability of the all the available dataset and thus avoiding biases in Q_{10} estimates due to the low amount of data available when analysing each experiment separately.

Data was fitted to an empirical model:

$$R = e^{aT+b} \qquad (4)$$

with R the relative grazing or growth rates (r_2/r_1), T the temperature difference (T_2-T_1) and a and b the parameters describing decay rate with temperature. Parameters and uncertainties were estimated using the same method applied to the estimates of the functional response. Values of Q_{10} can be estimated as $Q_{10} = e^{aT+b}$ for $T = 10$.

3- Results

3.1- Q_{10} estimate for grazing and growth

Data from 4 different experiments could be found to determine the temperature-effect on grazing and growth rates, respectively. Logarithmic plots of the rates versus temperature clearly show a linear trend for selected grazing and growth data (Figures 2 and 3).

Parameter estimates based on equation 3 and the normalised data were: a = 0.109 and b = 0.052, resulting in a Q_{10} of 3.1 ± 0.22 for the temperature dependence of grazing rates (Figure 4). For temperature dependence of growth rates parameter estimates were: a = 0.092 and b = 0.131, resulting in a Q_{10} of 2.8 ± 0.62 (Figure 5). Correlation coefficient between model and data is r^2 = 0.892 for grazing rates and r^2 = 0.565 for growth rates.

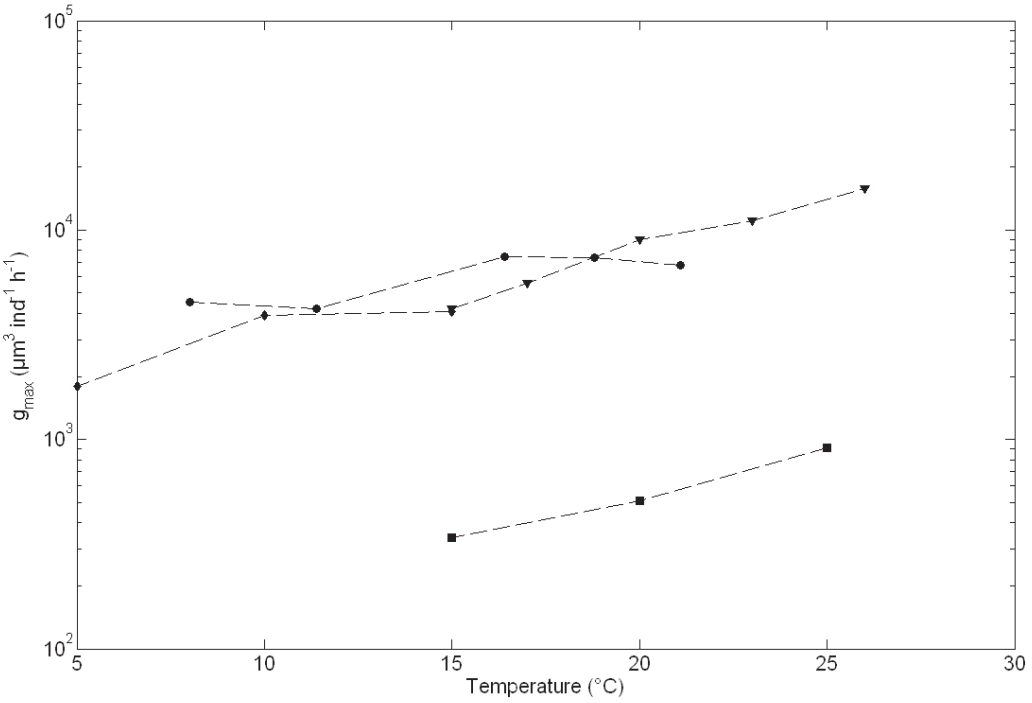

Figure 2: Variation of maximal grazing rate (pg C mL^{-1}) with temperature. Legend: (circle) Aelion and Chrisholm, (square) Verity tintinnid a, (diamond) Verity tintinnid b, (triangle) Rassoulzadegan

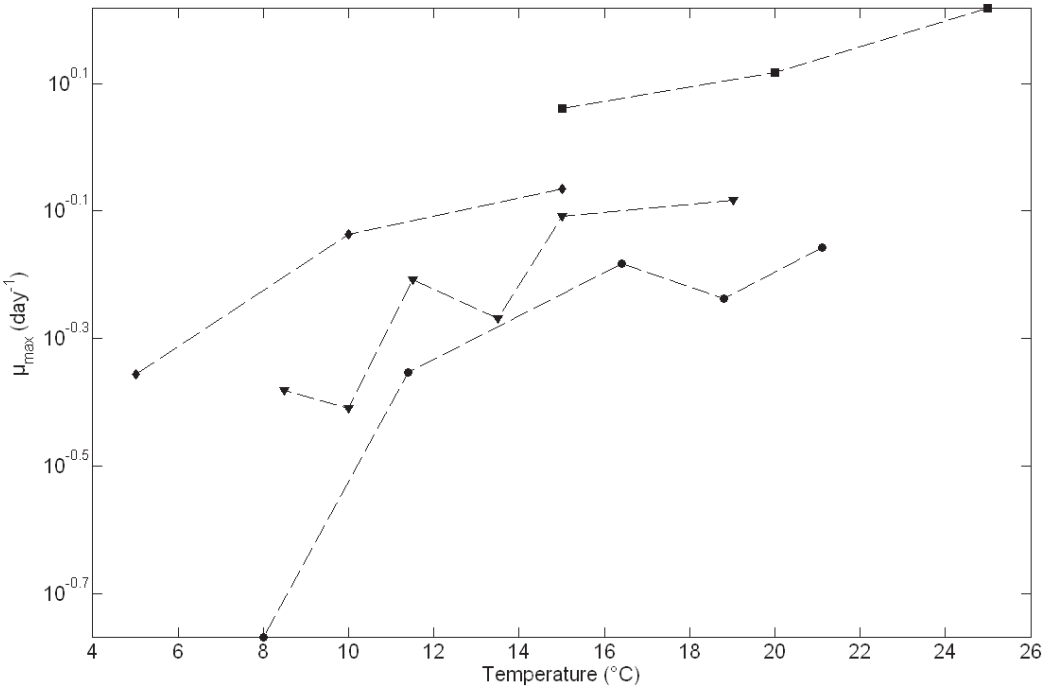

Figure 3: Variation of maximal growth rate (day^{-1}) with temperature. Legend: (circle) Aelion and Chrisholm, (square) Verity tintinnid a, (diamond) Verity tintinnid b, (triangle) Montagnes

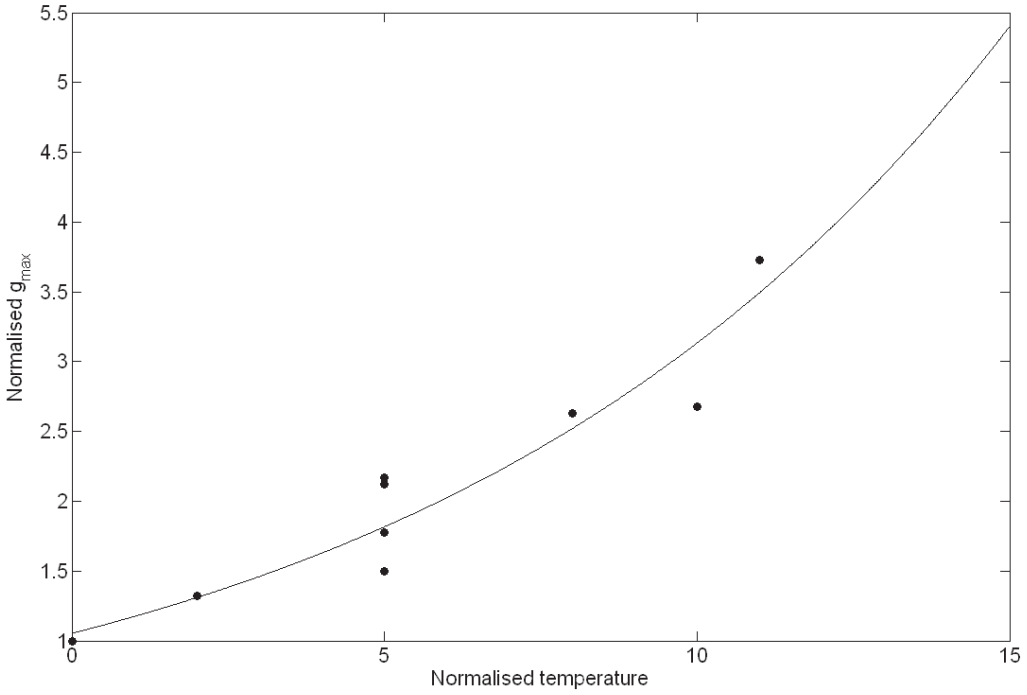

Figure 4: Variation of normalised grazing rate with temperature and modelled temperature dependence curve using optimised parameters for Equation 3. Correlation coefficient between model and data is $r^2 = 0.892$.

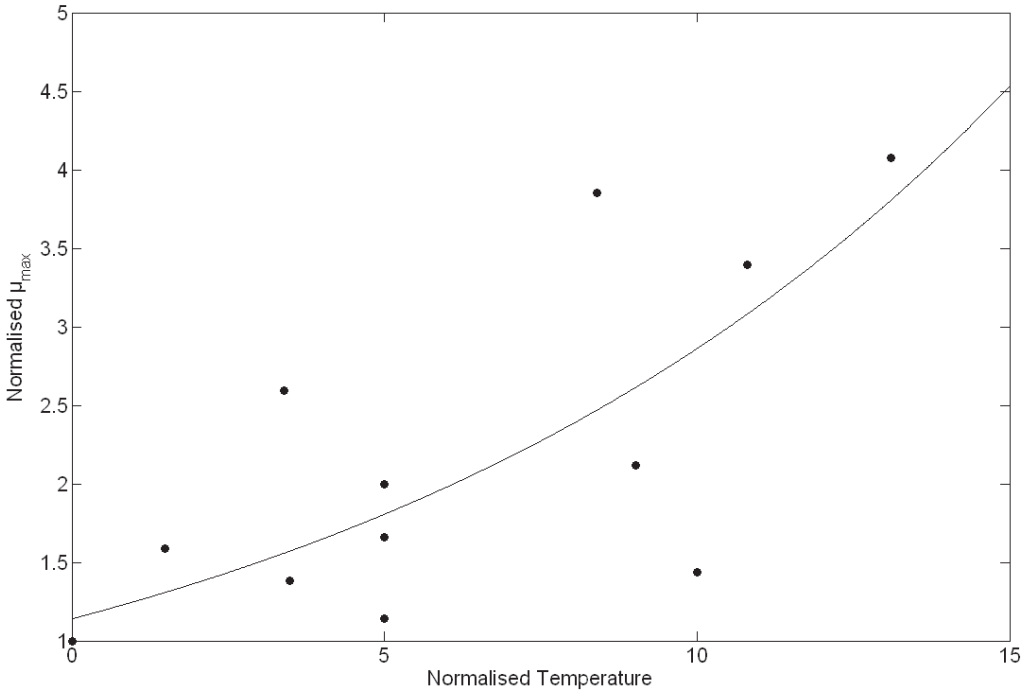

Figure 5: Variation of normalised growth rate with temperature and modelled temperature dependence curve using optimised parameters for Equation 3. Correlation coefficient between model and data is $r^2 = 0.64$.

3.2- Functional response

In order to investigate the influence of prey quality other than size and carbon content, prey taxa were grouped into Functional Types (PFT_s). Prey PFTs were defined according to Le Quéré et al., (2005). The phytoplankton PFT used are the following: silicifiers (diatoms), calcifiers (coccolithophores), pico-heterotrophs (bacteria), pico-autotrophs (cyanobacteria and non nitrogen fixing autotrophs), mixed phytoplankton (any phytoplankton that doesn't fit in a particular PFT), other phytoplankton PFT are defined but haven't been used as prey in the collected experiment (nitrogen fixers and DMSP producers).

Variation of maximum grazing rates (g_{max}) with increasing size of the ciliate as a function of prey:ciliates size ratios (as reflected in respective estimates of carbon content) are given in Figure 6. Ciliate maximum grazing rates increases both with ciliate carbon content and prey:ciliate carbon ratio. Adoubling in ciliate carbon contents leads to a six fold increase

in g_{max}. The increase in g_{max} with prey:ciliate size ratio is less uniform with a sharp increase until the ratio reaches a value of 0.1, no further increase or a decrease is noticed for higher prey:ciliate ratio. In contrast to g_{max} the half-saturation constant for grazing (Kg) doesn't show any significant change with increasing ciliate carbon content (Fig. 7), while Kg increases with prey:ciliate carbon ratio (Fig. 7). Whereby a doubling in prey:ciliate carbon ratio leads to an increase in Kg by a factor of 2.3 for prey:ciliate ratio equal or below 0.03. Above a prey:ciliate carbon ratio of 0.03 no changes in Kg are observed. Grazing threshold concentrations (P_tg) shows high variability depending on ciliate and prey species with 60% of the functional response experiments available for analysis of threshold concentrations showing some threshold value above zero. For threshold values above zero, no noticeable trend related to prey:ciliate carbon ratios is observed except for experiments with small ciliate species (Fig. 8). An increase in P_tg with ciliae carbon content can be observed within a ciliate carbon range of 226 to 8337 pg C ind^{-1}, whereby a doubling in ciliate carbon content leads to, roughly, a four-fold increase in P_tg (Fig. 8). There is no noticeable impact of prey PFT on g_{max} and Kg, but P_tg is higher for coccolithophores than for other prey PFT (Fig. 6, 7 and 8).

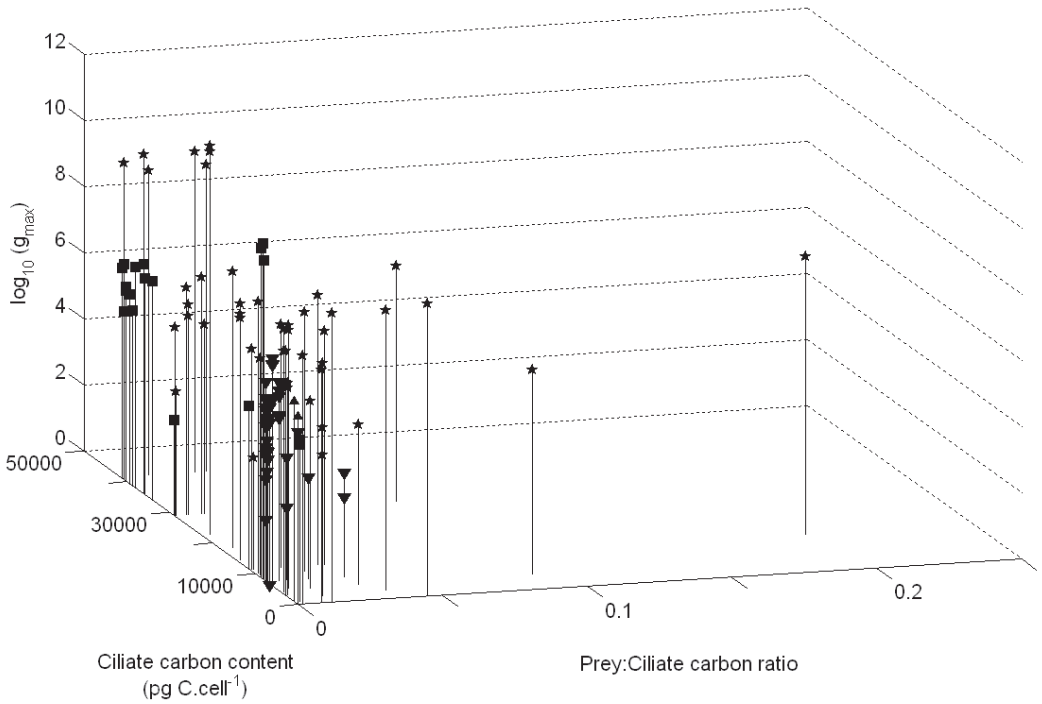

Figure 6: Variation of the maximal grazing rate (g_{max}) on a log scale versus the ciliate carbon content and the prey:ciliate carbon ratio. PFT legend: silicifiers (circle), calcifers (square), pico-autotrophs (downward triangle), mixed phytoplankton (star), other group exist but haven't been used as prey in the collected experiment.

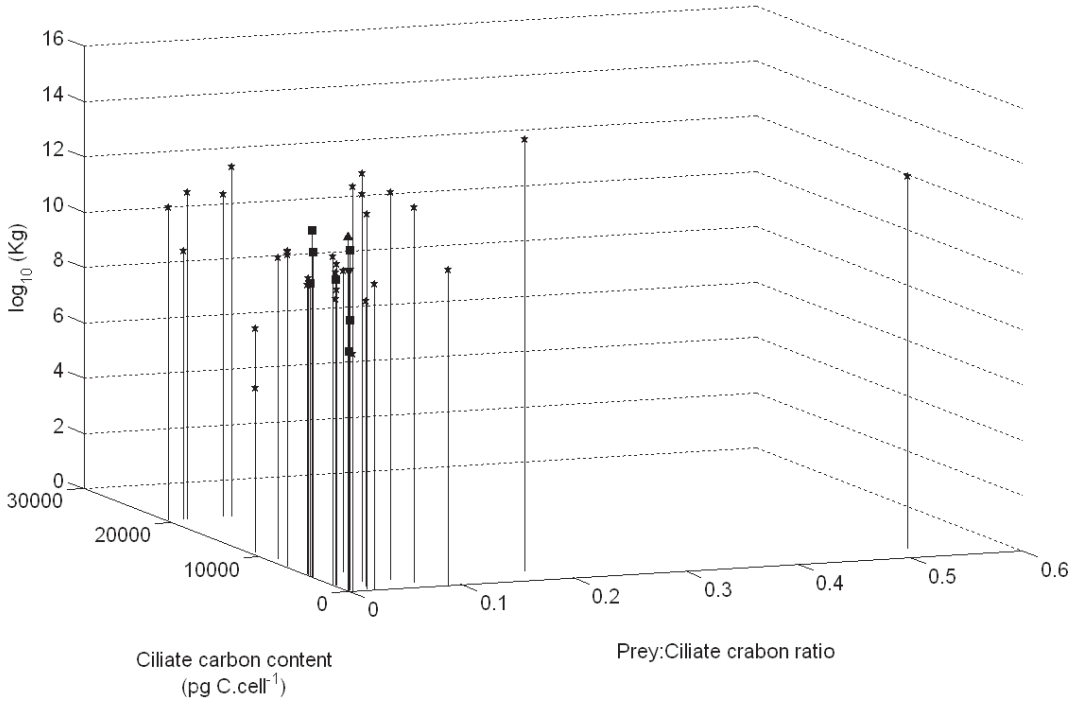

Figure 7: Variation of the grazing half-saturation (Kg) on a log scale versus the ciliate carbon content and the prey:ciliate carbon ratio. PFT legend: calcifers (square), pico-autotrophs (downward triangle), mixed phytoplankton (star), other group exist but haven't been used as prey in the collected experiment.

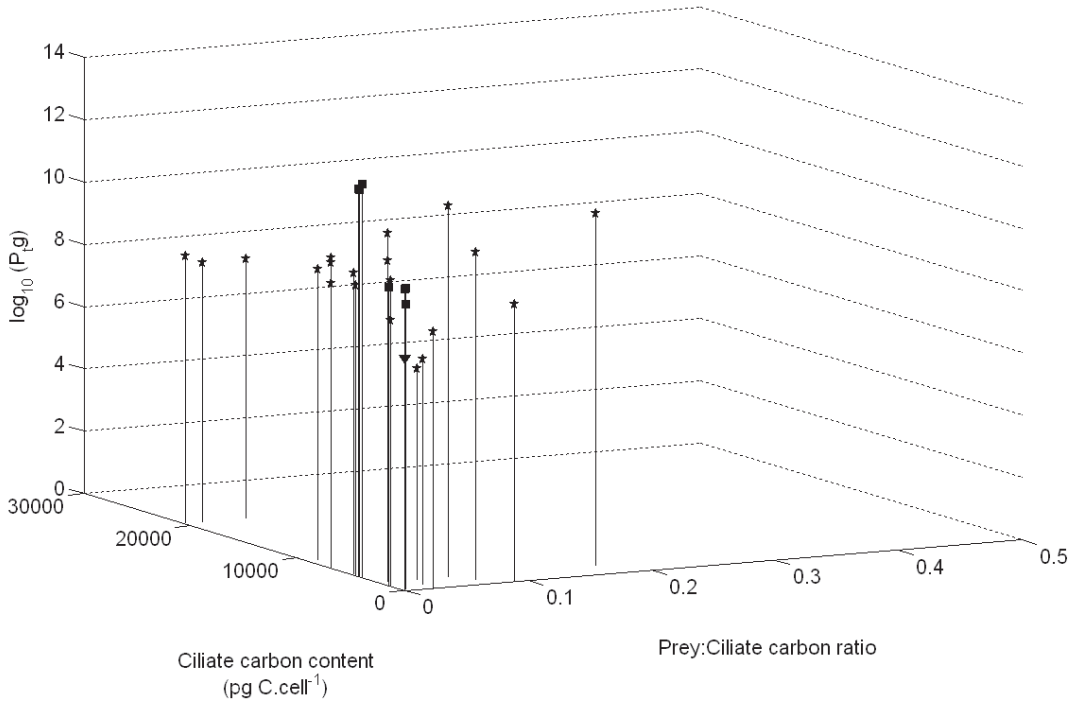

Figure 8: Variation of the grazing threshold concentration (P_tg) on a log scale versus evolution of the ciliate carbon content and the prey:ciliate carbon ratio. PFT legend: calcifers (square), pico-autotrophs (downward triangle), mixed phytoplankton (star), other group exist but haven't been used as prey in the collected experiment.

The values for μ_{max} are comprised between 0 and 2.7 day^{-1} (Fig. 9) with most of the value being below 1 day^{-1}, the highest values are when the offered prey is a pico-heterotroph (bacteria, ▲). μ_{max} does not increase with increasing ciliate size. μ_{max} increases with increasing prey:ciliate ratio, with highest values situated around a ratio of 0.03, for higher ratio there is too few value to judge if μ_{max} values are decreasing or increasing. All $K\mu$ values are situated around 10^{10} pg C ml^{-1} with no increase or decrease that can be related to size and size ratio (Fig. 10). 88% of the growth experiments (43 out of 49 growth experiments) showed $P_t\mu$ values above zero and ranging from a log value of 10^8 to 10^{10} pg C ml^{-1} (Fig. 11). The amount of available data as well as the range in prey:ciliate ratio is too small to detect possible possible size related changes in $P_t\mu$. No effect of the prey PFT on $K\mu$ and $P_t\mu$ can be noticed.

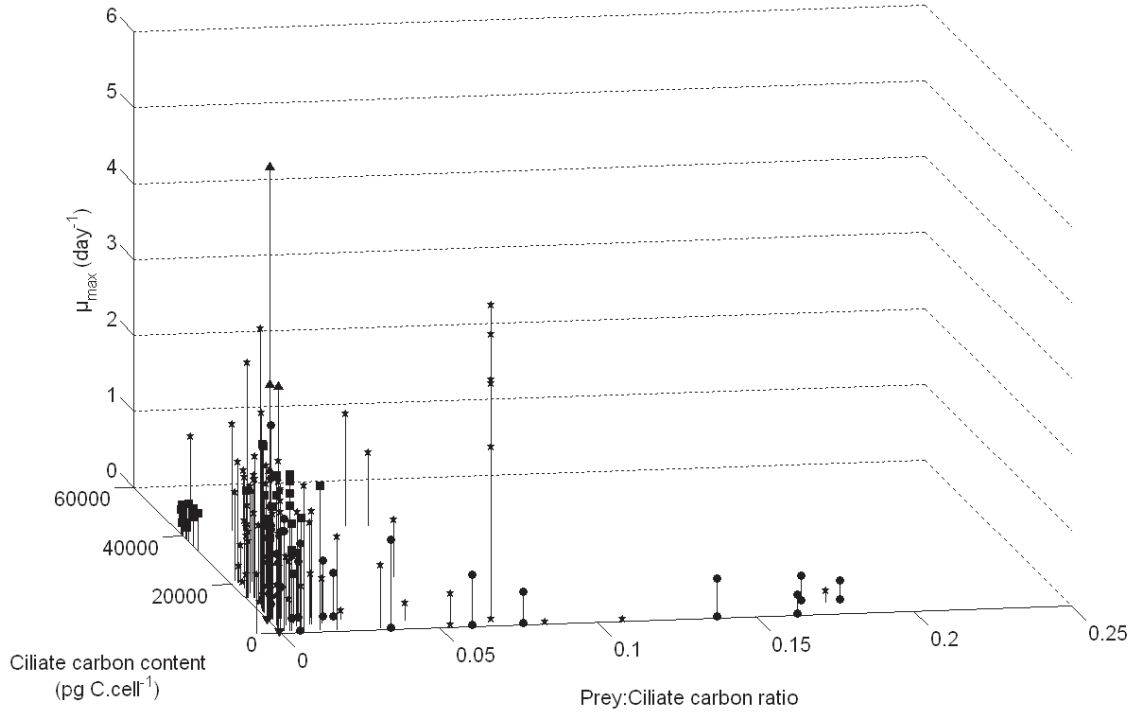

Figure 9: Variation of the maximal growth rate (μ_{max}) with the ciliate carbon content and the prey:ciliate carbon ratio. PFT legend: silicifiers (circle), calcifers (square), pico-heterotrophs (upward triangle), pico-autotrophs (downward triangle), mixed phytoplankton (star), other group exist but haven't been used as prey in the collected experiment.

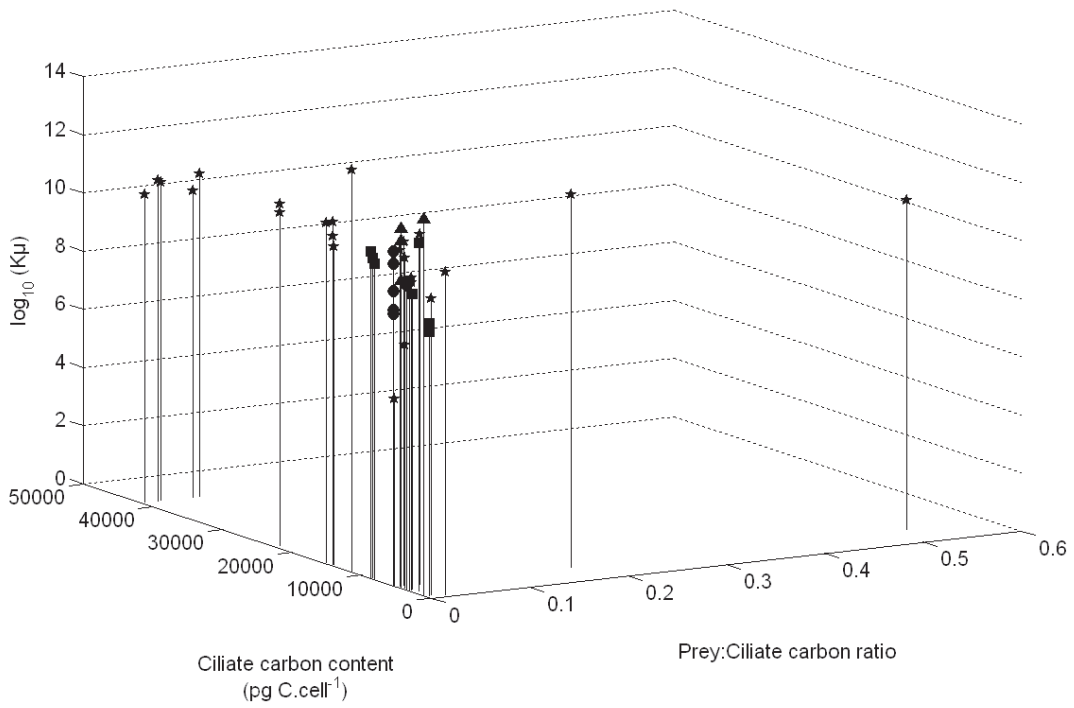

Figure 10: Variation of the growth half-saturation (Kμ) on a log scale versus the ciliate carbon content and the prey:ciliate carbon ratio. PFT legend: silicifiers (circle), calcifers (square), pico-heterotrophs (upward triangle), mixed phytoplankton (star), other group exist but haven't been used as prey in the collected experiment.

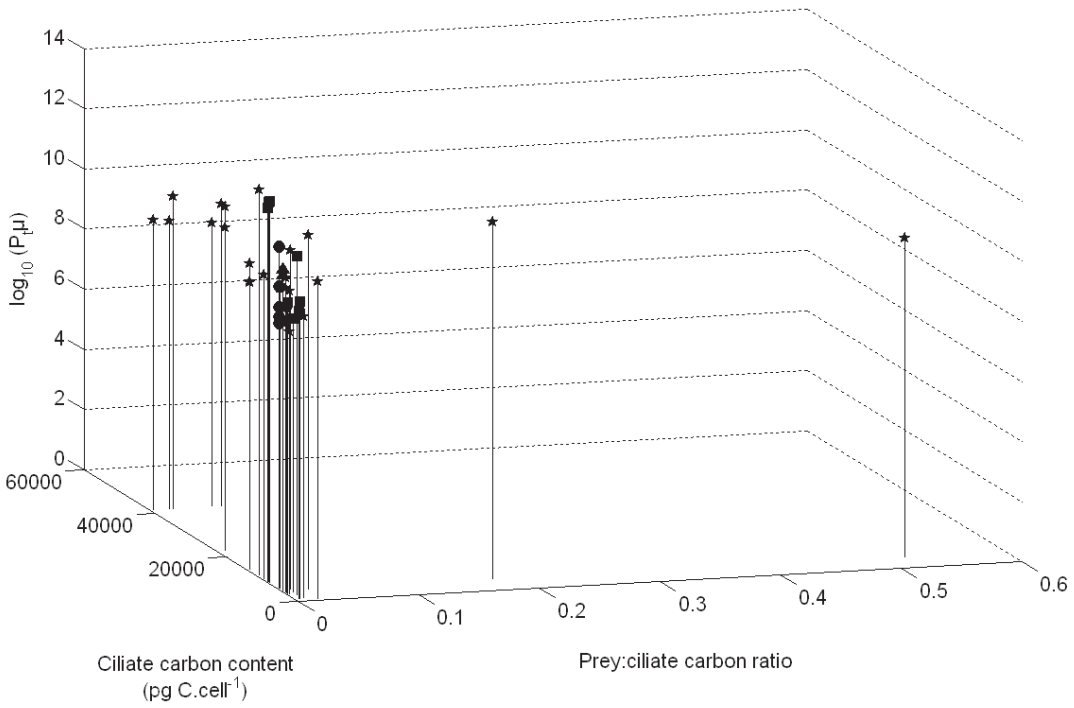

Figure 11: Variation of the growth threshold concentration ($P_t\mu$) on a log scale versus evolution of the ciliate carbon content and the prey:ciliate carbon ratio. PFT legend: silicifiers (circle), calcifers (square), pico-heterotrophs (upward triangle), pico-autotrophs (downward triangle), mixed phytoplankton (star), other group exist but haven't been used as prey in the collected experiment (nitrogen fixers and DMSP producers).

When comparing the value for K and P_t for grazing and growth, Kg is systematically superior to $K\mu$ sometimes by one order of magnitude, inversely P_tg is inferior to $P_t\mu$ by half an order of magnitude at the maximum (Table 2).

Table 2: Comparison between half-saturation and threshold concentration, in µg C mL^{-1} of grazing and growth.

Author	Kg	P_tg	Kµ	P_tµ
Gismervik 2005	776	0	66	38
	137	0	85	24
Heinbokel 1978	35	10	30	15
	33	5	4	2
	16	4	6	5
	440	0	7	0
Jeong et al., 1999	16	4	60	14
	114	4	37	12
	300	0	66	23
	80	5	39	15
	131	0	56	32
Jeong et al., 2000	691	0	81	40
	1570	0	171	128
	6028	78	364	140
Jeong 2004	0.37	0	125	93
	3	0	94	46
Verity 1985	213	9	12	13
	17	15	9	19
	6	15	10	14
	126	290	51	324
	267	240	61	305
	39	246	74	247
Verity 1991	63	14	42	16
	111	5	46	6
	44	17	39	24
	79	20	56	26
	87	17	131	14
	87	9	81	14

The difference in response to variation of prey concentration is observable in the following equations obtained by fitting all the temperature corrected data:

$$g = 251000 \times \left(\frac{P}{8800000 + P} \right) \tag{7}$$

$$\mu = 1.1 \times \left(\frac{P - 15800}{41900 + (P - 15800)} \right) \tag{8}$$

3.3- Gross Growth Efficiency (GGE)

GGE is the expression of the amount of grazed biomass transformed into predator biomass (eq. 9).

$$GGE = \frac{\mu}{g} \tag{9}$$

Data from Verity (1985) and Rassoulzadegan (1982) were used to determine how the temperature variations affect GGE (Fig. 12). As for other parameter GGE data was normalised in order to estimate overall variations in GGE for ciliates (Fig. 13). GGE decreases with temperature with a Q_{10} of 0.72 although large variability is observed.

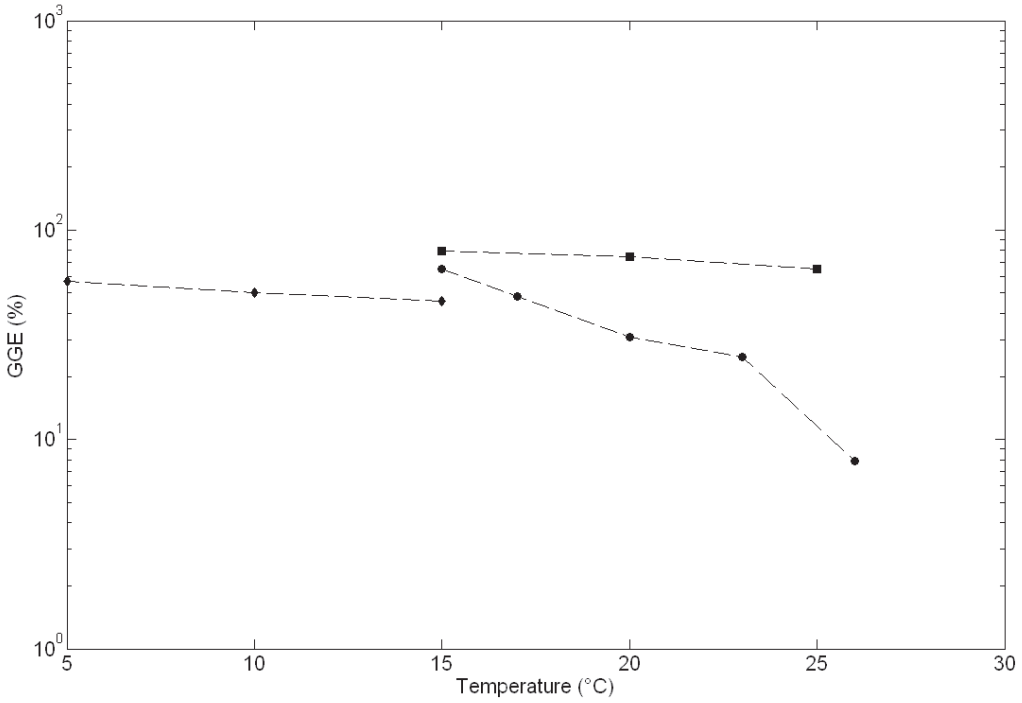

Figure 12: Variation of GGE with temperature. Verity 1985 Tintinnopsis acuminate (square), Verity 1985 Tintinnopsis vasculum (diamond), Rassoulzadegan 1982 Lohmaniella spiralis (circle).

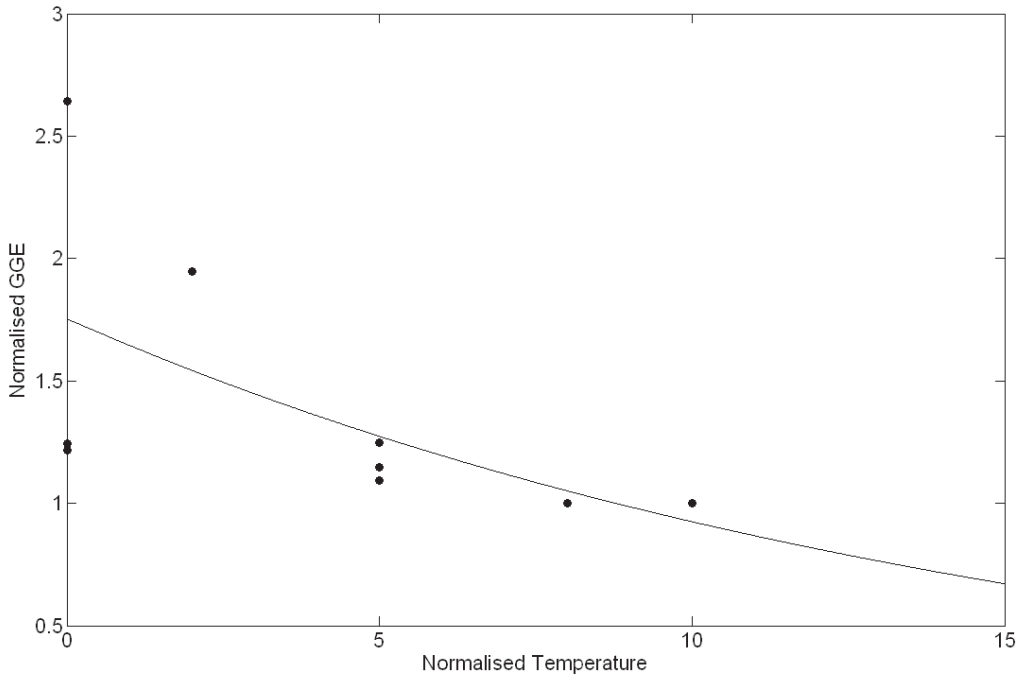

Figure 13: Variation of GGE in function of temperature and modelled temperature dependence curve using optimised parameters for Equation 3. Correlation coefficient between model and data is $r^2 = 0.45$. a = -0.042; b = 0.094; $Q_{10} = 0.72 \pm 0.45$

Comparison of prey concentration and GGE (Fig. 14) indicates high variability and no trend. GGE seems, however, to partially be influenced by cilate:prey carbon ratios as at low ratio (corresponding to large prey) GGE decreases to a value close to zero (Fig. 15). The GGE values for a ciliate:prey ratio superior to 230 have a mean of ~ 40%; while the GGE value for a ratio below 230 have a mean of about 10%. Comparison between variations in GGE with g_{max} and μ_{max} (Fig. 16) indicates that GGE increases with increasing μ_{max} and decreasing g_{max}.

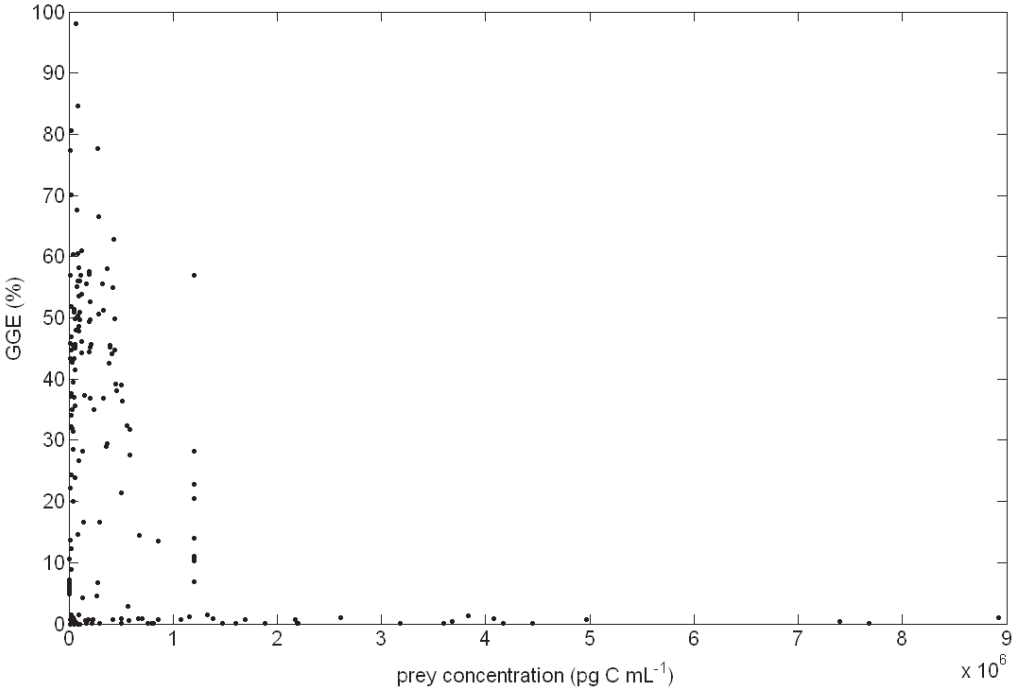

Figure 14: Variation of GGE in relation to change in prey concentration.

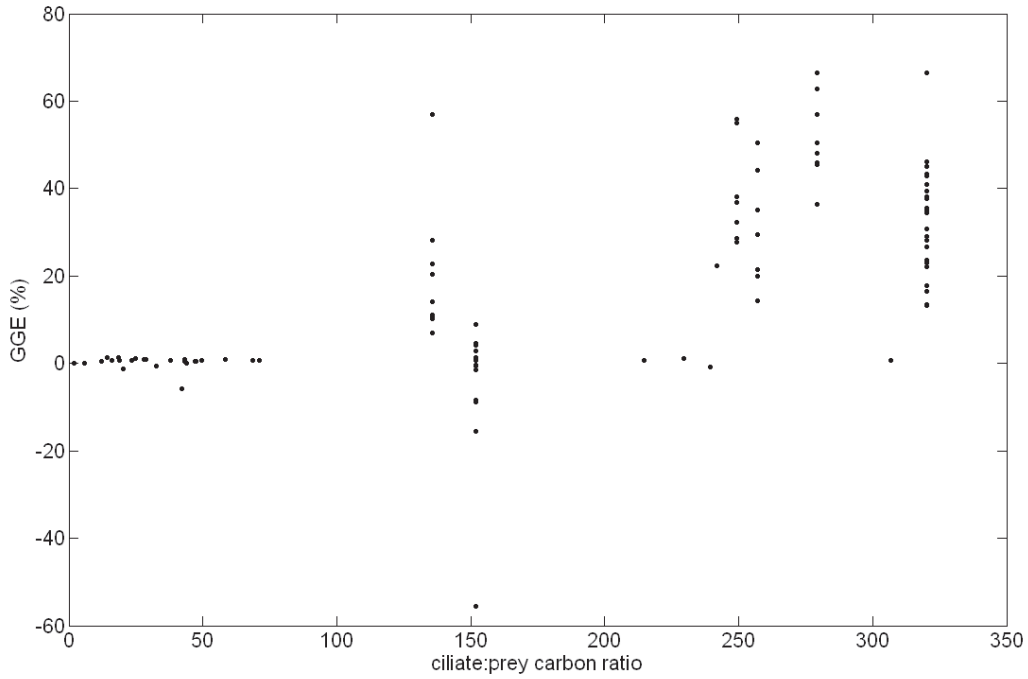

Figure 15: Variation of GGE (calculated from grazing and growth expressed in carbon per hour) with the ciliate to prey carbon ratio. (GGE = 0.137*ratio – 5.935)

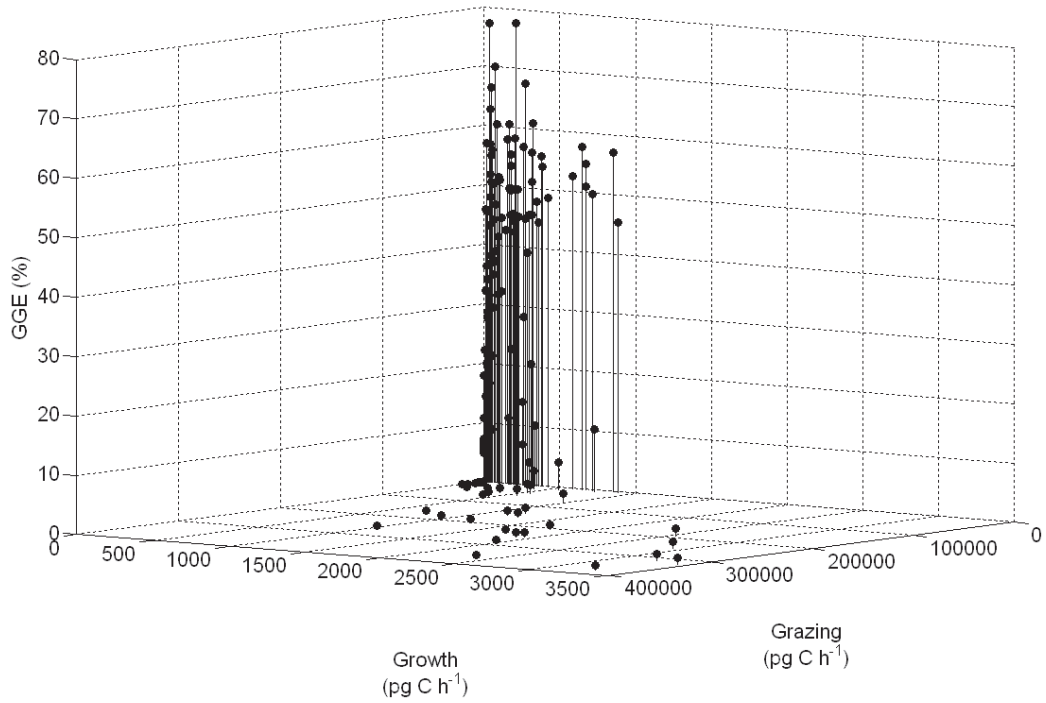

Figure 16: Variation of GGE with the specific grazing and growth rates.

4-Discussion

4.1- Temperature effects

Estimates of Q_{10} for grazing and growth give slightly different values (higher for grazing than for growth). However, the uncertainties found in these Q_{10} estimates suggest that there might be no differences. However, the analysis of the variation in GGE with temperature supports the notion of a small temperature effect on GGE (Q_{10} = 0.72 ± 0.45) similar to findings by Straile (1997), although this effect is complicated by the fact that temperature effects on GGE might also be affected by species-specific characteristics of ciliates and prey food offered in the experiments.

4.2- Functional response and GGE.

GGE increases with the ciliate:prey ratio and maximum growth rate and decreases with maximal grazing. These trend with size ratio can be interpreted as an optimisation of the resources when they are somehow scarce and is consistent with the trend in GGE and maximum grazinf rates. Below a ciliate:prey carbon ratio of 250, corresponding to an Estimated Spherical Diameter (ESD) prey:ciliate ratio of approximately 0.1, a shift in GGE to

low values (around 10%) is observed. The ratio of 0.1 is the ratio of the optimal prey:ciliate size ratio determined from previous studies using latex beads (Hansen et al., 1994). This shift is accompagnied by high grazing rates but low maximum growth rates. These results indicate that optimal ciliate to prey size ratio, when using living organisms as food cannot be determined by ingestion rates alone. However, the combinations of high grazing and low GGE for large prey indicates that these prey are ingested but possibly not properly digested or assimilated.

An effect of size cannot be seen on the half-saturation concentration and threshold concentration for both the grazing and growth. In general the grazing threshold is lower than the growth threshold, while the half-saturation for grazing is higher than for the growth (Table 2, Eq. 7 and 8). The difference between grazing and growth threshold are consistent with the fact that not all food ingested is assimilated for growth. However, the large differences (up to two orders of magnitudes) between grazing and growth half-saturation is surprising. In the case of grazing, the half-saturation constant decreases as maximum clearance rate and handling time increase. A low half-saturation constant reflects, therefore, the combination of ability to encounter, capture and handle the prey. Hence, not large differences between half-saturation constants of growth and grazing would be expected. The results obtained in this study, therefore suggest that factors determining success in prey acquisition do not influence growth.

If plotting the grazing and growth as a function of prey concentration following the equations (7) and (8) the grazing rate would be increasing linearly while the growth rate reached the saturation point. The difference in grazing and growth response to changing prey concentration, hint toward a GGE that is far from being stable (Straile, 1997). This result is supported by the experiment of Verity (1985) where grazing and growth response is decoupled. In addition, the GGE slightly decreases then show a sharp increase at low concentration, followed by slow decrease (Fig. 17).

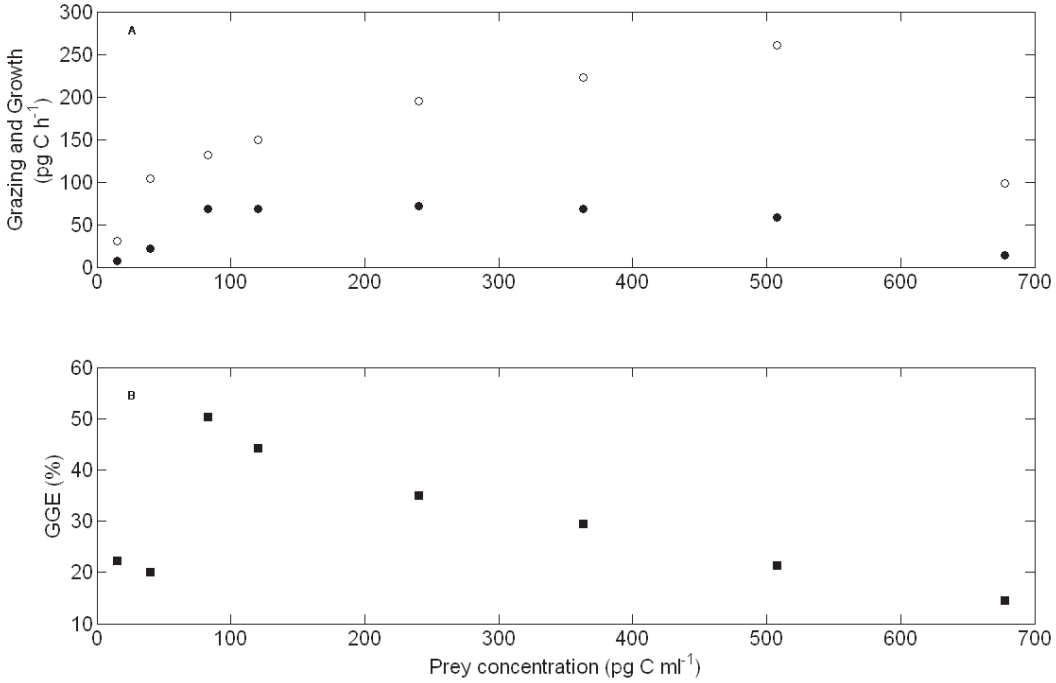

Figure 17: Variation of grazing and growth rates with prey concentration (A), in parallel to change in GGE (B). Data from Verity (1985) Tintinnopsis acuminate feeding on Isochrysis galbana at 25°C.

An attempt was made at making a quantitative description of the variation of grazing and growth maximal rates as a function of ciliate size and the prey:ciliate size ratio. To do this the value plotted against the predator size and the prey:predator ratio were fitted to a variety of relationship (log-linear, log-power and a Gaussian equation were tried) in order to find the more appropriate. None of the fits was satisfying in that they all overestimate the lowest value and underestimate the higher ones. However one feature was common to all the fits: the impact of the predator size is some order of magnitude less than the impact of the prey:predator size ratio.

5- Conclusion

This study brings out some points that can be of interest for future experiments on ciliates as well as for ecosystem models that include microprotozoa. One of them is the optimal size of prey for ciliates. Maximal grazing and growth rates increase above the optimum prey:predator size ratio determined during previous studies (Jonsson, 1986). This is consistent with studies where large ciliates of the genera Strobilidiid and Strombidiid are

found to be able to feed on prey item from the microphytoplankton (Kahl 1932; Smetacek 1981; Montagnes et al., 1988; Jakobsen and Hansen 1997). Calbet and Saiz (2005) found that ciliates consume around 30% of the primary production produced by large phytoplankton, similar tograzing impact of copepods. Hence, the view that ciliates grazing impact is mainly on bacteria, pico-autotrophs or nanoflagellates, *i.e.* the microbial loops (Pomeroy 1974; Azam 1983) might be misleading. Larger prey should be considered in future feeding and growth experiments in order to cover the whole prey size spectrum and also obtain more data on the GGE. Also, doing experiments with larger prey will allow to determine the maximal prey:ciliate size ratio and allow a better representation in conceptual food-web and models. Nevertheless, GGE at high prey:ciliate size ratios tend to be very low, indicating that although ciliates consumme large prey their growth should be limited.

Results from the analysis of available experimental data indicate the prey:predator size ratio have a larger effect on maximal grazing and growth rate than ciliate size. These results show that prey characteristic is a determinant factor when trying to estimate maximal grazing and growth rates in pelagic ciliates species and populations. This is further complicated by the fact that no relationship between taxonomic affiliation of prey and maximal grazing and growth rates could be found, indicating that the understanding of factors determining suitability of prey for a given ciliate species are complex and not understood.

Feeding threshold reveals behavioural traits and trade-offs in energy allocation in ciliates. However, neither size (as proxy for metabolic rates) nor prey PFTs had a visible impact on the feeding threshold or even the growth threshold. These results suggest that feeding threshold could be the result of species-specific ciliate-prey combinations. The opposite trends in GGE observed when comparing to maximum grazing and growth rates indicates that for a given ciliate species high maximum grazing rates (lower handling times) does reflect does not reflect better prey quality and suitability but seems to be rather the result of resource optimization. Hence, estimating growth from grazing using a fixed GGE leads to inaccurate and possibly misleading results.

More laboratory experiments are needed in order to better understand factors defining the determining of food preferences in ciliates, as well as their functional response and the decoupling between grazing and growth. Modellers might want to review the way ciliates impact pelagic ecosystems.

6-References

Aelion CM, Chisholm SW (1985) Effect of temperature on growth and ingestion rates of Favella sp. *J. Plankton Research,* 7:821-830

Aumont O, Maier-Reimer E, Blain S, Monfray P (2003) An ecosystem model of the global ocean including Fe, Si, P colimitations. *Global Biogeochemical cycles,* 17(2)

Azam F, Fenchel T, Field JG, Gray JS, Meyer-Reil LA and Thingstad F (1983) The ecological role of water-column microbes in the sea. *Mar. Ecol. Prog. Ser.,* 10:257-263

Banse K (1982) Cell volumes, maximal growth rates of unicellular algae and ciliates, and the role of ciliates in the marine pelagial. *Limnol. Oceanogr.*, 27(6):1059-1071

Bernard, C and Rassoulzadegan, F (1990) Bacteria or microflagellates as a major food source for marine ciliates: possible implications for the microzooplankton. *Mar. Ecol. Prog. Ser.,* 64:147-155

Buskey, EF and Stoecker, DK (1988) Locomottory patterns of the planktonic ciliate *Favella sp.*: adaptations for remaining within food patches. *Bulletin of Marine Science,* 43(3):783-796

Calbet A, Landry MR (2004) Phytoplankton growth, microzooplankton grazing, and carbon cycling in marine systems. *Limnol. Oceanogr.,* 49:51-57

Calbet A, Saiz E (2005) The ciliate-copepod link in marine ecosystems. *Aquat. Microb. Ecol.,* 38:157-167

Cristaki U, Dolan, JR, Pelegri, S and Rassoulzadegan F (1998) Consumption of picoplankton-size particles by marine ciliates: Effects of physiological state of the ciliate and particle quality. *Limnol. Oceanogr.,* 43(3):458-464

Eppley, RE (1972) Temperature and phytoplankton growth in the sea. *Fishery Bulletin,* 70(4):1063-1085

Evans TE, Paranjape MA (1992) Precision of estimates of phytoplankton growth and microzooplankton grazing when the functional response of grazers may be nonlinear. *Mar. Ecol. Prog. Ser.,* 80:285-290

Fenchel, T (1980)a, Suspension feeding in ciliated protozoa: Functional response and particle size selection. *Microb. Ecol.,* 6:1-11

Fenchel, T (1980)b, Suspension feeding in ciliated protozoa: Feeding rates and their ecological significance. *Microb. Ecol.,* 6:13-25

Gentleman W, Leising A, Frost B, Strom S, Murray J (2003) Functional responses for zooplankton feeding on multiple resources: a review of assumptions and biological dynamics. *Deep Sea Research II*, 50:2847-2875

Gismervik I (2005) Numerical and functional responses of choreo- and oligotrich planktonic ciliates. *Aquat. Microb. Ecol.,* 40:163-173

Granely, E and Johansson, N (2003) Effects of the toxic haptophyte *Prymnesium parvum* on the survival and feeding of a ciliate: the influence of different nutrient conditions. *Mar. Ecol. Prog. Ser.,*254:49-56

Hansen B, Bjoernsen PK, Hansen PJ (1994) The size ratio between planktonic predators and their prey. *Limnol. Oceanogr.*, 39(2):395-403

Hansen PJ, Bjornsen PK, Hansen BW (1997) Zooplankton grazing and growth: scaling within the 2-2,000- µm body size range. *Limnol. Oceanogr.*, 42(4):687-704

Heinbockel, JF (1978) Studies on the functional role of tintinnids in the southern California bight. I. Grazing and growth rates in laboratory cultures. *Marine Biology,* 47:177-189

Holling, CS (1959) Some characteristics of simple types of predation and parasitism. *Canadian Entomologist,* 91, 824–839.

Jakobsen HH, Hansen PJ (1997) Prey size selection, grazing and growth response of the small heterotrophic dinoflagellate Gymnodinium sp. and the ciliate Balanion comatum—a comparative study. *Mar. Ecol. Prog. Ser.,* 158:75–86

Jeong, HJ, Shim, JH, Lee, CW, Kim, JS and Koh, SM (1999) Growth and grazing rates of the marine planktonic ciliates *Strombidinopsis sp.* On red-tide and toxic dinoflagellates. *J. Euk. Microbiol.*, 49:69-76.

Jeong, HJ, Yoon, JY, Kim, JS, Yoo, YD and Seong, KA (2002) Growth and grazing rqtes of the prostomatid ciliate *Tiarina fusus* on red-tide and toxic algae. *Aquat. Microb. Ecol.,* 28:289-297

Jeong, HJ, Yoo, YD, Kim, JS, Kang, NS, Kim, TH, Kim, JH (2004) Feeding by the marine planktonic ciliate *Strombidinopsis jeokjo* on common heterotrophic dinoflagellates. *Aquat. Microb. Ecol.,* 36: 181-187.

Johansson M, Gorokhova E, Larsson U (2004) Annual variation in ciliate community structure, potential prey and predators in the open northern Batlic Sea proper. *J. Plankton. Res.,* 26:67-80

Jonsson R (1986) Particle size selection, feeding rates and growth dynamics of marine planktonic oligotrichous ciliates (Ciliophoa: Oligotrichina) *Mar. Ecol. Prog. Ser.,* 33:265-277

Kahl A (1932) Urtiere oder Protozoa I. Wimpertiere oder Ciliata (Infusoria). In: Dahl F (ed) Tierwelt Deutschlands und der angrenzenden Meeresteile 18:1–886

Kamiyama, T and Arima, S (2001) Feeding characteristic of two tintinnid ciliate species on phytoplankton including harmful species: effects of prey size on ingestion rates and selectivity. *Journal of Experimental Marine Biology and Ecology*, 257:281-296

Kiørboe, T(2008) A mechanistic approach to plankton ecology. Princeton, Univ. Press

Le Quéré C, Harrison SP, Prentice IC, Buitenhuis ET, et al (2005) Ecosystem dynamics based on plankton functional types for global ocean biogeochemistry models. *Global change biology*, 11:2016-2040

Lee JJ (1980) Informational energy flow as an aspect of protozoan nutrition. *J. Protozool.,* 27:5-9

Menden-Deuer S, Lessard EJ (1995) Carbon to volume relationships for dinoflagellates, diatoms, and other protist plankton. *Limnol. Oceanogr.,* 45:569-579

Montagnes DJS, Lynn DH, Roff JC, Taylor WD (1988) The annual cycle of heterotrophic planktonic ciliates in the waters surrounding the Isles of Shoals, Gulf of Maine: an assessment of their trophic role. Mar Biol 99:21–30

Montagnes DJS, Lessard EJ (1999) Population dynamics of the marine planktonic ciliate Strombidinopsis multiauris: its potential to control phytoplankton blooms. *Aquat. Microb. Ecol.,* 20:167-181

Montagnes DJS, Lynn DH, Roff JC, Taylor WD (1988) The annual cycle of heterotrophic planktonic ciliates in the waters surrounding the Isles of Shoals, Gulf of Maine: an assessment of their trophic role. *Mar. Biol.,* 99:21–30

Montagnes DJS, Berger JD and Taylor FJR (1996) Growth rate of the marine planktonic ciliate *Strombidinopsis cheshiri* Snyder and Ohman as a function of food concentration and interclonal variability. *Journal of Experimental Marine Biology and Ecology,* 206:121-132

Montagnes DJS, Kimance SA, Atkinson D (2003) Using Q10: can growth rates increase linearly with temperature? *Aquat. Microb. Ecol.*, 32:307-313

Mullin MM, Stewart EF, Fuglister FJ (1975) Ingestion by planktonic grazers as a function of concentration of food. *Limnol. Oceanogr.,* 20:259-262

Peters F (1994) Prediction of protistan grazing rates. *Limnol. Oceanogr.,* 39(1):195-206

Pomeroy LR (1974) The Ocean's food web, a changing paradigm. Bioscience 24:499-504

Rassoulzadegan F (1982) Dependence of grazing rate, gross growth efficiency and food size range on temperature in a pelagic oligotrichous ciliate Lohmaniella spiralis Leeg., fed on naturally occurring particulate matter. *Ann. Inst. Océanogr.,* Paris 58:177-184

Rivier A, Brownlee DC, Sheldon RW and Rassoulzadegan F (1985) Growth of microzooplankton: a comparative study of bacterivorious zooflagellates and ciliates. *Marine Microbial Food Webs*, 1:51-60

Scott JM (1985) The feeding rates and efficiencies of a marine ciliate, *Strombidium sp.*, grown under chemostat steady-state conditions. *J. Exp. Mar. Biol. Ecol.,* 90:81-95

Setälä O, Autio R, Kuosa H (2005) Predator-prey interactions between a planktonic ciliate Strombidium sp. (Ciliophora, Oligotrichida) and the dinoflagellate Pfiesteria piscida (Dinamoebiales, Pyrrophyta). *Harmful algae,* 4:235-247

Sherr EB, Sherr BF (2002) Significance of predation by protests in aquatic microbial food webs. *Antonie Leeuwenhoeck.*, 81:293-308

Sivia, D.S., Skilling, J. (2006) Data analysis – A bayesian Tutorial, Second edition, Clarendon Press, Oxford.

Stoecker D, Guillard RRL and Kavee RM (1981) Selective predation by *Favella ehrenbergii* (Tintinnia) on and among dinoflagellates. *Biol. Bull.,* 160:136-145

Stoecker D (1988) Are Marine planktonic ciliates suspension-feeders? *J. Protozool.,* 35(2):252-255

Stoecker D and Evans GT (1985) Effects of protozoan herbivory and carnivory in a microplankton food-web. *Mar. Ecol. Prog. Ser.,* 25:159-167

Stoecker DK, Stevens K, Gustavon Jr DE (2000) Grazing on *Pfiesteria piscida* by microzooplankton. *Aquat. Microb. Ecol.*, 22:261-270

Smetacek V (1981) Annual cycle of protozooplankton in the Kiel Bight. *Mar. Biol.,* 63:1–11

Straile D (1997) Gross growth efficiencies of protozoan and metazoan zooplankton and their dependence on food concentration, predator-prey weight ratio, and taxonomic group. *Limnol. Oceanogr.,* 42(6):1375-1385

Verity PG (1985) Grazing, respiration, excretion, and growth rates of tintinnids. *Limnol. Oceanogr.,* 30:1268-1282

Verity PG (1991) Feeding in planktonic protozoans: Evidence for non-random acquisition of prey. *J. Protozool.*, 38(1):69-76

Verity PG and Villareal TA (1986) The relative food value of diatoms, dinoflagellates, flagellates, and cyanobacteria for tintinnid ciliates. *Arch. Protistenkd.,* 131:71-84

Weisse T (2002) The significance of inter-and intraspecific variation in bacterivorous and herbivorous protists. *Antonie van Leeuwenhoek,* 81:327-341

Weisse T, Lettner S (2002) The ecological significance of intraspecific variation among freshwater ciliates. *Verh. Internat. Verein. Limnol.*, 28:1880-1884

CHAPTER 3:

Heterotrophic dinoflagellate feeding behaviour and growth rates. An analysis based on laboratory results.

1- Introduction

Microprotozooplanktonic organisms have been recognized as an important part of planktonic food webs. Their high growth rates enable them to closely follow changes in phytoplankton concentration (Banse 1982), and they play an essential role in transferring energy from the microbial loop to higher levels (Azam 1983). The two main groups of organisms composing microprotozooplankton are the pelagic ciliates and the heterotrophic dinoflagellates (dinoflagellates). Dinoflagellates can constitute a substantial part of the biomass, at times even exceeding that of other zooplankton groups (Smetacek 1981; Carreto et al., 1986; Lessard 1991). In early studies, dinoflagellates have been ignored in favour of ciliates, because their feeding ecology was mostly unknown until the early 1980s (Gaines and Taylor 1984; Gaines and Elbrätcher 1987; Jacobson and Anderson 1986). Dinoflagellates are raptorial feeders which demonstrate three main modes of prey consumption: (i) external digestion with a pallium, (ii) sucking the prey cell content with a peduncle (both methods mainly occurring in thecate dinoflagellate) or (iii) engulfing the prey cell. These modes of feeding allow them to eat prey as big as themselves or even larger (Hansen et al., 1994), including whole diatoms chain (Buck et al., 1990; 2005). However the functional response (variation of grazing and growth rates) is not as well known as that of pelagic ciliates and they are often absent from conceptual food-web models (Sherr and Sherr 2007). The functional response varies primarily with food concentration, but other factors can affect this, such as the size of the organism (both the dinoflagellate and the prey) or the quality of the offered prey (defined as the taxonomic affiliation of the prey). Our study is based on laboratory results of feeding and growth experiments found in the literature with the aim of describing heterotrophic dinoflagellates feeding behaviour and growth response depending on prey type, food preference, temperature impact in an effort to summarise actual knowledge and derive a

conceptual representation of the pelagic food-web by highlighting their predating impact on diatoms and other kinds of prey, as well as a quantitative description of dinoflagellates grazing and growth. Furthermore a comparison with ciliates will highlight the difference between these two groups of organisms of the microprotozooplankton.

2- Data and Method

2.1- Data selection and acquisition

The functional response of heterotrophic dinoflagellates is primarily affected by changes in food concentration. In order to elucidate the effect of food concentration on feeding and growth behaviour we collected data on characteristic parameters of the functional response as a function of food concentration, namely, maximum growth, grazing and clearance rate of heterotrophic dinoflagellates feeding on single prey types. When available individual data points on growth and grazing rates (or alternatively clearance rate) as function of prey concentration were collected and parameters of the functional response estimated. No article had been intentionally omitted, but some could have been overlooked. A total of 22 articles were selected with 161 laboratory experiments results (Table 1). If data was only available as graphics, the values were extracted using the ImageJ software of the National Health Institute (http://rsb.info.nih.gov/ij/download.html). In addition, for each experiment, ancillary information was collected encompassing experimental conditions, prey and predator information (i.e. species name, strain information, cell size, volume, carbon content) together with the corresponding method, when available (Database is available at: PANGAEA, http://www.pangaea.de). When not available, size, carbon content (C in pg C $cell^{-1}$) and volume (V in μm^3 $cell^{-1}$) of prey and predators were estimated from available ancillary information using appropriate geometrical shapes for conversion of size to volume or volume to size, respectively and volume – carbon conversion equations ($C = a * V^b$; with a and b being group specific) of Menden-Deuer and Lessard (1995). Food concentration can be expressed in number of prey cells, biovolume of prey or prey carbon. Dinoflagellates are not strictly preying on a single size class of organisms rather on a large spectrum. In addition, they display mechanoreceptors and chemoreceptors as well as a complex behaviour where they circle a potential prey before trying to capture it. It suggests active selection based not only on size but also on the potential nutritional value of the prey. Carbon is a measure of the nutritional value of a prey organism (Lee 1980). For this reason, the sizes of the organisms as well as grazing and clearance rates are expressed in carbon units.

Table 1: List of the articles used to collect data, dinoflagellate species used and rates provided.

Author	Dinoflagellate species	Information provided	Number of data (maximal rate)
Buskey et al., 1994	Protoperidinium huberi	grazing and growth as a function of prey concentration	1
Buskey and Hyatt., 1995	Noctilluca scintillans	grazing and growth as a function of prey concentration	2
	Oxhyrris marina	grazing and growth as a function of prey concentration	2
Buskey 1997	Protoperidinium pellucidum	grazing and growth as a function of prey concentration	4
Egerton and Marshall 2006	Pfiesteria piscida	grazing and growth as a function of prey concentration	
Goldmann et al., 1989	Oxhyrris marina	maximal grazing and growth rate	3
Hansen 1992	Gyrodinium spirale	maximal grazing and growth rate	1
	Gyrodinium spirale	grazing and growth as a function of prey concentration	10
	Anphidinium crassum	maximal grazing and growth rate	1
	Gyrodinium dominans	maximal grazing and growth rate	1
	Gyrodinium spirale	maximal grazing and growth rate	1
	Gyrodinium sp	maximal grazing and growth rate	1
	Protoperidinium pellucidum	maximal grazing and growth rate	1
Jacobson and Anderson 1993	Protoperidinium hirobis	grazing and growth as a function of prey concentration	1
Jeong et al., 2006	Pfiesteria piscida	grazing and growth as a function of prey concentration	5
	Pfiesteria piscida	maximal grazing and growth rate	9
Jeong et al., 2005a	Prorocentrum donghaiense	grazing as a function of prey concentration	1
	Prorocentrum micans	grazing as a function of prey concentration	1
	Lingulodinium polyedrum	maximal grazing rate	1
	Akashiwo sanguinea	maximal grazing rate	1
	Gonyaulax polygramma	maximal grazing rate	1
	Cochlodinium polykrikoides	maximal grazing rate	1
	Prorocentrum micans	maximal grazing rate	1
	Gymnodinium catenatum	maximal grazing rate	1
	Alexandrium catenella	maximal grazing rate	1
	Gonyaulax spinifera	maximal grazing rate	1
	Alexandrium tamarense	maximal grazing rate	1
	Gymnodinium impudicum	maximal grazing rate	1
	Scrippsiella trochoidea	maximal grazing rate	1
	Karenia brevis	maximal grazing rate	1
	Alexandrium minutum	maximal grazing rate	1
	Heterocapsa triquetra	maximal grazing rate	1
	Prorocentrum donghaiense	maximal grazing rate	1

Table 1 : continued

	Prorocentrum minimum	maximal grazing rate	1
	Heterocapsa rotunda	maximal grazing rate	1
Jeong et al., 2005b	Stoeckeria algicida	grazing and growth as a function of prey concentration	1
Jeong et al., 1999	Fragilidium cf. mexicanum	grazing and growth as a function of prey concentration	1
Jeong et al., 2003	Oxhyrris marina	grazing and growth as a function of prey concentration	1
Jeong et al., 2004a	Protoperidinium bipes	grazing and growth as a function of prey concentration	1
Jeong et al., 2005d	Prorocentrum donghaiense	grazing and growth as a function of prey concentration	1
	Heterocapsa triquetra	grazing and growth as a function of prey concentration	1
	Prorocentrum micans	grazing and growth as a function of prey concentration	1
	Lingulodinium polyedrum	grazing and growth as a function of prey concentration	2
	Lingulodinium polyedrum	maximal grazing rate	2
	Gonyaulax polygramma	maximal grazing rate	1
	Cochlodinium polykrikoides	maximal grazing rate	1
	Prorocentrum micans	maximal grazing rate	1
	Heterocapsa triquetra	maximal grazing rate	1
	Prorocentrum donghaiense	maximal grazing rate	1
Jeong et al., 2005e	Gonyaulax polyedra	grazing and growth as a function of prey concentration	1
Jeong et al., 2007a	Luciella masanensis	grazing and growth as a function of prey concentration	4
Jeong et al., 2007b	Oxhyrris marina	grazing and growth as a function of prey concentration	1
	Gyrodinium cf. guttula	grazing and growth as a function of prey concentration	1
	Pfiesteria piscida	grazing and growth as a function of prey concentration	1
Jeong and Latz 1994	Protoperidinium cf divergens	grazing and growth as a function of prey concentration	2
	Protoperidinium crassipes	grazing and growth as a function of prey concentration	2
Kim and Jeong 2004	Gyrodinium dominans	grazing and growth as a function of prey concentration	1
	Gyrodinium spirale	grazing and growth as a function of prey concentration	1
Menden-Deuer et al., 2005	Protoperidinium conicum	growth as a function of prey concentration	1
	Protoperidinium depressum	growth as a function of prey concentration	1
	Protoperidinium excentricum	growth as a function of prey concentration	1
Nakamura et al., 1992	Gyrodinium dominans	maximal growth rate	4
Nakamura et al., 1995	Gyrodinium dominans	grazing as a function of prey concentration	2
Naustvoll 1998	Diplopsalis lenticula	maximal growth rate	

Table 1: continued

Naustvoll 2000	Zygabikodinium lenticulatum	maximal growth rate	19
	Protoperidinium pallidum	maximal growth rate	20
	Protoperidinium steinii	maximal growth rate	14
Strom and Buskey 1993	Oblea rotunda	grazing and growth as a function of prey concentration	2
Tillmann and Reckermann 2002	Oblea rotunda	grazing and growth as a function of prey concentration	1

2.2- Modelling the functional response

Ingestion rates of food items depend on several factors: detecting, encountering, handling and ingesting the prey. Although prey encounter rate increases in proportion to prey density, the functional response of ingestion typically saturates at high prey densities. Based on the work of Holling (1959) one can distinguish three types of functional responses: a linear increase (Holling I), a decelerating increase (Holling II), and an S-shape increase (Holling III) of ingestion rate with prey concentration (each of these functional response type is characterised by a different variation of the clearance rate). The functional response of dinoflagellates is a Holling type II response: an increase followed by a saturation of the grazing rate.

Several mathematical expressions exist to represent the Holling II response (e.g. Michaelis-Menten, Ivlev, and rectilinear). However, on a statistical basis they usually give equally good fits (Mullin et al., 1975; Gentleman et al., 2003; personal unpublished results). The Michaelis-Menten function was chosen for fitting the data sine this choice allows comparison with previous studies since they all used this equation. Further, present mechanistic understanding of the grazing process as well as observational evidence supports the use of the Michaelis-Menten model (Kiørboe, 2008).

Grazing and growth response to food concentration in dinoflagellates might, however, present threshold concentrations bellow which no grazing or growth occurs. Therefore, when fitting the data, we include a threshold concentration (P_t) by modifying the Michaelis-Menten as follows:

$$r = r_{\max} \times \left(\frac{P - P_t}{K + (P - P_t)} \right) \quad (1)$$

with: r corresponding to the rate of grazing or growth at a given prey concentration P, r_{max} the maximal rate, K the half-saturation concentration and P_t the threshold concentration. Grazing and growth follow the same function but with different value for K, P_t and r_{max}, depending on the conversion efficiency of food ingestion into ciliate biomass.

2.2.a- Grazing

$$g(P) = g_{\max} \times \left(\frac{P - P_t g}{Kg + (P - P_t g)} \right) \quad (2)$$

In the case of the grazing response g_{max} is also equivalent to the inverse of the handling time for one prey ($\tau = 1/ g_{max}$): corresponding to the time needed to ingest and digest a prey at saturating concentration. The half-saturation concentration is the concentration at which the grazing or growth rates are half the maximum rate. The half saturation constant for grazing, g_{max} and the maximal clearance rate (F_{max}) are related through Equation 2. F_{max} is the maximum amount of suspension volume that individual grazers (in this case dinoflagellates) can clear of prey items.

$$K = \frac{g_{\max}}{F_{\max}} \quad (3)$$

F_{max} is equivalent to the encounter rate kernel (β) for a given grazer and prey system when the grazer capture all prey encountered (Kiørboe, 2008). If a grazer is not 100% efficient at catching its prey, F_{max} is equivalent to the encounter kernel times the capture efficiency (α). Encounter and capture efficiency are the limiting process at low prey concentration, while handling time is the limiting process at saturating food.

2.2.b Growth

Growth rate (μ) in protozoa follows the similar response to food concentration as grazing rate (g) whereby:

$$\mu = g \times GGE \quad (4)$$

with GGE (Gross Growth Efficiency) representing the efficiency of conversion of ingested food into biomass of grazer. GGE will depend on the energetic demands of the grazer and food quality but can also vary with food concentration depending on the feeding strategy of grazers (Jakobsen and Hansen, 1997).

$$\mu(P) = \mu_{\max} \times \left(\frac{P - P_t \mu}{K\mu + (P - P_t \mu)} \right) \quad (5)$$

Note that the earlier definitions are for the grazing parameters, their meaning is different for growth parameters.

The data collected were fitted to the modified Michaelis-Menten (Equation 1), parameter estimates μ_{max}, g_{max}, as well as respective threshold concentration and half-saturation constant, and their uncertainties were estimated using a Bayesian approach (Sivia and Skilling 2006) assuming flat priors and additive Gaussian noise. A detailed explanation is to be found in the Annex B. The estimated parameters (r_{max}, K and P_t) where then used to determine how size and prey type affect the functional response.

2.3- Correction for temperature effects and estimation of Q_{10}

Compiled grazing experiments were all conducted at 20ºC so temperature effect on grazing could not be estimated. In the compiled growth experiments temperature vary and one of the experiments (Nakamura 1995) includes measures of growth rate at different temperatures but similar experimental conditions and the same prey-dinoflagellates pair. The temperature dependence of metabolic rates in protozoa usually follows an exponential decay with decreasing temperature within the range best tolerated by the organisms (Montagnes et al., 2003). Here we use this relationship for our estimate of Q_{10}. The data from Nakamuraon the temperature dependence of growth was plotted on a log scale and visually examined, data points on the lower or upper temperature range that did not follow the linear relationship were flagged and not included in the following analysis. For the remaining data points, temperatures were adjusted by subtraction of the lowest temperature value (T_{min}) resulting in temperatures ranging from 0 to the maximum temperature range investigated (T_{min}- T_{max}). Similarly the growth or grazing rates were normalised by dividing by the grazing,

respectively, growth rates (r) obtained at the lowest temperature studied for each dataset (r_{min}) resulting in rates ranging from 1 to the maximum relative rates (r_{max}/r_{min}) for each set of experiments. This procedure has the advantage of giving a Q_{10} estimate for growth and grazing, respectively, by combining data on different species and experimental set-up in one single analysis that contains the variability of the all the available dataset and thus avoiding biases in Q_{10} estimates due to the low amount of data available when analysing each experiment separately.

Data was fitted to an empirical model:

$$R = e^{aT+b} \qquad (6)$$

with R the relative grazing or growth rates (r_2/r_1) , T the temperature difference (T_2-T_1) and a and b the parameters describing decay rate with temperature. Parameters were estimated using the same method applied to the estimates of the functional response. Values of Q_{10} can be estimated as $Q_{10} = e^{aT+b}$ for $T = 10$.

3-Results

3.1- Temperature

The data from Nakamura (1995) were normalized (Fig. 1) and the Q_{10} calculated. The parameters of the temperature dependence were a = 0.042 and b =0.007 , resulting in a Q_{10} of 1.53 ± 0.06, with a correlation coefficient of 0.998 used to transform all the maximal growth rates to their analogous values for a temperature of 20°C.

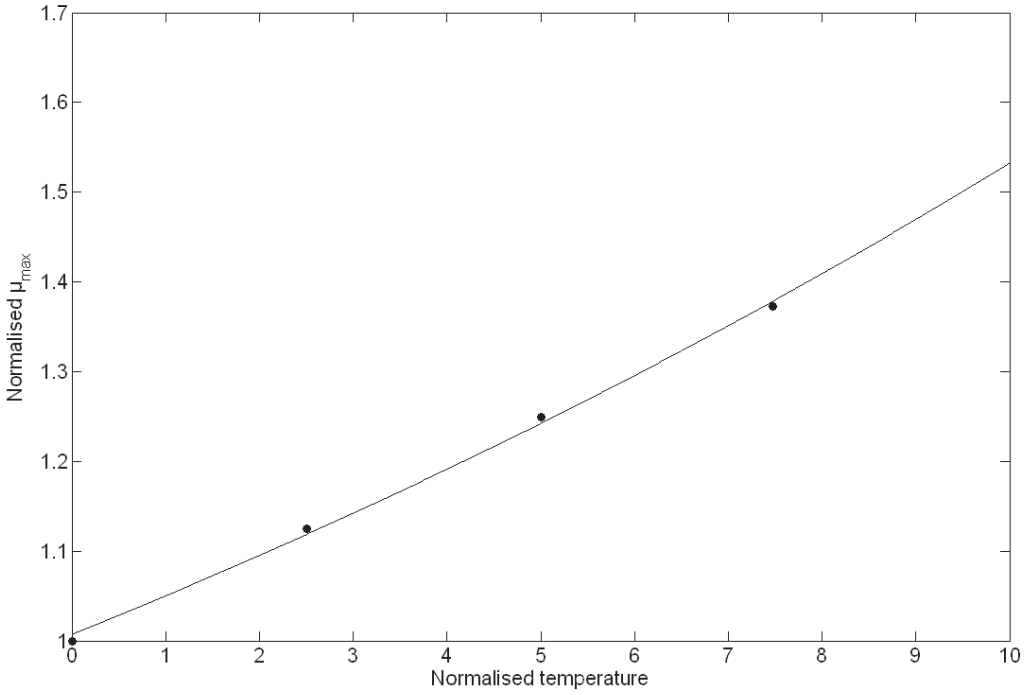

Figure 1: Variation of normalised growth rate with temperature and modelled temperature dependence curve using optimised parameters for Equation 3. Correlation coefficient between model and data is $r^2 = 0.998$. a =0.042; b = 0.007; Q_{10}=1.53 ± 0.06

3.2- Size and prey PFT impact

Dinoflagellates have different maximal grazing and growth rates depending on their size and the size of their food. The maximal grazing (g_{max}) value obtained increase with the size of dinoflagellates, the increase is particularly obvious for the series of experiments done with cyanobacteria as prey (▼, Fig. 2). g_{max} increases also with increasing value of the prey:dinoflagellate ratio. The highest value is reached for a carbon ratio of ~0.3 (diameter ratio of ~0.6). The grazing half-saturation (Kg) also increases with the size of the dinoflagellate and the carbon ratio to the prey (Fig. 3). The grazing threshold (P_tg) does not vary with size, whether dinoflagellate or prey size (Fig. 4), and in many cases the threshold is equal to zero, and is always equal to zero if the prey is a diatom, these value are not visible in figure 4 because of the logarithmic scale used.

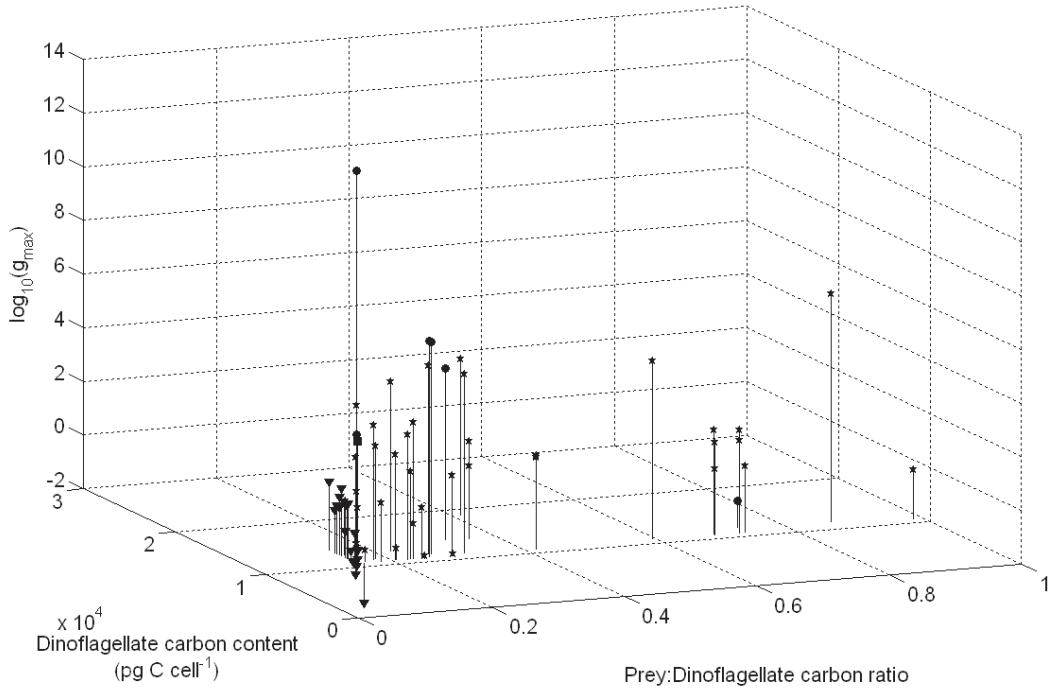

Figure 2: Variation of the logarithm of the maximal grazing rate (g_{max}) as a function of the prey:dinoflagellates carbon content and the dinoflagellates carbon content. PFT legend: diatoms (circle), cocolithophores (square), nanoflagellates and bacteria (upward triangle), pico-eucaryote and photosynthetic bacteria unable to fixe N_2 (downward triangle), mixed phytoplankton composed of autotrophic dinoflagellates and chrysophytes (star).

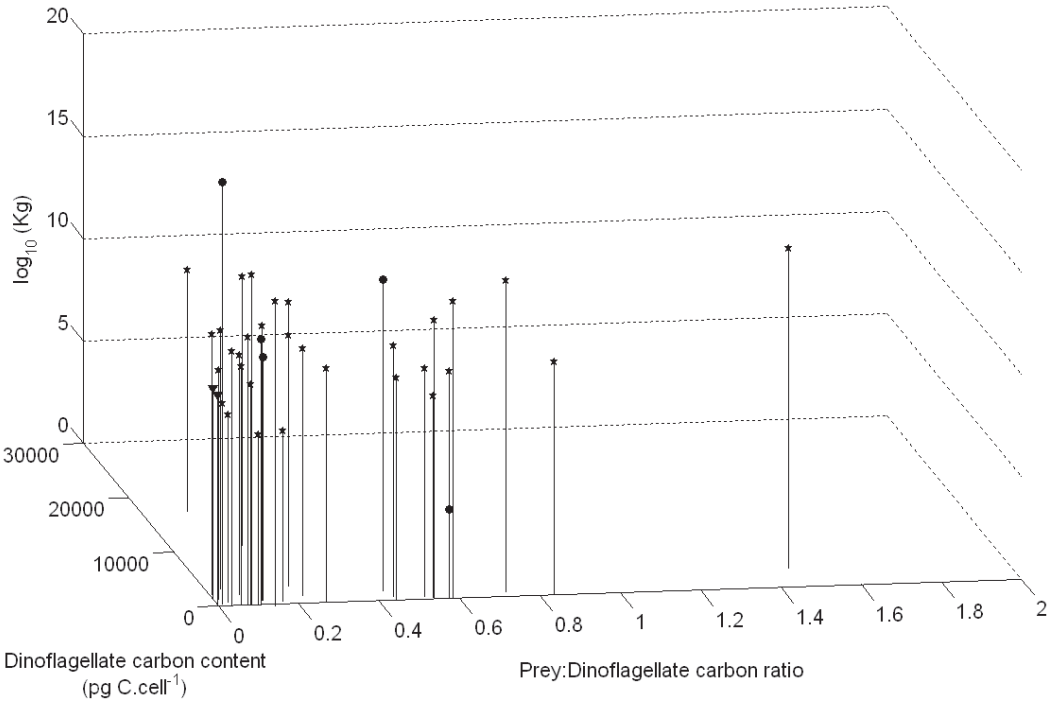

Figure 3: Variation of the logarithm of the grazing half saturation concentration (Kg) as a function of the prey:dinoflagellates carbon content and the dinoflagellates carbon content. PFT legend: diatoms (circle), cocolithophores (square), nanoflagellates and bacteria (upward triangle), pico-eucaryote and photosynthetic bacteria unable to fixe N_2 (downward triangle), mixed phytoplankton composed of autotrophic dinoflagellates and chrysophytes (star).

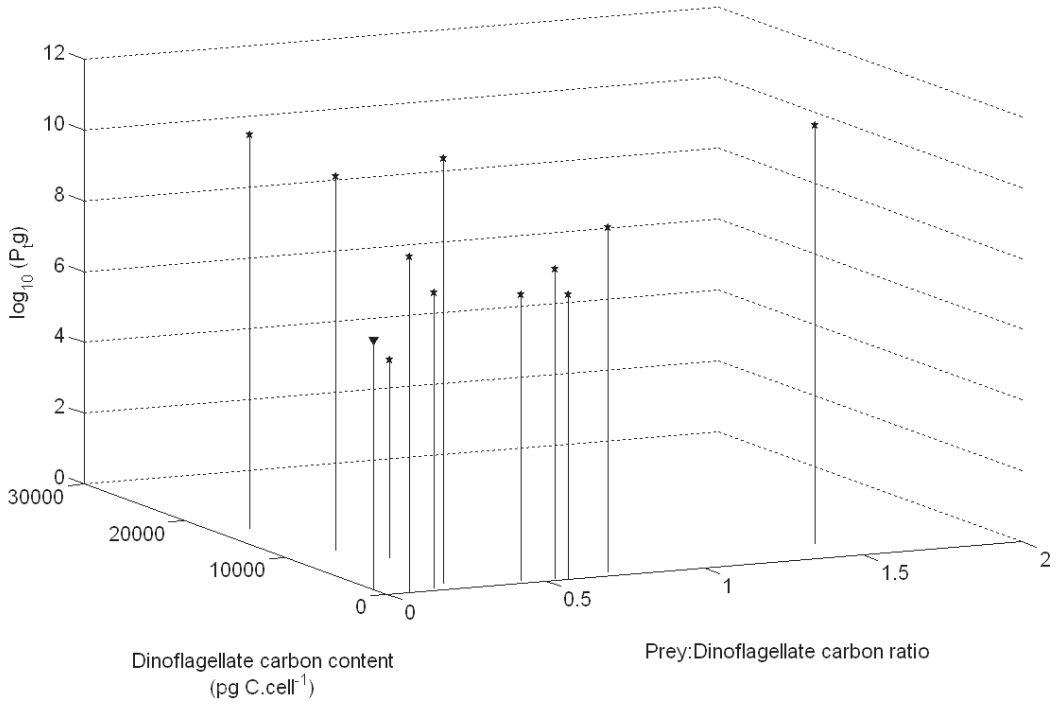

Figure 4: Variation of the grazing threshold concentration (P_tg) as a function of the prey:dinoflagellates carbon content and the dinoflagellates carbon content. Please note that several P_tg with a value of zero are not displayed because of the logarithmic scale. PFT legend: diatoms (circle), cocolithophores (square), nanoflagellates and bacteria (upward triangle), pico-eucaryote and photosynthetic bacteria unable to fixe N_2 (downward triangle), mixed phytoplankton composed of autotrophic dinoflagellates and chrysophytes (star).

The maximal growth (μ_{max}) values collected and calculated include some negative values (Fig. 5) when the prey wouldn't sustain the growth of the dinoflagellate. μ_{max} increases with the size of the dinoflagellate and the size ratio to the prey. The highest values are for a carbon ratio of ~2.3 (diameter ratio of ~1.8), increasing sharply before this ratio and slowly decreasing after. Growths half-saturation ($K\mu$) presents a small answer to size increase (Fig. 6). The growth threshold ($P_t\mu$) increases clearly with increasing carbon ratio and increasing dinoflagellate size (Fig. 7)

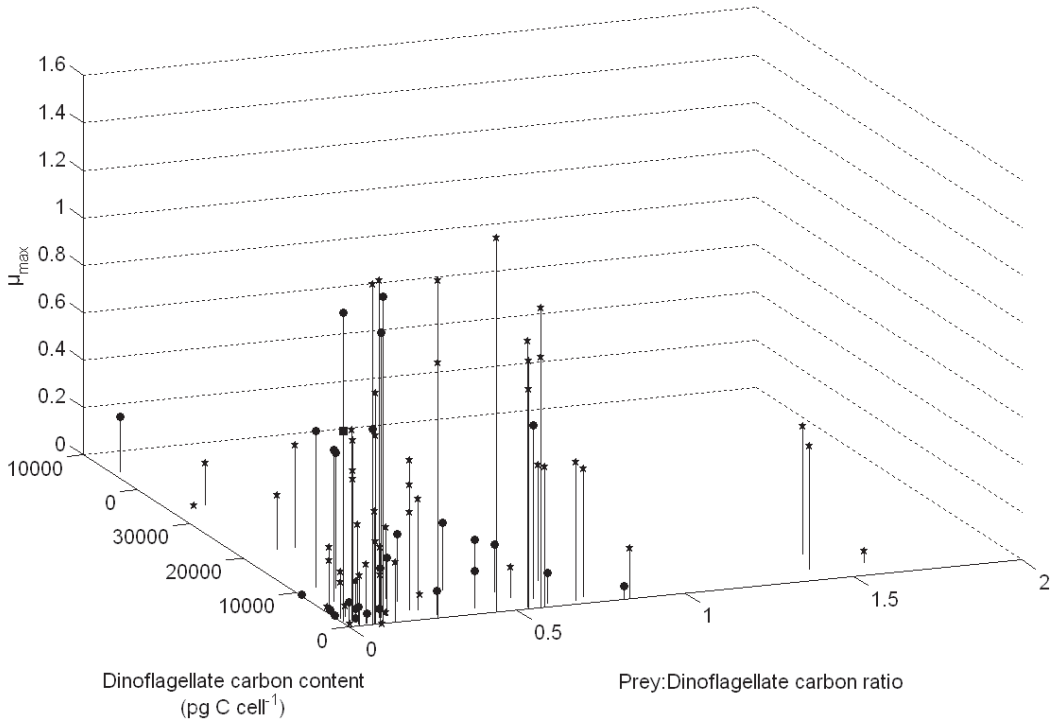

Figure 5: Variation of the maximal growth rate (μ_{max}) as a function of the prey:dinoflagellates carbon content ratio and the dinoflagellates carbon content. PFT legend: diatoms (circle), cocolithophores (square), nanoflagellates and bacteria (upward triangle), pico-eucaryote and photosynthetic bacteria unable to fixe N_2 (downward triangle), mixed phytoplankton composed of autotrophic dinoflagellates and chrysophytes (star).

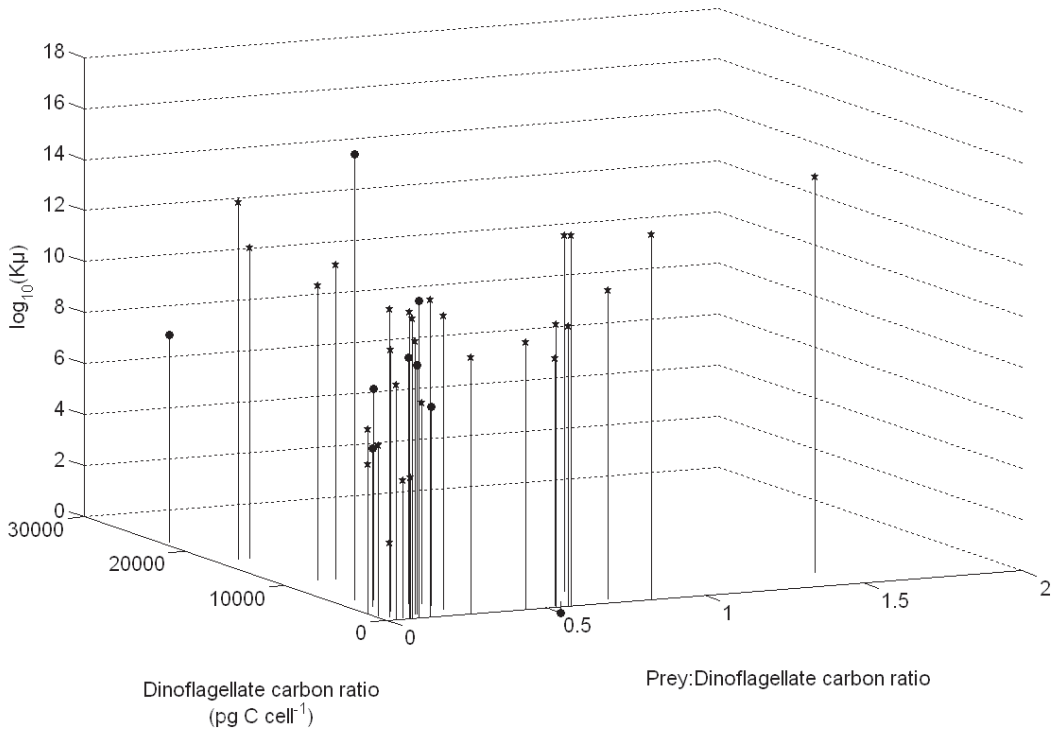

Figure 6: Variation of the logarithm of the growth half-saturation concentration (Kμ) as a function of the prey:dinoflagellates carbon content ratio and the dinoflagellates carbon content. PFT legend: diatoms (circle), cocolithophores (square), nanoflagellates and bacteria (upward triangle), pico-eucaryote and photosynthetic bacteria unable to fixe N_2 (downward triangle), mixed phytoplankton composed of autotrophic dinoflagellates and chrysophytes (star).

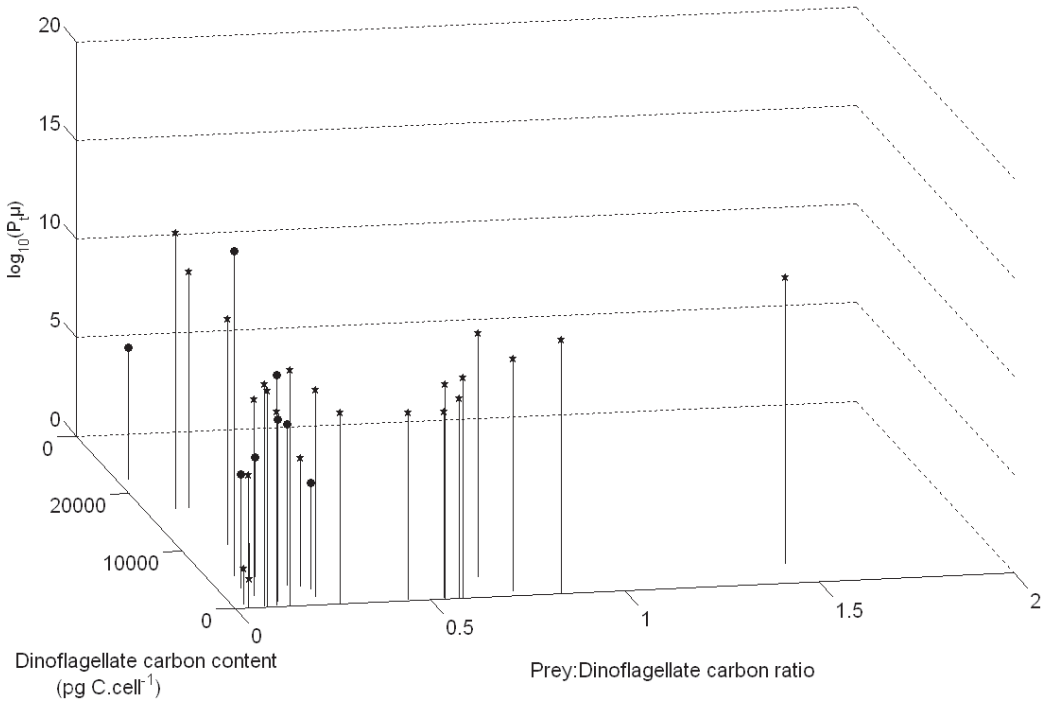

Figure 7: Variation of the logarithm of the growth threshold concentration ($P_t\mu$) as a function of the prey:dinoflagellates carbon content ratio and the dinoflagellates carbon content. PFT legend: diatoms (circle), cocolithophores (square), nanoflagellates and bacteria (upward triangle), pico-eucaryote and photosynthetic bacteria unable to fixe N_2 (downward triangle), mixed phytoplankton composed of autotrophic dinoflagellates and chrysophytes (star).

The main type of prey offered to heterotrophic dinoflagellates in the experiments compiled in this study are diatoms and autotrophic dinoflagellates. Differences are observed in parameters values for grazing and growth between these two groups are observed (Table 2). A median test at the 90% confidence interval is used to confirm this observation. Diatoms are grazed at a higher g_{max} (mean of 2.8 pg C dinoflagellates^{-1} time^{-1} against a mean of 0.064 pg C dinoflagellates^{-1} time^{-1} for autotrophic dinoflagellates and chrysophytes) with all the $P_t g$ equal to zero, in comparison to other prey type (Fig. 4). There is no significant difference between Kg for different prey PFT. On the contrary, μ_{max} is not significantly different when the prey is a diatom or an autotrophic dinoflagellate or chrysophytes (mean growth rate of 0.42 day^{-1} against a mean of 0.34 day^{-1} when diatoms are the offered prey), however $K\mu$ and the $P_t\mu$ are significantly lower when diatoms are offered as prey compared to another prey species, $K\mu$ and $P_t\mu$ mean are 10 time smaller for diatoms than for another prey type.

Comparing the grazing and the growth response to prey concentration variations shows that the half-saturation constants both for grazing and growth, Kg and $K\mu$, respectively, are usually different from each other; the same applies for the threshold values $P_t g$ and $P_t\mu$ (Table 2). The differences between Kg and $K\mu$ vary from absent up to one order of magnitude with Kg being higher than $K\mu$. Many values of $P_t g$ are equal to zero (23 out of 32 experiment with both grazing and growth) and $P_t\mu$ values are in the majority of cases higher when there is a threshold for both the grazing and the growth.

Table 2: Half-saturation and threshold concentration, in µg C mL^{-1}, for grazing and growth of dinoflagellates: estimates from compilled data.

Author	Kg	P_tg	Kµ	P_tµ
Buskey et al., 1994	223516	0	37643	14197
Buskey, 1997	0.07 10^{-3}	0	15	4
	6108	134	5316	1890
Hansen, 1992	177	160	100	35
Jacobson and Anderson, 1993	142	0	17	10
Jeong et al., 2006	156	19	73	9
	91	0	22	15
	64	3	55	24
	800	0	62	50
	9700	0	121	54
Jeong et al., 2005b	50	0	33	13
Jeong et al., 1999	57	0.27	51	0
Jeong et al., 2003	657	0	44	15
Jeong et al., 2004a	417	0	238	114
Jeong et al., 2005c	45	0	0.24	0
	111	0	0.22	0
	72	0	0.79	0
	296	0	1.12	0
	1054	0	2.62	0.65
Jeong et al., 2005d	340	0	0.33	0
Jeong et al., 2007a	482	13	160	75
	1928	0	1965	68
	2644	0	242	150
	84	0	1595	363
Jeong et al., 2007b	241	0	9	0.80
Jeong and Latz, 1994	492	38	216	0.0002
	136	67	189	156
Kim and Jeong, 2004	19	6	16	12
	119	0	28	20
Strom and Buskey, 1993	0.06	0	0.001	0
	10	0	0.018	0.006
Tillmann and Reckermann, 2002	4016	17	184	126

3.3- Gross Growth Efficiency (GGE)

GGE is the expression of the quantity of the grazed biomass transformed into predator biomass (Eq. 7). It has been shown to vary with temperature, prey to predator weight ratio and especially the prey concentration (Straile 1997).

$$GGE = \frac{\mu}{g} \tag{7}$$

The obtained values vary between 0% and 100%, with a mean of 16% if negatives values are not taken in account (negative growth). The GGE calculated from g_{max} and μ_{max} decreases exponentially with increasing prey:dinoflagellate ratio (Fig. 8). The highest value for GGE are found when the ratio is smaller than 0.2. The tendancy of GGE is opposite to that observed for g_{max} and μ_{max} who increase with increasing ratio (Fig. 2 and 5). Comparing GGE variation to value of g_{max} and μ_{max}, the highest value of GGE occur for the lowest value of g_{max} (Fig. 9).

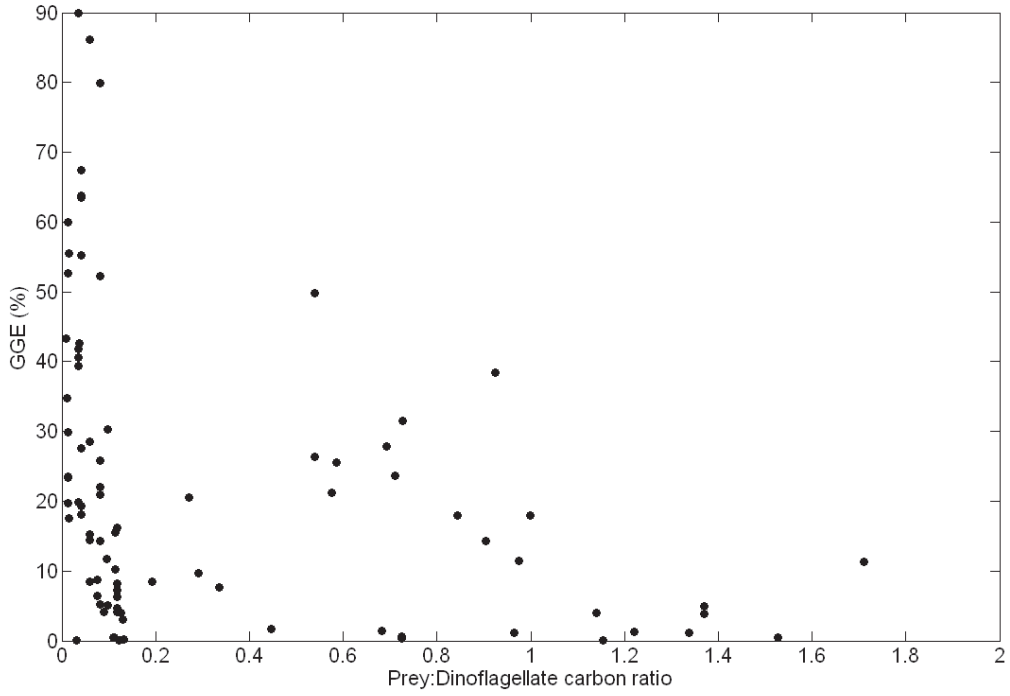

Figure 8: Variation of the GGE with the carbon ratio between the prey and the dinoflagellate.

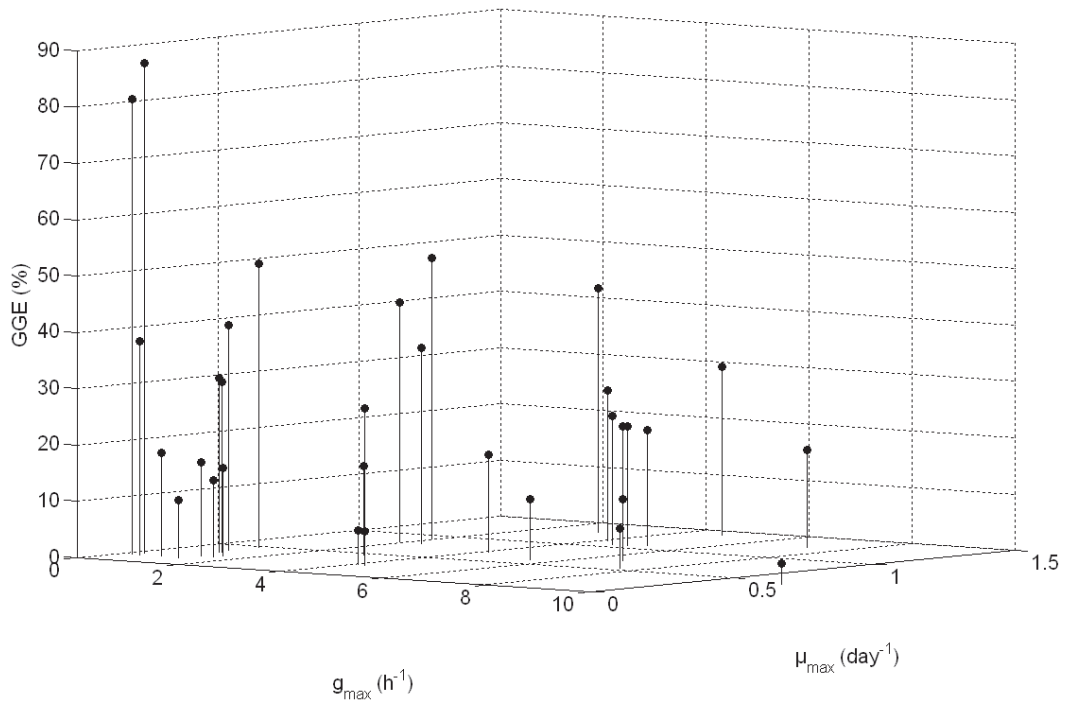

Figure 9: GGE and maximal grazing and growth rates variations.

3.4- Comparison with ciliates

Ciliate and dinoflagellate g_{max} increases with organism size, and the size ratio with their prey (Fig. 10). Under similar conditions of predator size and size ratio to their prey, dinoflagellate g_{max} are lower than that of ciliates. Kg and P_tg of both organisms do not show a dependence on either their size or the size ratio. Kg for ciliates tends to be lower than that of the dinoflagellates (Fig. 11). P_tg for grazing is usually slightly higher for ciliates than for dinoflagellates (Fig. 12) and $P_tg = 0$ is observed in various cases for heterotrophic dinoflagellates.

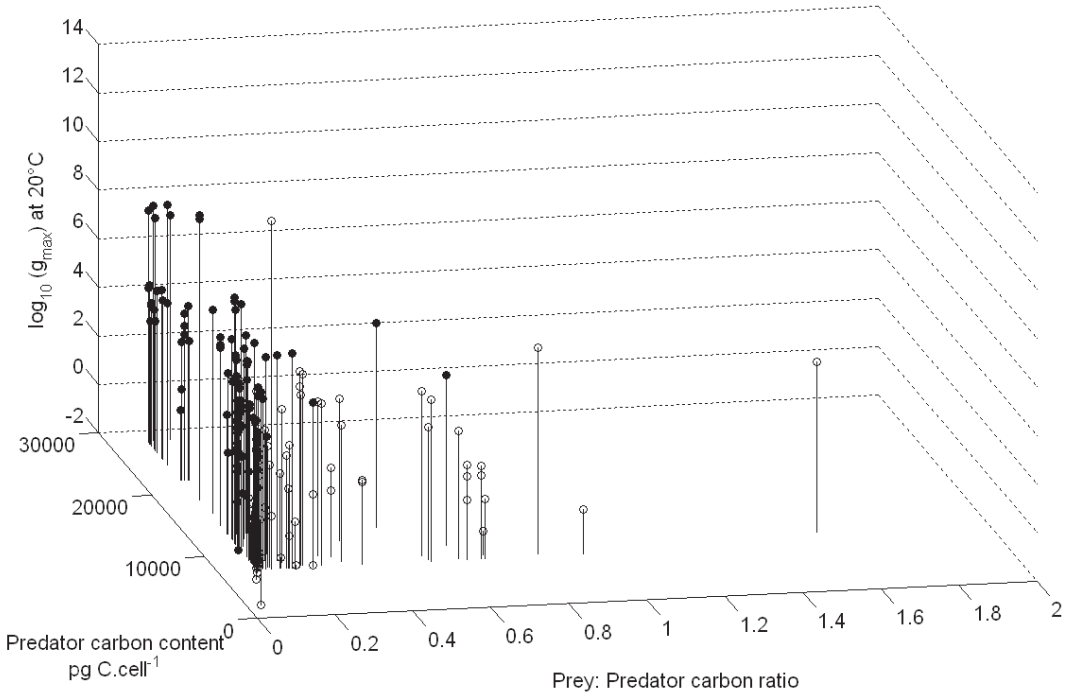

Figure 10: Variation of the logarithm of 'g_{max}' with predator carbon content and prey to predator carbon ratio; ciliates (●) dinoflagellates (○).

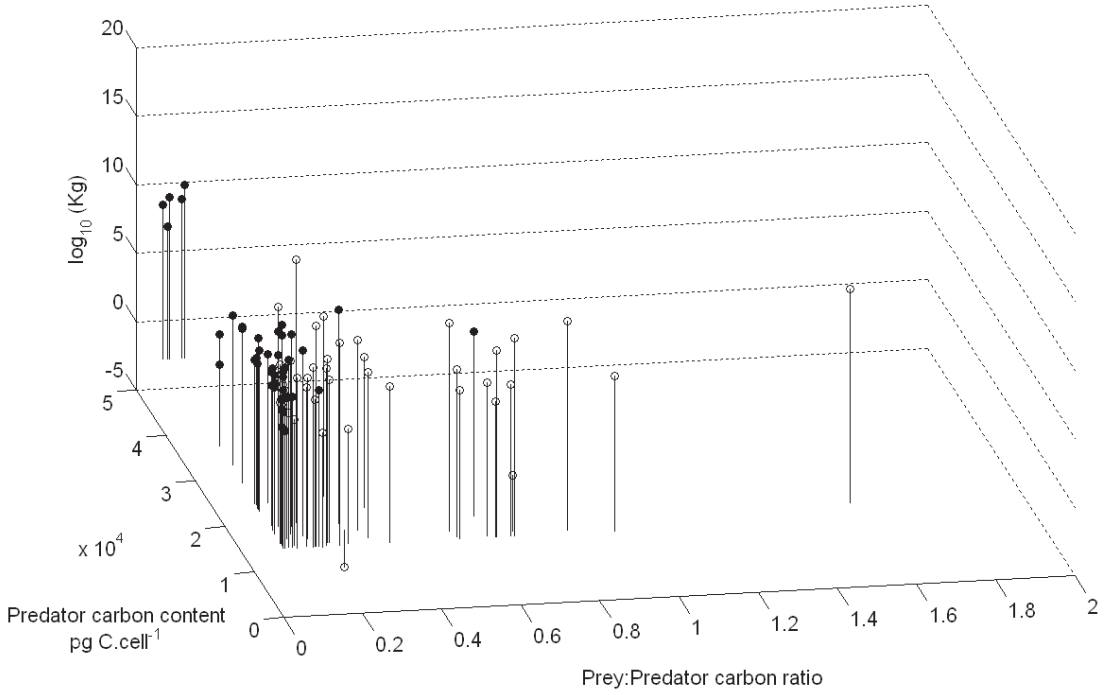

Figure 11: Variation of the logarithm of the half-saturation concentration 'Kg' with predator carbon content and prey to predator carbon ratio; ciliates (●) dinoflagellates (○).

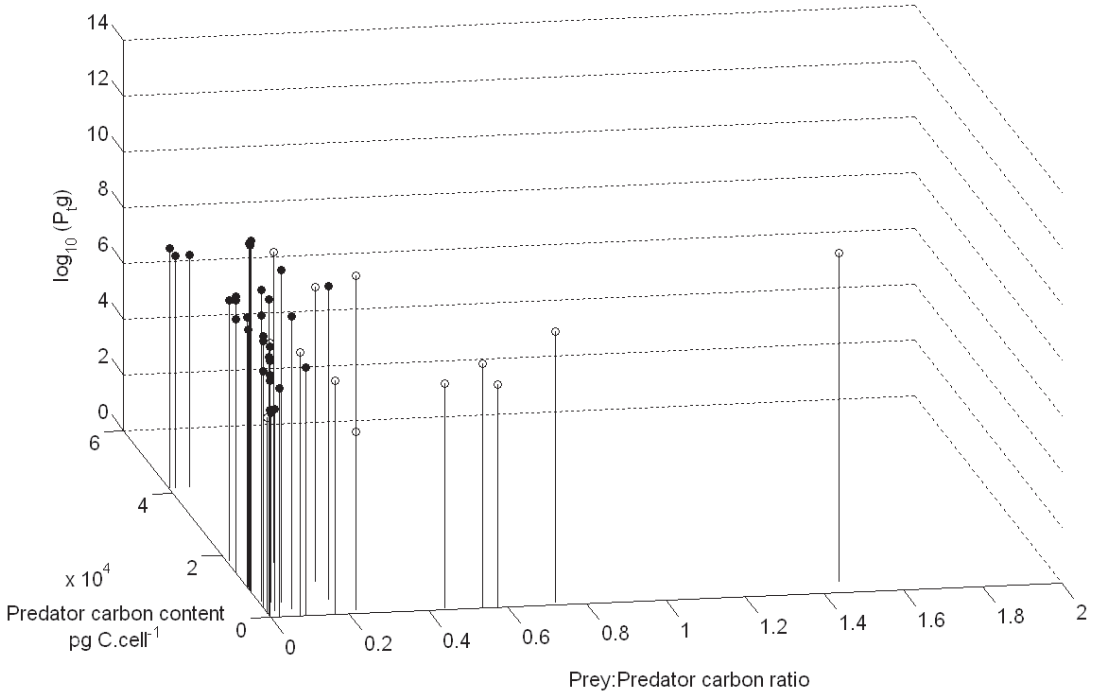

Figure 12: Variation of the logarithm of the threshold concentration '$P_t g$' with predator carbon content and prey to predator carbon ratio; ciliates (●) dinoflagellates (○).

.

Ciliate and dinoflagellate μ_{max} increases with organism size, and the size ratio with their prey (Fig. 13). Under similar conditions of predator size and size ratio to their prey, dinoflagellate μ_{max} are lower than that of ciliates. $K\mu$ and $P_t\mu$ of both organisms do not show a dependence on either their size or the size ratio. Ciliates $K\mu$ is higher than that of the dinoflagellates in similar size and ratio conditions (Fig. 14), whereas ciliates $P_t\mu$ is lower or equal to that of dinoflagellates (Fig. 15). The differences in mean K and P_t both the grazing and the growth for ciliates and dinoflagellates are summarized in Table 3.

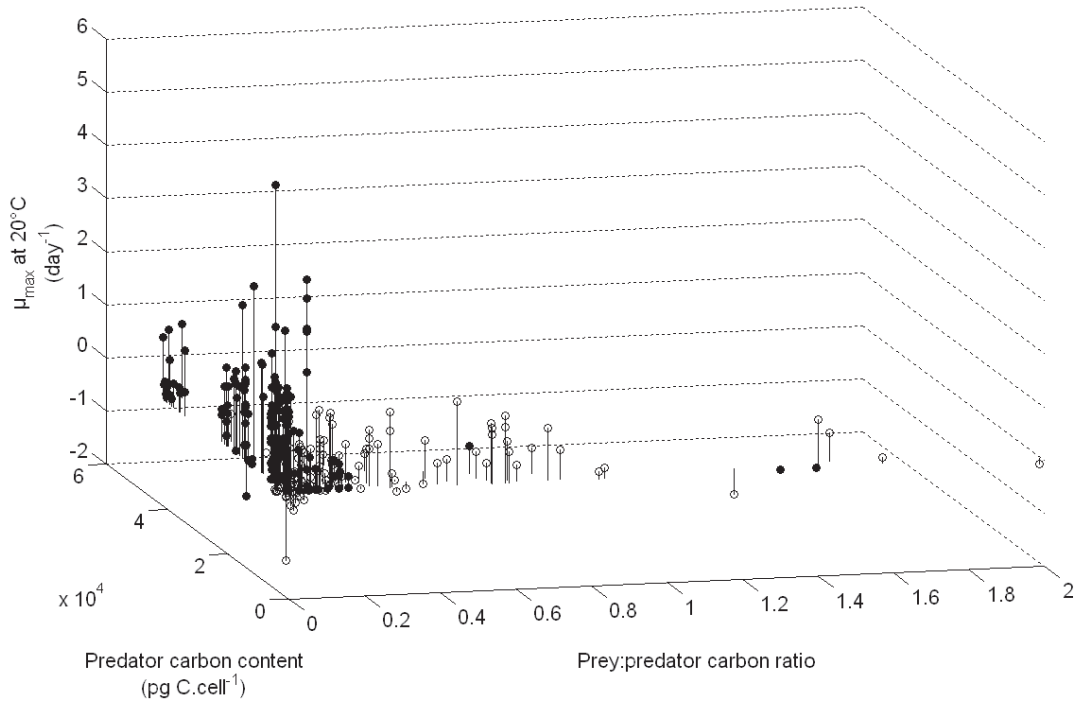

Figure 13: Variation of the logarithm of the maximal growth rate 'μ_{max}' with predator carbon content and prey to predator carbon ratio; ciliates (●) dinoflagellates (○).

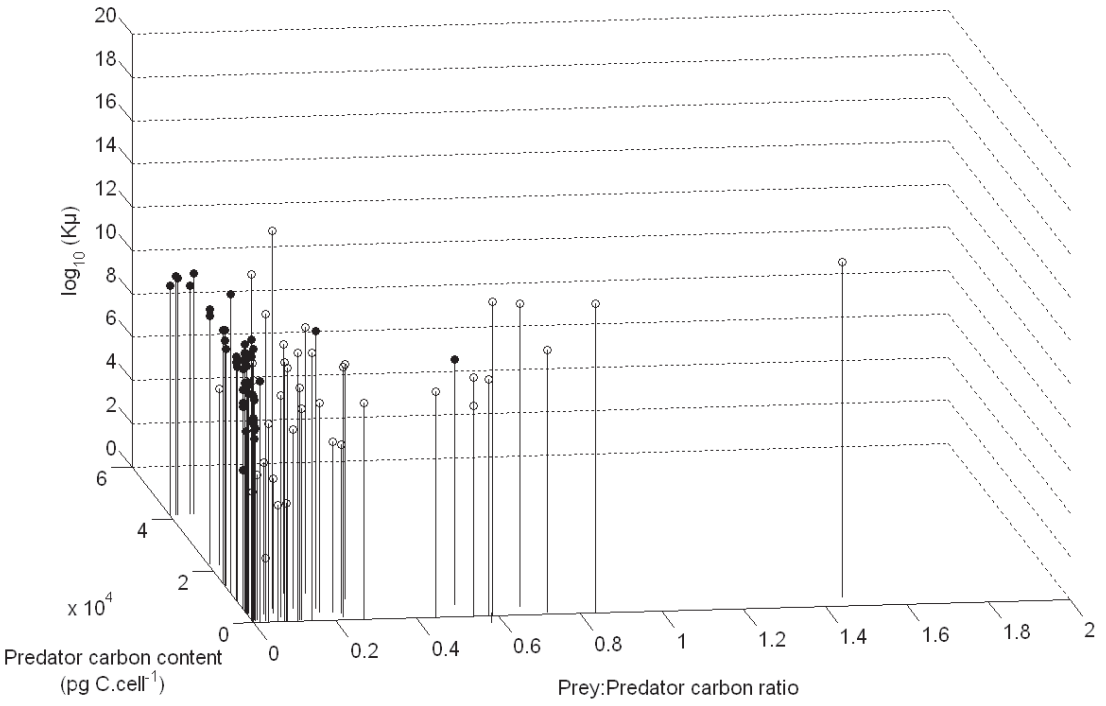

Figure 14: Variation of the logarithm of the half-saturation concentration 'Kμ' with predator carbon content and prey to predator carbon ratio; ciliates (●) dinoflagellates (○).

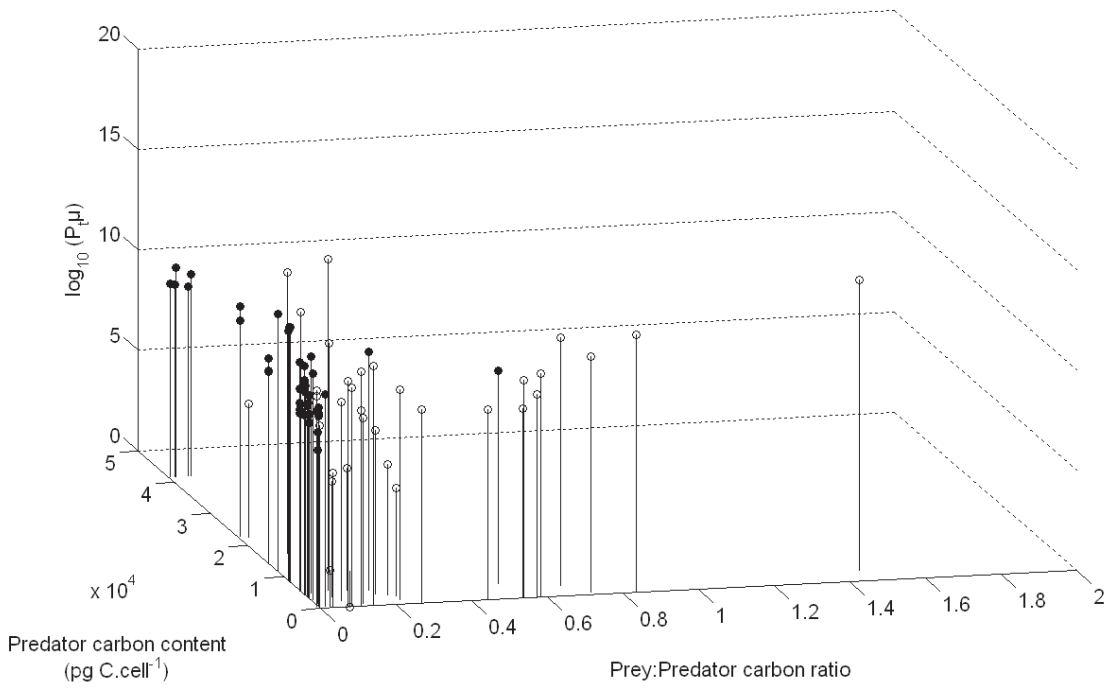

Figure 15: Variation of the logarithm of the threshold concentration 'P_t' with predator carbon content and prey to predator carbon ratio; ciliates (●) dinoflagellates (○).

Table 3: Mean of the K and P_t (standard deviation)

Concentrations ($\mu g\ C\ L^{-1}$)	Ciliates	Dinoflagellates
Kg	400 (974)	5531 (32902)
Kμ	95 (152)	1039 (5404)
$P_t g$	36 (80)	13 (36)
$P_t \mu$	59 (90)	512 (2440)

4- Discussion

4.1- Functional response

The limited amount of data allowed to estimate the half-saturation constants and thresholds for both grazing and growth of both the heterotrophic dinoflagellates and ciliates. However, the estimated uncertainties in the parameter values are large (Table 3). These large uncertainties are unavoidable and should be kept in mind when nterpreting the results of the data analysis. Despite a limited amount of data for grazing and growth a few trends of functional response can be recognised. Dinoflagellates grazing and growth parameter values increase with dinoflagellate size and prey:dinoflagellates size ratio. Heterotrophic dinoflagellates can eat prey that is up to 10-30 times bigger in terms of carbon content (or about 5 fold prey:dinoflagellate Estimated Spherical Diameter, ESD). These high ratios occur at the extreme end of the prey size spectrum, where maximal grazing rates are low (not shown). Maximal rates – g_{max} and μ_{max} – are increasing as expected with prey size. No slowing or a decrease of the increasing maximal rates can be seen, a prey:dinoflagellate size ratio of 0.3 is reached in the grazing experiments and 2.3 for the growth experiments (ESD ratio of respectively 0.6 and 1.8). This is in agreement with the 3:1 dinoflagellate:prey optimal ESD ratio found by Hansen et al. (1994).

The prey:dinoflagellate ratio for maximum GGE is about 0.2 or lower, ratio value at which the maximal grazing and growth rates are small. In addition GGE maximal values are obtained with the lowest g_{max}. This suggests the possibility that dinoflagellates are able to optimize their resources or reduce their basal metabolism under scarce food conditions. This optimisation ability under scarce food conditions may help dinoflagellates surviving near starvation conditions.

Additional information on the functional response is contained in the difference between grazing and growth P_t and K. The difference between P_t is towards a higher value of the growth threshold has expected, representing the basal metabolism of dinoflagellates. The difference of K between grazing and growth was not expected to be so large (Table 2), with $K\mu$ being sometimes several orders of magnitude lower than Kg. This could be due to the high uncertainty on the calculated value of half-saturation, as well as simply a consequence of a strong decoupling between grazing and growth.

4.2- Prey selection

Due to their sophisticated feeding behaviour, prey selection by dinoflagellates is a recurrent question. Grazing threshold and half-saturation concentration determine how fast a dinoflagellate will react to an increase in the concentration of prey and how efficient it will be in catching that prey. If both are low then the maximal grazing and growth rate on this prey are reached quickly and this prey is considered to be preferred over other prey with higher threshold and half-saturation constants. Dinoflagellates have a low feeding threshold, which is equal to zero when offering diatoms as prey items. The growth threshold is also significantly lower when offering diatoms as prey. This lower threshold on diatoms is coupled to higher maximal grazing, arguing for diatoms being the preferred prey type of dinoflagellates, even if more diatoms must be eaten to produce the same maximal growth rate as when autotrophic dinoflagellates are consumed. Naustvoll (2000) also found that some species prefer autotrophic dinoflagellates or will not preferentially eat the species that can sustain their maximal growth rate, preferring rather the prey found in their natural environment. Jeong (2006; 2007) offered fish blood cells as prey, resulting in higher maximal grazing and growth rates, coupled to high threshold and half saturation constant (data not included in current analysis). In addition it has been reported that heterotrophic dinoflagellates are able to feed on copepod eggs and nauplii, as well as on invertebrate larvae (Jeong 1994; Jonhson and Shanks 2003), with the possibility of more than one dinoflagellates feeding on the same egg or nauplii. It seems that even if dinoflagellates have a preference for diatoms or autotrophic dinoflagellates, they can feed on other types of prey when their preferred prey is not available. Dinoflagellates might also simply be opportunistic predators switching to other kinds of prey when their concentration increases or when locating the preferred prey is time and energy consuming compared to feeding on the available prey. This conclusion is supported by the absence of feeding threshold concentrations when their preferred prey is offered, while other kinds of food do have a threshold even if they can sustain higher growth rates than diatoms, like fish blood cells, which are less likely to be present in sufficient quantities in the environment to support the dinoflagellate community. The maximal growth rate values for dinoflagellates on fish blood cells is 1.5 to 1.7 d^{-1} whereas the highest maximal growth rate on diatoms is of 1.4 d^{-1} for the collected experiments. The maximal growth rate reached by the dinoflagellates used by Jeong in his experiments is of the order of 1 d^{-1} or lower when they are fed diatoms. This flexibility in prey choice is an advantage for dinoflagellates should their preferred prey disappear from the plankton community. This, coupled with the production of cysts and swarmers, will ensure survival of the heterotrophic dinoflagellates until better food

conditions. For that reason their low grazing and growth rate compared to other protozooplankton gives them an advantage in water poor in potential prey.

4.3- Comparison to ciliates

Heterotrophic dinoflagellates are, with pelagic ciliates, the predominant microprotozooplankton in the world oceans. The first difference between dinoflagellates and ciliates is anatomical and results in different feeding modes, one being a filter feeder and the other a raptorial feeder. The different feeding modes are associated with different prey range, ciliates feeding on prey ten times smaller in size, while dinoflagellates have a prey:dinoflagellate estimated spherical diameter ratio from 1:1 to 3:1 to even 10:1 (Hansen et al., 1994).

Another difference between the two species is that dinoflagellates grazing and growth rates are lower when comparing dinoflagellates and ciliates of the same size and with similar prey:predator size ratios. Dinoflagellates also have a higher basal metabolism (higher $P_t\mu$) and K than ciliates for both the grazing and the growth, resulting in different functional response. GGE, g_{max} and μ_{max} (Hansen 1992) are lower for dinoflagellates. These low rates and the high $P_t\mu$ can be seen as a disadvantage for dinoflagellates when feeding, but they are coupled to different food preferences. The dinoflagellates prefer large or chain forming diatoms to the picophytoplankton preferred by ciliates, resulting in different impacts on the ecosystem. Heterotrophic dinoflagellates preference for diatoms or potentially toxic autotrophic dinoflagellates is also a way to avoid competition for prey (Lessard 1991) and to increase survival prospects for dinoflagellates when ciliates can outgrow them (Jakobsen and Hansen 1997). Competition for prey of the nanozooplankton size class (2-20 µm diameter) can be assumed for a dinoflagellate with an ESD of approximately 20 µm or less and a ciliate of 100 µm ESD (Goldman and Dennett 1990). In this size range the dinoflagellate is also a potential prey of the ciliate and vice-versa. However the capacity of dinoflagellates for burst swimming allow them to escape predation by the ciliate or they can also turn out as a predator for the ciliate who capture them (Hansen 1991).

Discussing the trophic role of dinoflagellates would be more relevant when compared to copepods due to their similar prey (Naustvoll 2000). In addition, when dinoflagellates are included in copepods diet, copepods present better reproduction rates as when on a diatom only diet (Castellani et al., 2005).

4.4- Impact on food web representation and models

In conceptual representations of the marine pelagic food-web and thus in models including microzooplankton, there is no distinction between dinoflagellates and ciliates, and the microzooplankton is more ciliate like than a group representing the two (Sherr and Sherr 2007). This microzooplankton is considered as a part of the microbial loop, i.e. eating nanophytopankton and bacteria. Yet these organisms do not cover the prey size range of dinoflagellates, which feed on prey at least three times bigger than themself with a preference for diatoms. None of the collected feeding experiments were carried out using chain forming diatoms, although diatom chains are not out of the dinoflagellates prey size range, especially the thecate form with external feeding mode and the capacity to "share prey" offered by these feeding modes (external pallium and feeding tube). Dinoflagellates have been reported to feed on diatoms chain (Buck et al., 1990; Buck and Newton 1995; Buck et al., 2005) only leaving empty frustules behind, or packed chains. A top-down control of heterotrophic dinoflagellates on diatoms via the grazing pressure can be assumed to be coupled to a disruption of the carbon and silicate cycle. The fecal pellets of dinoflagellates have a low sinking rate and can remain in the water column for quite a long time due to vertical mixing affecting the export of biogenic silica toward deeper water level. The preference of dinoflagellates for diatoms as prey, especially the larger dinoflagellates, marks them as a food competitor to copepods.

5- Conclusion

This compilation and analysis of literature data revealed a need for more experiments and data on dinoflagellates, in order to better constrain their feeding behaviour and growth response. However a few important points were drawn from the data analysis. One is the apparent preference of dinoflagellates for diatoms; the other is the decoupling between grazing and growth (different threshold and half-saturation concentration) with a GGE varying with the food concentration. Dinoflagellates are quite different from the ciliates in their functional response, in addition to their different feeding mode that enables them to prey on different size classes of phytoplankton, giving them different food niches.

6-References

Azam F, Fenchel T, Field JG, Gray JS, Meyer-Reil LA and Thingstad F (1983) The ecological role of water-column microbes in the sea. *Mar. Ecol. Prog. Ser.* 10:257-263

Banse K (1982) Cell volumes, maximal growth rates of unicellular algae and ciliates, and the role of ciliates in the marine pelagial. *Limnol. Oceanogr*., 27(6):1059-1071

Buck KR, Bolt PA, Garrison DL (1990) Phagotrophy and fecal production by an athecate dinoflagellate in Antarctic sea ice. *Mar. Ecol. Prog. Ser.* 60:75-84

Buck KR, Newton J (1995) Fecal pellet flux in Dabob Bay during a diatom bloom: contribution of microzooplankton. *Limnol. Oceanogr.,* 40:306–315

Buck, K.R., Marin III, R., Chavez, F.P. (2005) Heterotrophic dinoflagellate fecal pellet production: grazing of large, chain-forming diatoms during upwelling events in Monterey Bay, California. *Aquat. Microb. Ecol.,* 40: 293-298

Buskey EJ, Coulter CJ and Brown SL (1994) Feeding, growth and bioluminescence of the heterotrophic dinoflagellate *Protoperidinium huberi*. *Mar. Biol.,* 121:373-380

Buskey EJ and Hyatt CJ (1995) Effect of the Texas (USA) "brown-tide" alga on planktonic grazer. *Mar. Ecol. Prog. Ser.,*126:285-292

Buskey EJ (1997) Behavioral components of feeding selectivity of the heterotrophic dinoflagellate Protoperidinium pellucium. *Mar. Ecol. Prog. Ser.,153:77-89*

Carreto, J.I., Benavides, H.R., Negri, R.M., Glorioso, P.D. (1986). Toxic red-tide in the Argentina sea. Phytoplankton distribution and survival of the toxic dinoflagellates Gonyaulax excavate in a frontal area. *J. Plankton Res.*, 8:15-28

Castellani C, Irigoien X, Harris R, Lampitt R (2005) Feeding and egg production of Oithona similis in the North Atlantic. *Mar. Ecol. Prog. Ser.,* 228:173–182

Egerton TA and Marshall HG (2006) Feeding preferences and grazing rates of *Pfiesteria piscida* and a cryptoperidiniopsoid preying on fish blood cells and algal prey. *Harmful algae*, 5:419-426

Gaines, G., Taylor, F.J.R. (1984). Extracellular digestion in marine dinoflagellates. *J. Plankton Res.*, 6:1057-1061

Gaines, G., Elbrätcher, M. (1987). Heterotrophic nutrition. In Taylor, F.J.R. (ed.) The biology of dinoflagellazes. Blackwell, Oxford, p. 224-268

Gentleman W, Leising A, Frost B, Strom S, Murray J (2003) Functional responses for zooplankton feeding on multiple resources: a review of assumptions and biological dynamics. *Deep Sea Research II,* 50:2847-2875

Goldman, JC, Dennett, MR (1990) Dynamics of prey selection by an omnivorous flagellate. *Mar. Ecol. Prog. Ser.,* 59:183-194

Hansen B, Bjoernsen PK, Hansen PJ (1994) The size ratio between planktonic predators and their prey. *Limnol. Oceanogr.*, 39(2):395-403

Hansen PJ (1991) Quantitative importance and trophic role of heteotrophic dinoflagellates in a coastal pelagic food web. *Mar. Ecol. Prog. Ser.,* 73:253–261

Hansen PJ (1992) Particle size selection, feeding rates and growth dynamics of marine heterotrophic dinoflagellates, with special emphasis on Gyrodinium spirale. *Mar. Biol.,* 114: 327–334

Hansen PJ, Bjornsen PK, Hansen BW (1997) Zooplankton grazing and growth: scaling within the 2-2,000- µm body size range. *Limnol. Oceanogr.*, 42(4):687-704

Holling, C.S., 1959. Some characteristics of simple types of predation and parasitism. *Canadian Entomologist,* 91, 824–839.

Jacobson DM, Anderson DM (1986) Thecate heterotrophic dinoflagellates: feeding behavior and mechanisms. *J. Phycol.*, 22:249–258

Jakobsen HH, Hansen PJ (1997) Prey size selection, grazing and growth response of the small heterotrophic dinoflagellate Gymnodinium sp. and the ciliate Balanion comatum—a comparative study. *Mar. Ecol. Prog. Ser.,* 158:75–86

Jeong HJ (1994) Predation by the heterotrophic dinoflagellate Protoperidinium cf. divergens on copepod eggs and early naupliar stages. *Mar. Ecol. Prog. Ser.,* 114:203-208

Jeong HJ, Yoo YD, Kim ST and Kang NS (2004) Feeding by the heterotrophic dinoflagellate *Protoperidinium bipes* on the diatom *Skeletonema costatum*. *Aquat. Microb. Ecol.,* 36:171-179

Jeong HJ, Shim JH, Kim JS, Park JY, Lee CW and Lee Y (1999) Feeding by the mixotrophic thecate dinoflagellate *Fragilidium* cf. *mexicanum* on red-tide and toxic dinoflagellates. *Mar. Ecol. Prog. Ser.,*176:263-277

Jeong HJ, Kim JS, Yoo YD, Kim ST, Kim TH, Park MG, Lee CH, Seong KA, Kang NS and Shim JH (2003) *J. Eukaryot. Microbiol.,* 50(4):274-282

Jeong HJ, Park JY, Nho JH, Park MO, Ha JH, Seong KA, Jeng C, Seong CN, Lee KY and Yih WH (2005a) Feeding by the red-tide dinoflagellates on the cyanobacteria *Synechococcus*. *Aquat. Microb. Ecol.* 41:131-143

Jeong HJ, Kim JS, Kim JH, Kim ST, Seong KA, Kim TH, Song JY, Kim SK (2005b) Feeding and grazing impact of the newly described heterotrophic dinoflagellate *Stoeckeria algicida* on the harmful alga *Heterosigma akashiwo*. *Mar. Ecol. Prog. Ser.,*295:69-78

Jeong JH, Yoo YD, Park JY, Song JY, Kim ST, Lee SH, Kim KY and Yih WH (2005c) Feeding by the phototrophic red-tide dinoflagellates: five species newly revealed ans six species previously known to be mixotrophic. *Aquat. Microb. Ecol.* 40:133-150

Jeong HJ, Yoo YD, Seong KA, Kim JH, Park JY, Kim S, Lee SH, Ha JH and Yih WH (2005d) Feeding by the mixotrophic red-tide dinoflagellate *Gonyaulax polygramma*: mechanisms, prey species, effect of prey concentration, and grazinf impact. *Aquat. Microb. Ecol.,* 38:249-257

Jeong HJ, Ha, JH, Park, JY, Kim, JH, Kang, NS, Kim, S, Kim, JS, Yoo, YD, Yih, WH (2006) Distribution of the heterotrophic dinoflagellate Pfiesteria piscicida in Korean waters and its consumption of mixotrophic dinoflagellates, raphidophytes and fish blood cells. *Aquat. Microb. Ecol.,* 44:263-278

Jeong HJ, Ha JH, Yoo YD, Park JY, Kim JH, Kang NS, Kim TH, Kim HS and Yih WH (2007a) Feeding by the *Pfiesteria*-like hetrotrophic dinoflagellates *Luciella masanensis*. *J. Euk. Microbiol.,* 54(3):231-241

Jeong HJ, Song JE, Kang NS, Kim S, Yoo YD and Park JY (2007b) Feeding by the heterotrophic dinoflagellates on the common marine heterotrophic nanoflagellate *Cafeteria sp. Mar. Ecol. Prog. Ser.,*333:151-160

Johnson, KB, Shanks, AL (2003) Low rates of predation on planktonic marine invertebrate larvae. *Mar. Ecol. Prog. Ser.,* 248:125-139

Jonsson R (1986) Particle size selection, feeding rates and growth dynamics of marine planktonic oligotrichous ciliates (Ciliophoa: Oligotrichina). *Mar. Ecol. Prog. Ser.,* 33:265-277

Kim JS and Jeong HJ (2004) Feeding by the heterotrophic dinoflagellates *Gyrodinium dominans* and *G. spirale* on the red-tide dinoflagellate *Prorocentrum minimum*. *Mar. Ecol. Prog. Ser.,* 280:85-94

Kiørboe, T.(2008) A mechanistic approach to plankton ecology. Princeton, Univ. Press

Landry MR, Ondrusek ME, Tanner SJ, Brown SL, Constantinou J, Bidigare RR, Coale KH, Fitzwater S (2000) Biological response to iron fertilization in the eastern equatorial Pacific (IronEx II). I. Microplankton community abundances and biomass. *Mar. Ecol. Prog. Ser.,* 201:27–42

Lee JJ (1980) Informational energy flow as an aspect of protozoan nutrition. *J. Protozool.,* 27:5-9

Lessard EJ (1991) The trophic role of heterotrophic dinoflagellates in diverse marine environments. *Mar. Microb. Food. Webs,* 5:49–58

Menden-Deuer S, Lessard EJ (1995) Carbon to volume relationships for dinoflagellates, diatoms, and other protist plankton. *Limnol. Oceanogr.,* 45:569-579

Menden-Deuer S, Lessard EJ, Satterberg J and Grünbaum D (2005) Growth rate and starvation survival of three species of the pallium-feeding, thecate dinoflagellate genus *Protoperidinium. Aquat. Microb. Ecol.,* 51:154-152

Montagnes DJS, Kimance SA, Atkinson D (2003) Using Q10: can growth rates increase linearly with temperature? *Aquat. Microb. Ecol.*, 32:307-313

Mullin MM, Stewart EF, Fuglister FJ (1975) Ingestion by planktonic grazers as a function of concentration of food. *Limnol. Oceanogr.,* 20:259-262

Nakamura Y, Yamazaki Y and Hiromi J (1992) Growth and grazing of a heterotrophic dinoflagellate, *Gyrodinium dominans*, feeding on a red tide flagellate, Chattonella antique. *Mar. Ecol. Prog. Ser.,* 82:275-279

Nakamura Y, Suzuki S and Hiromi J (1995) Growth and grazing of a naked heterotrophic dinoflagellates, Gyrodinium dominans. *Aquat. Microb. Ecol.,* 9: 157-164

Naustvoll L (1998) Growth and grazing by the thecate heterotrophic dinoflagellate *Diplopsalis lenticula* (Diplopsalidaceae, Dinophyceae). *Phycologia* 37(1):1-9

Naustvoll L (2000) Prey size spectra and food preferences in thecate heterotrophic dinoflagellates. *Phycologia,* 39(3): 187-198

Sherr, E.B., Sherr, B.F. (2007) Heterotrophic dinoflagellates: a significant component of microzooplankton biomass and major grazers of diatoms in the sea *Mar. Ecol. Prog. Ser.*, 352: 187-197

Sivia, DS, Skilling, J. (2006) Data analysis – A bayesian Tutorial, Second edition, Clarendon Press, Oxford.

Smetacek V (1981) Annual cycle of protozooplankton in the Kiel Bight. *Mar. Biol.,* 63:1–11

Straile D (1997) Gross growth efficiencies of protozoan and metazoan zooplankton and their dependence on food concentration, predator-prey weight ratio, and taxonomic group. *Limnol. Oceanogr.,* 42(6):1375-1385

Strom SL and Buskey EJ (1993) Feeding growth and behaviour of the thecate heterotrophic dinoflagellate *Oblea rotunda*. *Limnol. Oceanogr.,* 38(5):965-977

Tillmann U and REckermann M (2002) Dinoflagellate grazing on the raphidophyte *Fibrocapsa japonica*. *Aquat. Micron. Ecol.,* 26:247-257

CHAPTER 4:

Microzooplankton Representation in Model: Comparison of Pelagic Ciliates and Heterotrophic Dinoflagellates.

1-Introduction

The ocean carbon cycle modulates global climate by acting as a source and/or sink for atmospheric carbon dioxide (Siegenthaler and Sarmiento 1993). The climate in turn impacts the functioning of the ocean by alterating the magnitude and sign of physico-chemical and biotic carbon sinks (Woodwell et al., 1998). Experiments using coupled biogeochemical ocean general circulation models (BOGCM) provide a method for assessing marine biogeochemical responses to and feedbacks on future climate change (Sarmiento et al., 1998; Joos et al., 1999). Physico-chemical carbon sinks are readily incorporated into BOGCM as the dependence of surface pCO_2 on temperature (Joos et al., 1999) and carbonate chemistry (Kleypas et al., 1999) are well known. The likely effects of global warming on oceanic biota, and hence the biological pump, are tested using simple biogeochemical parameterisations (Sarmiento et al., 1998; Joos et al., 1999) or simple ecosystem (so-called NPZD) models (Cox et al., 2000). Biogeochemical models initially only simulated the cycles of C and P to describe the role of the ocean ecosystem in exporting matter from the surface to the deep sea (Najjar et al., 1992; Maier-Reimer 1993). These initial models used simple parameterisation that restore nutrient fields to observed values in order to calculate biological activity, but did not represent the organisms themselves. More recent biogeochemical models explicitly represent autotrophic and heterotrophic production based on measured rates (e.g. *in situ* measurements to constrain fluxes and laboratory measurements to constrain parameterisations). These different approaches are now converging in Dynamic Green Ocean Models, which incorporate into BOGCMs the current conceptual understanding of ocean ecosystems (Le Quéré et al., 2005).

These ecosystem models include organisms or groups of organisms based on their impact on biogeochemical cycles and their importance in term of biomass (Plankton

Functional Types or PFTs; Le Quéré et al., 2005). The microzooplankton (heterotrophs 20 to 200 µm in size) is represented in ecosystem models because of the high biomasses and growth rates (close to that of phytoplankton) attained by this group allowing it to follow fluctuations in phytoplankton biomass and possibly to regulate phytoplankton blooms. Microzooplankton is composed of a large variety of protozoans, nauplii and larvae of metazoans. A diverse assemblage of protozoa and metazoan both contribute to the microzooplankton but ciliates and heterotrophic and mixotrophix dinoflagellates tend to largely dominate this group both numerically and in biomass.

Ciliates are filter feeders, sieving the surrounding water to find and capture their prey and are known to have an optimal prey size roughly one tenth of their own diameter. The lower limit of ciliate prey size spectrum is possibly determined by the spacing between the rows of ciliated organelles (polykinetids) surrounding the cytostome (cell mouth). The upper size-limit of prey consumed is thought to be constrained by the cytostome or cell diameter (Heinbokel 1978; Jonsson 1986; Hansen et al., 1994). Field observations suggest much larger maximum prey size than values estimated from laboratory experiments, however, quantitative information this aspect of ciliate feeding behaviour is still lacking. Heterotrophic and mixotrophic dinoflagellates are raptorial feeders: they actively swim around in search of prey items that are either engulfed or digested externally (palium and peduncle feeding; Jacobson 1999). The variety of feeding modes found in dinoflagellates allows this group to feed on a wide range of prey and particle sizes up to five times larger than their own size (Hansen 1994). The differences in feeding mode and prey size spectrum between ciliates and dinoflagellates results in different grazing selectivity on phytoplankton communities with dinoflagellates consuming diatoms and ciliates primarily nanophytoplankton. Metabolic rates of similar-sized ciliates and dinoflagellates are also different with higher grazing and growth rate in ciliates than dinoflagellates (Strom 1998). These differences in traits indicate that these two groups should have a different impact and role in the marine pelagic foodwebs.

One of the major challenges, in the context of understanding feedbacks between climate and ocean biogeochemistry using PFT-based ecosystem model is to determine the biological complexity required for numerical models to accurately capture climate change impacts and subsequent biotic feedbacks (Anderson 2005; Doney 1999). Microzooplankton, through its large impact on phytoplankton biomass and nutrient recycling, is a key aspect in this issue. What are the impacts of ciliates and dinoflagellates on a model's ecosystem, and are these close enough that a mixed microzooplankton group yields similar results to modelling the groups separately? This question is the one addressed in this study, using the

PlankTOM5 BOGCM (Buitenhuis et al., 2006). The model is used to compare the differences between a mixed-microzooplankton (composed of an equal mixture of ciliates and dinoflagellates), ciliates and dinoflagellates. The comparison is done in two steps, by investigating the effect of differences in the functional grazing response and the effect of differences in food preferences. Grazing parameters and food preferences were obtained from an extensive literature search and analysis of data (Sailley et al., in prep). The grazing parameters were modified resulting in three representations of microzooplankton: mixed microzooplankton (original reference parameters), ciliates and dinoflagellates. Finally, the importance of prey preferences was tested by using different specific food preferences for the ciliate and dinoflagellate runs.

2- Model description

2.1-PlankTOM5 biogeochemical model

The PlankTOM5 model used here is the same as in Buitenhuis et al., (subm.). The equations governing the microzooplankton are briefly presented and explained below. Documentation of the other components can be found at http://lgmacweb.env.uea.ac.uk/green_ocean/.

The change in the concentration of microzooplankton is calculated using the following equation:

$$\delta MIC/\delta t = \Sigma grazing_F^{mic} \times MGE - \text{basal respiration} - grazing_{mic}^{mes} \quad (1)$$

where MIC is the microzooplankton concentration, MGE is the model growth efficiency, $grazing_F^{mic}$ the grazing of microzooplankton on a given type of food or PFT. In PlankTOM5 four different food are represented namely, small particulate organic carbon (POC_s), coccolithophores (COC), diatoms (DIA) and mixed phytoplankton (MIX). MIX encompass all of the phytoplankton that is not COC or DIA. $Grazing_{mic}^{mes}$ is the grazing pressure of mesozooplankton on microzooplankton . Microzooplankton mortality is only due to starvation and grazing by mesozooplankton. There is no internal grazing in the microzooplankton or mortality due to diseases.

2.2- Grazing

The microzooplankton grazing rate ($grazing_F^{mic}$) on any one food (F) is described by the following equation:

$$grazing_F^{mic} = G_{0°C}^{mic} \times Q_{10,gr}^{\wedge T/10} \times \frac{p_F^{mic} C_f}{K_{½}^{mic} + \Sigma p_F^{mic} C_f} \times MIC \quad (2)$$

Where $G_{0°C}^{mic}$ is the maximum grazing rate at 0 °C, $Q_{10,gr}$ is the temperature dependence of grazing, T is the temperature, p_F^{mic} is the preference for food F, C_f is the concentration of the food F and $K_{½}^{mic}$ is the half saturation constant for grazing. A preference superior to one results in this food being eaten preferentially to other type of food at equal concentration or even slightly lower.

2.3- Partitioning of grazing

The net growth of an organism can be calculated as being:

net growth = grazing x GGE (3)

where GGE (gross growth efficiency) is the part of grazing that is incorporated into biomass. The grazed matter is partitioned between the biomass of microzooplankton (GGE), respiration, unassimilated matter and dissolved matter as follows:

GGE + unassimilated matter + dissolved matter + respiration = 1 (4)

Unassimilated matter and respiration are held constant and correspond to the fractions of grazing that are partitioned to POCs, DOC and DIC. To allow the model to subtract basal respiration whether net growth occurs or not, a model growth efficiency (MGE) is defined (Buitenhuis et al., 2006) and used instead of the GGE. The formulation provides a continuous function of biomass change with changing food concentration, from net loss at low food concentration to a net gain at high food concentration.

MGE + unassimilated matter + dissolved matter + feeding respiration = 1 (5)

In addition, to accommodate the fixed Fe:C ratio in zooplankton and variable Fe:C ratio in the foods, the MGE is decreased when the zooplankton are iron rather than carbon limited:

$$\text{MGE} = \min(1\text{-unass}, \text{GGE} + \text{basal respiration} / \Sigma\text{grazing}_F^{mic}, \Sigma\text{grazing}_F^{mic}{}_{Fe} * (1\text{-unass})/(\Sigma\text{grazing}_F^{mic}{}_C * \text{Fe:C}^{mic})) \quad (6)$$

Equation 5 introduces a feeding respiration, which is proportional to grazing and which is not measurable as a separate quantity: only the sum of feeding respiration and basal respiration is measurable. However, feeding and basal respiration could be separated as the slope and ordinal intercept of respiration plotted as a function of grazing (Verity 1985). Feeding respiration is introduced as a programming convenience so that the model does not have to decide every time and place whether the zooplankton are starving. It is equivalent to introducing a threshold food concentration for growth.

2.4- Basal respiration

The basal respiration was calculated as:

$$\text{basal respiration} = \text{res}_{0°C}^{mic} \times Q_{10,res}{}^{\wedge T/10} \times \text{MIC} \quad (7)$$

Where $\text{res}_{0°C}^{mic}$ is the feeding respiration at 0 °C, MIC is the microzooplankton concentration and $Q_{10,res}$ is the temperature dependence of respiration.

2.5- Fluxes of dissolved and particulate egestion and respiration

The other microzooplankton mediated fluxes are:

$$\delta\text{DOC}/\delta t = (1\text{ -inorg}) \times (1\text{ –unassimilated matter -MGE}) \times \Sigma\text{grazing}_F^{mic} \times \text{MIC} \quad (8)$$

$$\delta\text{POC}_s/\delta t = \text{unassimilated matter} \times \Sigma\text{grazing}_F^{mic} \times \text{MIC} \quad (9)$$

$$\delta PO_4^{3-}/\delta t = \text{inorg} \times (1 - \text{unassimilated matter -MGE}) \times \Sigma\text{grazing}_F^{mic} \times \text{MIC} + \text{res}_{0°C}^{mic} \times Q_{10,res}{}^{\wedge T/10} \times \text{MIC} \quad (10)$$

where *inorg* is a factor partitioning the ingested matter that is not used for growth or particulate egestion, between respiration to DIC, PO_4 and Fe, and dissolved egestion to DOC (Fig. 1).

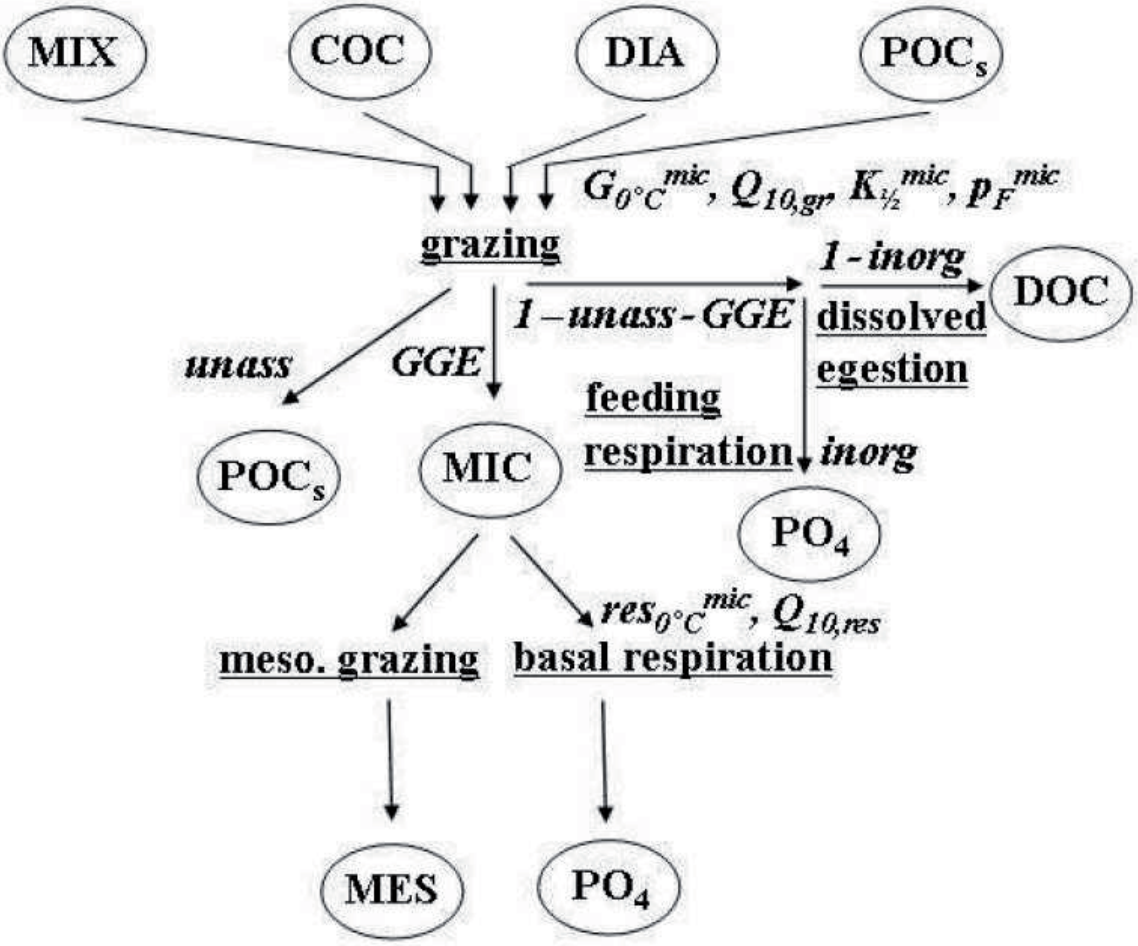

Figure 1: Fluxes through microzooplankton. Circles represent state variables (MIX = mixed-phytoplankton, COC = coccolithophores, DIA = diatoms, POCs = small particulate organic carbon, DOC = dissolved organic carbon, MIC = microzooplankton, PO_4 = nutrients (including dissolved organic carbon), MES = mesozooplankton), underlined text represent fluxes and italic texts represent parameters.

Microzooplankton mortality was only included for starvation (basal respiration below the threshold food concentration) and grazing by mesozooplankton. There's no internal grazing in the microzooplankton or mortality due to diseases.

3- Physical model and model forcing

PlankTOM5 is coupled to the global ocean general circulation model (GCM) NEMOv2.3 (Buitenhuis et al., subm; Madec 2008). It has a horizontal resolution of 2° in longitude and on average 1.1° in latitude, and a vertical resolution of 10 m in the top 100 m, the vertical resolution increases to 500 m from 5 km depth. The NEMO model was forced by daily wind and precipitation from NCEP reanalysis (Kalnay et al., 1996) from 1990 to 2000. The PlankTOM5 model was forced by river input of DIC, alkalinity, DOC, PO_4, SIO_3 and Fe (da Cunha et al., 2007), sediment input of Fe and dust input of Fe and SIO_3 (Aumont et al., 2003).

The model was initialised with observations from the World Ocean Atlas 2005 (T, S, PO_4^{3-}, SiO_3^{-} and O_2), GLODAP (DIC and alkalinity), and Zhang & Rothrock (2003, ice extent and thickness and snow thickness). Other tracers were initialised with the steady-state fields generated by a run from a previous model version (Manizza et al,. in preparation).

4- Parameterisation

Parameters of microzooplankton are extracted from the work of Buitenhuis et al., (subm). For the representation of ciliates and dinoflagellates the changed parameters are: $G_{0°c}^{mic}$, $K_{1/2}$, Q_{10}, the feeding respiration and the food preferences. The values for these parameters are obtained from an extensive compilation and analysis of measurements from laboratory experiments on grazing and growth of ciliates and dinoflagellates found in the literature (database available at www.pangeae.de). As in Buitenhuis et al., (subm), the collected growth rates were fitted to the following equation with F the food concentration:

$$\mu = \frac{\mu_{0°C} \times Q_{10}^{\wedge T/10} \times F}{K_{1/2} + F} \qquad (11)$$

That gave computed values for $\mu_{0°C}$, Q_{10} and $K_{1/2}$ for ciliates and dinoflagellates. The same GGE value is used for ciliates and dinoflagellates than for microzooplankton and used to obtain $G_{0°c}^{mic}$ from $\mu_{0°C}$. The feeding respiration or threshold is obtained from the following equation:

$$res = \frac{G_{0°C}^{\ mic} \times GGE \times P_t}{K_{1/2} + P_t} \quad (12)$$

Where P_t is the threshold concentration computed from the collected data by fitting all the growth rates to a Michaelis-Menten with threshold.

We calculated preferences with a phytoplankton biomass weighted mean of 1:

$$\frac{(p_{poc}^{\ mic} \text{ x } C_{poc} + p_{dia}^{\ mic} \times C_{dia} + p_{coc}^{\ mic} \times C_{coc} + p_{mix}^{\ mic} \times C_{mix})}{\Sigma C_{phytoplankton}} = 1 \quad (13)$$

The preference is a value obtained based on the variation of the maximal grazing rate with the size of the organism and the size ratio with its prey (Sailley et al., in prep a; b), literature knowledge of the size selectivity spectra of the organisms (Hansen et al., 1994) and the possible preference for a certain type of prey, *e.g.* dinoflagellates prefer diatoms over other prey type (Sherr and Sherr 2007). A preference superior to one results in this food being eaten preferentially to other type of food at equal concentration or even slightly lower, if the preference is inferior to one this food will be ignored for other present food. The phytoplankton biomasses (C_f and $C_{phytoplankton}$) use for the calculation of the food preferences are obtained from a database based on accessory pigments and size classes over the world ocean (Uitz et al., 2006). Diatoms are assumed to be 100% of microphytoplankton, 50% of nano phytoplankton is assumed to be coccolithophores, the remaining 50% plus the picophytoplankton compose the mixed phytoplankton.

5- Design of the model experiments

The model ecosystem, and upper layer reach a steady-state after 6 years of simulation. The model was run for ten years (1990-2000) to have a stable and functioning ecosystem in the upper-layer.

Three types of model configuration based on grazing parameters (Table 1) were used to compare the impact of ciliates and dinoflagellates: (i) a mixed-microzooplankton composed of both ciliates and dinoflagellates (MIC), (ii) a microzooplankton composed only of ciliates (CIL), (iii) a microzooplankton composed only of dinoflagellates (DIN). For each configuration three different runs (or experiments) were conducted as a sensitivity analysis to

see the impact of food preferences (Table 2): (a) the reference runs: food preferences are those of the mixed microzooplankton (MFP); (b) food preferences are those specifically for ciliates or for dinoflagellates (SFP); (c) the food preferences are all set to one: there are no food preferences (NFP).

6- Results

6.1- Parameterization.

For the MIC model the maximal grazing rate and half-saturation are higher than for CIL and DIN, while the respiration is about half of that for CIL, and the Q_{10} is close to that of DIN (Table 1). The MIC representation is not an intermediate group between CIL and DIN but a group on its own. The parameters for CIL show a maximal grazing rate that is about twice as that for DIN, a higher half-saturation by an order of magnitude of three, a lower feeding respiration by a factor of two and a higher Q_{10} than for DIN. These difference between the parameters reflect the difference in the functional response of ciliates and dinoflagellates (maximal rate and half-saturation) as well as their different metabolism (feeding respiration and Q_{10}).

Table 1: grazing parameters for the model

	MIC [§]	CIL	DIN	MESO[§]
Maximal grazing at 0°C (day^{-1})	0.92	0.75	0.39	0.31
Half saturation ($\mu g\ C\ L^{-1}$)	76.8	43.1	$24.0\ 10^{-3}$	3.12
Feeding respiration (day^{-1})	0.036	0.06	0.15	0.008
Q_{10} of grazing, growth and respiration	1.70	2.07	1.72	1.77

[§] Taken from Buitenhuis et al. (subm.)

The food preferences (Table 2) show the same as the grazing parameters: MIC is for a group on its own rather than a homogeneous mix between ciliates and dinoflagellates. The DIN food preferences reflect their large food size spectra without any marked preference for a prey size, it also shows the marked preference of dinoflagellates for diatoms. The CIL food preferences are a result of the small range it covers with a marked size preference for prey

from the picophytoplankton thus the mixed-phytoplankton, but no PFT preference. The preferences of mosozooplankton (MESO) are added for information.

Table 2: Food preferences for different representation of the microzooplankton

Food type or PFT	MIC[§] (MFP)	CIL (SFP)	DIN (SFP)	MESO[§] (all)
POC	0.13	0.27	0.28	0.51
Diatoms	0.26	0.53	2.78	2.54
Mixed phytoplankton	1.29	3.2	1.94	0.51
Coccolithophores	1.03	0.13	1.39	0.63
Microzooplankton	-	-	-	2.54

[§] Taken from Buitenhuis et al. (subm.)

6.2- Model simulation.

6.2.a- Simulations with different microzooplankton functional response parameterizations (MIC, CIL and DIN): MFP experiments.

The MIC_{MFP} has been used in previous studies (Buitenhuis et al., subm.) and will be considered as the standard run. The primary production is 50 Pg C y^{-1} (Table 3), well within the range of global estimates of derived from satellite imagery of 47-50 Pg C y^{-1} (Behrenfeld and Falkowski 1997). The geographical distribution of chlorophyll *a* (Chl*a*) is similar to values derived from SeaWifs (Fig. 2 and 3) albeit with lower values in high productivity regimes such as upwelling and coastal areas, as well as in high latitudes. The microzooplankton biomass in model runs is about half the value of observation (Table 4) and shows a different distribution to observations with higher values in the Southern Ocean and lower values between 20°N and 40° N (Fig. 2 and 3). The consumption of phytoplankton by microzooplankton is 24 Pg C y^{-1} (48% of the primary production), within the range estimated by Calbet and Landry (2004) (Table 3). Grazing impact of mesozooplankton is 12.8 Pg C y^{-1} (25.6% of the primary production), higher than estimates (Calbet 2001; Table 3) by a factor two. Mesozooplankton grazing impact is lower than microzooplankton grazing impact by a factor two. The highest microzooplankton biomasses occur in the Western Pacific and in the Southern Ocean (Fig. 2). With the exception of the Southern Ocean these are areas where

maximum phytoplankton growth and consumption by microzooplankton also occurs (Fig. 4). Figure 5 presents distribution of export fluxes at the surface for the different model runs. Areas of high export correspond to areas of high productivity and low microzooplankton grazing (i.e. between 30°N and 60°N, west African upwelling areas as well as between 30°S and 45°S; Fig. 3). Diatom biomass is equal to the biomass calculated from observations (Uitz et al., 2006), while that of coccolithophore is half of the observed values and biomass of mixed-microzooplankton about 1.5 times higher than observations (Table 4). Diatoms and mixed phytoplankton (excluding coccolithophores) dominate phytoplankton biomass in the Southern Ocean. Coccolithophores dominate in the North Atlantic south of 40°N, Indian Ocean and Western Pacific, and other mixed phytoplankton the remaining oceanic areas.

The CIL_{MFP} experiment results in similar microzooplankton biomass than in the MIC_{MFP} run (Table 4), however, the geographical distribution is different with higher values around the equator between 30°S and 30°N (Fig. 1) but more pronounced in the North Pacific and a reduction in polar areas. The distribution of ciliates is concurrent with a reduction in phytoplankton biomass around the equator (Fig. 1) in particular in the subtropical gyres. The yearly primary production decreases to 45.6 Pg C y^{-1}, closer to satellite-based estimates (Table 3). The grazing impact of microzooplankton in CIL_{MFP} is higher by 3.8 Pg C y^{-1} compared to that of MIC_{MFP}, while mesozooplankton grazing is reduced by 2.5 Pg C y^{-1} (Table 3). Locally the mortality of phytoplankton by microzooplankton is increased by a factor 2 and the grazing of microzooplankton extends over a larger area. Similar to MIC_{MFP}, the increase in grazing pressure leads to an increase in phytoplankton growth over ocean areas were grazing is higher while export decreases concomitantly (Fig. 3 and 4) resulting in an overall decrease in export of 1.9 Pg C y^{-1} (21% as compared to the MIC_{MFP} run, Table 3). The CIL_{MFP} run results in a significant reduction in average standing stocks of smaller phytoplankton (coccolithophores and mixed small phytoplankton) in the Southern Ocean and subtropical gyres while diatoms biomass increases as compared to the MIC_{MFP} run (Table 3). The increase in diatom biomass is accompanied by a shift in diatom distribution from the western Pacific, where high microzooplankton grazing rates are found, to the eastern equatorial pacific.

The DIN_{MFP} run has a yearly primary production of 47.8 Pg C similar to the other experiments (Table 3), although average phytoplankton biomass is significantly lower than for previous runs. Mesozooplankton biomass is also significantly lower (over 50% lower, Table 4). In the DIN_{MFP} run microzooplankton biomass increases roughly in a similar manner as in CIL_{MFP}, except at high latitudes (particularly in the Southern Ocean) where

concentrations decrease (Fig. 3). In contrast to CIL_{MFP}, however, higher concentrations of phytoplankton are found between 40°S and 40°N, in particular in the subtropical gyres, while at high latitudes concentrations are low and close to zero (Fig. 2). The DIN_{MFP} experiment results in an increase in microzooplankton grazing in high and mid-latitudes, with the exception of some pockets along the high latitude boundaries of the subtropical gyres dominated by mesozooplankton (Fig. s1). In contrast to MIC_{MFP} and in particular CIL_{MFP} grazing rates are lower in the western pacific, equatorial Atlantic and Indian Ocean. Hence, overall grazing impact on phytoplankton is close to values for MIC_{MFP} and CIL_{MFP} (25 Pg C y^{-1}) while mesozooplankton grazing is reduced by roughly a factor of 2 (Table 3). Compared to MIC_{MFP} and CIL_{MFP}, the local increase, respectively decrease, in grazing rate is accompanied by an increase, respectively decrease, in phytoplankton growth rates. The DIN_{MFP} parameterization leads to an increase in the consumption of POC (detritus) corresponding to roughly twice the increase found in the CIL_{MFP} run together with a decrease in export (Table 3, grazing on all food minus the grazing on phytoplankton). Pockets of high export correspond to area dominated by mesozooplankton (Fig. 4 and s1). In DIN_{MFP}, the biomass of all phytoplankton groups is strongly reduced as compared to MIX_{MFP} and CIL_{MFP} (Table 4) in descending order: coccolithophores (up to 99 % reductions) followed by diatoms (up to 42%) and finally mixed phytoplankton (up to 41% reduction). With the exception of coccolithophores, biomass reduction occurs mostly in the Southern Ocean (Fig. s2, s3 and s4).

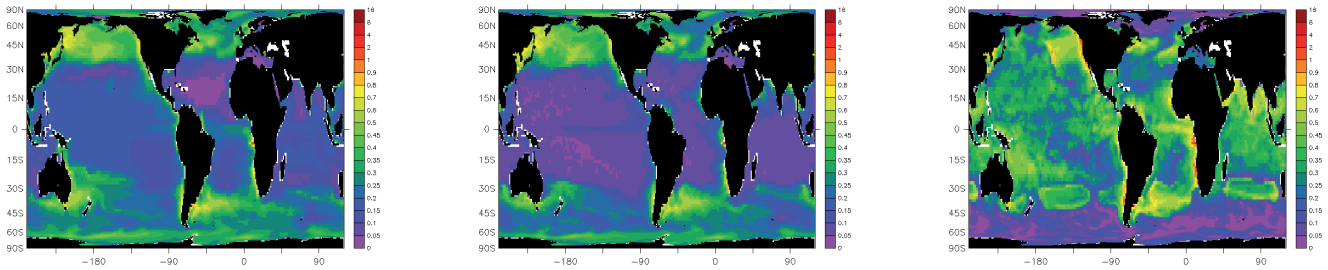

Figure 2: Annual mean of surface chlorophyll a (µg L^{-1}) (upper panel) in MFP experiments; from left to right MIC, CIL, DIN run. SeaWifs observation (lower panel)

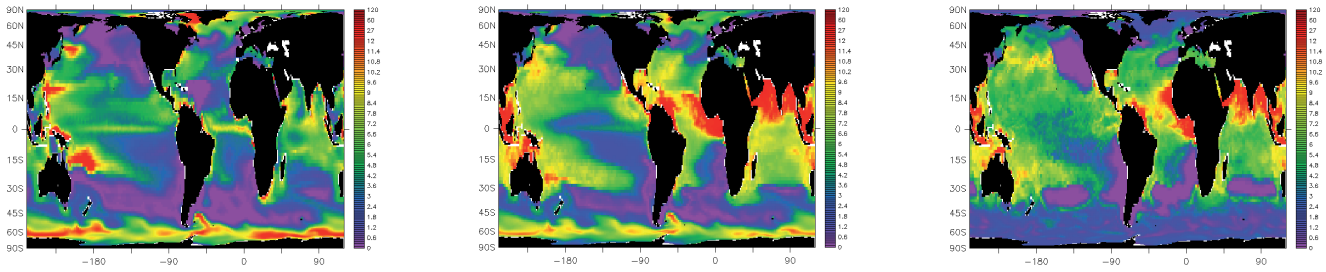

Figure 3: Annual mean of surface biomass of microzooplankton (µg C L^{-1}) in MFP experiments (upper panel) and mean of observed microzooplankton concentration (µg C L^{-1}) as a function of latitude (lower panel). From left to right MIC, CIL, DIN run.

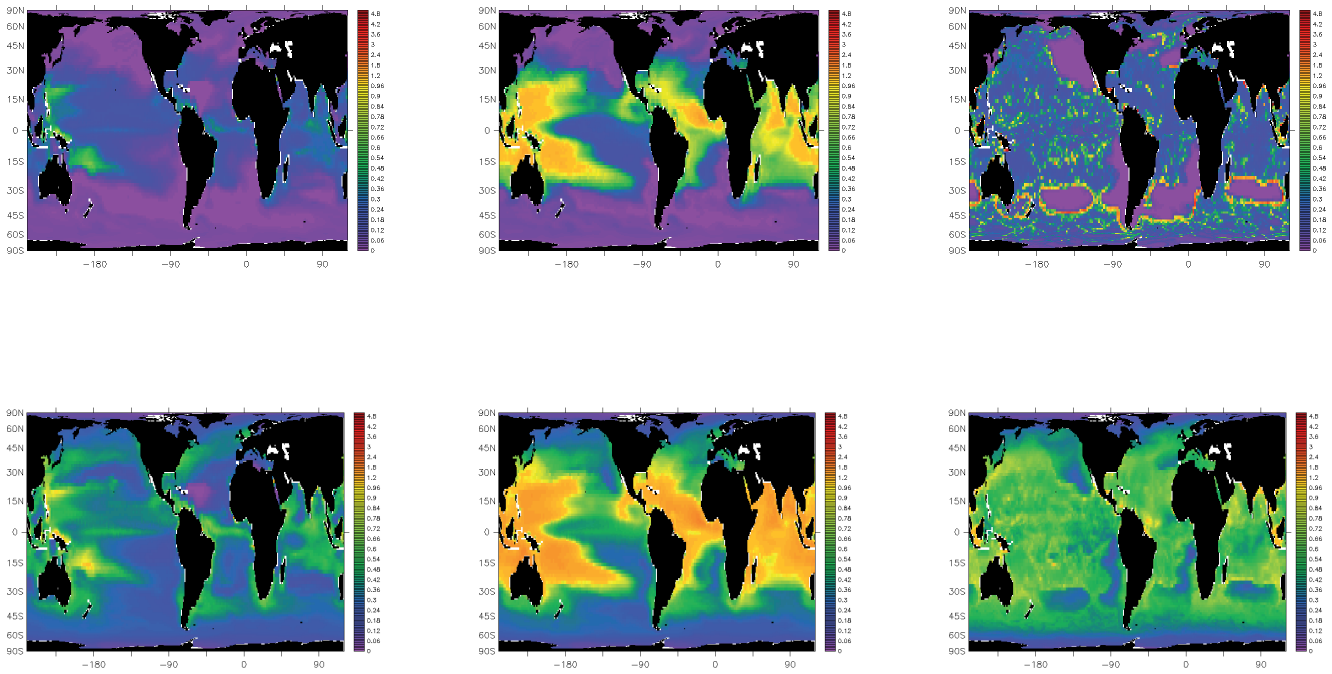

Figure 4: Phytoplankton mortality caused by microzooplankton grazing (upper panel) and phytoplankton growth (lower panel) in day^{-1}, model output for experiment MFP. From left to right: MIC, CIL and DIN run.

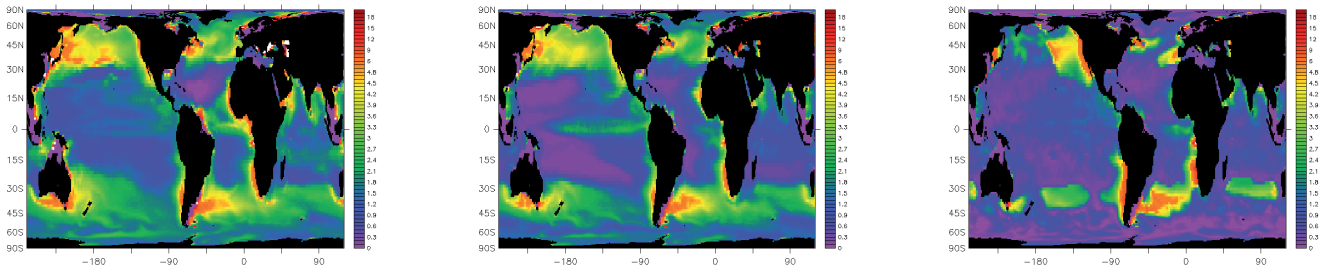

Figure 5: Export in mol m^{-2} $year^{-1}$, model output for experiment MFP. From left to right: MIC, CIL and DIN run.

6.2.b- Simulations with no food preferences: NFP experiments

Overall changes

The experiments with no differences in food preferences (NFP) show significant increase in microzooplankton biomass (Southern Ocean excepted) for the MIX and CIL runs, respectively (Fig. 1, 4 and 5). Biomass of microzooplankton increases in equatorial regions, western Pacific and Indian Ocean (between 15°S and 15°N), North Atlantic and Nordic seas and decreases in the Southern Ocean for MIX_{NFP} as compared to MIX_{MFP}. Similar changes occur for CIL_{NFP} but the increase in microzooplankton biomass is more marked and covers a broader area ranging between 30°S and 30°N. The same pattern of change between MIX_{NFP} and MIX_{MFP} is observed for phytoplankton growth and to a lesser extend for microzooplankton mediated grazing except in the polar areas were only minor changes occur (Fig. 3 and s5). The CIL_{NFP} configuration differs markedly from CIL_{MFP} by a large increase in phytoplankton growth and mortality in the eastern Pacific and western Atlantic between 30°S and 30°N (Fig. 3 and s2). The changes in microzooplankton grazing and phytoplankton growth results in slight increase in phytoplankton biomass (Southern Ocean excepted) for the MIX and CIL runs, respectively (Fig. 1, 4 and 5) accompanied by a slight reduction in export fluxes for MIX_{NFP} between 30°S and 30°N and in polar areas. For CIL_{NFP} similar trend in export is observed with larger reduction in fluxes between 30°S and 30°N.

The DIN_{NFP} run shows large reduction in phytoplankton and microzooplankton biomass as compared to DIN_{MFP} (Fig. 1, 2 and 5). Phytoplankton biomass decreases to zero levels in most ocean basins with the exception of the Subantarctic region, Subarctic Pacific, equatorial upwelling and North Atlantic while microzooplankton biomass decreases globally with the exception of the equatorial upwelling areas. Higher phytoplankton biomass is found mostly in areas where microzooplankton biomass is low (Fig. 5) and mesozooplankton abundances are high (Fig. s6).

Phytoplankton growth and mortality is higher in DIN_{NFP} as compared to DIN_{MFP}, in particular at low and mid-latitudes and areas with high microzooplankton grazing are also associated with equally high phytoplankton growth rates (Fig. 3 and s5, the grazing mortality is about 90% of the growth rate). Export fluxes are also strongly reduced with the exception of areas where mesozooplankton abundances are high (Fig. s6 and s7).

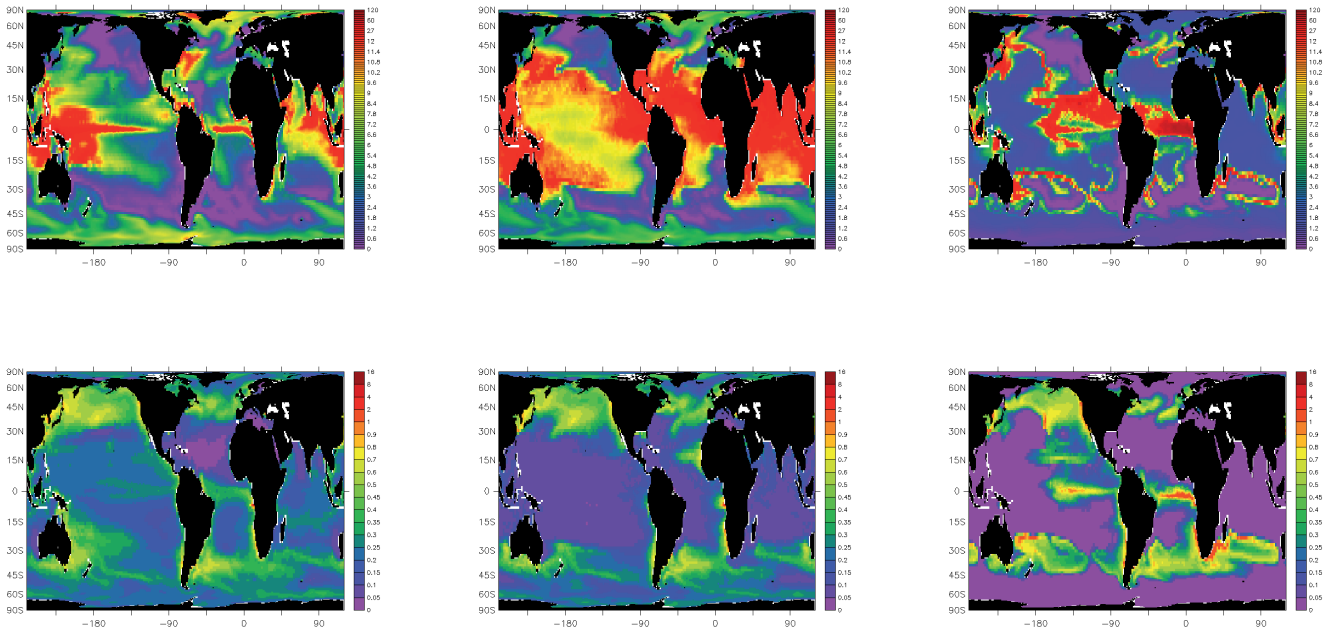

Figure 6: Distribution of microzooplankton (µg C L^{-1}) for the runs of experiment 'NFP' (upper panel) and surface chlorophyll a (µg L^{-1}) (lower panel). From left to right: MIC, CIL and DIN run.

Figure 6: Distribution of microzooplankton (µg C L^{-1}) for the runs of experiment 'NFP' (upper panel) and surface chlorophyll a (µg L^{-1}) (lower panel). From left to right: MIC, CIL and DIN run.

Changes in PFT distribution

The MIX_{NFP} and CIL_{NFP} configuration lead to a global decrease in diatom and coccolithophore biomass as compared to MIX_{MFP} and CIL_{MFP}, respectively. The decrease in diatom and coccolithophore biomass is somewhat compensated by an increase in mixed phytoplankton biomass (Fig. s2, s3 s8 and s9). Similar changes are observed between DIN_{MFP} and DIN_{NFP} although in this case they are accompanied by a decrease in mixed phytoplankton biomass in the Western Pacific, North Atlantic Gyre and Indian Ocean (Fig. s4 and s10).

6.2.c- Simulations with varying food preferences: SFP experiment

Overall changes

The change from standard microzooplankton food preferences (MFP) to SFP causes a global decrease in phytoplankton and microzooplankton biomass as well as growth and grazing rates (primarily by microzooplankton) in CIL (Fig. 1, 2, 6 and s11). These changes are associated to a shift in distribution patterns with higher microzooplankton in the Subantarctic and in the Subarctic Pacific. These shifts are accompanied by an increase in phytoplankton growth south of 30°S and north of 45°N concomitant with an increase in microzooplankton grazing rates in these two areas. A decrease in export is observed globally in the CIL_{SFP} run with the exception of the Equatorial Pacific (Fig. 4 and s12).

Main differences between DIN_{MFP} and DIN_{SFP} are a decrease in phytoplankton and microzooplankton biomass accompanied by a slight increase in phytoplankton growth rates and microzooplankton grazing rates in the Southern Ocean. Export decreases in the Southern Ocean (Fig. s12).

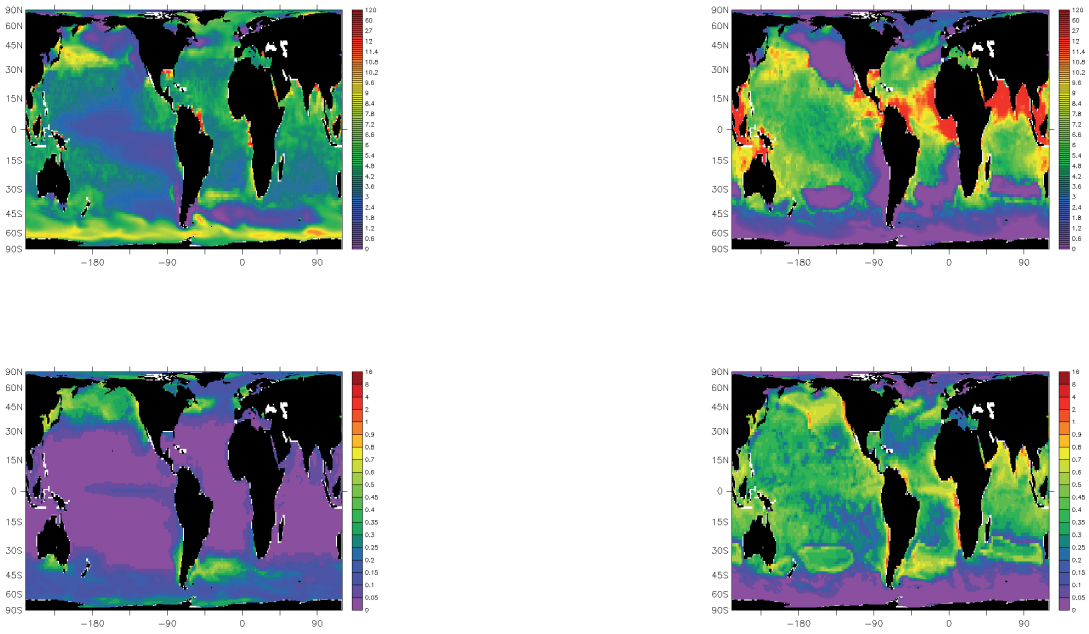

Figure 7: Distribution of microzooplankton (µg C L^{-1}) for the runs of experiment 'SFP' (upper panel) and surface chlorophyll a (µg L^{-1}) (lower panel). In order from left to right: CIL and DIN run

Changes in PFT distribution

The changes in food preferences between CIL_{MFP} and CIL_{SFP} results in a decrease in diatom biomass in the equatorial upwelling areas and an increase in diatom biomass in high latitudes (Fig. s3 and s13). Mixed phytoplankton biomass (excluding diatoms and coccolithophores) decreases between 30°S and 30°N as well as south of 50°S and coccolithophores are found only in the Mediterranean (Fig. s3 and s13). The DIN_{SFP} run results in a global decrease in diatom biomass and an increase in mixed phytoplankton except in polar areas were no mixed phytoplankton is found (Fig. s4 and s14).

Table 3: Primary production and different fluxes in Pg C $year^{-1}$.

		Primary Production	Export	Grazing on phytoplankton		Grazing on all foo
Observations and estimations	Food Preferences			microzooplankton	mesozooplankton	microzooplanktor
		46.5[#]	9.6 - 11.1[+]	25-33[#§]	5.5[$]	
MIC	MFP	50	9.1	24.0	12.8	25.2
	NFP	60	8.1	27.5	17.6	36.3
	SFP	-	-	-	-	-
CIL	MFP	45.6	7.2	27.8	10.3	30.3
	NFP	54.7	5.2	37.2	10.7	46.4
	SFP	27.6	4.7	17.3	5.1	19.7
DIN	MFP	47.8	4.9	25.0	6.2	36.9
	NFP	31.4	5.4	6.9	15.1	19.8
	SFP	52.4	4.6	26.4	7.6	40.3

[#] Behrenfeld & Falkowski (1997)

[§] Calbet and Landry (2004)

[$] Calbet (2001)

[+]Schlitzer (2004), Laws et al (2000)

Table 4: PFTs biomass in µg C L^{-1}.

	Food Preferences	Protozoo-plankton	Mesozoo-plankton	Diatoms	Coccolithophores	Mixed-phytoplankton
Observations		2.8[$]	7.1[§]	1.3[*]	2.4[*]	5.8[*]
		1.6				
	MFP	(1.8)’	1.3	1.3	1.3	8.8
MIC	NFP	1.8	1.7	0.4	0.8	10.3
	SFP	-	-	-	-	-
		1.9				
	MFP	(1.8)’	1.2	1.8	0.4	6.1
CIL	NFP	2.6	1.4	0.4	0.2	7.0
	SFP	1.6	0.7	2.5	0.2	2.6
		1.6				
	MFP	(1.2)’	0.7	0.7	0.1	5.2
DIN	NFP	11.04	1.7	0.0	0.0	4.2
	SFP	1.6	0.8	0.2	0.1	6.2

[$] Buitenhuis et al. (subm.)

[§] Buitenhuis et al. (2006)

[*] Le Quéré et al (2005).

’ Model values have been averaged at location were observation data

7- Discussion

7.1- Sensibility to grazing parameterisation.

The first set of experiments (MIX_{MFP}, CIL_{MFP} and DIN_{MFP}) was designed to test the sensitivity of biogeochemistry to different formulations of the functional response of microzooplankton growth (respiration, GGE) and grazing (g_{max} and half-saturation). Here we first highlight features of the model that provides some insights on the role of microzooplankton in PlankTOM 5 before discussing sensitivity to parameterization. One surprising feature of the different runs is that resulting increases in grazing rates are associated to increases in phytoplankton growth rates and decreases in export. These results indicate that, although grazing mortality of phytoplankton by microzooplankton is higher than by the mesozooplankton (50% against 24% in MIC_{MFP}), it promotes growth of phytoplankton by decreasing export. The increased phytoplankton growth rates tend to be compensated by microzooplankton grazing leading to little changes in primary production and a decrease in phytoplankton biomass in areas were grazing rate is highest (grazing mortality is 70% of the growth). Comparison between results obtained here and sensitivity analyses on the role of mesozooplankton using similar model (Buitenhuis et al., 2006) indicates that grazing by microzooplankton (in contrast to mesozooplankton) leads to higher recycling of organic matter (less export) in the surface ocean promoting higher phytoplankton growth. Because parameterization of mesozooplankton and microzooplankton tend to be similar in the model, theses differences can be attributed to the fact that egested material by microzooplankton enters the small POC pool (POC_s) while egested material by mesozooplankton enter the large POC pool (POC_l) which contribute most to sinking fluxes, added to the low respiration rate of mesozooplankton. The higher basal respiration rates for the dinoflagellates seem to further enhance recycling and phytoplankton growth rates at low and mid-latitudes while maintaining standing stocks similar to those in CIL. Theses conclusions are supported by the fact that areas of high export correspond almost exactly to areas where mesozooplankton is abundant.

In the simulations MIC_{MFP}, CIL_{MFP} and DIN_{MFP} maximum grazing rates but also half saturation constant for microzooplankton grazing gradually decrease while feeding respiration rates increase, remember that the feeding respiration is equivalent to a growth threshold. These changes results in an increase in microzooplankton grazing pressure and phytoplankton growth rates at low and mid-latitudes, even though maximum attainable grazing razes decrease. These results indicate that changes in maximum grazing rates do not significantly affect net biogeochemistry in the model (i.e. turnover rates are increased in the surface ocean but net loses do not change significantly). In contrast, changes in half-saturation constant for

microzooplankton grazing significantly affects spatial distribution of phytoplankton and vertical fluxes. High latitudes, especially in the Southern Ocean, are particularly sensitive to decrease in half-saturation constants for grazing as grazing rates increase markedly only in the DIN_{MFP} run even though microzooplankton biomass tends to decrease. Also, at high latitudes, the promotion of phytoplankton growth through microzooplankton grazing also occurs for the DIN_{MFP} run but not very markedly. Because temperature sensitivity of microzooplankton growth and grazing (Q_{10} between 1.7 and 2.07) is higher than for phytoplankton (Q_{10} = 1.89) one would expect tighter grazing control on phytoplankton by microzooplankton in warmer areas. This is the case for the CIL_{MFP} run but not for DIN_{MFP}. further, differences in half saturation constants are possibly responsible for this trend as microzooplankton in DIN_{MFP} can achieve maximum grazing rates at low biomass while MIC and CIL require higher phytoplankton biomass at low temperatures in order to achieve similar grazing rates to DIN (Figure 7). However, this cannot be the sole explanation since microzooplankton grazing at low latitudes tends to promote phytoplankton growth rates so that changes in phytoplankton abundances with increasing grazing remain small or even increase in the subtropical gyres for DIN_{MFP}. Comparison of PFT distribution in the Southern Ocean indicates that while mixed phytoplankton (excluding coccolithophores and diatoms) are abundant in the Southern Ocean for the MIC_{MFP} and CIL_{MFP} runs, they are completely absent in the DIN_{MFP} run. Hence, a combination of lower half saturation constant for grazing and other limiting factors seem to affect phytoplankton growth and biomass in the Southern Ocean. The most likely candidates are the combination of higher selectivity for non-diatom phytoplankton in MFP together with low light due to deep mixed layer depths that results in a penalty for growth of non diatom phytoplankton (Aumont et al., 2003). This combination results in the decrease of mixed phytoplankton in the Southern Ocean as opposed to low and mid-latitudes. The low half saturation constant in the DIN also leads to a decrease in diatoms in the southernmost part of the Southern Ocean while their range also expands globally as compared to MIC_{MFP} and CIL_{MFP}. Here again a combination of factors might explain this evolution: low half saturation constant lead to an increase in grazing pressure on diatoms, however this is compensated by a reduction in mesozooplankton. This is supported by the fact that areas were diatom biomass increase correspond to the locations where mesozooplankton decreases when comparing MIC_{MFP} and DIN_{MFP}. Also, rechanneling of nutrients from the other phytoplankton functional types favours growth of diatoms in these areas.

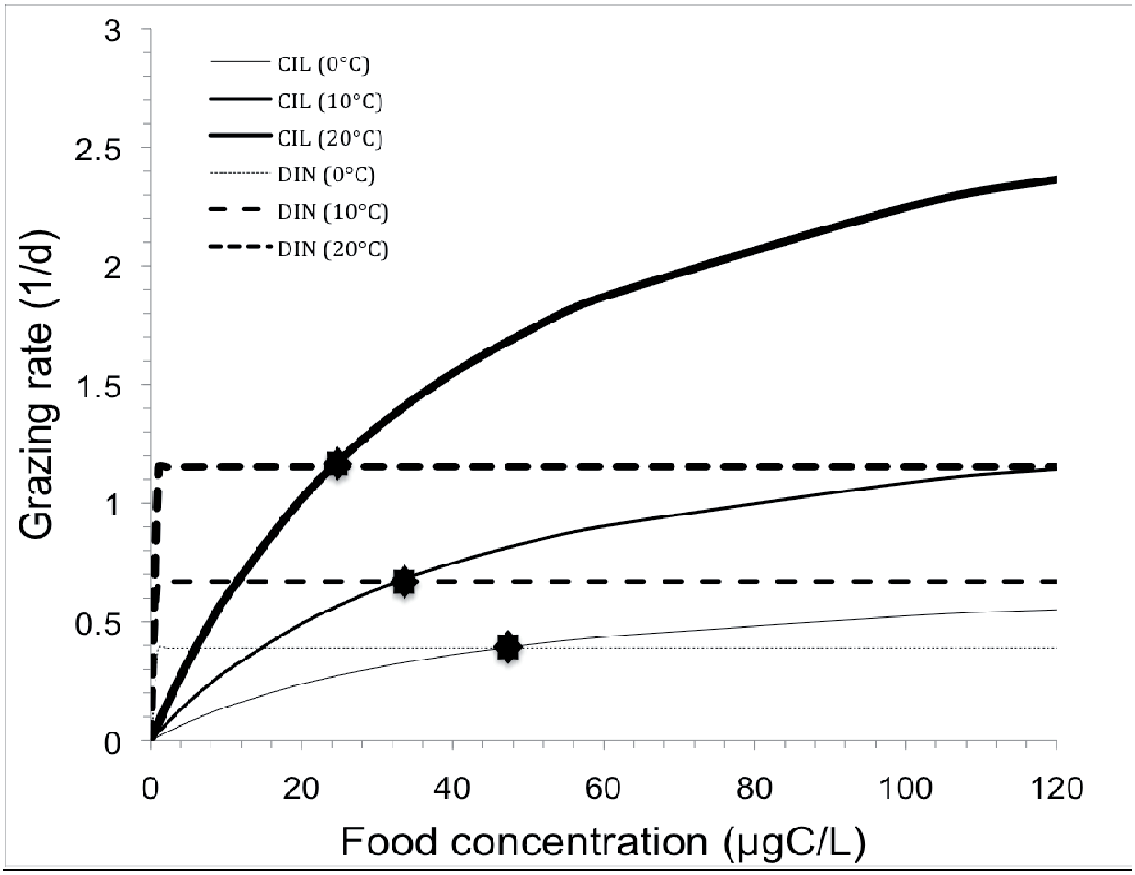

Figure 8: Temperature sensitivity of microzooplankton grazing for CIL and DIN as a function of food concentration. The stars mark the points in the curves where CIL grazing rates are similar to grazing rates for DIN.

7.2- Sensibility to food preferences

Changes in food selectivity between MFP standard runs and NFP (no food preferences) for MIX and CIL correspond primarily, to a relative increase in grazing rates of diatoms and POC_s and a relative decrease in maximum grazing rates of mixed phytoplankton and coccolithophores. Not surprisingly, these changes lead to a decrease in diatoms and a global increase in mixed phytoplankton. These changes are of similar magnitude for MIX and CIL (Table 4). Furthermore, both runs also result in strong reduction in coccolithophores. These results cannot be attributed solely to the direct effect of grazing on coccolithophores. This is in supported by the fact that the shift to SFP in CIL has the opposite effect than the shift to NFP, as expected, but only for diatoms and mixed phytoplankton. Hence, coccolithophore biomass is not directly sensitive to food preferences but rather parameters of the functional response (i.e. maximum grazing rates and half-saturation constant) as well as

competition with other phytoplankton groups for nutrient resources, in particular, distribution of PO_4 (Fig. s15; coccolithohores are advantaged in locations where PO_4 is limiting).

Food preferences changes from MFP to NFP for DIN results in pratically total consumption of phytoplankton biomass in areas were microzooplankton is present while the mixed phytoplankton increases in areas were microzooplankton is absent (also corresponding to the areas were mesozooplankton is abundant). This is the result of stronger grazing pressure on diatoms and coccolithophores (not surprising) but also on mixed phytoplankton. The higher grazing rates result also in strong increases in phytoplankton growth rates but not enough to compensate for grazing losses. The shift to SFP (higher selectivity for diatoms and lower selectivity for POC_s) revert the trend to conditions similar to the MFP configuration albeit with overall lower diatom concentrations and higher mixed phytoplankton concentrations at low and mid-latitudes. These results are at first glance counterintuitive and puzzling. The changes in food preferences should lead to higher maximum grazing rates for diatoms and POC_s in DIN_{NFP} (this is indeed the case as concentrations of both decrease), however diatoms decrease is more marked than in DIN_{SFP}. Furthermore, while little changes or a decrease in grazing on coccolithophores and mixed phytoplankton are expected, grazing rates on these too groups (in particular mixed phytoplankton) are so high as to significantly reduce their biomass even though the increase in microzooplankton concentrations are moderate. Furthermore export fluxes do not change significantly from other experiments. Figure 9 shows the differences in grazing rates on PFTs between NFP and MFP runs as well as SFP and MFP runs, respectively for varying biomass of PFTs and relative composition. As the biomass of diatoms, POCs and coccolithophores decrease the grazing on mixed phytoplankton increases for both DIN_{SFP} and DIN_{NFP}. However, the relative increase is higher for NFP than SFP (Fig. 9). Because of the low half saturation constant for DIN specific grazing rates are similar for all configurations changes, also given the larger sensitivity of diatoms and coccolithophores biomass to the DIN configuration, the NFP run should lead to a decrease in diatoms, POCs and coccolithophores, and as these plankton types are exhausted, to enhanced grazing on mixed phytoplankton until values reach levels below the very low half saturation levels for DIN.

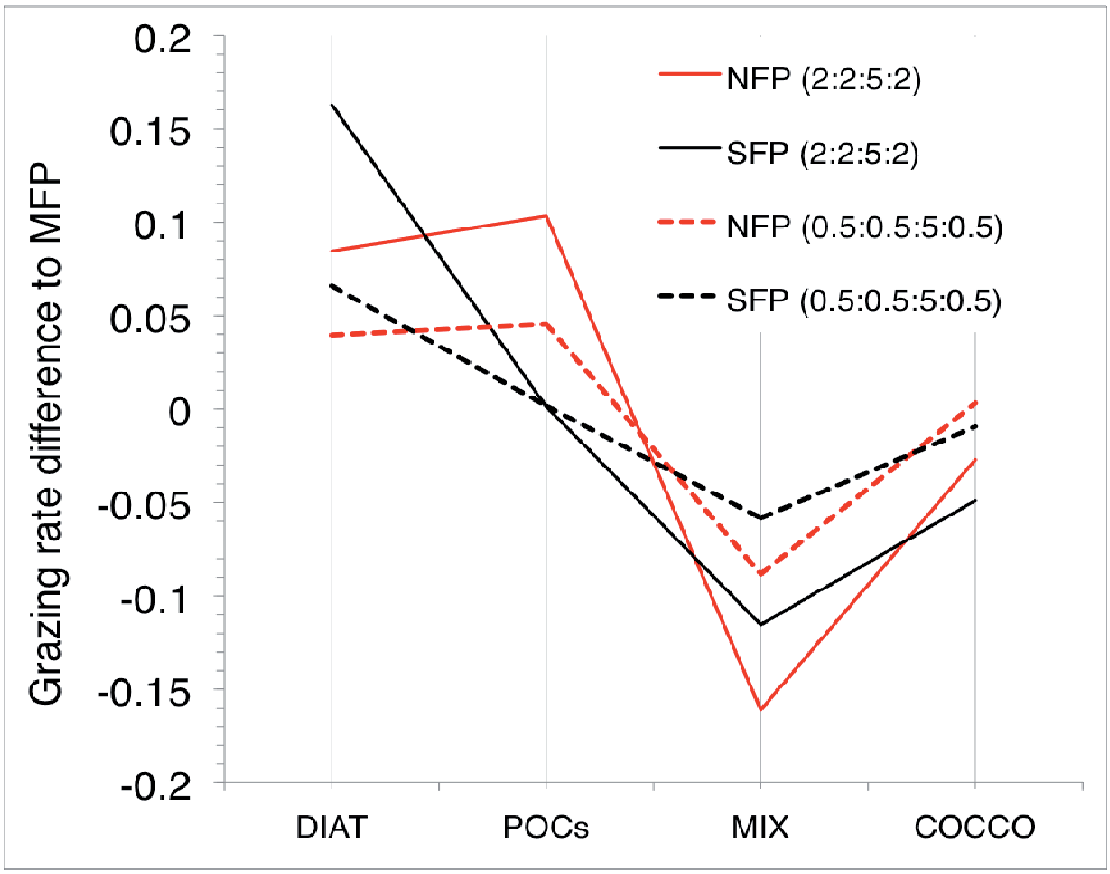

Figure 9: Differences in grazing rates between NFP and MFP and, SFP and MFP, respectively. Differences are shown for each plankton functional type: DIAT (diatoms), POCs (small POC), MIX (mixed phytoplankton excluding diatoms and coccolithophores), COCCO (coccolithophores). Grazing rates have been calculating assuming different phytoplankton biomass given in brackets in the legend and in following order diatoms:POCs:mixed phytoplankton:coccolithophores.

The effect on nutrient distribution of shifting preferences (MFP to NFP) is stronger than the changes in grazing parameterization (MIC, CIL and DIN; Fig. s.15 and s16) for silica. In contrast, other nutrients (phosphate and iron) seem more affected by changes in parameters of the grazing response in MIC, CIL and DIN with higher sensitivity to changes in respiration rate (Fig. s.15, s16 and s17). Increasing grazing pressure leads to higher nutrient content due to both reduced phytoplankton biomass as well as an increase in nutrient remineralisation.

7.3- Other features

Another surprising feature of model results is the fact that mesozooplankton and microzooplankton tend to exclude each other. This could be explained by the fact that mesozooplankton is assumed to graze preferentially on microzooplankton, however, it does not explain why mesozooplankton is scarcely found in other areas where microzooplankton thrives in the model. The model results rather suggest that in most areas, microzooplankton outcompete mesozooplankton because they have higher grazing rates or lower half saturation constant. Finally, the constant mortality rate for mesozooplankton possibly accentuates the trend (i.e. in contrast grazing by mesozooplankton on the microzooplankton is density dependent). These results indicate that the simple biology and trophic relationships in the model cannot fully represent planktonic interactions at higher trophic levels. Also, competitive exclusion tends to be strongest in the DIN_{MFP} as compared to CIL_{MFP} and MIC_{MFP} indicating higher sensitivity to lowering grazing half-saturation constants for grazing in the microzooplankton. Model results show similar sensitivity to shifts in food preferences as to decrease in half-saturation constants for microzooplankton grazing. Shifts in food preferences have similar effects than decrease in half saturation constants for microzooplankton grazing. In particular changes from MFP to NFP lead to an increase in mesozooplankton biomass with highest values for DIN followed by MIC and finally CIL. Changes in food preferences from MFP to SFP, on the other hand leads to a decrease in mesozooplankton biomass for CIL but hardly any change for DIN. These results are partly counter-intuitive as shifts from MFP to NFP increases significantly selectivity for small POC and diatoms while decreasing selectivity for coccolithophores and other phytoplankton. The results suggest that availability of phytoplankton other than diatoms and coccolithophores (due to their high abundances in low and mid-latitudes) determines changes in distribution of mesozooplankton, even though mesozooplankton has a preference for diatoms and tends to "survive" in areas were diatom production should be high (Subarctic Pacific, Subantarctic, North Atlantic and equatorial upwelling regions). This is confirmed by the fact that changes in food preferences between MFP and SFP does hardly affect mesozooplankton for the DIN run (with much higher selectivity for diatoms) while mesozooplankton biomass decreases significantly in CIL_{SFP} even though selectivity for diatoms and coccolithophores decrease in this model configuration.

The last feature is that total phytoplankton biomass is constituted up to more than 50% by mixed-phytoplankton (observation value in Table 3). As a consequence mixed-phytoplankton is the phytoplankton PFT that will regulate the primary production. Competition for nutrient and light with diatom and coccolithophores determines its

distribution, but the recycling of export of said nutrient due to microzooplankton grazing and respiration also play a role. The best example for that is what happened in the DIN_{MFP} run. Dinoflagellate grazing in the DIN_{MFP} run resulted in the lower mixed-phytoplankton biomass for all the MFP run, this was due to less nutrient recycling at latitudes higher than 45° leading to a decreases of surface chlorophylle in the Southern Ocean. The high grazing pressures below 45° latitude leads to an absence of export and renewed primary production.

8- Conclusion

The primary differences between ciliates and dinoflagellates lie in their different metabolic levels, grazing and growth rates. Ciliates have a lower metabolism than dinoflagellates, higher grazing rates, and by extension, higher growth rates. Ciliates have a different functional response to prey concentration being prone to starvation at low prey concentration while conversely attaining better rates at high prey concentration. Temperature dependences of these two organisms are also different. Transforming the microzooplankton into a ciliate or a dinoflagellate only group indicates how they have different impacts on model ecosystem, and occupy different niches. In reality, dinoflagellates and ciliates are not purely and simply separated, they are found in the same places, share some prey, and can feed on each other. Thus, the experiment with mixed microzooplankton is not the same as having the two groups present separately.

The combined decrease in parameters of the feeding response of microzooplankton as a function of food concentration (maximum grazing rates and feeding half saturation constant) leads to an increase in grazing pressure but also phytoplankton growth rates. This indicates that grazing pressure is more sensitive to changes in half saturation constant than changes in maximum grazing rates of the microzooplankton. Furthermore, increasing microzooplankton grazing pressure leads to an increase in nutrient recycling (partly through respiration) and phytoplankton growth rates in the surface ocean. Resulting net changes in phytoplankton biomass are, however, primarily sensitive to changes in half-saturation constant for grazing. Phytoplankton distribution in high latitude areas tend to be also more sensitive than other regions to changes in half saturation constant for grazing due to limitation of phytoplankton growth by light caused by deep mixing. Distributions of diatoms and mixed phytoplankton (excluding diatoms and coccolithophores) are equally sensitive to changes in grazing half saturation constant and food preferences and less so to changes in maximum grazing rates, while distribution of coccolithophores is primarily sensitive to both changes in half saturation

and maximum grazing parameters as a result of competition for resources with other phytoplankton.

Competitive exclusion between micro- and mesozooplankton in model indicates the presence of biological controls not properly represented in the model. This observation also puts into questions the necessity of having several zooplankton compartments in this and similar type of ecosystem models. In this model configuration, zooplankton faecal pellets seem the main contributors to vertical fluxes out of the mixed layer, indicating that the effect of aggregation might be largely underestimated in the model.

Another significant result is the tendency of dinoflagellates to be present in warmer water, contrary to the ciliates. Which of these two organisms would then dominate a warming ocean and what would the consequences be on the rest of the ecosystem and the biogeochemical cycles? With the current version of the model this question cannot be answered. Refinements, such as splitting the microzooplankton into a ciliate only and a dinoflagellate only PFT, will help improve our understanding of the ecosystem and prediction of the consequences of global warming. These experiments also highlight that with three phytoplankton PFTs most of the primary production ends up being the result of only one group: the mixed-phytoplankton. Thus more detail in phytoplankton representation is needed.

9- References

Aumont O, Maier-Reimer E, Blain S, Monfray P (2003) An ecosystem model of the global ocean including Fe, Si, P co-limitations. *GBC* 17 (2) 29, 15p. 2001GB001745

Anderson (2005) Plankton functional type modelling: running before we can walk? Journal of Plankton Research 27 (11) 1073-1081

Buitenhuis E T, P van der Wal, H J W de Baar (2001) Blooms of *Emiliania huxleyi* are sinks of atmospheric carbon dioxide; a field and mesocosm study derived simulation. *Glob. Biogeochem. Cycl.* 15 (3) 577-587

Buitenhuis, E. T., C. Le Quéré, O. Aumont, G. Beaugrand, A. Bunker, A. Hirst, T. Ikeda, T. O'Brien, S. Piontkovski, D. Straile (2006) Biogeochemical fluxes through mesozooplankton. *Global Biogeochemical Cycles* 20, GB2003, doi: 10.1029/2005GB002511

Buitenhuis ET, Rivkin R, Sailley S, Le Quéré C, (subm.) Global biogeochemical fluxes through microzooplankton. *Global Biogeochemical Cycles*

Behrenfeld M J and Falkowski PG (1997), Photosynthetic rates derived from satellite-based chlorophyll concentration, *Limnol. Oceanogr.,* 42(1), 1-20.

Calbet, A. (2001), Mesozooplankton grazing effect on primary production: A global comparative analysis in marine ecosystems, *Limnol. Oceanogr*., *46*, 1824-1830.

Calbet, A., and M. R. Landry (2004), Phytoplankton growth, microzooplankton grazing, and carbon cycling in marine systems, *Limnol. Oceanogr., 49*, 51-57.

Cox P M et al., Acceleration of global warming due to carbon-cycle feedbacks in a coupled climate model, *Nature*, 408, 184– 187, 2000.

Da Cunha LC, Le Quéré C, Buitenhuis ET, Giraud X, Ludwig W (2007) Potential impact of changes in river nutrient supply on global ocean biogeochemistry. *Global Biogeochem. Cycles* GB4007, doi:10.1029/2006GB002718

Doney SC, Major challenges confronting marine biogeochemical modelling, *Global Biogeochem. Cycles*, 13, 705– 714, 1999.

Falkowski P, et al., The global carbon cycle: A test of our knowledge of earth as a system, *Science*, 290, 291– 296, 2000.

Gaspar P, Gregoris Y, Lefèvre JM (1990) A simple eddy kinetic energy model for simulations of the oceanic vertical mixing: Tests at station Papa and Long-Term Upper Ocean Study site. *J. Geophys. Res., 95* (16), 179-193.

Gent PR and JC McWilliams (1990), Isopycnal mixing in the ocean circulation models, *J. Phys.Oceanogr.*, 20, 150-155.

Hansen B, Bjoernsen PK, Hansen PJ (1994) The size ratio between planktonic predators and their prey. *Limnol. Oceanogr.* 39(2):395-403

Heinbockel, JF (1978) Studies on the functional role of tintinnids in the southern California bight. I. Grazing and growth rates in laboratory cultures. *Marine Biology,* 47:177-189

Jacobson, DM (1999) A brief history of dinoflagellates feeding research. *J. Eukaryot. Microbiol.*, 46(4): 376-381

Jonsson R (1986) Particle size selection, feeding rates and growth dynamics of marine planktonic oligotrichous ciliates (Ciliophoa: Oligotrichina) *Mar. Ecol. Prog. Ser.,* 33:265-277

Joos F, et al., Global warming and marine carbon cycle feedbacks on future atmospheric CO2, *Science*, 284, 464– 467, 1999.

Kalnay, E., M. Kanamitsu, R. Kistler, W. Collins, D. Deaven, L. Gandin, M. Iredell, S. Saha, G. White, J. Woollen, Y. Zhu, M. Chelliah, W. Ebisuzaki, W. Higgins, J. Janowiak, K. C. Mo, C. Ropelewski, J. Wang, A. Leetmaa, R. Reynolds, R. Jenne, and D. Joseph (1996), The NCEP/NCAR 40-year reanalysis project, *Bull. Am. Meteorol. Soc., 77*(3), 437-471.

Kleypas JA, et al., Geochemical consequences of increased atmospheric carbon dioxide on coral reefs, *Science*, 284, 118–120, 1999.

Laws, E. A., P. G. Falkowski, W. O. Smith Jr., H. Ducklow, and J. J. McCarthy (2000), Temperature effects on export production in the open ocean, *Global Biogeochem. Cycles, 14*, 1231-1246.

Le Quéré, C, Harrison SP, Prentice IC, Buitenhuis ET, Aumont O, Bopp L, Claustre H, Cotrim da Cunha L, Geider R, Giraud X, Klaas C, Kohfeld KE, Legendre L, Manizza M, Platt T, Rivkin RB, Sathyendranath S, Uitz J, Watson AJ, Wolf-Gladrow D (2005) Ecosystem dynamics based on plankton functional types for global ocean biogeochemistry models. *Global Change Biol.,* 11, 1-25.

Madec G (2008) NEMO ocean engine, Institut Pierre-Simon Laplace (IPSL), France, No 27 ISSN No 1288-1619 http://www.nemoocean.eu/index.php/content /download/2702/18843/file/NEMO_book.pdf

Maier-Reimer, E (1993) Geochemical cycles in an ocean general circulation model. Preindustrial tracer distributions. *Global Biogeochem. Cycles*, 7:645-677

Manizza M, Le Quéré C, Buitenhuis ET. Sensitivity of global ocean biogeochemical dynamics to ecosystem structure in a future climate. *Geophysical Research Letters* submitted doi:10.1029/2008GL036694

Najjar R, Sarmiento JL and Toggweiler JR (1992) Downward transport and fate of organic matter in the ocean: Simulations with a general circulation model, *Global Biogeochem. Cycles,* 6: 45-76

Roullet G, and Madec G (2000), Salt conservation, free surface, and varying levels: a new formulation for ocean general circulation models, *J. Geophys. Res.,* 105(C10), 23927-23942.

Sailley S, Klaas C, Wolf-Gladrow D, (in prep. a) Pelagic ciliate feeding behaviour and growth rate. An analysis based on laboratory experiments

Sailley S, Klaas C, Wolf-Gladrow D,(in prep. b) Heterotrophic dinoflagellate feeding behaviour and growth rate. An analysis based on laboratory experiments

Sarmiento JL, Hughes TMC, Stouffer RJ, and Manabe S, Simulated response of the ocean carbon cycle to anthropogenic climate warming, *Nature*, 393, 245–249, 1998.

Schlitzer, R. (2004), Export production in the equatorial and North Pacific derived from dissolved oxygen, nutrient and carbon data, *J. Oceanogr.,* 60**,** 53-62.

Siegenthaler U, and Sarmiento JL, Atmospheric carbon dioxide and the ocean, *Nature*, 365, 119– 125, 1993.

Strom, SL, Morello, TA (1998) Comparative growth rates and yields of ciliates and heterotrophic dinoflagellates. *Journal of Plankton Research,* 20(3):571-584

Timmermann R, Goosse H, Madec G, Fichefet T, Ethe C, and Dulière V (2005), On the representation of high latitude processes in the ORCA-LIM global coupled sea ice-ocean model, *Ocean Modelling, 8*, 175-201.

Uitz, J., H. Claustre, A. Morel, and S. B. Hooker (2006), Vertical distribution of phytoplankton communities in open ocean: an assessment based on surface chlorophyll, *J. Geophys. Res., 111*, C08005, 2005JC003207.

Verity, P. G. (1985), Grazing, respiration, excretion and growth rates of tintinnids, *Limnol. Oceanogr., 30*, 1268-1282.

Woodwell GM, et al., Biotic feedbacks in the warming of the earth, *Climatic Change*, 40, 495– 518, 1998.

Yang EJ, Choi JK, Hyun J (2008) Seasonal variation in the community and size structure of nano- and microzooplankton in Gyeonggi Bay, Yellow Sea. *Estuarine, Coastal and Shelf Science* 77: 320-330.

Zhang, Jinlun and Rothrock DA (2003) Modelling global sea ice with a thickness and enthalpy distribution model in generalized curvilinear coordinates, *Mon. Wea. Rev*. 131(5), 681-697.

10- Supplementary Figures

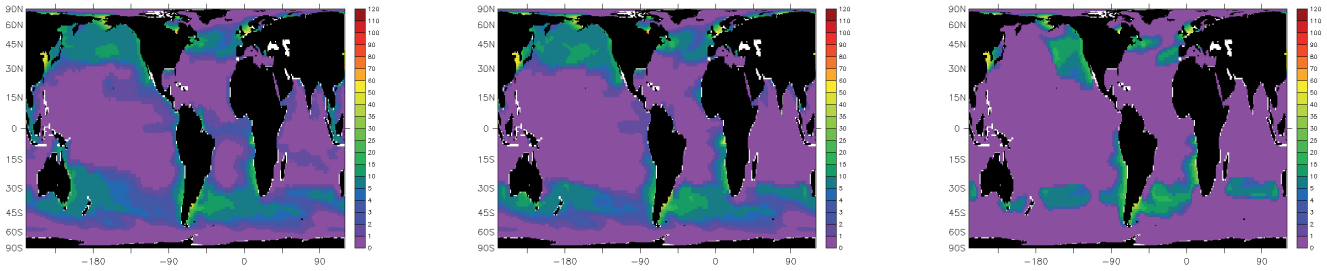

Figure s1: Annual mean of mesozooplankton surface concentration in µg C L^{-1} for the MFP runs, from left to right: MIC, CIL and DIN.

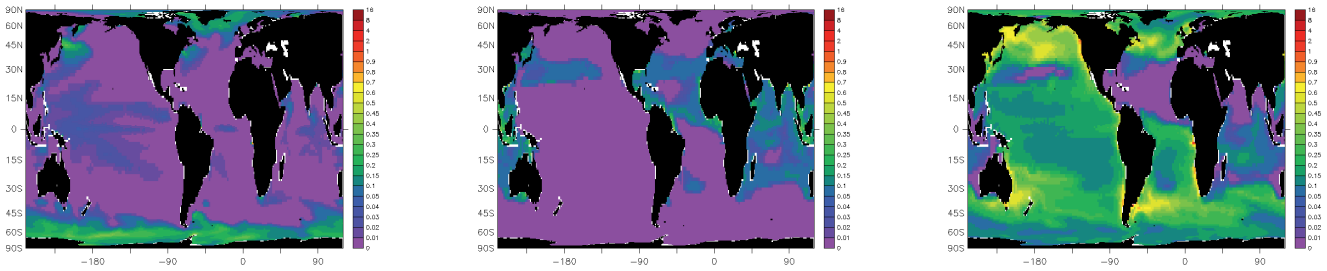

Figure s2: Annual mean of phytoplankton's PFT surface concentration in chlorophyll a (µg L^{-1}) for the MIC_{MFP} runs, from left to right: DIA, COC and MIX.

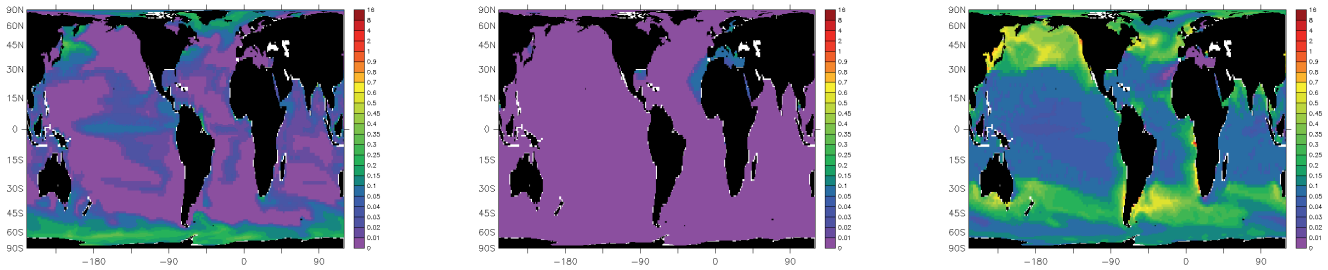

Figure s3: Annual mean of phytoplankton's PFT surface concentration in chlorophyll a (µg L^{-1}) for the CIL_{MFP} runs, from left to right: DIA, COC and MIX.

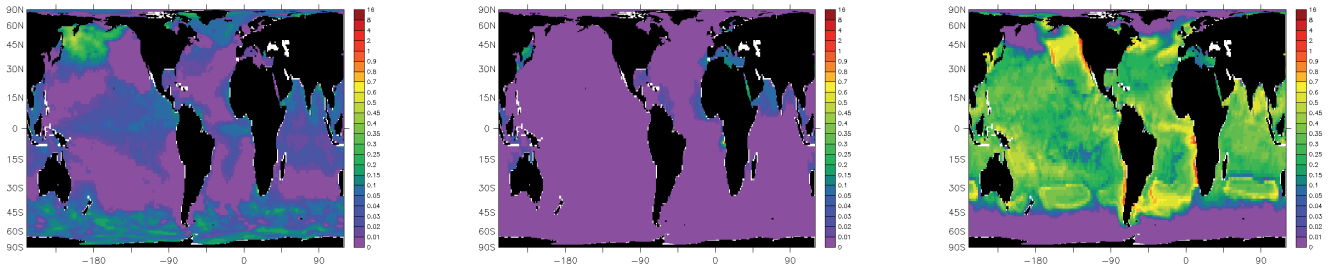

Figure s4: Annual mean of phytoplankton's PFT surface concentration in chlorophyll a (µg L^{-1}) for the DIN_{MFP} runs, from left to right: DIA, COC and MIX.

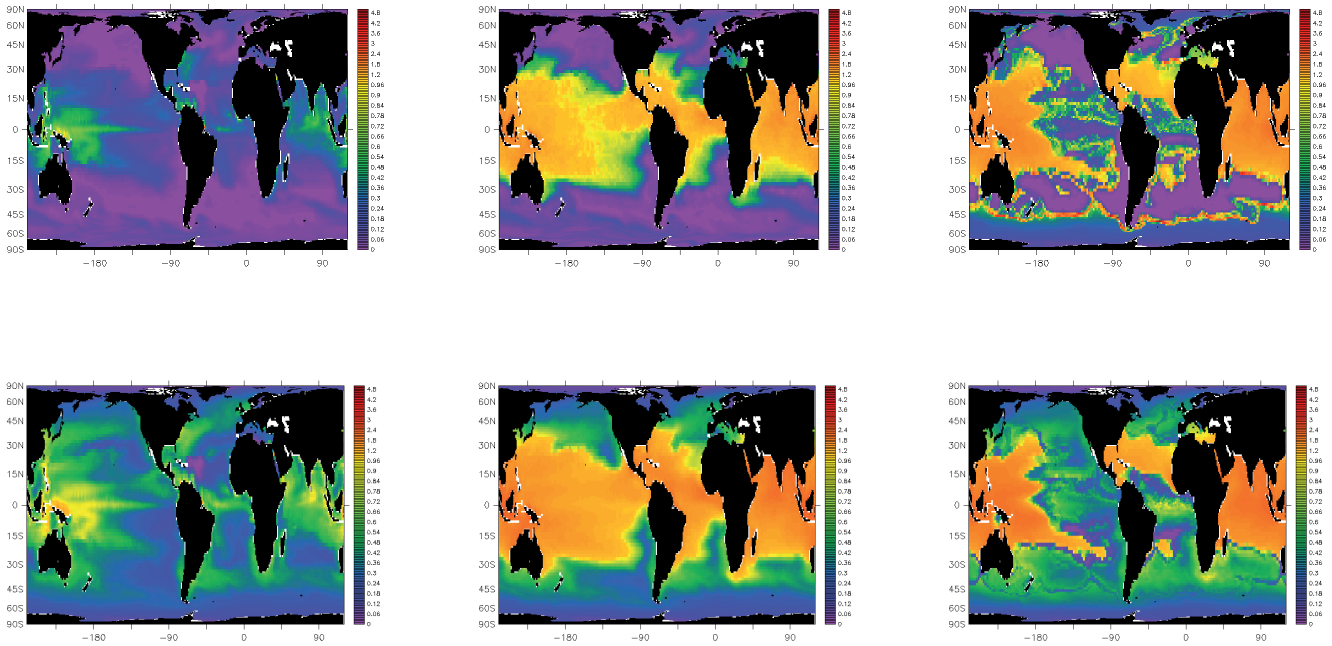

Figure s5: Phytoplankton mortality caused by microzooplankton grazing (upper panel) and phytoplankton growth (lower panel) in day^{-1}, NFP model output. From left to right: MIC, CIL and DIN run. Note the different maximum on the scale for the DIN run.

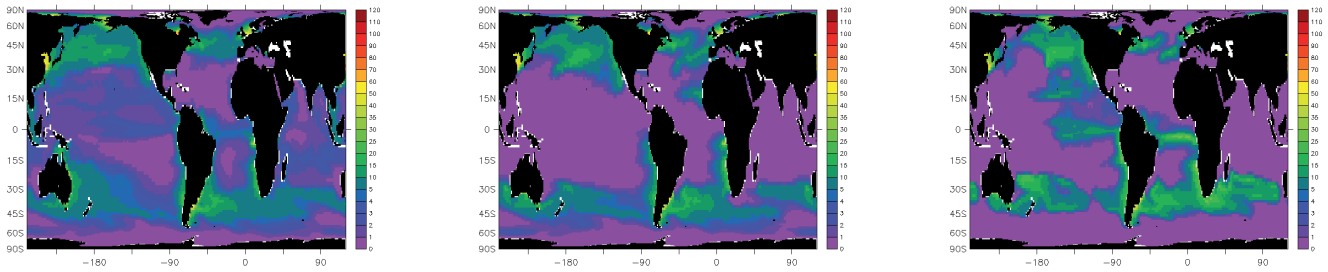

Figure s6: Annual mean of mesozooplankton surface concentration in µg C L^{-1} for the NFP runs, from left to right: MIC, CIL and DIN.

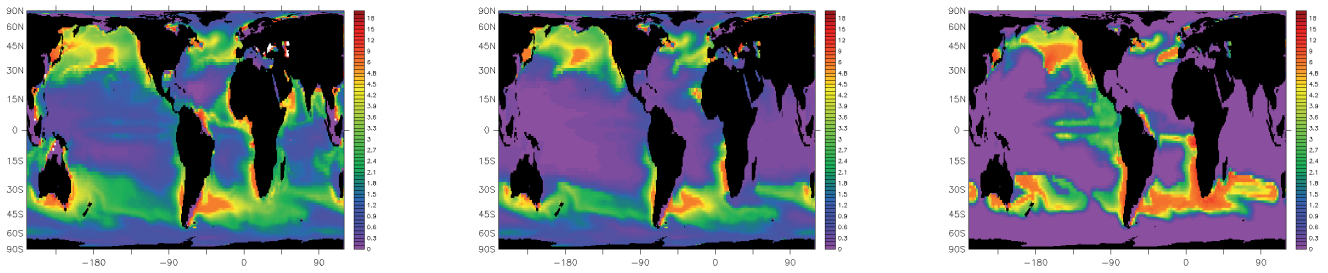

Figure s7: Export in mol m^{-2} $year^{-1}$, NFP model output. From left to right, and top to bottom: MIC, CIL and DIN run.

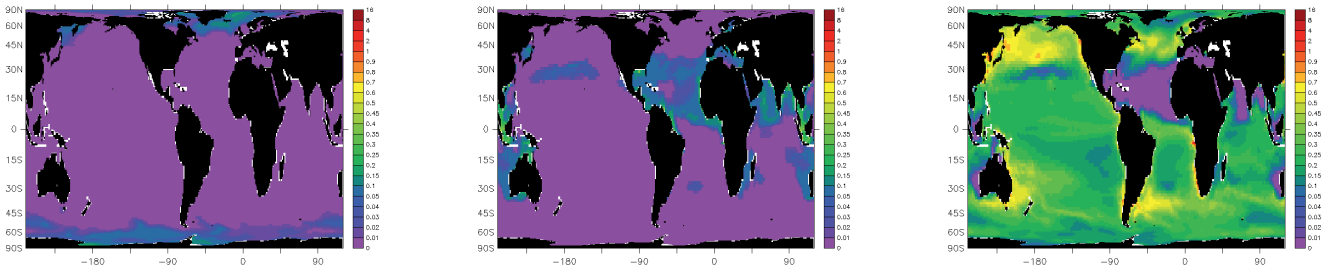

Figure s8: Annual mean of phytoplankton's PFT surface concentration in chlorophyll a (µg L^{-1}) for the MIC_{NFP} runs, from left to right: DIA, COC and MIX.

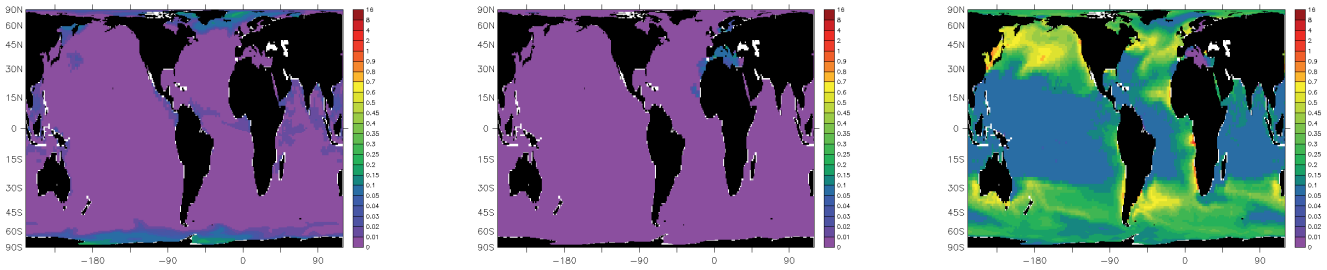

Figure s9: Annual mean of phytoplankton's PFT surface concentration in chlorophyll a (µg L^{-1}) for the CIL_{NFP} runs, from left to right: DIA, COC and MIX.

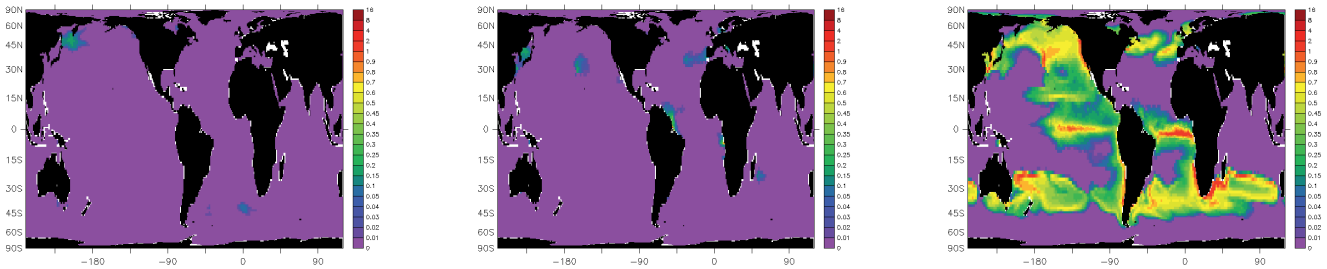

Figure s10: Annual mean of phytoplankton's PFT surface concentration in chlorophyll a (μg L^{-1}) for the DIN_{NFP} runs, from left to right: DIA, COC and MIX.

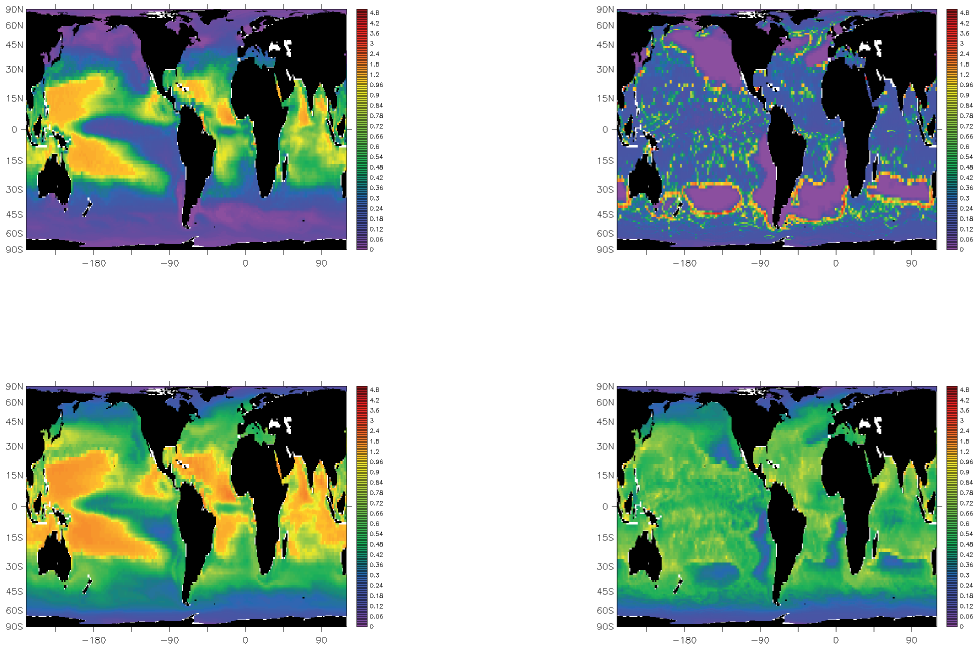

Figure s11: Phytoplankton mortality caused by microzooplankton grazing (upper panel) and phytoplankton growth (lower panel) in day^{-1}, SFP model output. CIL run (left panel) and DIN run (right panel).

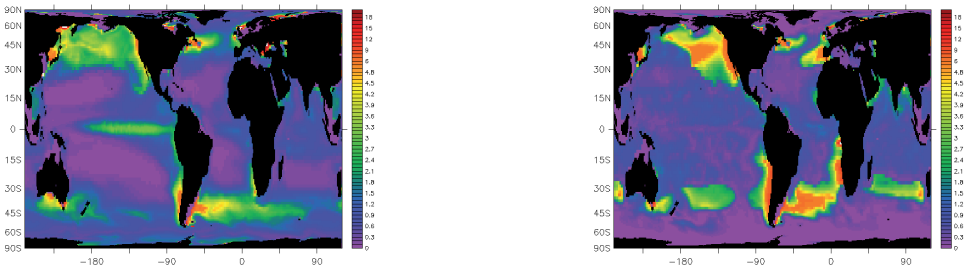

Figure s12: Export in mol m^{-2} $year^{-1}$, SFP model output. CIL run (left panel) and DIN run (right panel).

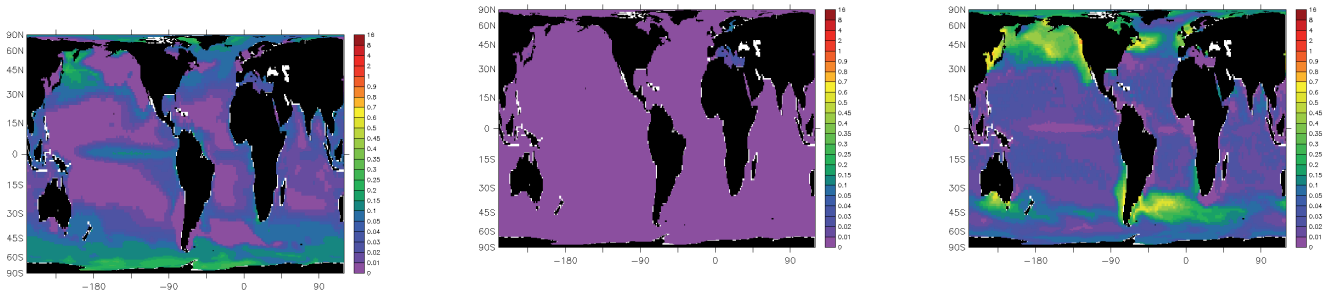

Figure s13: Annual mean of phytoplankton's PFT surface concentration in chlorophyll a (µg L^{-1}) for the CIL_{SFP} runs, from left to right: DIA, COC and MIX.

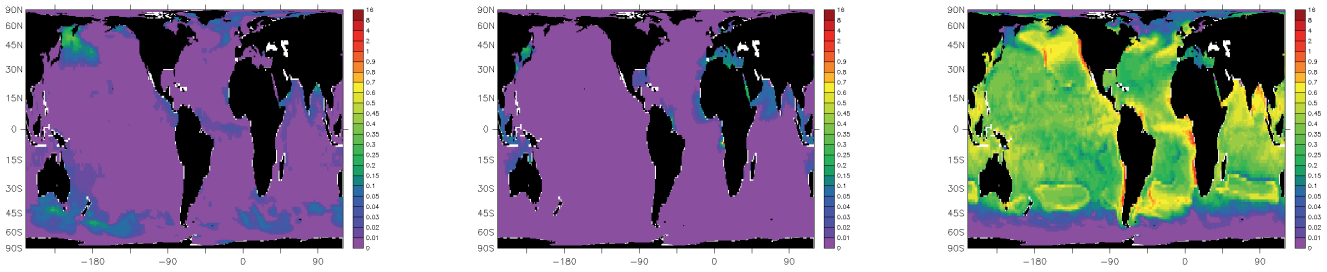

Figure s14: Annual mean of phytoplankton's PFT surface concentration in chlorophyll a (µg L^{-1}) for the DIN_{SFP} runs, from left to right: DIA, COC and MIX.

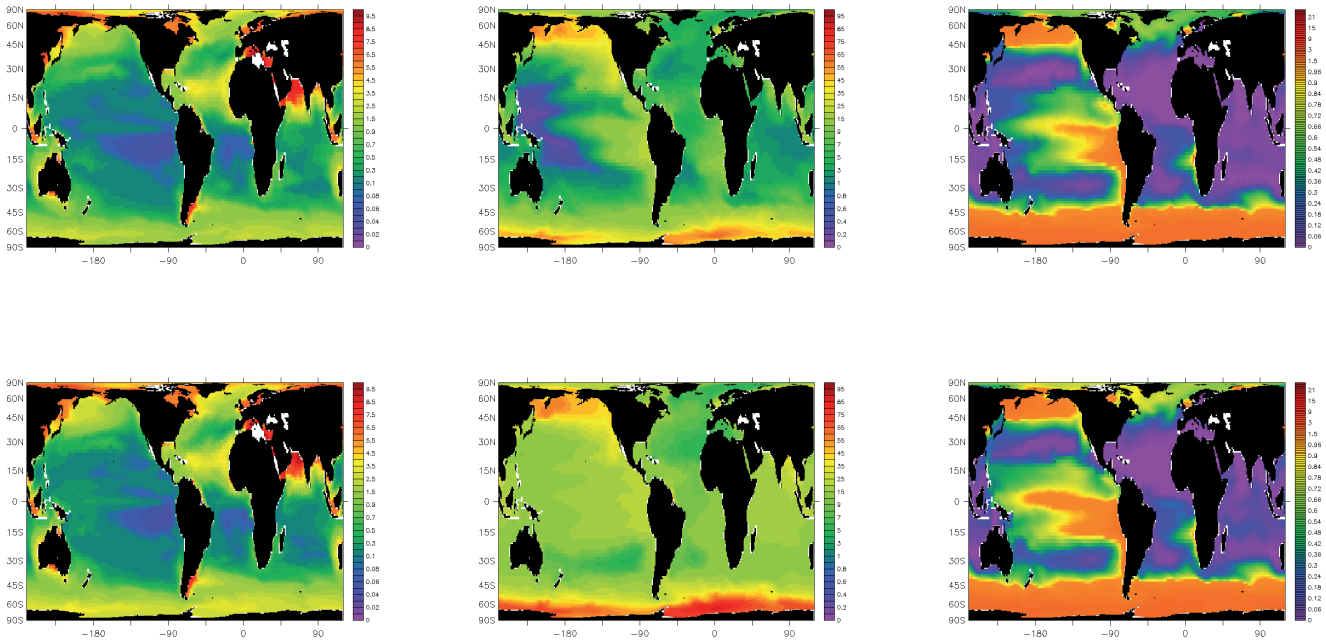

Figure s15: Surface concentration of (from left to right) iron, silica and PO_4 for the MIC run. Upper panel: MFP, lower panel: NFP.

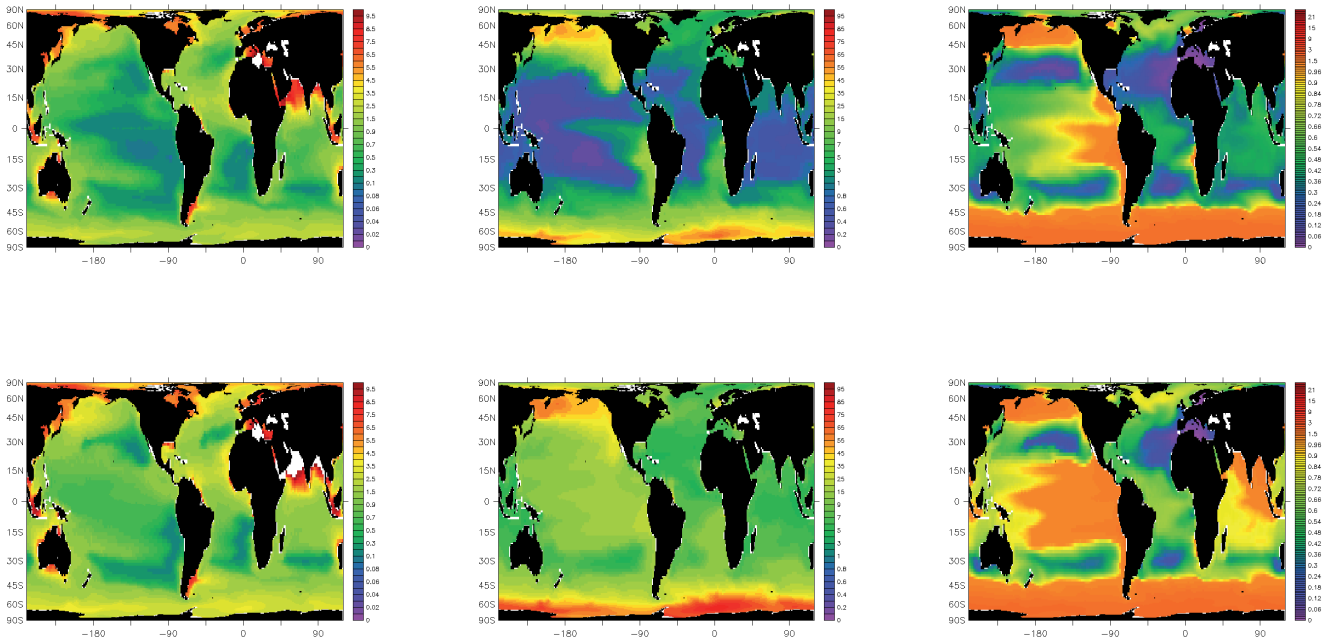

Figure s16: Surface concentration of (from left to right) iron, silica and PO_4 for the CIL run. Upper panel: MFP, lower panel: NFP.

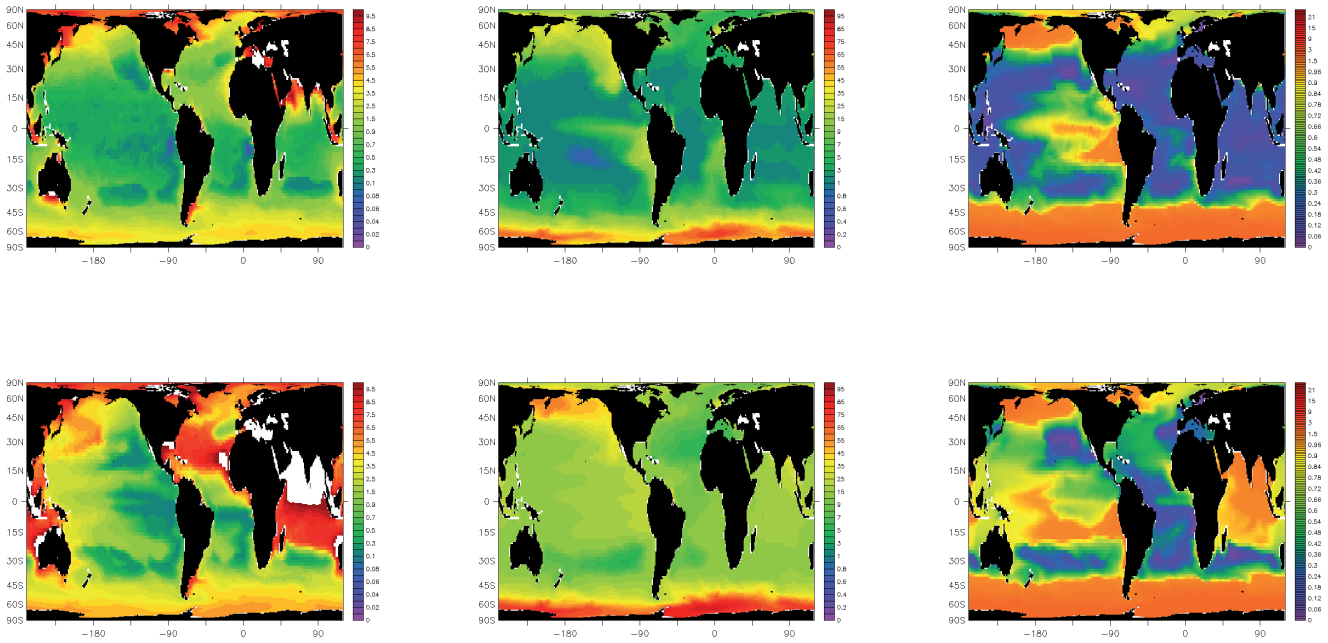

Figure s17: Surface concentration of (from left to right) iron, silica and PO_4 for the DIN run. Upper panel: MFP, lower panel: NFP.

Chapter 5:

General Conclusion and Outlook

1- Conclusions

Rather than discussing and reiterating the conclusions from every chapter, some important points regarding not only this work but also future work will be discussed.

1.1- Main steps.

Finding and collecting the data was done with new interactive search tools (e.g. Google Scholar and Web of Science/ISI Web of Knowledge). Selection criteria were for laboratory experiments with one prey and one predator. The collected data were not homogeneous in measures (cell number, volume or carbon). Choosing a single measure to make the data comparable was the first step needed after collecting the data. Measures and units had to be converted accordingly. Volume and estimated diameter of a cell are the most often used measures to describe and explore prey-predator relationship. However, we decided to use the cellular carbon content. The carbon content is related to the size of the organisms and to the taxonomy of the organism. This is an important point in that two phytoplankton cells of the same diameter but of different group (e.g. a small diatom and a *Phaeocystis* cell) will have different carbon content. Thus prey selection based on food quality and not on prey size will be more noticeable by using the cellular carbon content as unit for the functional response of ciliates and dinoflagellates, size relationships are still visible.

To analyze the data, a suitable mathematical relationship describing the functional response was needed. The Michaelis-Menten is an obvious choice for describing the functional response with small rates at low prey concentration and saturation at high concentrations. However, after looking at several of the collected datasets it appeared that the Michaelis-Menten function could not describe all sets, especially for the growth response. A

threshold concentration was observed in more than two third of the growth datasets for both ciliates and dinoflagellates; a grazing threshold was also observed in about half of the ciliates datasets, and more than half of the dinoflagellates datasets. Thus the question was: which equation should be used to best describe each and every dataset? The equation had to obey two conditions, (i) the quality of the fit to the data and (ii) the parameters had to give significant information on the functional response mechanism. Using the Bayesian method (described in detail in Annex A) we tested the goodness-of-fit of different equations (Michaelis-Menten, Ivlev, and Rectilinear). It appeared that the goodness-of-fit of these equations was equal, the choice was then down to the second points. Thus the Michaelis-Menten equation with threshold was choosen. It is a well studied equation (Fenchel 1980; Kiørboe 2008) and broadly used by other authors. A parameter was added to the classic Michaelis-Menten to account for the threshold. Adding another parameter to account for decrease in grazing or growth for very large prey concentration, *i.e.* beyond the saturation plateau was considered for a while, however, finally abandoned because only 3 out of 500 datasets showed this feature.

1.2- Relationship between grazing and growth

Throughout this thesis, the functional response of grazing and growth to prey concentration was represented by using a Michaelis-Menten equation with threshold (Eq. 1)

$$r = r_{\max} \times \left(\frac{P - P_t}{K_m + (P - P_t)} \right) \qquad (1)$$

'r' is the rate (grazing or growth) at a given prey concentration 'P', 'r_{max}' the maximal rate, 'K_m' the half-saturation concentration and 'P_t' is the threshold concentration; K, P and P_t are in pg C mL^{-1}. Grazing and growth follow the same function with different value for K and P_t. The maximal grazing rate is the inverse of the handling time, *i.e.* the time needed to ingest and digest the prey. Grazing half-saturation is related to the encounter rate and capture efficiency (Kiørboe 2008). The grazing threshold can be related to the capacity of the organism to detect his prey. For growth the half-saturation and threshold concentration are related to the assimilation rate of the prey and the basal metabolism.

In field studies the measurement of both grazing and growth rates at the same site is beyond the working capacity of the investigator (Vézina and Platt 1988). It has been

suggested that growth rates can be estimated from grazing rates by applying a multiplication factor called gross growth efficiency (GGE):

$$GGE = \frac{growth \quad rate}{grazing \quad rate} \tag{2}$$

This approach implies that the GGE of a single organism is constant through the functional response. A constant GGE implies that both the half-saturation and the threshold concentration must have equal values for both grazing and growth. Our data analysis shows that the grazing half-saturation is higher than for the growth, and the grazing threshold concentration is lower than for growth. It means that with increasing prey concentration the grazing will occur earlier, but will reach the saturation point later than growth. Consequently, GGE will decrease, increase and then decrease again before stabilising, once both processes have reached their saturation concentrations (Fig. 1). The amplitude of variation of GGE is probably be dependent on the organism itself, food type and water temperature. In the case of *T. acuminate* (Fig. 1, based on data from Verity) GGE varies between 15 and 50%. When using a "rule" value of 30% the actual values might be half or double as much.

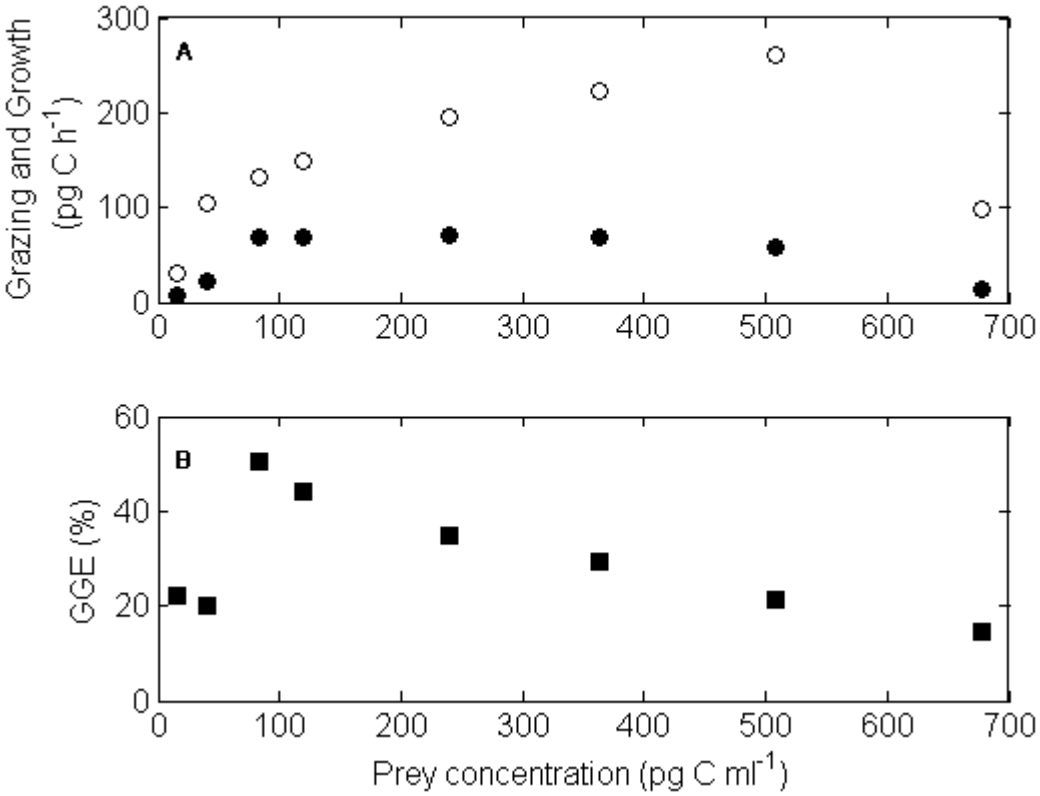

Figure 1: Variation of grazing and growth rates with prey concentration (A), in parallel to change in GGE (B). Data from Verity (1985) *Tintinnopsis acuminate* feeding on *Isochrysis galbana* at 25°C. Graphic from chapter 1 (Fig. 17, page 37)

1.3- Feeding behaviours

Due to their anatomy and feeding modes, ciliates and dinoflagellates naturally target prey of different sizes. Yet in ecosystem representation and modelling, they are often lumped together under the name of "microzooplankton" and their major role in the pelagic food-web is simply to be a link between the microbial loop and the rest of the food-web. As such they are considered as feeding primarily on nanozoo- and nanophytoplankton. Yet as was demonstrated through this study, they are not limited to this size class for food. Furthermore, ciliates and dinoflagellates have different optimal size classes of food. According to the data collected, ciliates are more specialised and preferentially feed on prey around half of their own diameter, with a range of 10 to 90% of their own diameter respectively. In contrast, dinoflagellates have a broad prey size spectrum ranging from a diameter 10% their own size, to prey with a diameter approximately 1.5 times larger and with no definite optimal size ratio. Within these size classes there can be an additional preference for a particular prey type, which is not based on the size, but on nutritional value and PFT. This preference was

highlighted using maximal rate, half-saturation concentration and threshold concentration for both the grazing and the growth. It appeared that ciliates choose the organisms they prey on based mostly on size, with no preference for one type of organism over another. Conversely, dinoflagellates have a marked preference for diatoms over other prey from the same size class (e.g. autotrophic dinoflagellates) ingesting them with higher rates, a lower half-saturation concentration and an absence of threshold.

As a result the role of microzooplankton in the pelagic ecosystem cannot be relegated as being a link between the microbial loop and the rest of the food-web. Ciliates and dinoflagellates prey on nanoplankton but not to the extent they prey on prey of larger sizes. As a result, the ecosystem representation (Introduction, Fig. 3, page 8) should be modified to include a microzooplankton box in the food-chain based on a diatom dominated phytoplankton. Microzooplankton would prey on phytoplankton and be preyed upon by copepods adding an additional step in energy transfer. Of course, copepods will still be able to prey directly on phytoplankton (Fig. 2).

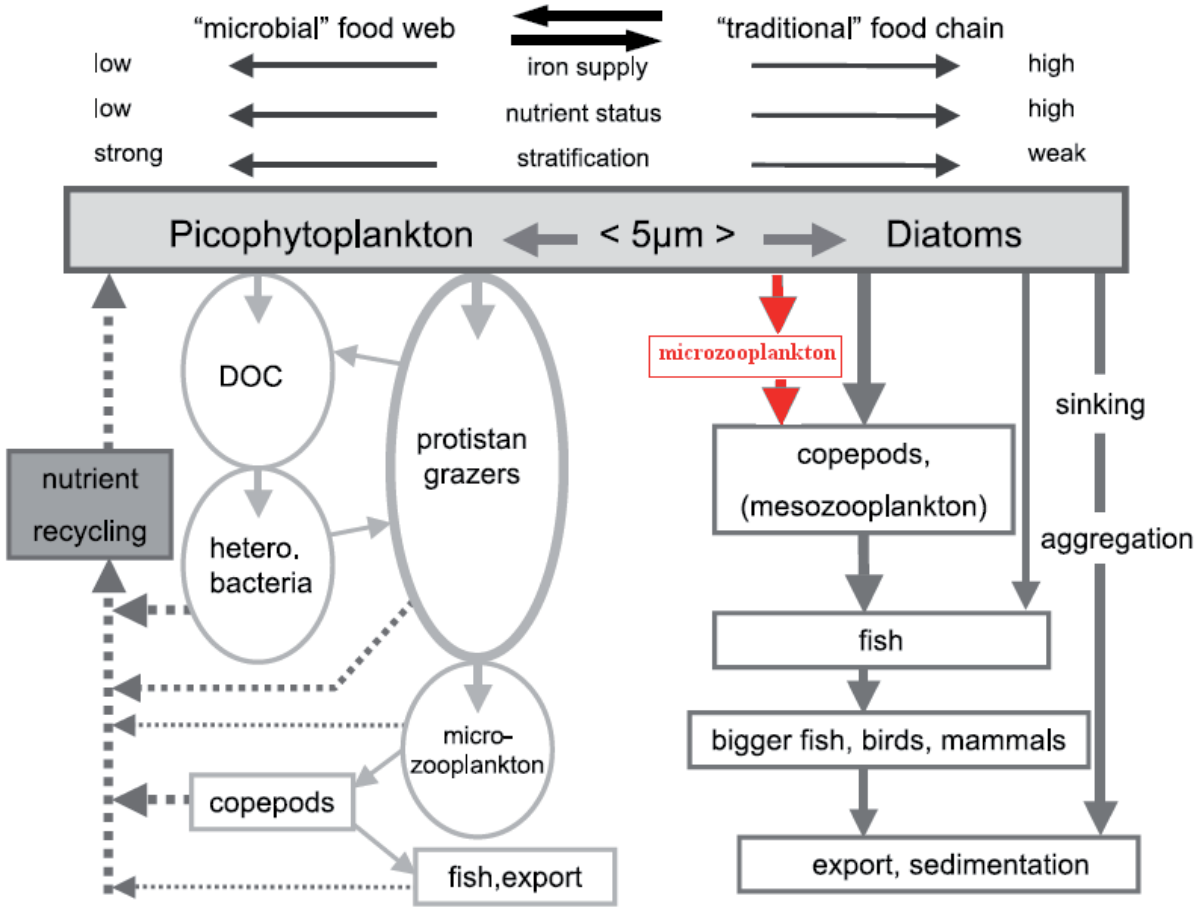

Figure 2: Modified food web representation.

1.4- Temperature

In the global warming context, it is important to know how organisms respond to temperature. Ciliates have a higher Q_{10} than dinoflagellates. However ciliates grazing Q_{10} is lower than their growth Q_{10}. The collected data didn't allow us to calculate a grazing Q_{10} for dinoflagellates. However, Straile (1997) found that both organisms have a GGE that varies with temperature. The correlation between GGE and temperature of ciliates and dinoflagellates differs. Ciliate GGE decreases with temperature. Dinoflagellate GGE increases with temperature. One conclusion can be drawn from this: even though dinoflagellates have lower grazing rates at 0°C and a lower Q_{10}, with a GGE that increases with temperature they should be able to compete with ciliates at higher temperature and even out-compete them. Based on data from Straile (1997) that give a GGE of 30% for ciliates and 26% for dinoflagellates at a temperature of 15°C, the critical temperature can be expected to be situated between 15 and 20°C.

1.5- Modelling of microzooplankton.

3D simulations using the PlankTOM 5 model to compare mixed-microzooplankton, (MIC), ciliate (CIL) and dinoflagellate (DIN), brought out some interesting features. Ciliate and dinoflagellates runs (CIL and DIN) are different from mixed-microzooplankton run (MIC) with only changing the grazing parameters (MFP runs). MIC, CIL and DIN run show different impact on the ecosystem through different distribution of the mixed-microzooplankton, ciliates and dinoflagellates. The ecosystem will shift from an export to a recycling systems depending on the grazing impact of microzooplankton. Areas of high density of microzooplankton are highly regenerative with low to no export. Changing the food preferences (SFP runs) or suppressing them (NFP runs) enhance the differences between MIC, CIL and DIN run.

From the analysed runs it is difficult to conceive that the generic microzooplankton reflect completely the range of ciliates and dinoflagellates behaviour, and their impact on ecosystems. A separation of both organisms in future model versions appears necessary. Food preferences are also an important part of the differentiation between the organisms and modulate the intensity of the impact of the grazer on the ecosystem. In future model version with additional phytoplankton functional types (*e.g.* PlankTOM 10, with 7 phytoplankton functional types) will be even more critical and important in influencing the ecosystem.

2- Outlook

To pursue the description of the functional response started in this thesis more data are needed to cover the whole range of size relationships between prey and predator. We need more data on both grazing and growth functional responses of both organisms. A series of laboratory experiments using a wide range of prey (minimum ten different types, from bacteria to diatoms) and different type of ciliate and dinoflagellates (at least three species of each with different size; more would be needed for dinoflagellates to take into account the potential impact of their feeding mode). Having these experiments done under similar conditions will allow us to develop a clearer picture of size effects. Some experiments with a mixture of prey would need to be designed to explore possible active selection of prey by both the ciliates and dinoflagellates. These could be complemented with competition experiments where different mixture of ciliates and dinoflagellates (ciliates being a fraction of the total microzooplankton concentration like 0, ¼, ½, ¾, 1) preying on a single prey species culture. Predation of ciliates on dinoflagellates and vice-versa will have to be taken in account and different ciliate:dinoflagellate size ratio will have to be tried out. If the experiments are a success and improve the understanding of ciliate and dinoflagellate, as well as allow tentative prediction on grazing and growth rate, the ideal would be to design mesocosm experiments where the microzooplankton is the highest predator and compare the mesocosm results with the experiments predictions.

The decoupling between grazing and growth in terms of response to temperature change and variation of food concentration opens different horizons:

(i) Verification and comparison with other organisms to establish if the separation between grazing and growth is as strong as for ciliates and dinoflagellates and what Q_{10} they have.

(ii) Since the work of Straile (1997) there has been no further large scale compilation and analysis of data on GGE, it would be interesting and potentially important to expand this work by incorporating the data created in the last 10 years.

(iii) The approach of having a constant GGE is questionable in term of response to temperature variation, and the variation at low food concentration. The method used in PlankTOM 5 of having a model growth efficiency (MGE, that varies with food concentration and the stochiometry of the prey) in addition to the GGE is a good starting point and could be further developed to include a response to temperature.

(iv) If there is enough data to parameterize a growth equation for zooplankton, the way growth is modelled could be modified. The general approach is to apply an equation for

grazing. A constant fraction of the energy gained by grazing is allocated to growth using a GGE. Instead, separate equations could be used for grazing and growth, with both process would also have a different Q_{10}. However, the allocation of energy to the other process (e.g. respiration, egestion, basal metabolism) would have to have priority on the growth, making the partitioning of energy more complicated to represent in models, compared to the current approach.

(v) The parameters of the growth equation (K and P_t) and their mechanistic interpretation (prey assimilation and basal metabolism) should be examined in more details, to see how they can be.

This study highlights the fact that microzooplankton is not a homogeneous group as is assumed in current ecosystems models. The next step of the modelling work conducted in this thesis would be to use the PlankTOM 10 model with three zooplankton compartments, *i.e.* ciliates, dinoflagellates, and mesozooplankton. To check for possible improvement and modification a reference run would be designed with only mesozooplankton and a mixed-microzooplankton. This would clarify two things, (i) establish whether separating ciliates and dinoflagellates is required to improve the cycling of biogenic elements and (ii) appoint a temporary limit to the level of difference needed between two zooplankton type to separate them in a model: not size class but a taxonomical group based on the class level (Ciliatea and Dinophyceae in this case).

3- References

Fenchel, T (1980), Suspension feeding in ciliated protozoa: Feeding rates and their ecological significance. *Microb. Ecol.,* 6:13-25

Kiørboe, T.(2008) A mechanistic approach to plankton ecology. Princeton, Univ. Press

Straile D (1997) Gross growth efficiencies of protozoan and metazoan zooplankton and their dependence on food concentration, predator-prey weight ratio, and taxonomic group. *Limnol. Oceanogr*., 42(6):1375-1385

Vézina, AF, Platt, T (1988) Food web dynamics in the ocean. I. Best-estimates of flow networks using inverse methods. *Mar. Ecol. Prog. Ser.,* 42:269-287

ANNEXES

Annexe A:

Biogeochemical Fluxes through Microzooplankton.

Buitenhuis, Erik[1,5], Richard Rivkin[2], Sévrine Sailley[3], Corinne Le Quéré[1,4]

[1] University of East Anglia, Norwich

[2] University of Newfoundland, Canada

[3] Alfred-Wegener Institute for Polar Research, Bremerhaven, Germany

[4] British Antarctic Survey, Cambridge, United Kingdom

[5] corresponding author: martinburo@email.com

Index terms: 0414, 0434, 4805, 4815, 4890

Key words: ciliates, dinoflagellates, heterotrophic nanoflagellates, dynamic green ocean model (DGOM)

Submitted to Global Biogeochemical Cycles 10 June 2009, doi:10.1029/2009GB003601

Running title: Global microzooplankton biogeochemistry

Abstract

Microzooplankton ingest a significant fraction of primary production in the ocean and thus remineralise nutrients and stimulate regenerated primary production. While their role in ocean biogeochemical cycles is well recognised, information is scattered throughout the literature and not readily accessible for global analysis. We synthesised observations on microzooplankton specific grazing rate, partitioning of grazed material, respiration rate, microzooplankton biomass, microzooplankton mediated phytoplankton mortality rate and phytoplankton growth rate. We used these observations to parameterise and evaluate the microzooplankton compartment in a global biogeochemical model that represents five plankton functional types (PFTs). Microzooplankton biomasses predicted in this simulation are closer to the independently derived evaluation data than in the previous model version. Most rates, including primary production, microzooplankton grazing, and export of sinking detritus are within observational constraints. However, the model underestimates micro- and mesozooplankton biomasses and chlorophyll concentrations. Thus, we propose that sufficient carbon enters the model ecosystem, but insufficient is retained. By taking into account the model underestimation of biomass, we estimate that the ocean inventory of microzooplankton biomass is 0.24 Pg C, which is similar to the biomass of mesozooplankton.

1. Introduction

Simplified representations of ocean ecosystems have divided the complex predator prey dynamics into two generalized trophic pathways: the classical food chain (i.e. large phytoplankton and planktonic metazoans), which has been studied from a fisheries perspective for over 120 years [*Mills*, 1989], and the microbial loop (i.e. small autotrophs and heterotrophs and their protistan grazers), which has been studied from the perspective of elemental and energy cycling for approximately 30 years [*Pomeroy*, 1974; *Azam et al.*, 1983]. Recent estimates of grazing for the herbivores that dominate in these two pathways suggest that mesozooplankton directly consume ~10-15 % of particulate primary production in the surface ocean [*Calbet*, 2001; *Behrenfeld and Falkowski*, 1997], while microzooplankton consume 59-75 % [*Calbet and Landry*, 2004]. Over large spatial scales, and in steady state, the particulate primary production that is not respired would be available for vertical export out of the surface ocean. *Bacteria* and *Archaea* consume the dissolved organic carbon (DOC) released by phytoplankton (which is about 5% of particulate primary production for exponentially growing phytoplankton and up to 40% under suboptimal conditions [*Nagata*, 2000]) as well as the DOC produced by the rest of the food web.

Biogeochemical models initially only simulated the cycles of C and P to describe the role of the ocean ecosystem in export from the surface to the deep sea [*Najjar et al.*, 1992; *Maier-Reimer*, 1993]. These early models used observed nutrient fields to calculate biological activity, but did not represent the organisms themselves. More recent biogeochemical models are now explicitly representing autotrophic and heterotrophic production based on measured rates (e.g. *in situ* measurements to constrain fluxes and laboratory measurements to constrain parameterisations), which allows the nutrient fields to be used for model evaluation.

These different approaches are now converging in Dynamic Green Ocean Models, which incorporate into global ocean biogeochemical models [*Le Quéré et al.*, 2005] the current conceptual understanding of ocean ecosystems, with biologically mediated transfer rates that are parameterized with measured values. This approach has the major advantage that the models can directly benefit from the laboratory- and field-derived information available for different planktonic organisms to formulate equations and evaluate results. In this paper we have synthesized observations on the key rate processes and the biomass distribution of microzooplankton, the major consumers of the autotrophic and heterotrophic microbes that dominate the cycling of carbon and nutrients in the upper ocean. We use this information to assess the role of microzooplankton in regulating biogeochemical fluxes.

2. Model description

2.1 PlankTOM5 biogeochemical model

The PlankTOM5.2 model was developed from the 5 PFT (plankton functional type) Dynamic Green Ocean Model of *Le Quéré et al.* [2005] by merging it with the ballasting effect and separate treatment of attached and detached coccoliths as in *Buitenhuis et al.* [2001], with the mesozooplankton equations and parameterisations of the standard run in *Buitenhuis et al.* [2006] and the river nutrient inputs as in the TODAY run in *da Cunha et al.* [2007]. Here, we present only the equations governing the microzooplankton. To a large extent, these equations use the same structure as for mesozooplankton [*Buitenhuis et al.*, 2006]. Documentation of the other compartments can be found at http://lgmacweb.env.uea.ac.uk/green_ocean/.

The change in the biomass of microzooplankton (Figure 1) is calculated as follows:

$$\delta MIC/\delta t = \Sigma grazing_F^{mic} \times \text{model growth efficiency - basal respiration} - grazing_{mic}^{mes} \quad (1)$$

where MIC is the microzooplankton biomass. The food sources F for microzooplankton are mixed phytoplankton (MIX), coccolithophores (COC), diatoms (DIA) and small particulate organic carbon (POC_s). The model does not include bacterial biomass.

2.1.1 Grazing

The microzooplankton grazing rate on any one food is described by the following equation:

$$grazing_F^{mic} = G_{0°C}^{mic} \times Q_{10,gr}^{\wedge T/10} \times \frac{p_F^{mic} F}{K_{½}^{mic} + \Sigma p_F^{mic} F} \times MIC \quad (2)$$

where $G_{0°C}^{mic}$ is the maximum grazing rate at 0 °C, $Q_{10,gr}$ is the temperature dependence, T is the temperature, p_F^{mic} is the preference for food F, and $K_{½}^{mic}$ is the half saturation constant for grazing. In this formulation a decrease in the preference p_F^{mic} increases the $K_{½}^{mic}$ for that food.

2.1.2 Partitioning of grazing

In field and laboratory experiments, net growth of microzooplankton is given by:

$$\begin{aligned} \text{net growth} &= \text{grazing} - \text{egestion} - \text{respiration} \\ &= \text{grazing} \times \text{GGE} \end{aligned} \quad (3)$$

where *GGE* (gross growth efficiency) is the part of grazing that is incorporated into biomass, egestion is partitioned between particulate egestion to POC_s and dissolved egestion to DOC, and respiration produces dissolved inorganic nutrients and DIC. During experiments in which net growth occurs, egestion and respiration are typically scaled in proportion to grazing [*Nagata*, 2000; *Stoecker*, 1984; *Verity*, 1985] which makes it possible to formulate a dimensionless partitioning of grazing:

$$\text{GGE} + \text{unass} + \text{dis} + \text{res} = 1 \quad (4)$$

where *GGE*, *unass*, *dis* and *res* are the fractions of grazing that are partitioned to MIC, POC_s, DOC and DIC. To allow the model to subtract basal respiration whether net growth occurs or not, we define a model growth efficiency as for mesozooplankton [*Buitenhuis et al.*, 2006]. The formulation provides a continuous function of biomass change with changing food concentration, from net loss at low food concentration to a net gain at high food concentration. In addition, to accommodate the fixed Fe:C ratio in zooplankton and variable Fe:C ratio in the foods, the model growth efficiency is decreased when the zooplankton are iron rather than carbon limited:

$$\text{model growth efficiency} + \text{unass} + \text{dis} + \text{feeding res} = 1 \quad (5)$$

$$\begin{aligned} \text{model growth efficiency} = \text{MIN}[&1\text{-unass}, \text{GGE} + \text{basal respiration} / \Sigma\text{grazing}_F^{\text{mic}}, \\ &\Sigma\text{grazing}_F{}^{\text{mic}}{}_{\text{Fe}} * (1\text{-unass})/(\Sigma\text{grazing}_F{}^{\text{mic}}{}_{\text{C}} * \text{Fe:C}^{\text{mic}})] \end{aligned} \quad (6)$$

Equation 5 introduces a feeding respiration, which is proportional to grazing and which is not measurable as a separate quantity; only the sum of feeding respiration and basal respiration is measurable. However, feeding and basal respiration could be separated as the slope and ordinal intercept of respiration plotted as a function of grazing [cf. *Verity*, 1985]. Feeding respiration is introduced as a programming convenience so that the model does not have to decide at every time and place whether the zooplankton are starving. This formulation is equivalent to introducing a threshold food concentration for growth, which will be used in section 3.1.3 to fit basal respiration to observed threshold concentrations.

2.1.3 Basal respiration

The basal respiration was calculated as:

$$\text{basal respiration} = res_{0°C}^{mic} \times Q_{10,res}^{\wedge T/10} \times MIC \quad (7)$$

where $res_{0°C}^{mes}$ is the respiration rate at 0 °C.

2.1.4 Fluxes of dissolved and particulate egestion and respiration

The other microzooplankton mediated fluxes are:

$$\delta DOC/\delta t = (1 - inorg) \times (1 - unass - \text{model growth efficiency}) \times \Sigma grazing_F^{mic} \times MIC \quad (10)$$

$$\delta POC_s/\delta t = unass \times \Sigma grazing_F^{mic} \times MIC \quad (11)$$

$$\delta PO_4^{3-}/\delta t = inorg \times (1 - unass - \text{model growth efficiency}) \times \Sigma grazing_F^{mic} \times MIC + res_{0°C}^{mic} \times Q_{10,res}^{\wedge T/10} \times MIC \quad (12)$$

where *inorg* partitions the ingested matter that is not used for growth or particulate egestion between respiration to DIC, PO_4 and Fe, and dissolved egestion to DOC.

We included microzooplankton mortality from starvation (basal respiration below the threshold food concentration) and grazing by mesozooplankton, and not grazing by other microzooplankton or viral lysis

2.2 Physical model

We used the global ocean general circulation model (GCM) NEMOv2.3 [*Madec*, 2008]. It has a horizontal resolution of 2° longitude and on average 1.1° latitude, and a vertical resolution of 10 m in the top 100 m, increasing to 500 m at 5 km depth. The model has a free surface height [*Roullet and Madec*, 2000], and is coupled to a thermodynamic sea ice model [*Timmermann et al.*, 2005]. The vertical mixing is calculated at all depths using a turbulent kinetic energy model [*Gaspar et al*., 1990], and sub grid eddy induced mixing is parameterized according to *Gent and McWilliams* [1990].

NEMO is a development of OPA. The latter was used by *Buitenhuis et al.* [2006] to

run the previous version of the biogeochemical model PISCES-T, to which we compare our present results. OPA had all of the features mentioned in the previous paragraph, but it should be realised that the differences between PlankTOM5 and PISCES-T will be a combination of the progress made in the physics and in the biogeochemistry.

2.3 Model forcing

The PlankTOM5 model was forced by river inputs of DIC, alkalinity, DOC, PO_4, SiO_3 and Fe [*da Cunha et al.*, 2007], sediment input of Fe and dust input of Fe and SiO_3 [*Aumont et al.*, 2003]. In contrast to *Buitenhuis et al.* [2006], we did not use nutrient restoring. Therefore, we compare our results with the run of PISCES-T-OPA8 that also didn't use nutrient restoring. The NEMO model was forced by daily wind and precipitation from NCEP reanalysis [*Kalnay et al.*, 1996] from 1948 to 2007. Sensible and latent heat fluxes are calculated with a bulk formula, using the temperature difference between the modelled sea surface temperature and the daily air temperature from NCEP reanalysis. The latent heat flux also provides evaporation. At the end of each year the water budget is calculated. From this, a water flux correction is calculated that is applied over the course of the next year.

The model was initialised with observations of T, S, PO_4^{3-}, SiO_3^{-} and O_2 from the World Ocean Atlas 2005, DIC and alkalinity outside the Arctic Ocean with GLODAP gridded data, DIC in the Arctic Ocean with GLODAP bottle data (http://cdiac.ornl.gov/ftp/oceans/GLODAP_bottle_files/Atlantic.GLODAP.V1.1.Z Observations North of 60°N were horizontally averaged and then applied over the Arctic Ocean), and ice extent and thickness and snow thickness [*Zhang and Rothrock*, 2003]. DIC concentrations were corrected for anthropogenic increases since 1948. Other tracers were initialised with the output of the previous model version.

The standard simulation was run from 1948 to 2007. Sensitivity analyses were initialized with the output of the standard simulation and were run from 1994 to 1999 and all results, including of the standard simulation, are of 1999. The 60 year standard simulation of the PlankTOM5-NEMO model will be included in the Primary Production Algorithm Round Robin 4 (Saba et al. manuscript in preparation, 2009).

3. Data synthesis of microzooplankton flux rates and biomasses

We compiled databases of microzooplankton specific grazing rates from field experiments, growth rates from laboratory experiments, DOC egestion as a fraction of grazing, threshold food concentration, microzooplankton caused phytoplankton mortality

rates, phytoplankton growth rates and field measured microzooplankton biomass.

Microzooplankton can be defined either taxonomically as a diverse grouping of heterotrophic protists, or operationally as a size class, typically < 200 µm. The difference between the taxonomic and operational definitions is that the latter includes the smaller life-stages of metazoans such as copepod nauplii. For our purpose of global biogeochemical modelling of plankton functional types we have used the taxonomic approach. In a previous model version [*Buitenhuis et al.*, 2006] we have included data on copepod nauplii in the parameterisation of mesozooplankton. This avoids the complication of having to transfer biomass from micro- to mesozooplankton when the nauplii grow out of the microzooplankton size class. The larger than 20 µm protistan fraction mostly consists of ciliates and dinoflagellates, and the smaller fraction mostly consists of nanoflagellates. We synthesized all data that we could find. There was more process data on ciliates (n=1044) and dinoflagellates (n=507), than flagellates (n=132).

These newly compiled databases were complemented by the database of microzooplankton GGE by *Straile* [1997], respiration of starving microzooplankton by *Fenchel and Finlay* [1983], while we could find only one paper each on POC egestion and respiration as a fraction of grazing. The complete databases is located at (http://lgmacweb.env.uea.ac.uk/green_ocean/.micro.html), including references to the papers that were used to compile each of the databases.

3.1 Parameterisation of the biogeochemical model

3.1.1 Grazing

The field observations of microzooplankton grazing of phytoplankton were fit to the *Michaelis and Menten* [1913] kinetic equation including an exponential increase with temperature:

$$\text{grazing}^{mic} = G_{0°C}{}^{mic} \times Q_{10.gra}{}^{\wedge T/10} \times \frac{\text{Chl } a}{K_{½,chl}{}^{mic} + \text{Chl } a} \quad (13)$$

This gave computed $G_{0°C}{}^{mic}$ = 3.5 d^{-1}, $Q_{10,gra}$ = 2.2 and $K_{½,chl}{}^{mic}$ = 3.29 µg Chl·L^{-1}. The $K_{½}$ for food was converted to carbon using a C/Chl ratio of 55 [g/g] , giving 180 µg C·L^{-1} (Figure 2A,B, see Table 1 for a summary of parameter values and the number of observations). This compares reasonably well with a $K_{½}$ of 240 µg C·L^{-1} that was reported by *Hansen et al.* [1997] for all sizes of zooplankton. In Table 1, all temperature dependent rates have been reported at 20 °C to make them easier to compare to typical surface ocean conditions.

The laboratory derived growth rates of microzooplankton were fit to the same equation. Food concentrations (F) were expressed in carbon units:

$$\mu^{mic} = \mu_{0°C}{}^{mic} \times Q_{10,gro}{}^{\wedge T/10} \times \frac{F}{K_{½,C}{}^{mic} + F} \quad (14)$$

This gave computed $\mu_{0°C}{}^{mic}$ = 0.28 d^{-1}, $Q_{10,gro}$ = 1.7 and $K_{½,C}{}^{mic}$ = 77 µg $C \cdot L^{-1}$. The carbon specific grazing rate was calculated from the laboratory growth rate divided by the gross growth efficiency (Figure 2C,D).

As was done for mesozooplankton [*Buitenhuis et al.*, 2006], we calculated food preferences using a phytoplankton biomass weighted mean of 1:

$$\frac{p_{dia}{}^{mic} \times biomass^{dia} + p_{coc}{}^{mic} \times biomass^{coc} + p_{mix}{}^{mic} \times biomass^{mix}}{\Sigma biomass^{phytoplankton}} = 1 \quad (15)$$

$$p_{dia}{}^{mic} = p_F{}^{mic} \times \text{relative preference} \quad (16)$$

Food selection has been studied both in the field and in the laboratory. However, at present there is both evidence for little [e.g. *Palomares-Garcia et al.*, 2006] and significant selection of food species [e.g. *Verity et al.*, 1991; *Sun et al.*, 2007]. This lack of consistency may reflect competing contributions from size selection, biochemical composition of the food, differences among the different zooplankton, and in the case of field studies concomitant changes in food and zooplankton communities. A synthesis on size selection by *Straile* [1997] shows that dinoflagellate GGE is highest when their prey are of similar size as themselves, such as diatoms, while ciliate GGE is highest when their prey are 3 orders of magnitude smaller, i.e. about 10 times smaller in diameter. Qualitatively based on these preferred predator:prey ratios, the relative microzooplankton preference for diatoms: coccolithophores: mixed phytoplankton: POC_s were taken as 1:4:5:0.5. The global average phytoplankton biomasses were taken from a database based on accessory pigments over the world ocean [*Uitz et al.,* 2006]. We assumed that diatoms are 100% of the microphytoplankton, coccolithophores are 50% of the nanophytoplankton, and mixed phytoplankton are the remaining 50% of the nanophytoplankton plus 100% of the picophytoplankton.

3.1.2 Partitioning of grazed food

The grazed food is partitioned among the increase in grazer biomass, dissolved egestion

to DOC, unassimilated fecal material, and respiration that is associated with feeding (i.e. respiration that supports energetic costs of searching for and digesting food). The GGE that we used were all measurements of protozoans compiled by *Straile* [1997] (Figure 2E). This database includes freshwater microzooplankton. Most of the data for DOC egestion [*Nagata*, 2000] was expressed relative to grazing (Figure 2F), but, following previous work on mesozooplankton [*Buitenhuis et al.*, 2006], we converted this to a fraction of DOC egestion plus feeding respiration (*1-inorg* in Equation 10). We could only find one published measurement of the unassimilated fraction for microzooplankton [*Stoecker*, 1984] and one published measurement of respiration as a fraction of grazing [*Verity*, 1985]. We used GGE and DOC egestion as the average of the measurements, and divided the remaining fraction of grazing over unassimilated fraction and feeding respiration in the ratio of their respective measurements (i.e. $unass_{model} = unass_{measured} / (feeding\ res + unass_{measured}) * (1 - GGE - dis)$).

3.1.3 Basal respiration

We used two independent sets of observations to constrain basal respiration. One set of parameterisations was calculated by equating basal respiration (Equation 7) to the growth rate (Equation 14) at the threshold food concentration, at which the change in microzooplankton biomass is 0. By solving for the food concentration, we get:

$$\text{threshold} = \frac{K_{½}^{mic} \times res_{0°C}^{mic} \times Q_{10,res}^{\wedge T/10}}{\mu_{0°C}^{mic} \times Q_{10,gr}^{\wedge T/10} - res_{0°C}^{mic} \times Q_{10,res}^{\wedge T/10}} - 1) \quad (17)$$

We fit basal respiration to laboratory measured threshold food concentrations (Figure 2G). This situation is not ideal, because the observed threshold concentrations fell into two distinct ranges. There was no consistently low quality food type for all grazers. In addition, because both the numerator and the denominator of Equation 17 are temperature-dependent, the basal respiration rate is very sensitive to the increase in threshold with temperature. Therefore, the basal respiration rates that were fit to the low threshold concentrations had a high Q_{10}. We therefore compared these basal respiration rates to the respiration rates of starving protozoans that were compiled by *Fenchel and Finlay* [1983] (Figure 2H). We estimated the range of basal respiration in the same way as was done for mesozooplankton [*Buitenhuis et al.*, 2006]: the dataset is bisected into two parts by the fitted line to equation 17. These two parts are then used for parameter fits to the high and low parts of the dataset. We used these parameters in the sensitivity study (Figure 5).

3.1.4 POC degradation

The POC degradation rate at 0°C was adjusted to give a reasonable ocean-atmosphere CO_2 flux.

3.2 Evaluation data

We produced three evaluation datasets (Figure 3). The first one is of microzooplankton biomass. The database contains both measurements of individual species/taxonomic groups or size classes and of reported total biomass: It contains 4629 observations of total biomass, and 3859 observations on the model grid with a climatological year of 12 months. 90% of data were collected in the top 180 m of the ocean. The second dataset is the rate of microzooplankton-mediated phytoplankton mortality: It contains 1405 observations and 1087 on the model grid. The third dataset is of phytoplankton growth rate determined during the same dilution assay from which mortality was estimated: It contains 1393 observations and 1036 on the model grid. The latter two datasets were obtained from field measurement of microzooplankton grazing using the dilution technique [*Landry and Hassett*, 1982]. 90% of these datasets were collected in the top 50 m of the ocean.

In the standard simulation, the observations that were used for the parameterisation were independent of the evaluation datasets. However, in the sensitivity simulation with the field derived grazing rate, the measurements that were used for the parameterisation were part of the evaluation datasets. The field-derived carbon specific microzooplankton grazing rates (Figure 2A,B) were computed from the phytoplankton mortality rate and the microzooplankton biomass, but the number of dilution experiments for which we have concurrent measurements of microzooplankton biomass is much smaller (n=36) than the number of phytoplankton mortality observations (n=1405). To keep the evaluation of this simulation consistent with the standard simulation, and because 97% of the phytoplankton mortality and growth measurements and 99% of the biomass measurements were independent of the parameterisation, we included the parameterisation measurements in the evaluation datasets.

The model output and evaluation data were compared using the cost function:

$$\text{cost function} = 10^{\text{average}(|\log(\text{model}/\text{data})|)} \qquad (18)$$

We used this formulation because it is an estimate of relative error, in contrast to e.g. the sum of squared residuals, which measures absolute error and is thus biased towards the error in the larger values. A perfect model would give a cost function of 1, and a model that is either half or double the observations would give a cost function of 2. Thus, the cost function measures the distance between model and observations, but not the bias. We also report average concentrations and global rates as a measure of bias.

We calculated the global biomass of microzooplankton by using the model results to extrapolate the observed concentrations to the global ocean:

$$\text{global biomass} = \text{model global biomass} * \frac{\text{average observed biomass}}{\text{average model biomass}} \quad (19)$$

in which the average model biomass is calculated at the same places and months as the observations.

4 Results

We compiled the first global database of microzooplankton biomass (Figure 3, all data available at http://lgmacweb.env.uea.ac.uk/green_ocean/.micro.html). The average microzooplankton biomass is 2.8 µg C·L^{-1}. This is less than half of the average mesozooplankton biomass (Table 2), but we will argue in the discussion that this is due to relatively more mesozooplankton observations in high productivity regions.

The microzooplankton biomass is about equally divided among dinoflagellates (38 ± 28%, n=539, Figure 4) flagellates (34 ± 30%) and ciliates (28 ± 26%). Thus, we can confirm the results of *Sherr and Sherr* [2007] with a substantially larger database that dinoflagellate biomass is at least as high as ciliate biomass (dinoflagellate/(dinoflagellate+ciliate) = 58 ± 30%, n=1412).

We compiled both field and laboratory derived grazing rates. The curve fits find a higher maximum grazing rate and half-saturation concentration for the field data ($G_{15°C}^{mic}$ = 17.0 ± 1.0 d^{-1}, $K_{½}^{mic}$ = 180 ± 8 µg C•L^{-1}) than for the laboratory data ($G_{15°C}^{mic}$ = 2.7 ± 0.2 d^{-1}, $K_{½}^{mic}$ = 77 ± 1 µg C•L^{-1}). However, there are fewer observations in the field (36 vs. 1297), so that the parameters are not as well constrained. Because of the higher standard deviations of the parameters, and our assessment of the trade-off between cost functions and chlorophyll distribution (see Discussion), we used the laboratory derived grazing rate with the starved respiration rate as the standard simulation (Figures 3 and S8), and performed a sensitivity analysis using the field-derived grazing rate (Table 2, 3).

The standard simulation was parameterised based on the observations without model

tuning (bold parameters in Table 1). In the standard simulation, the modelled microzooplankton biomasses in the low latitudes have a lower bias relative to the observations than in the high latitudes (Figure 3, Figure 7B). There is no discernable bias in the seasonality in either hemisphere (data not shown). On average, the cost function indicates that there is a 2.8 fold difference between modelled and observed biomass (Table 3, Figure 5).

The model primary production closely matches the observed global rate, export is reasonably reproduced, microzooplankton grazing on phytoplankton is slightly underestimated, and mesozooplankton grazing on phytoplankton is substantially overestimated (Table 3). The cost functions are 3.4 for primary production and 2.1 for export. The model underestimates the average chlorophyll concentration and microzooplankton and mesozooplankton biomasses (Table 2, Figures 5A,D, 6A), but all are improved relative to the previous model version [*Buitenhuis et al.*, 2006]. The cost function is 5.1 for chlorophyll and 6.7 for mesozooplankton (Table 3, Figure 5).

There is no clear trend in either observations or model of rates of phytoplankton growth or mortality with latitude between 50°S and 60°N (Figure 3). The model uses an exponential temperature function for both phytoplankton growth rate and microzooplankton grazing rate, so this relative constancy shows that the model correctly predicts a general increase in phytoplankton nutrient limitation and microzooplankton food limitation at lower latitudes (data not shown). The cost functions in the standard simulation are 2.5 for phytoplankton growth and 41 for phytoplankton mortality (Table 3, Figure 5).

We performed sensitivity analyses of all microzooplankton parameters including a range of values of basal respiration and grazing rate (Figures 5, 6, Tables 2, 3). The sensitivity analysis of respiration rate was done separately using the laboratory and field derived grazing rates (Table 1, Figure 5). The sensitivity analysis of grazing rate was done with parameters that were intermediate between the laboratory and field derived values ($K_{½}$ = 128 µg C·L^{-1}, Q_{10}=1.95). The modelled global rates of primary production, microzooplankton grazing on phytoplankton, mesozooplankton grazing on phytoplankton and export spanned the observed rates of about 47, 30, 6 and 10 Pg C/y, respectively (Figures 5B,E, 6B, Table 2). Not surprisingly, microzooplankton biomass decreased with an increase in basal respiration rate. This also led to a decrease in microzooplankton grazing on phytoplankton and an increase in chlorophyll concentration, mesozooplankton grazing on phytoplankton and mesozooplankton biomass. However, primary production decreased, consistent with a decrease in turnover rate of phytoplankton. As was found for mesozooplankton [*Buitenhuis et al.*, 2006], changing the grazing rate showed an optimum in microzooplankton biomass and globally integrated

grazing. The initial increase, despite a steady decline in chlorophyll concentration, seems to be due primarily to an increase in phytoplankton turnover rate. Between a grazing rate of 2 and 2.5 d^{-1} the global microzooplankton grazing decreases while microzooplankton biomass increases. This is caused by a steady phytoplankton-driven decline in mesozooplankton biomass that results in a decline in mesozooplankton grazing on microzooplankton despite the increase in microzooplankton biomass.

As noted above, the standard simulation has a latitudinal gradient in model/data mismatch for microzooplankton biomass (Figure 3, 7B). Since there are general latitudinal gradients in both food concentrations and temperature, the mismatch could be due to several reasons. We tested one of the possible reasons, namely that GGE has been found to decrease with temperature in some types of marine organisms (e.g. bacteria and a smaller dataset of microzooplankton in *Rivkin and Legendre* [2001]). Temperature explained none of the variability of the whole database, but there was a negative trend in GGE for ciliates and a positive trend for both dinoflagellates and flagellates. We combined the measurements for dinoflagellates and flagellates, and performed sensitivity analyses with the two different trends of GGE with temperature (Table 2, 3). As expected from the underestimation of microzooplankton biomass at high latitudes in the standard simulation, the simulation with a lower GGE at low temperature gave a higher cost function and a bigger underestimation of microzooplankton biomass than the standard simulation (Table 2, 3). The simulation with the ciliate GGE has average microzooplankton biomass that match the observations (Table 2, Figure 7A), and also has very little latitudinal gradient in the cost function (Figure 7B). The phytoplankton growth cost function is improved from 40 to 33, there is a small improvement in microzooplankton biomass cost function from 2.8 to 2.7, and small deteriorations in the other cost functions.

In the sensitivity simulation with a lower $K_{½}$, the model is closer to the observations for microzooplankton biomass, micro- and mesozooplankton grazing, while there is a deterioration in chlorophyll concentration, mesozooplankton biomass, and export. It gives a lower cost functions for microzooplankton biomass, phytoplankton growth and mortality rates and export and a higher cost functions of chlorophyll concentration and mesozooplankton biomass (Table 2, 3). Increasing the $K_{½}$ leads to the opposite effects, except for a deterioration in mesozooplankton biomass and higher cost functions of chlorophyll concentration and mesozooplankton biomass.

Setting all microzooplankton food preferences to 1 has a major impact on the relative contribution of the phytoplankton functional types to total chlorophyll with a near complete

loss of diatoms (data not shown). This decrease in diatoms leads to a decrease in export and an increase of the smaller phytoplankton, primary production and grazing rates of both micro- and mesozooplankton (Table 2). We tested two cases of repartitioning microzooplankton grazing. Increasing GGE at the expense of DOC production leads to higher microzooplankton biomass and grazing with less export. This was accompanied by only a small decrease in primary production and mesozooplankton biomass. Increasing the unassimilated fraction to POC_s (to that observed by *Stoecker* [1984]) at the expense of feeding respiration had a smaller effect in the opposite direction with an increase in export and decrease in primary production and grazing rates.

We calculated the globally integrated microzooplankton biomass in the model (Σlocal biomass*grid box volume). We correct for the bias in the model, using equation 19, by multiplying this model result by the ratio between the average local biomass in the evaluation database (2.8 µg $C \cdot L^{-1}$) and the average local biomass in the model at the same places and months as the evaluation data (1.6 µg $C \cdot L^{-1}$ in the standard simulation). From this, we estimate that the annual average inventory of microzooplankton biomass is 0.24 Pg C. We also estimated the range around this value from the 19 sensitivity simulations as 0.14 – 0.33 Pg.

5 Discussion

Unlike in terrestrial ecosystems, herbivory plays a fundamental role in ocean biogeochemical cycles, and leads to much higher primary production through nutrient recycling than could be supported on external nutrient supply from the deep sea, rivers and dust alone. Herbivory leads to lower standing stocks of primary producers, and to accurately model biogeochemical fluxes it is thus necessary to achieve realistic results for both standing stocks and turnover rates. The standard simulation underestimates the concentration of chlorophyll and biomasses of both micro- and mesozooplankton (Figure 5A,E, 6A, Supplementary Figure S8). Primary production in the model was close to observations: with the modelled rates (48.3 Pg C/y in the standard simulation) being very close to the most thoroughly validated remote sensing estimate of *Behrenfeld and Falkowski* [1997] of 46.5 Pg C/y. This suggests that the ecosystem loss rates are too high, because enough carbon enters the ecosystem, but insufficient carbon is retained. None of the sensitivity studies on microzooplankton parameters simultaneously increased the concentration of chlorophyll and biomasses of both micro- and mesozooplankton. We provisionally conclude that the underestimations are not due to a single cause. For chlorophyll concentrations, preliminary

results suggest this can be improved by replacing the steady state photosynthesis model with a dynamical iron-light colimitation model [*Buitenhuis and Geider*, subm.], an adaptation of the *Geider et al*. [1998] nitrogen-light colimitation model. For microzooplankton, the most significant improvement was obtained by using the ciliate GGE that decreases with temperature. This same pattern of an inverse relationship between temperature and growth efficiency was reported for both bacteria and protists by *Rivkin and Legendre* [2001] based on a meta-analysis of published information. The improvement in microzooplankton biomass argues for the importance of ciliates as opposed to dinoflagellates, which is consistent with a maximum growth rate at 15 ºC that is higher for ciliates (2.3 ± 0.2 d^{-1}) than for dinoflagellates (0.9 ± 0.2 d^{-1}, Figure 2D), despite their contributing only $28 \pm 26\%$ of the microzooplankton biomass. For mesozooplankton, *Buitenhuis et al.* [2006] have shown that the model can be brought closer to the observed biomass by increasing the grazing rate within the uncertainty of the observed grazing rates.

In the parameterisation datasets (Figure 2), there is considerable unexplained variability around the fitted functional relationships. In addition to the normal measurement uncertainty, this is due to the use of measurements on different species from different taxonomic groups in a single fit. Despite obvious shortcomings, there are some hopeful signs from this first effort to compile an almost complete representation of microzooplankton mediated biogeochemical fluxes. For example, the field and laboratory grazing rates fall into the same range despite their being derived with very different methodologies (Figure 2A-D), the partitioning of grazing is broadly consistent with that of mesozooplankton (though the unassimilated fraction of 0.13 for microzooplankton is both poorly constrained and considerably smaller than the value of 0.31 for mesozooplankton [*Buitenhuis et al.*, 2006]), and the basal respiration rate that was calculated from the threshold concentrations and the laboratory derived grazing rate are broadly consistent with the starved respiration rates (Figure 2G-H).

Food preferences have a major impact on the phytoplankton PFT (plankton function type) distributions, and on the proportions of primary production that are exported or remineralised. However, information on food preferences is not generally reported for natural microzooplankton populations, and the information that is available in the literature for laboratory experiments does not cover the naturally occurring range of foods. We have parameterised food preference in the model based on general information concerning predator:prey size ratios (cf. Section 3.1.1). More observations will be needed before this can be resolved in the model.

The cost function for microzooplankton biomass changed less than 2-fold (max/min = 1.8) in the sensitivity studies of basal respiration and grazing rates (Figures 5C,F, 6C), even though the biomass itself changed substantially (max/min = 6.4). This was in contrast to the sensitivity of the microzooplankton mediated phytoplankton mortality (max/min = 75) to microzooplankton basal respiration and grazing rates (Figures 5C,F, 6C) and of the mesozooplankton biomass cost function (max/min = 8) to mesozooplankton grazing rate [*Buitenhuis et al.* 2006, Figure 6]. This suggests that there is a relatively wide region of parameter space in which the cost function is not very sensitive to changes in microzooplankton basal respiration and grazing. The cost function using observed phytoplankton mortality rates is lower for the lower microzooplankton respiration rates, which were fit to the lower half of the observed threshold concentrations (Figure 5C,F); consistent with the independent observations of starved respiration (Figure 2H). The cost function of phytoplankton mortality is also lower for the higher microzooplankton grazing rates, but at an increasing cost function of mesozooplankton biomass.

Thus, there are clear tradeoffs in the tested range of model parameterizations with respect to cost functions (Figures 5C,F, 6C). For instance, the combination of the field measured grazing rate, with the low threshold concentrations, lowers the cost function for microzooplankton-mediated phytoplankton mortality rates, but it deteriorates the cost function for mesozooplankton biomass, and does not reproduce the low chlorophyll that is a distinct feature of the subtropical gyres. The combination of high grazing rates with low threshold allows microzooplankton to effectively suppress phytoplankton blooms, so that nutrients are unused in regions outside the subtropical gyres, and these nutrients are then transported into the subtropical gyres, leading to the homogeneous distribution of chlorophyll (data not shown). There are compensating improvements to the chlorophyll outside the subtropics, so that there is a small decrease in the cost function for chlorophyll in this simulation. We conclude that the more realistic surface chlorophyll field, as well as higher average mesozooplankton biomass and chlorophyll concentration in the standard simulation were more important than the substantial increase in the cost function for phytoplankton mortality. We propose that the trade-off in the different cost functions indicates that for some parts of the model, the parameterisation was inadequate, and that larger parameterisation datasets would improve model performance.

We also find a trade-off between the standard PlankTOM5 simulation and PISCES-T [*Buitenhuis et al.*, 2006]. PlankTOM5 shows improvements without model tuning, in both the cost function of microzooplankton and the average biomass of microzooplankton. There are

also improvements in the mesozooplankton biomass, global primary production, chlorophyll concentration and global export, but deteriorations in the cost function of mesozooplankton, chlorophyll and export and in global mesozooplankton grazing (Figure 5, Table 2). The model results can be further improved by tuning within the range of uncertainty of the parameters, suggesting that increased data constraints or better model structure (e.g. adding nanozooplankton) in the future will contribute to improved model results.

Using the model to extrapolate the observations of microzooplankton biomass we calculate a global biomass of 0.24 Pg C. *Buitenhuis et al.* [2006] estimated mesozooplankton biomass as 0.16 Pg C, also using Equation 19. We calculated global microzooplankton biomass for the sensitivity simulations, which gave a range of 0.14 – 0.33 Pg. Thus, we conclude that the difference in global biomass between micro- and mesozooplankton should not be seen as a significant difference. It does suggest that the difference in average observed local biomass (Table 2) between microzooplankton (2.8 μg C L^{-1}) and mesozooplankton (7.1 μg C L^{-1}) is probably due to observational bias, with relatively more observations in high productivity regions for mesozooplankton.

While the biomass of the two zooplankton types is thus similar, globally integrated grazing is higher for microzooplankton than for mesozooplankton, particularly for the extrapolated observations: 25-33 vs. 5.5 Pg C·y^{-1}, but also in the standard simulation: 20.3 vs. 14.6 Pg C·y^{-1} as a consequence of, amongst others, the higher biomass specific maximum grazing rates: 0.92 vs. 0.31 d^{-1} at 0 °C.

Conclusion

In summary, when our model uses equations and parameters from observations, the global fluxes are in reasonable agreement with observations of primary production, grazing of micro- and mesozooplankton on phytoplankton and export. The model underestimates the concentrations of chlorophyll and the biomass of microzooplankton and in particular mesozooplankton, but the incorporation of new observations has led to improvements relative to the previous model version.

Based on the low discriminative power of the cost function for microzooplankton biomass over a wide range of parameter values, we suggest that the most effective progress which can be made in defining the role of microzooplankton in global biogeochemical cycles is to make microzooplankton biomass a standard oceanographic measurement, in particular during dilution grazing experiments.

Acknowledgements

We thank Clare Enright for making the forcing and restart files and other technical support. We thank Heather Bussey for compiling the grazing database and Candice Way for compiling the biomass database. We thank the Laboratoire d'Océanographie et du Climat for making the code of the NEMO model available. We thank the members of the Dynamic Green Ocean Project for their input throughout this project. We thank Bablu Sinha for identifying a problem in the previous model version with the closure of the iron budget of zooplankton. EB thanks the NERC for financial support through MarQuest NE/C516079/1 and the EU through CarboOcean 511176[GOCE]. RR thanks the Natural Science and Engineering Research Council of Canada for financial support. SS thanks the EU for financial support through EurOceans 511106-2. The grazing database assembly was supported by the Max Planck institute for biogeochemistry, Germany, and the biomass database assembly was supported by EurOceans. For details on the model equations, flux rate and microzooplankton biomass observations, simulation results, and general model documentation see the additional information at: http://lgmacweb.env.uea.ac.uk/green_ocean/.micro.html.

Literature

Aumont, O., E. Maier-Reimer, S. Blain, and P. Monfray (2003), An ecosystem model of the global ocean including Fe, Si, P co-limitations, *Global Biogeochem. Cycles, 17*, 1060, 2001GB001745.

Azam, F., T. Fenchel, J. G. Field, J. S. Gray, L. A. Meyer-Reil, and F. Thingstad (1983), The ecological role of water-column microbes in the sea, *Mar. Ecol. Progress Ser., 10*, 257-263.

Behrenfeld, M. J., and P. G. Falkowski (1997), Photosynthetic rates derived from satellite-based chlorophyll concentration, *Limnol. Oceanogr., 42***,** 1-20.

Buitenhuis E. T., P. van der Wal, and H. J. W. de Baar (2001), Blooms of *Emiliania huxleyi* are sinks of atmospheric carbon dioxide; a field and mesocosm study derived simulation, *Global Biogeochem. Cycles, 15*, 577-587.

Buitenhuis, E. T., C. Le Quéré, O. Aumont, G. Beaugrand, A. Bunker, A. Hirst, T. Ikeda, T. O'Brien, S. Piontkovski, and D. Straile (2006), Biogeochemical fluxes through mesozooplankton, *Global Biogeochem. Cycles, 20,* GB2003, doi: 10.1029/2005GB002511.

Calbet, A. (2001), Mesozooplankton grazing effect on primary production: A global comparative analysis in marine ecosystems, *Limnol. Oceanogr.*, *46*, 1824-1830.

Calbet, A., and M. R. Landry (2004), Phytoplankton growth, microzooplankton grazing, and carbon cycling in marine systems, *Limnol. Oceanogr., 49*, 51-57.

da Cunha, L. C., C. Le Quéré, E. T. Buitenhuis, X. Giraud, and W. Ludwig (2007), Potential impact of changes in river nutrient supply on global ocean biogeochemistry, *Global Biogeochem. Cycles, 21*, GB4007, doi:10.1029/2006GB002718

Fenchel, T., and B. J. Finlay (1983), Respiration rates in heterotrophic, free-living protozoa, *Microb. Ecol., 9*, 99-122.

Gaspar P., Y. Gregoris, and J. M. Lefèvre (1990), A simple eddy kinetic energy model for simulations of the oceanic vertical mixing : Tests at station Papa and Long-Term Upper Ocean Study site, *J. Geophys. Res., 95*, 179-193.

Geider, R. J., H. L. MacIntyre, and T. M. Kana (1998), A dynamic regulatory model of phytoplanktonic acclimation to light, nutrients, and temperature, *Limnol. Oceanogr., 43*, 679-694.

Gent, P. R., and J. C. McWilliams (1990), Isopycnal mixing in the ocean circulation models, *J. Phys. Oceanogr., 20***,** 150-155.

Hansen, J., P. K. Bjørnsen, and B. W. Hansen (1997), Zooplankton grazing and growth: scaling within the 2-2000 µm body size range, *Limnol. Oceanogr., 42*, 687-704.

Kalnay, E., M. Kanamitsu, R. Kistler, W. Collins, D. Deaven, L. Gandin, M. Iredell, S. Saha, G. White, J. Woollen, Y. Zhu, M. Chelliah, W. Ebisuzaki, W. Higgins, J. Janowiak, K. C. Mo, C. Ropelewski, J. Wang, A. Leetmaa, R. Reynolds, R. Jenne, and D. Joseph (1996), The NCEP/NCAR 40-year reanalysis project, *Bull. Am. Meteorol. Soc., 77*, 437-471.

Landry, M. R., and R. P. Hassett (1982), Estimating the grazing impact of marine micro-zooplankton, *Mar. Biol., 67*, 283-288.

Laws, E. A., P. G. Falkowski, W. O. Smith Jr., H. Ducklow, and J. J. McCarthy (2000), Temperature effects on export production in the open ocean, *Global Biogeochem. Cycles, 14*, 1231-1246.

Le Quéré, C., S. P. Harrison, I. C. Prentice, E. T. Buitenhuis, O. Aumont, L. Bopp, H. Claustre, L. Cotrim da Cunha, R. Geider, X. Giraud, C. Klaas, K. E. Kohfeld, L. Legendre, M. Manizza, T. Platt, R. B. Rivkin, S. Sathyendranath, J. Uitz, A. J. Watson, and D. Wolf-Gladrow (2005), Ecosystem dynamics based on plankton functional types for global ocean biogeochemistry models, *Global Change Biol., 11*, 1-25.

Madec G. (2008), NEMO ocean engine, *No 27* ISSN No 1288-1619 http://www.nemo-ocean.eu/index.php/content/download/2702/18843/file/NEMO_book.pdf, Institut Pierre-Simon Laplace (IPSL), France.

Maier-Reimer, E. (1993), Geochemical cycles in an ocean general circulation model. Preindustrial tracer distributions, *Global Biogeochem. Cycles, 7*, 645-677.

Manizza, M., C. Le Quéré, and E. T. Buitenhuis, Sensitivity of global ocean biogeochemical dynamics to ecosystem structure in a future climate, *Geophysical Research Letters* submitted doi:10.1029/2008GL036694.

Michaelis, L., and M. L. Menten (1913), Die Kinetik der Invertinwirkung, *Biochem. Zeitschrift, 49*, 333-369.

Mills, E. (1989), *Biological oceanography. An early history, 1870-1960*, Cornell University Press, Ithaca, USA

Nagata, T. (2000), Production mechanisms of dissolved organic matter, in *Microbial ecology of the ocean*, edited by D. L. Kirchmann, Wiley-Liss, New York, USA

Najjar, R. G., J. L. Sarmiento, and J. R. Toggweiler (1992), Downward transport and fate of organic matter in the ocean: simulations with a general circulation model, *Global Biogeochem. Cycles, 6*, 45-76.

Palomares-García, R., J. J. Bustillos-Guzmán, and D. López-Cortés (2006), Pigment specific rates of phytoplankton growth and microzooplankton grazing in a subtropical lagoon, *J. Plankton Res., 28***,** 1217-1232.

Pomeroy L. R.(1974),The ocean's food web, a changing paradigm, *Bioscience, 24*, 499-504.

Rivkin, R. B., and L. Legendre (2001), Biogenic carbon cycling in the upper ocean: effects of microbial respiration, *Science, 291*, 2398-2400.

Roullet, G., and G. Madec (2000), Salt conservation, free surface, and varying levels: a new formulation for ocean general circulation models, *J. Geophys. Res., 105***,** 23927-23942.

Schlitzer, R. (2004), Export production in the equatorial and North Pacific derived from dissolved oxygen, nutrient and carbon data, *J. Oceanogr.,* 60**,** 53-62.

Sherr, E. B., and B. F. Sherr (2007), Heterotrophic dinoflagellates: a significant component of microzooplankton biomass and major grazers of diatoms in the sea, *Mar. Ecol. Progres Ser., 352***,** 187-197.

Stoecker, D. K. (1984), Particle production by planktonic ciliates, *Limnol. Oceanogr., 19*, 930-940.

Straile, D. (1997), Gross growth efficiencies of protozoan and metazoan zooplankton and their dependence of food concentration, predator-prey weight ratio, and taxonomic group, *Limnol. Oceanogr., 42***,** 1375-1385.

Sun, J., Y. Feng, Y. Zhang, and D. A. Hutchins (2007), Fast microzooplankton grazing on fast-growing, low-biomass phytoplankton: a case study in spring in Chesapeake Bay, Delaware Inland Bays and Delaware Bay, *Hydrobiologia, 589***,** 127-139.

Timmermann, R., H. Goosse, G. Madec, T. Fichefet, C. Ethe, and V. Dulière (2005), On the representation of high latitude processes in the ORCA-LIM global coupled sea ice-ocean model, *Ocean Modelling, 8*, 175-201.

Uitz, J., H. Claustre, A. Morel, and S. B. Hooker (2006), Vertical distribution of phytoplankton communities in open ocean: an assessment based on surface chlorophyll, *J. Geophys. Res., 111*, C08005, 2005JC003207.

Verity, P. G. (1985), Grazing, respiration, excretion and growth rates of tintinnids, *Limnol. Oceanogr., 30*, 1268-1282.

Zhang, J., and D.A. Rothrock (2003), Modeling global sea ice with a thickness and enthalpy distribution model in generalized curvilinear coordinates, *Mon. Wea. Rev.*, *131***,** 681-697.

Tables

Table 1. Microzooplankton and POC degradation rate parameters in the model (value formatting corresponds to the simulations in Tables 2 and 3, note that the temperature dependent values have been given at 20 °C)

flux	parameter (Figure 1)	value	st.err.	organisms	n
field derived specific grazing	$G_{20°C}^{mic}$	17 d^{-1}	1.0	field populations	36
Q_{10} grazing	$Q_{10,gra}$	2.2	0.2		
half saturation grazing	$K_{½}^{mic}$	180µg C·L^{-1}	8		
threshold		84 µg C·L^{-1}	11	ciliates, (dino)flagellates	37
basal respiration from threshold	$res_{20°C}^{mic}$	1.9 d^{-1}		field populations	
Q_{10} basal respiration	$Q_{10,res}$	3.46			
laboratory derived specific grazing	$G_{20°C}^{mic}$	**2.7 d^{-1}**	0.2	ciliates, dinoflagellates	1297
Q_{10} grazing	$Q_{10,gro}$	**1.7**	0.2		
half saturation grazing	$K_{½}^{mic}$	**77 µg C·L^{-1}**	1.1		
basal respiration from threshold	$res_{20°C}^{mic}$	*0.49 d^{-1}*		ciliates, dinoflagellates	37
Q_{10} basal respiration	$Q_{10,res}$	*2.3*			
gross growth efficiency	*GGE*	**0.3**	0.17	ciliates, (dino)flagellates	305[a]
basal respiration from starved respiration	$res_{20°C}^{mic}$	**0.21 d^{-1}**		ciliates, flagellates, amoebae	28[b]
Q_{10} starved respiration	$Q_{10,res}$	**2.4**			
particulate egestion	*unass*	**0.13**		ciliate	1
inorganic fraction of excretion	*inorg*	**0.66**		ciliate	22,1
preference for mixed phytoplankton	p_{mix}^{mic}	**1.29**			
preference for diatoms	p_{dia}^{mic}	**0.26**			
preference for coccolithophores	p_{coc}^{mic}	**1.03**			
preference for POC_s	p_{poc}^{mic}	**0.13**			
POC_l & POC_s degradation		**0.04 d^{-1}**			
Q_{10} POC_l & POC_s degradation		**1.89**			

[a]) Straile (1997)

[b]) Fenchel and Finlay (1983)

Table 2. Average concentrations and globally integrated rates for sensitivity tests.

	changed rate	parameter values	microz[ab] µg C·L^{-1}	micphy[c] Pg C·y^{-1}	chl[d] µg·L^{-1}	PP[e] Pg C·y^{-1}	mesoz[af] µg C·L^{-1}	mesphy[g] Pg C·y^{-1}	export[h] Pg C·y^{-1}
observ.			2.8	25-33	0.22	46.5	7.1	5.5	9.6-11.1
PISCES-T		Buitenhuis et al. 2006	1.0		0.10	64.0	2.0	10.6	8.2
standard	lab. graz. starv. resp.	**Table 1**	1.6	20.3	0.12	48.3	2.2	14.6	9.0
sensitivity (See also Fig. 5 & 6)	lab. graz. thr. resp.	*Table 1*	0.9	12.4	0.15	48.9	2.0	13.9	10.4
	field graz. thr. resp.	Table 1	0.7	17.4	0.14	51.5	1.7	12.7	9.5
	(dino) flagellate GGE	0.046 +0.014T	0.8	19.5	0.14	58.7	2.2	14.4	9.7
	ciliate GGE	0.68 -0.022T	2.9	17.6	0.11	46.8	2.0	15	8.7
	low $K_{½}^{mic}$	31 µg C·L^{-1}	2.1	24.6	0.08	42.4	1.9	10.1	7.0
	high $K_{½}^{mic}$	180 µg C·L^{-1}	0.7	8.5	0.15	45.9	2.1	14.5	10.7
	$p_{all\ food}^{mic}$	1	1.7	23.5	0.12	56.5	2.7	18.8	8.2
	GGE DOC	0.43 0.06	2.3	22.0	0.11	47.7	2.1	14.0	8.5
	unass. inorg.	0.21 0.60	1.5	19.0	0.12	46.9	2.1	14.5	9.2

[a] For zooplankton biomasses, the model was sampled where evaluation data was available.

[b] Microzooplankton biomass.

[c] Microzooplankton grazing on phytoplankton, calculated as the fraction of PP eaten by microzooplankton [*Calbet and Landry,* 2004] × PP$^{\bullet}$.

[d] Chlorophyll, SeaWiFS satellite.

[e] Particulate primary production [*Behrenfeld and Falkowski*, 1997].

[f] Mesozooplankton biomass [*Buitenhuis et al.*, 2006].

[g] Mesozooplankton grazing on phytoplankton [*Calbet*, 2001].

[h] Export at 100 m [*Schlitzer*, 2004; *Laws et al.*, 2000].

Table 3. Cost functions for sensitivity tests (Equation 18)

	changed rate	parameter values	microz	phymor	chl[a]	PP	phygro	mesoz	export
PISCES-T		Buitenhuis et al. 2006	4.0		3.1	3.4		4.0	1.9
standard	lab. graz. starv. resp.	**Table 1**	2.8	41	5.1	3.4	2.5	6.7	2.1
sensitivity (See also Fig. 5 & 6)	lab. graz. thr. resp.	*Table 1*	2.9	92	5.1	3.6	3.1	8	2.1
	field graz. thr. resp.	Table 1	2.6	14	4.8	3.5	2.6	8.9	2
	(dino) flagellate GGE	0.046 +0.014T	3.2	127	5.1	3.5	2.6	6.2	2
	ciliate GGE	0.68 -0.022T	2.7	33	5.1	3.5	2.6	6.9	2.3
	low $K_{½}^{mic}$	31 $\mu g\ C \cdot L^{-1}$	2.4	10	5.5	3.4	2	11.4	2.5
	high $K_{½}^{mic}$	180 $\mu g\ C \cdot L^{-1}$	3.1	579	5.2	3.7	3.7	7	2.1
	$p_{all\ food}^{mic}$	1	2.7	46	5.5	3.9	2.5	4.9	2.4
	GGE DOC	0.43 0.06	2.7	19	5	3.5	2.4	6.6	2.2
	unass. inorg.	0.21 0.60	2.8	51	5.1	3.6	2.8	6.7	2.1

[a] Using World Ocean Atlas 2005 *in situ* chlorophyll concentrations in order to include subsurface chlorophyll concentration

Figures and captions

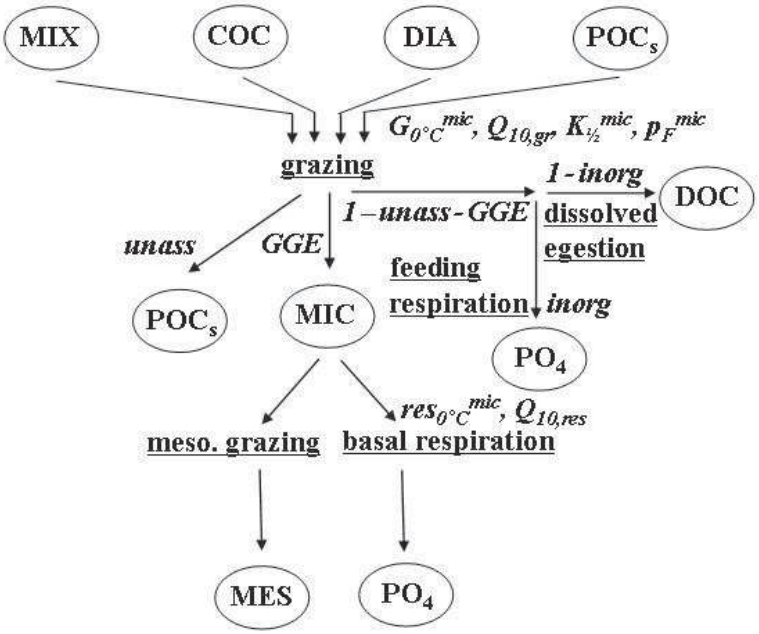

Figure 1. Microzooplankton mediated fluxes. Circles represent state variables (MIX = mixed phytoplankton, COC = coccolithophores, DIA = diatoms, POC_s = small particulate organic carbon, DOC = dissolved organic carbon, MIC = microzooplankton, PO_4 = nutrients (including dissolved inorganic carbon), MES = mesozooplankton), underlined texts represent fluxes, and italic texts represent parameters (see Table 1 for explanations and values).

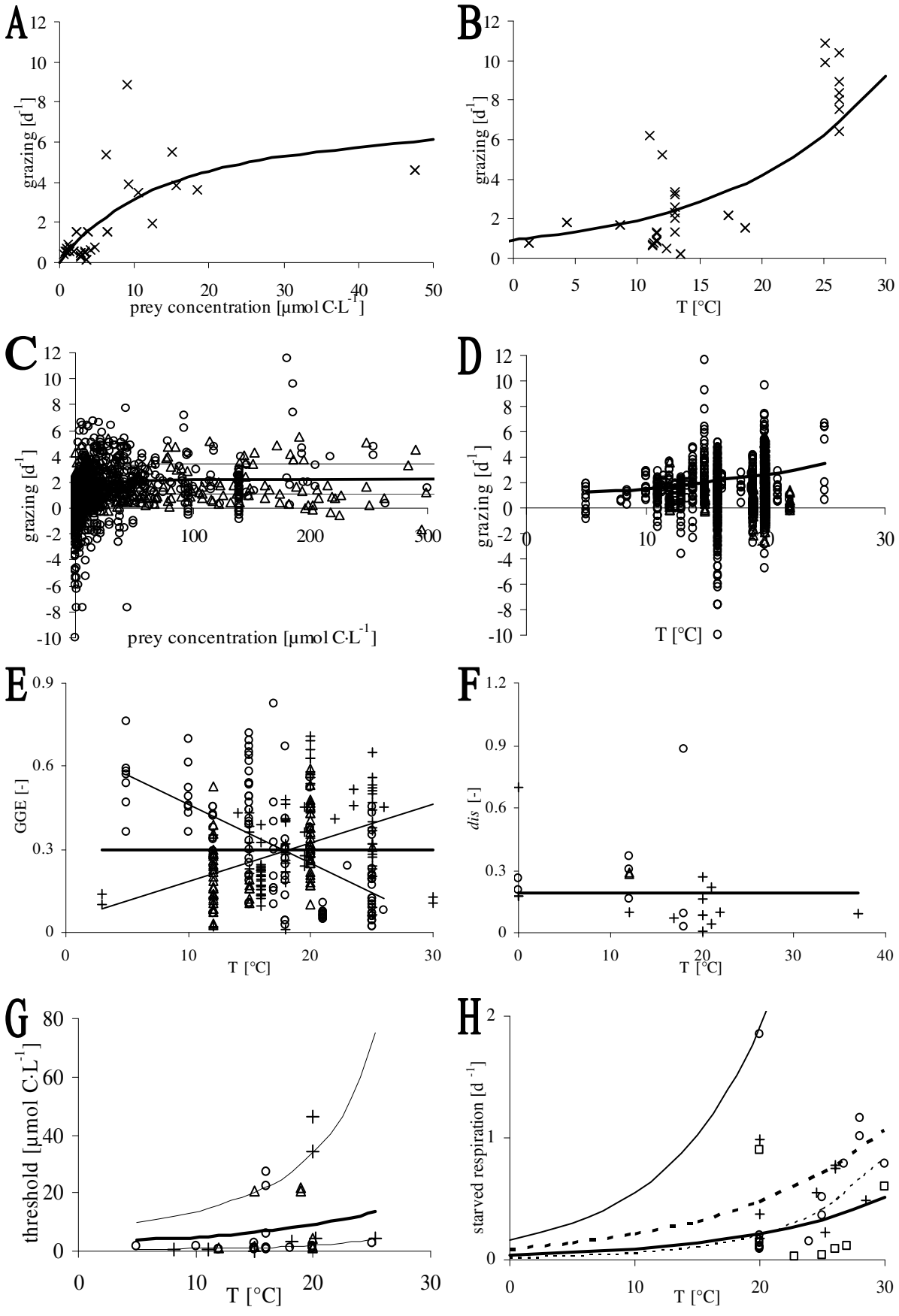

Figure 2. Databases used for calculating parameter values. Crosses are field measurements, circles are ciliates, triangles are dinoflagellates, plusses are flagellates, squares are amoeba. A) Field

measurements of grazing rate as a function of phytoplankton concentration (converted from chlorophyll *a* for comparison to panel C) corrected to the average temperature of 10.5 °C. B) Field measurements of grazing rate as a function of temperature corrected to the average chlorophyll *a* concentration of 1.1 $\mu g \cdot L^{-1}$ (Same data as A, the uncorrected data was fit to Equation 13). C) Laboratory measurements of grazing rate (converted from growth rate for comparison to panel A) as a function of food concentration (45 measurements at high food concentrations are not plotted, but were included in the fit to the data). D) Laboratory measurements of grazing rate as a function of temperature (Same data as A, the data were fit to Equation 14). E) Gross growth efficiency [*Straile*, 1997]. Horizontal line is the average, not calculated as a function of temperature (Temperature explains less than 2% of GGE variability of the combined data). Downward sloping line: ciliate linear regression (GGE=0.68 -0.022T, n=132 , r^2=0.36). Upward sloping line: dinoflagellate and flagellate linear regression (GGE=0.046 +0.014T, n=173 , r^2=0.18). F) Fraction of grazing that is converted to DOC (*dis* in Equations 4 and 5). Horizontal line is the average, not calculated as a function of temperature (Temperature explains less than 10% of *dis* variability). G) Threshold concentration as a function of temperature (the data were fit to Equation 17. The basal respiration rate is different when using the grazing rate from field or laboratory observations (Figure 2H, Table 1), but the fitted lines to the threshold are the same). Thick line was fit to all measurements. Thin lines are fit to the data that lie above and below the fit to all measurements, approximately corresponding to the high and low halves of the data. H) Respiration of starved microzooplankton [*Fenchel and Finlay*, 1983]. Thick solid line was fit to Equation 7. Thin solid line: respiration fit to all threshold concentrations for field measured grazing. Thick dashed line: respiration fit to all threshold concentrations for laboratory derived grazing rates. Thin dashed line: respiration fit to low threshold concentrations for laboratory derived grazing rates.

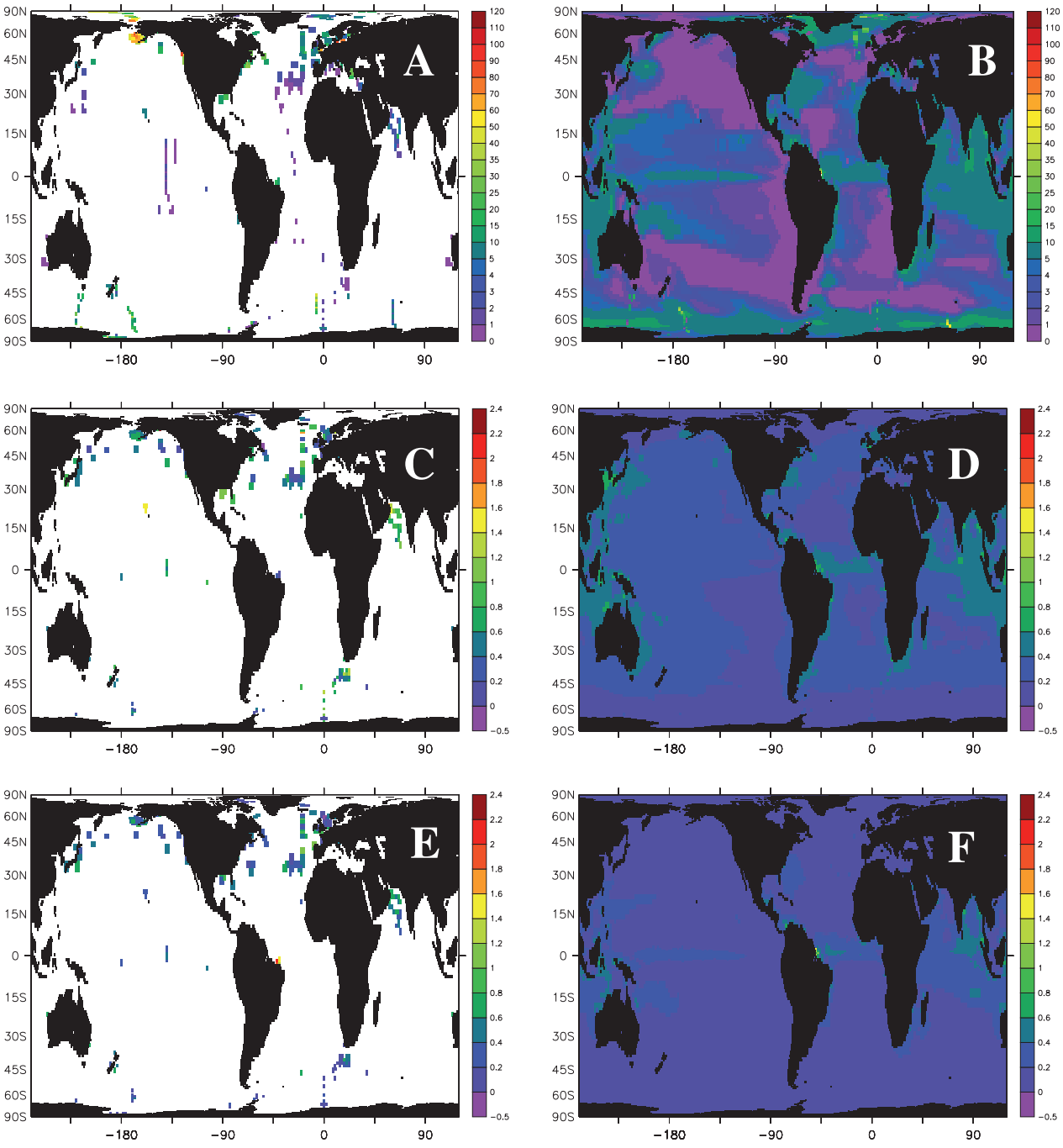

Figure 3. A, B) Microzooplankton biomass [µg C·L^{-1}], C, D) phytoplankton growth rate [d^{-1}], E, F) microzooplankton caused phytoplankton mortality rate [d^{-1}]. A, C, E) Observations. B, D, F) Model results standard simulation. Model results are for the same months and depths where there are observations and annual averages over the top 50 m everywhere else.

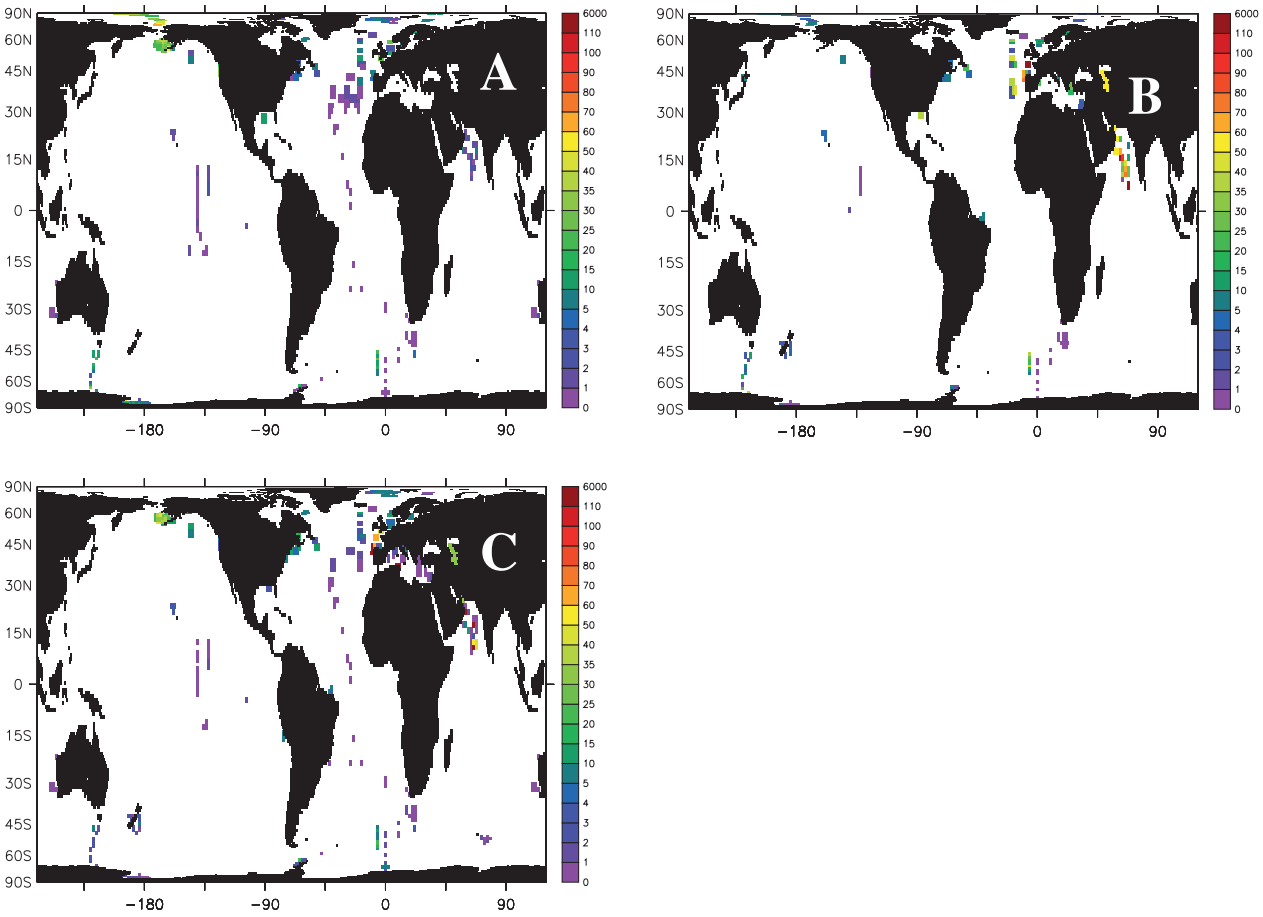

Figure 4. Observed biomass of the three main taxonomic groups of microzooplankton [µg C·L^{-1}]. A) dinoflagellates, B) flagellates and C) ciliates.

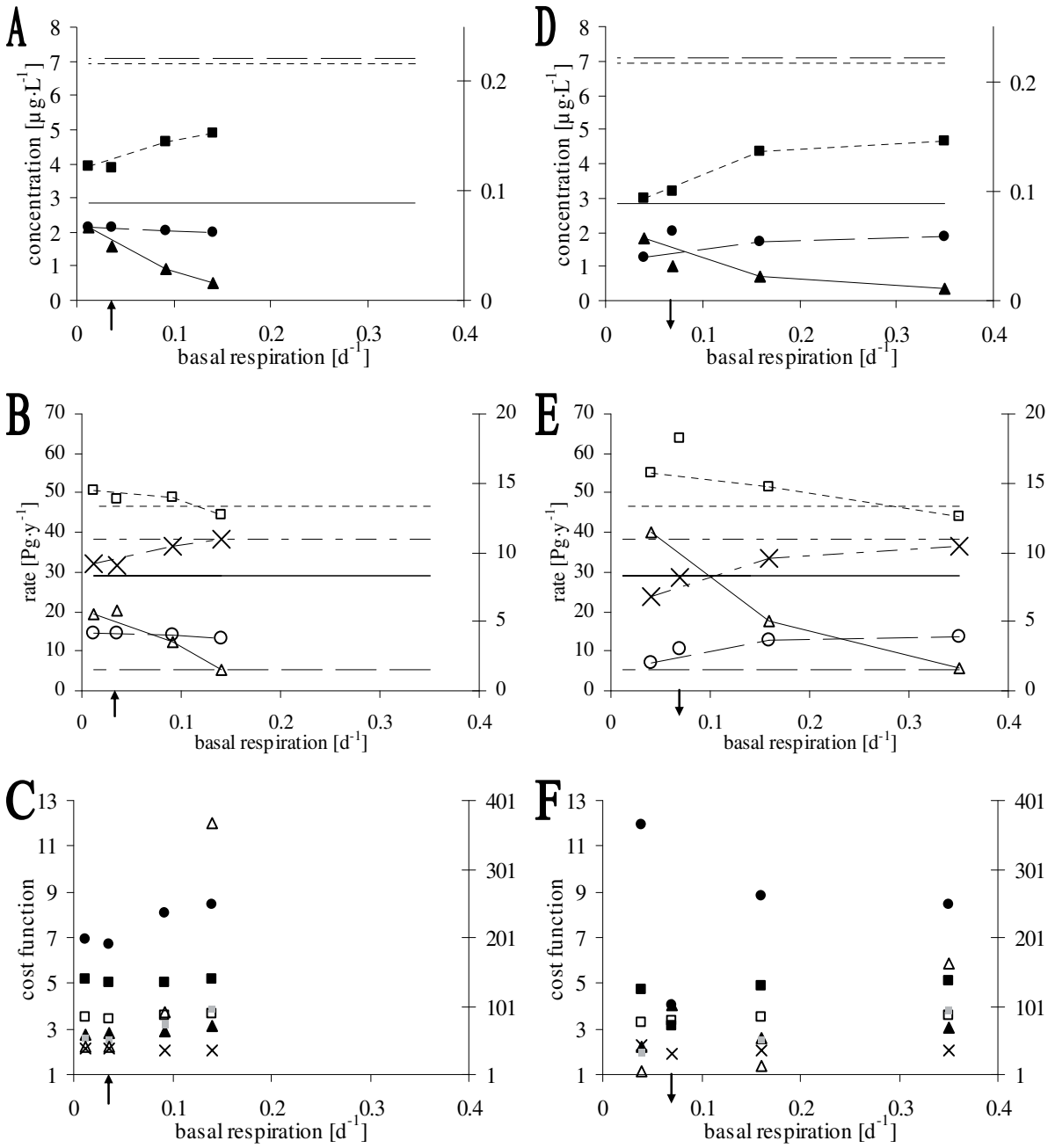

Figure 5. Sensitivity analysis of microzooplankton basal respiration. Horizontal lines are evaluation data (with references in parenthesis). A-C) Laboratory growth rates with low, all and high threshold concentrations. Arrow up: standard simulation. D-F) Field grazing rates with low, all and high threshold concentrations. Arrow down: PISCES-T. A, D) Left y-axis: Solid line and triangles: microzooplankton, dashed line and circles: mesozooplankton [*Buitenhuis et al.*, 2006]. Right y-axis: Dotted line and squares: chlorophyll [µg·L^{-1}; *World Ocean Atlas*, 2005]. The model was sampled at the same places (and months for microzooplankton and chlorophyll) as the observations. B, E) Left y-axis: Solid line and

triangles: microzooplankton grazing on phytoplankton [*Calbet and Landry*, 2004], dashed line and circles: mesozooplankton grazing on phytoplankton [*Calbet*, 2001], dotted line and squares: primary production [*Behrenfeld and Falkowski*, 1997]. Right y-axis: Dash-dotted line and crosses: export at 100 m [*Schlitzer*, 2004]. C, F) Cost function (10^ave(abs(log(model/observation)))). Left y-axis: symbols as in A and B, grey squares: phytoplankton growth rate. Right y-axis: Triangles: microzooplankton caused phytoplankton mortality rate.

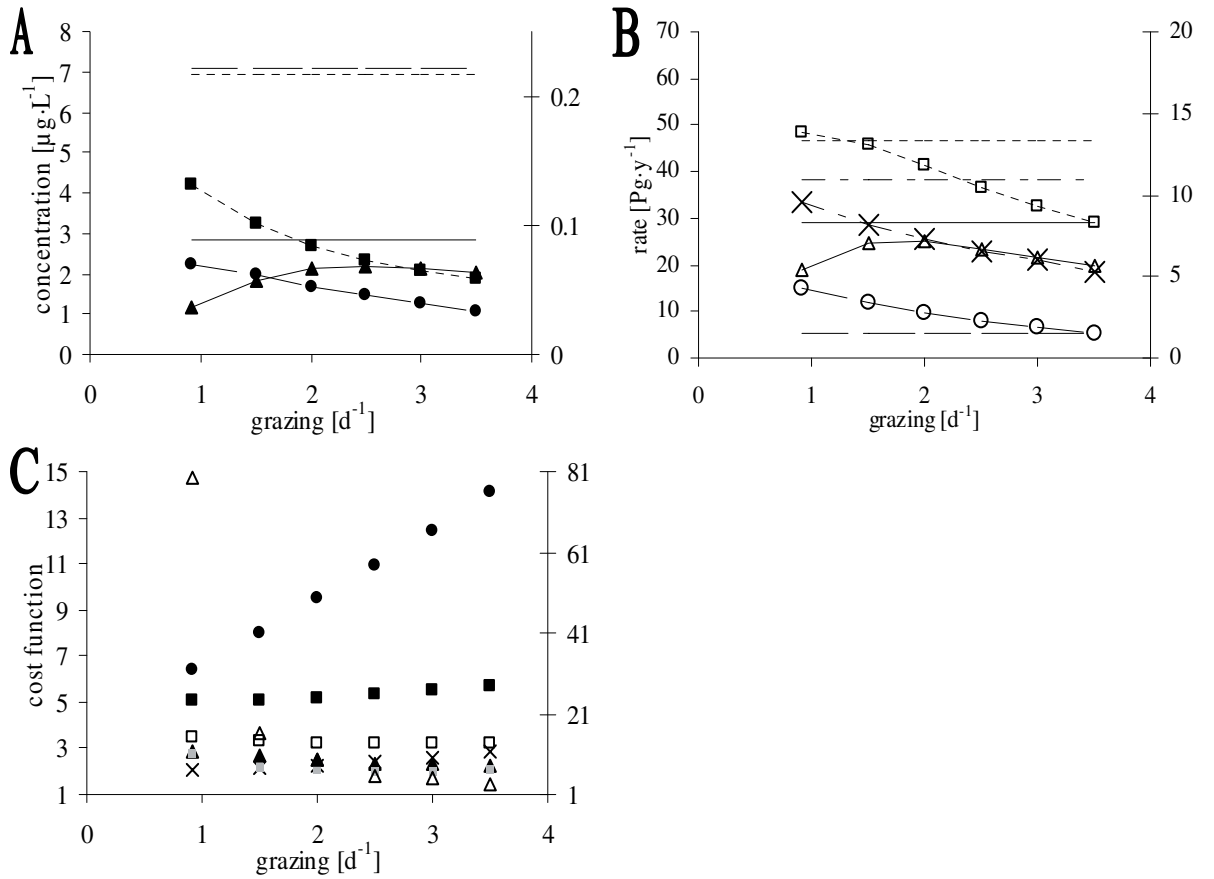

Figure 6. Sensitivity analysis of microzooplankton grazing. Symbols as in Figure 5

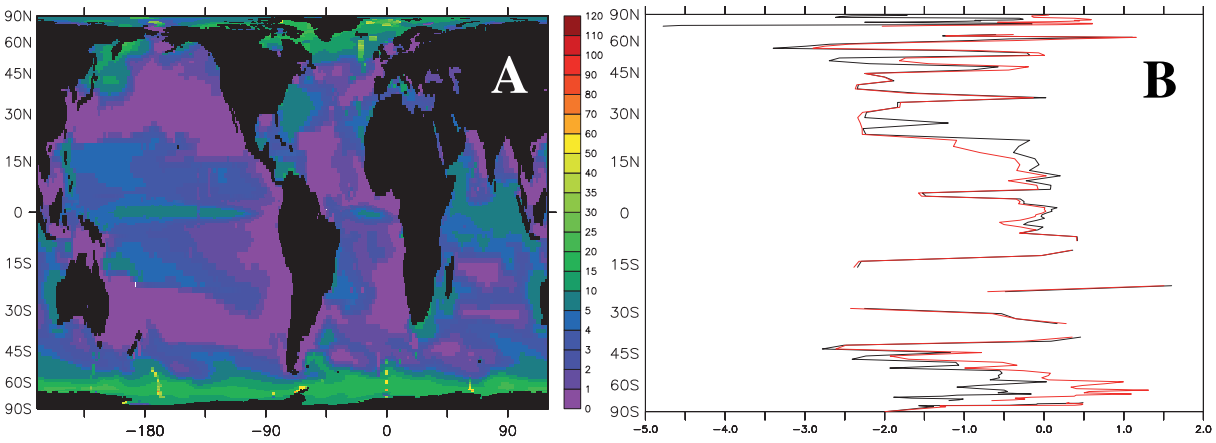

Figure 7. A) Microzooplankton biomass simulated with ciliate GGE. Model results are for the same months and depths where there are observations and annual averages over the top 50 m everywhere else. B) Zonal average of log(model/observed microzooplankton biomass) for the standard simulation (black line) and simulation with ciliate GGE (red line). Positive (negative) values indicate that the model overestimates (underestimates) observed microzooplankton biomass.

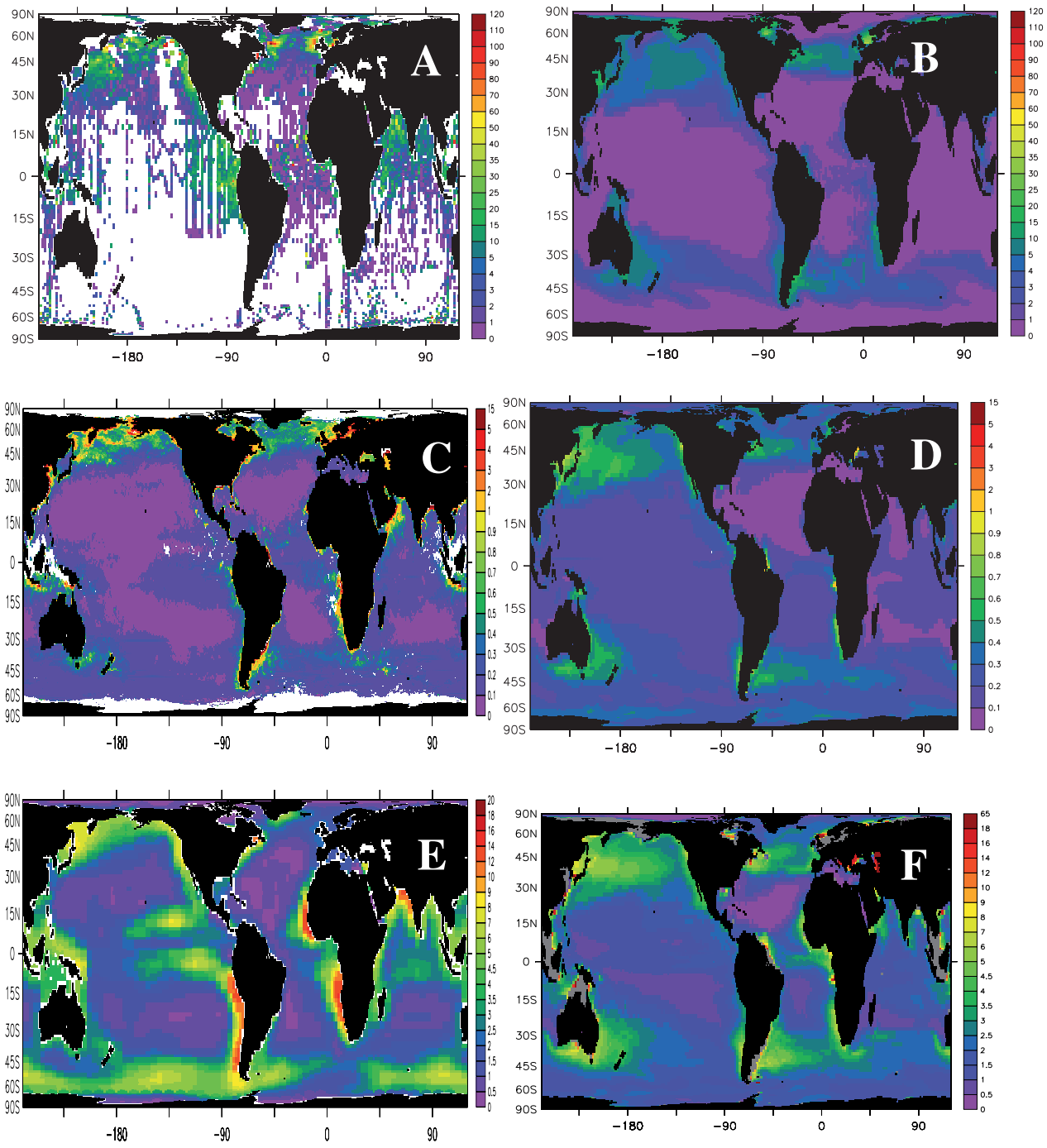

Supplementary Figure S8. A, B) Mesozooplankton biomass [µg C·L^{-1}; *Buitenhuis et al.*, 2006]. Model results were averaged over the same depth ranges as the observations and over the top 200m where no observations were available. C, D) Surface chlorophyll *a* [g L^{-1}] (SeaWIFS). E, F) export at 100 m [mol m^{-2} y^{-1}] [*Schlitzer*, 2004]. A, C, E) Observations. B, D, F) Model results standard simulation

Annexe B: Bayesian parameter estimation.

B.1- Theory

Two models – based on the Michaelis-Menten equation – were used to describe the functional response (feeding and growth) of ciliates and dinoflagellates:

$$r = r_{\max} \times \frac{P}{K_m + P} \qquad (1)$$

and

$$r = r_{\max} \times \frac{P - P_t}{K_m + P - P_t} \qquad (2)$$

with r_{max} the maximal rate (growth or grazing), P the food concentration and K_m the half-saturation constant . Equation (2) represents a similar response but includes a threshold food concentration (P_t) for feeding or growth.

Model parameters for equation (1), namely r_{max} and K_m, can be estimated by using the inverse of equation (1):

$$\frac{1}{r} = \frac{1}{r_{\max}} + \frac{K_m}{r_{\max}} \times \frac{1}{P} \qquad (1b)$$

Plotting 1/r as a function of 1/P yield the so-called *Lineweaver-Burk* plot. Parameters r_{max} and K_m can be estimated through linear regression of 1/r *vs.* 1/P. This method, however, cannot be applied to solve for parameters in equation (2). In addition, in order to apply the regression analysis, the variances of the dependent variable (1/r) should be equal over the whole data range.

Parameters of equation (1) and (2) were, therefore, estimated using a Bayesian approach in order to obtain unbiased estimates of parameters as well as an estimate of uncertainties for each parameter.

The Bayesian approach is based on the Bayes theorem for conditional probabilities:

$$P(B \mid A \cap I) = \frac{P(A \mid B \cap I) \times P(B \mid I)}{P(A \mid I)} \qquad (3)$$

which can be easily derived from the product rule of probabilities (Jaynes 2003)

$$P(A \cap B \mid I) = P(B \mid A \cap I) P(A \mid I) = P(A \mid B \cap I) P(B \mid I) \quad (4)$$

P(A ∩ B | I) is the conditional probability that both propositions A and B are true given the background information I. P(B| A∩ I) is the conditional probability for proposition B to be true given that A and I are true and P(A|I) is the conditional probability for proposition A to be true given the background information I. Similarly, P(A| B∩ I) is the probability for proposition A to be true given that B and I are true and P(B|I) is the conditional probability for proposition B to be true given the background information I.

In the context of parameter estimation the Bayes theorem can be rewritten as follows (compare, for example, Wolf-Gladrow 2008)

$$P(parameters \mid data \cap I) = \frac{P(data \mid parameters \cap I) \times P(parameters \mid I)}{P(data \mid I)} \qquad (5)$$

Where P(parameters | data ∩ I) is the posterior probability distribution (`posterior´ for short) for the model parameters given the data (observations) and background information I, P(data | parameters ∩ I) is the probability to observe the data given a model with specified model parameters (`likelihood´ for short), P(parameters | I) is the probability distribution for the model parameters given the background information I only (`prior´ for short), i.e. without taking into account the data (apriori), and P(data | I) is the probability to observe the data given the background information only, *i.e.* without taking into account the data. In the context of parameter estimation the term P(data | I) is not specified explicitly and used as a normalization factor only. The prior P(parameters | I) can be specified in various ways, for example:

Flat prior:

$$P(parameters \mid I) = const \qquad (6)$$

Jeffreys prior:

$$P(parameters \mid I) \propto 1 / (K_m \times g_{max}) \qquad (7)$$

Priors based on equation (6) and (7) are used when little or no prior information on values of model parameters is available. A flat prior expresses our ignorance about the values of parameters (‘*i.e.* all values within a given range have the same probability’). Jeffreys prior is applied when the model parameters are positive and finite.

As a model we assume a Michaelis-Menten function (Eq. 1) plus additive Gaussian noise for the grazing (g). The likelihood to observe an individual datum, d_k, is given by the Gaussian distribution

$$P(d_k \mid \text{parameters} \cap I) = 1/\{\sigma_k \sqrt{(2\,\pi)}\} \exp\{-[g(g_{max}, K_m) - d_k]^2 / (2\,\sigma_k^2)\} \qquad (8)$$

where σ_k^2 is the variance. Assuming further that all deviations between model and observation are independent of each other, one can write the likelihood for the whole data set as the product of the probabilities for each data and obtains:

$$P(\text{data} \mid \text{parameters} \cap I) \propto \exp(-\zeta^2/2) \qquad (9)$$

where

$$\zeta^2 = \Sigma_{k=1}^{N} \{[g(g_{max}, K) - d_k]/ \sigma_k\}^2 \qquad (10)$$

ζ^2 is the sum over the squared deviations between the Michaelis-Menten function (`model´) and the data weighted by the variances.

Application of the flat prior together with the likelihood (Eq. 9) leads to the posterior

$$P(\text{parameters} \mid \text{data} \cap I) = \text{const.}\ \exp(-\zeta^2/2) \qquad (11)$$

The posterior is maximal when ζ^2 is minimal. The optimal model parameters, $g_{max,o}$ and $K_{m,o}$, are estimated by maximizing the posterior (minimizing the least-squared error). This is the `least-squared method´.

A further simplification results from the assumption that all variances σ_k^2 are equal and thus

$$P(\text{data} \mid \text{parameters} \cap I) \propto \exp(-\zeta^2/2) \qquad (12)$$

where

$$\zeta^2 = \Sigma_{k=1}^{N} [g(g_{max}, K_m) - d_k]^2 \qquad (13)$$

(the variance is hidden in the normalization constant of the posterior).

In addition to the optimal parameter values one can also derive their uncertainties from the posterior (Eq. 11). For the model without threshold effect, uncertainties for parameter estimates of g_{max} and K_m are estimated from the second derivatives of the least-square sum L (Eq. 14) with respect to the model parameters as follows (we use the notation L, a, b instead of P(data | parameters), g_{max} and K_m to simplify notation)

$$L(a,b) = L\,(g_{max}, K_m) = -\,\zeta^2/2 \qquad (14)$$

The second derivatives of L(a,b) at the optimal values $a_o = g_{max,o}$ and $b_o = K_{m,o}$, are denoted by A, B, C:

$$A = (\partial^2 L/\partial a^2)_{ao,bo} \qquad (15)$$

$$B = (\partial^2 L/\partial b^2)_{ao,bo} \qquad (16)$$

$$C = (\partial^2 L/\partial a \partial b)_{ao,bo} \qquad (17)$$

The next step is to form the matrix M of all these second derivatives:

$$M = \begin{Bmatrix} A & C \\ C & B \end{Bmatrix} \qquad (17a)$$

The negative of the inverse of M is the covariance matrix S. The square roots of the diagonal elements of S are the estimates of the uncertainties (standard deviations) of the model parameters (Sivia and Skilling 2006).

Uncertainty of the optimal value of g_{max}:

$$\sigma_a^2 = -B/(A*B-C^2) = \sigma_{gmax}^2 \qquad (18)$$

Uncertainty of the optimal value of K_m:

$$\sigma_b^2 = -A/(A*B-C^2) = \sigma_{Km}2 \qquad (19)$$

Covariance:

$$\sigma_{ab}^2 = C/(A*B-C^2) = \sigma_{gmax,Km}^2 \qquad (20)$$

B.2- Example

In order to illustrate the method I have created an artificial data set using the Michaelis-Menten equation without threshold (Eq. 1). P is the prey concentration, g the grazing rate. In this dataset g_{max} = 10 (all units are left out on purpose for the artificial data set) and K_m = 4. The dataset was generated by adding Gaussian noise with $\mu = 0$ and $\sigma = 1$ to exact model values. The data obtained is listed in Table 1 and plotted in Fig. 1.

As mentioned earlier we assume a flat prior ($P(g_{max},K_m \mid I)$ = constant) and P(data | I) is a normalisation factor. Consequently, the posterior probability is essentially given by the likelihood (Eq. 13, simplified version Eq. 21):

$$P(g_{\max}, K_m \mid data \cap I) = c * \exp\left\{-0.5\sum_{K=1}^{N}\left[g_K - g_{\max} \times P_K / (K_m + P_K)\right]^2\right\} \quad (21)$$

A rough estimate of the value for g_{max} and K_m can be obtained by looking at the data (10 and 5 respectively). We specify ranges around these 'estimates by eye' (9 to 12 and 2 to 8, respectively) and calculate ζ^2 at various points inside these ranges (equidistant in each quantity, with resolution equal to the desired accuracy of the parameter value estimate). The optimal values $g_{max,o}$ = 10.6 and $K_{m,o}$ = 5.1 are derived from the location of the minimum of ζ^2 (equivalent to the maximum of posterior probability distribution) in the g_{max}-K_m-plane (Fig. 2 and 3). The model parameters uncertainties are calculates from the second derivatives of ζ^2 (Eqs. 14 to 20).

Table 1: Artificial dataset.

P	1	2	3	4	5	6	7	8	9	10	11	12	13	14	15	16	17	18	19	20
g	0.4	3.6	3.2	6.4	4.8	6.5	6.6	5.7	4.8	7.1	6.3	8.1	8.2	9.5	8.5	7.4	8.5	7.2	8.2	8.3

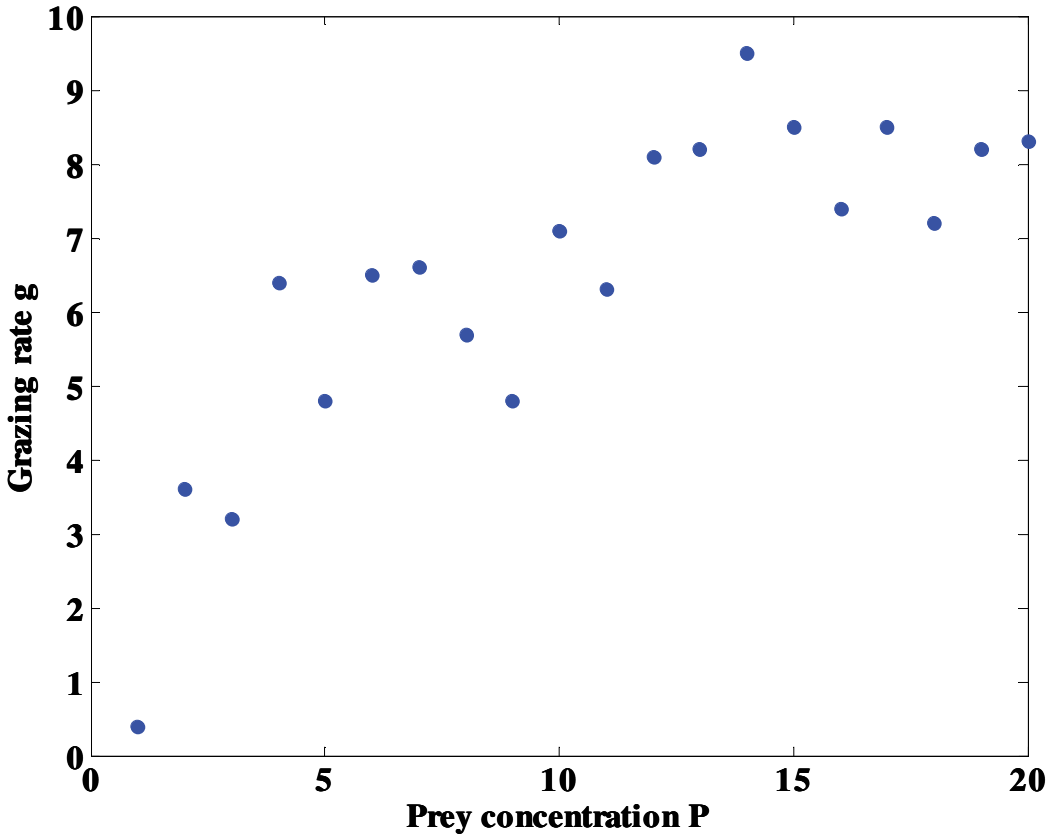

Figure 1: Plot of the grazing rates (g_k) as a function of the prey concentration (P_k); artificial data.

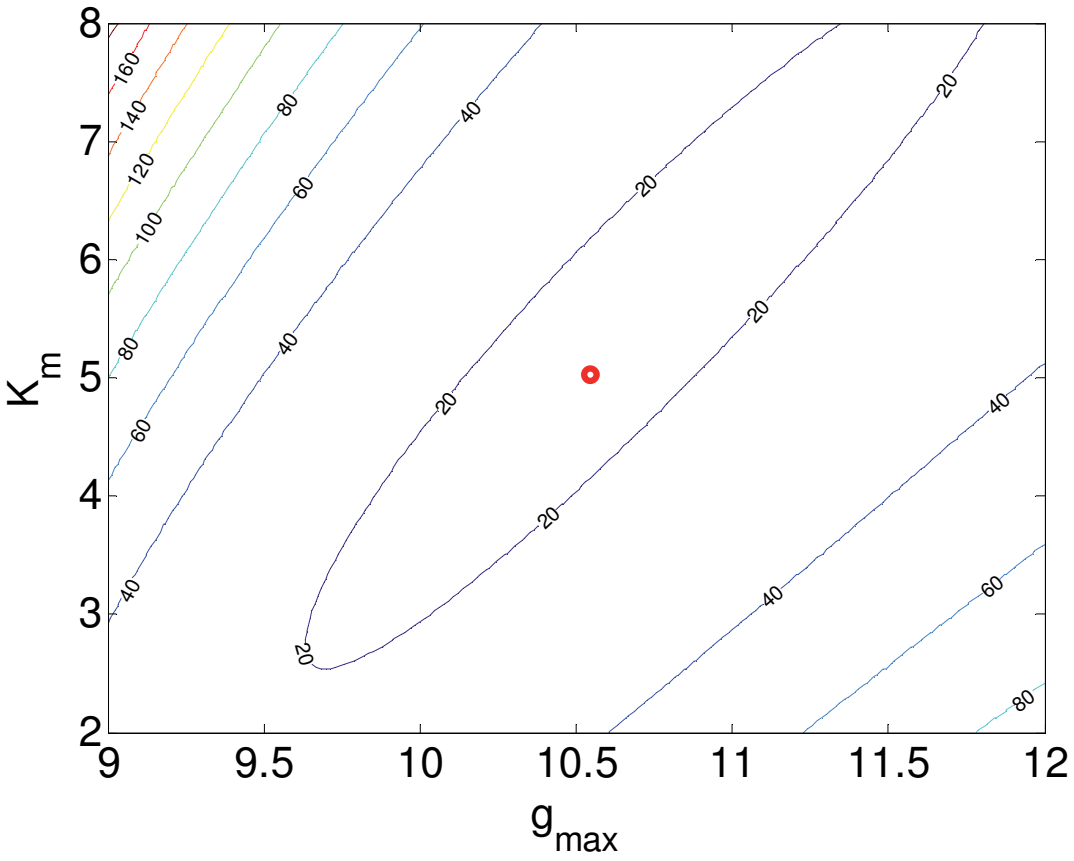

Figure 2: Isocontours of ζ^2 showing the location of the least-squares minimum (red 'o') as a function of the possible value of g_{max} and K_m

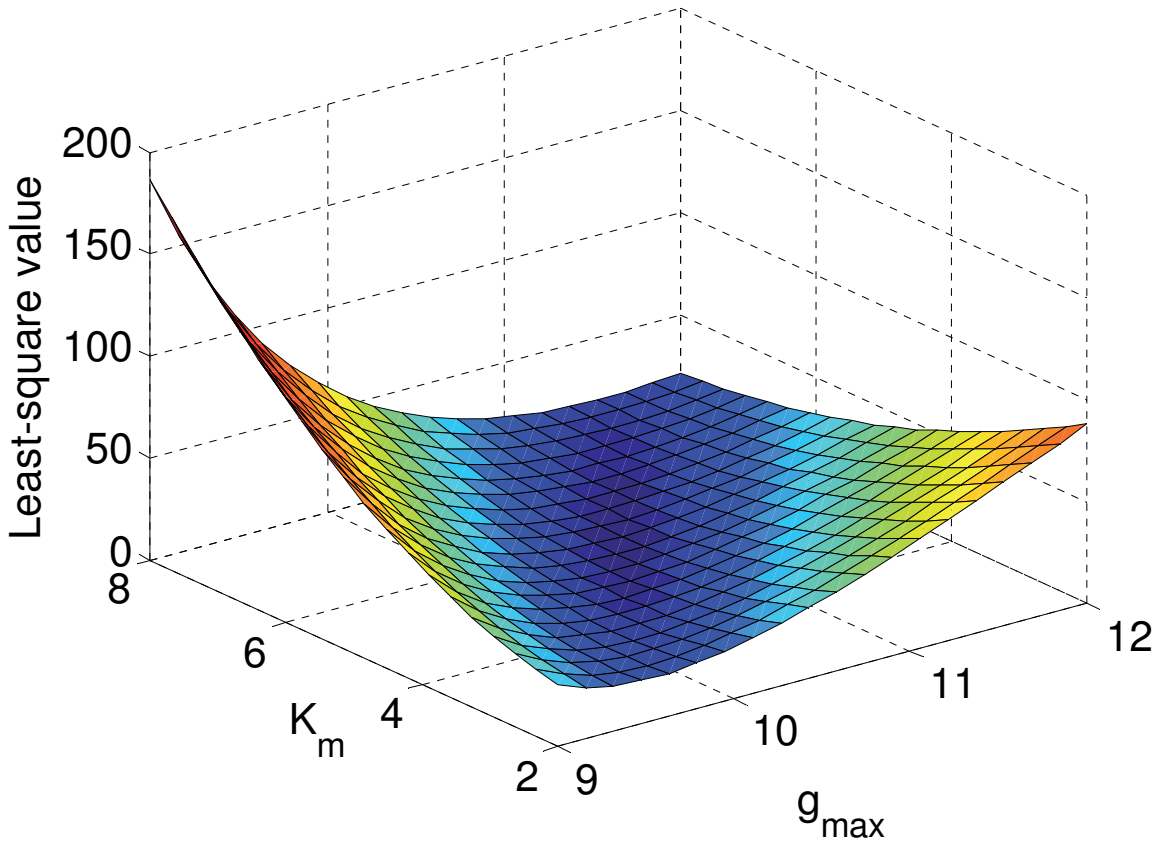

Figure 3: Location of the least-square minimum as a function of the possible value of g_{max} and K_m

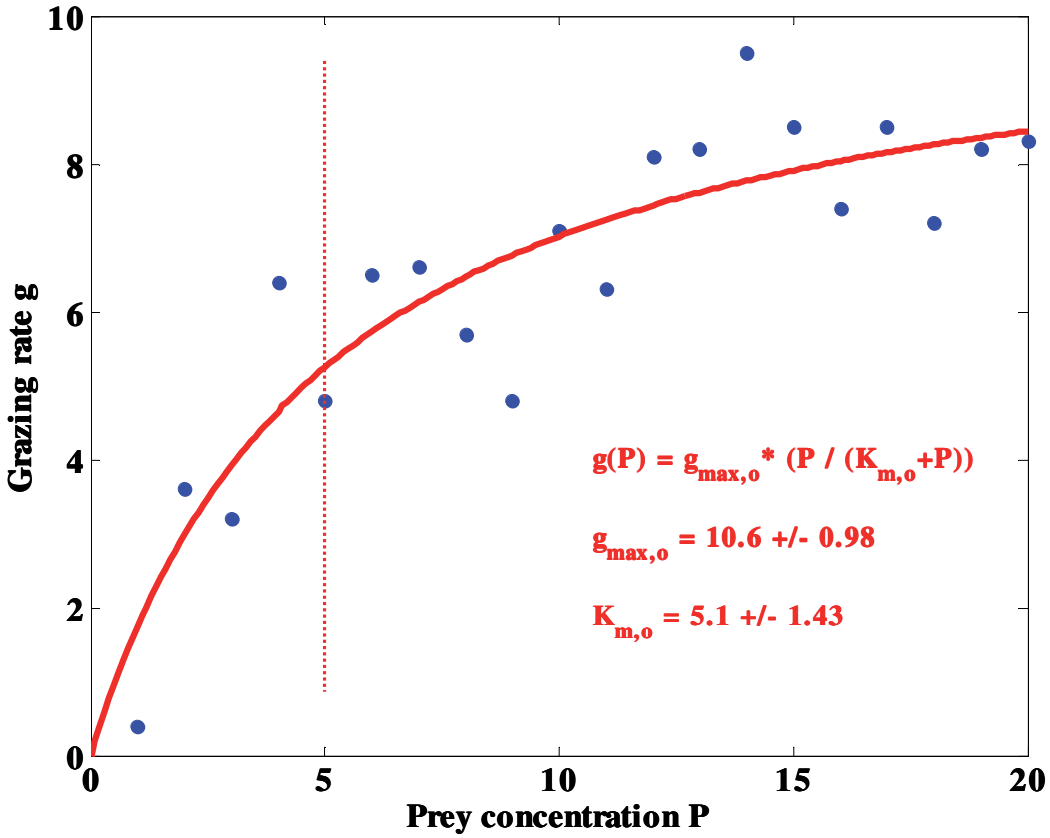

Figure 4: Dataset and the fit with the optimal values.

To estimate parameters for the Michaelis-Menten equation with threshold (Eq. 2), the procedure is analogue. Annex B contains the Matlab code, with annotations used to realise the fit and parameter estimations for a Michaelis-Menten with threshold.

References

Sivia, D.S., Skilling, J. (2006) Data analysis – A Bayesian Tutorial, Second edition, Clarendon Press, Oxford.

Wolf-Gladrow, DA (2008) Probability and Statistics - An Introduction, Lecture notes. Version 2.01. Open access publication, available by request to the author (Dieter.Wolf-Gladrow@awi.de).

Annexe C: Matlab codes used for parameter estimation.

Note: annotations

Code explanations are be in green with each line commencing with a "%" symbol.

To apply the code simply "copy-paste" the lines below and run it without removing the explanations. No graphic code has been included.

C.1- Main code.

```
%-------------------------------------------------------------------------
%
%Estimation of the parameter for a Michaelis-Menten type equation with
%threshold, plus calculation of the incertitude of the parameter.
%
%-------------------------------------------------------------------------

display('------------------parameter estimation-------------------------')

global conc g L
%these variables (conc, g and L) are global, therefore they can be used
%with other codes without being reloaded or redefined.


load conc.txt
load graz.txt
%load .txt file where the data set for concentration (conc.txt) and grazing
%(graz.txt) (or growth if you don't want to recreate a growth.txt file) are
%saved


g=graz;
%define the rates from the graz.txt file as the 'g' data


L= length (conc);
%L is the number of data points in the conc.txt file
```

```
gmaxa = 0:0.01:2.5;
Ka = 10000:5000:1500000;
xa = 1000:100:10000;
%definition of the array of possible values for the maximal rate (gmaxa),
%half-saturation concentration (Ka) and threshold (xa); vary with datasets.
%minimal value : step : maximal value


N = length (gmaxa);
M = length (Ka);
P = length (xa);
%calculate the length of each array of value defined previously

nmin=0;
mmin=0;
pmin=0;
Lmin=1e20;
%sets a minimal value to variables n, m and p related to N, M and P. Also
%defines a variable Lmin.

for n=1:N
    for m=1:M
        for p=1:P
        gmax=gmaxa(n);
        K=Ka(m);
        x=xa(p);
        s=0;
        for i=1:L;
            s=s+((gmax*(conc(i)-x)/(K+conc(i)))-g(i))^2;
        end

%This code defines a loop, calculating the least square for each
%combination of parameters in the defined array.

        La(n,m) = s;
        if s<Lmin
            Lmin=s;
            nmin=n;
            mmin=m;
            pmin=p;
```

```
        end
        end
    end
end
%The lowest least-square value, 's', will determine the optimal combination
%of parameter values to obtain the best-fit.

gmaxopt=gmaxa(nmin)
Kopt=Ka(mmin)
xopt=xa(pmin)
%optimal parameter value




s=0; gmax=gmaxopt; y=Kopt; x=xopt;
 for i=1:L;
     s=s+((gmax*(conc(i)-x)/(y+conc(i)))-g(i))^2;
 end
 s;
 sige=sqrt(s/L)
 %Calculation of the standard deviation (sige)




%The next part section of code consist of the calculation of parameters
%uncertainties, using the covariance matrix method.
%The second derivatives are calculated for each parameter using the
%parallel code MMtrchsq.m (see next code).
%The covariance matrix was calculated and inverted.

gmax=gmaxopt; K=Kopt; x=xopt;


change = 0.01;
glow = (1-change)*gmax; ghigh = (1+change)*gmax; dg = (ghigh-glow)/2;
Klow = (1-change)*K; Khigh = (1+change)*K; dK = (Khigh-Klow)/2;
xlow = (1-change)*x; xhigh = (1+change)*x; dx = (xhigh-xlow)/2;
xa = xlow:dx:xhigh;      N = length(xa);
```

```
dxx = 6.6459e-004;
chixx = (MMtrchsq(gmaxopt+dg,Kopt,xopt) ...
      -2*MMtrchsq(gmaxopt,Kopt,xopt) ...
      +MMtrchsq(gmaxopt-dg,Kopt,xopt))/dg/dg/sige^2;

dyy = 8.5050e-009;
chiyy = (MMtrchsq(gmaxopt,Kopt+dK,xopt) ...
      -2*MMtrchsq(gmaxopt,Kopt,xopt) ...
      +MMtrchsq(gmaxopt,Kopt-dK,xopt))/dK/dK/sige^2;

dzz = 1.6516e-007;
chizz = (MMtrchsq(gmaxopt,Kopt,xopt+dx) ...
      -2*MMtrchsq(gmaxopt,Kopt,xopt) ...
      +MMtrchsq(gmaxopt,Kopt,xopt-dx))/dx/dx/sige^2;

dxy = -2.3523e-006;
chixy = (MMtrchsq(gmaxopt+dg,Kopt+dK,xopt) ...
        -MMtrchsq(gmaxopt-dg,Kopt+dK,xopt) ...
        -MMtrchsq(gmaxopt+dg,Kopt-dK,xopt) ...
        +MMtrchsq(gmaxopt-dg,Kopt-dK,xopt))/4/dg/dK/sige^2;

dxz = -5.0305e-006;
chixz = (MMtrchsq(gmaxopt+dg,Kopt,xopt+dx) ...
        -MMtrchsq(gmaxopt-dg,Kopt,xopt+dx) ...
        -MMtrchsq(gmaxopt+dg,Kopt,xopt-dx) ...
        +MMtrchsq(gmaxopt-dg,Kopt,xopt-dx))/4/dg/dx/sige^2;

dyz = 2.1103e-008;
chiyz = (MMtrchsq(gmaxopt,Kopt+dK,xopt+dx) ...
        -MMtrchsq(gmaxopt,Kopt-dK,xopt+dx) ...
        -MMtrchsq(gmaxopt,Kopt+dK,xopt-dx) ...
        +MMtrchsq(gmaxopt,Kopt-dK,xopt-dx))/4/dK/dx/sige^2;

% A=(1/2)* [dxx dxy dxz ; dxy dyy dyz ; dxz dyz dzz];
A = [chixx chixy chixz; chixy chiyy chiyz; chixz chiyz chizz]/2;
sigma=inv(A);
siggmax=sqrt(sigma(1,1))
sigK=sqrt(sigma(2,2))
sigx=sqrt(sigma(3,3))
```

C.2- Parallel code (MMtrchsq.m).

```
%-----------------------------------------------------------------
%Program MMtrchsq.m , used for data incertitude estimation
%
%-----------------------------------------------------------------


function xdot = fct(gmax,K,x)
% MMtrchisq.m

global conc g L
s=0;
for i=1:L;
    s=s+((gmax*(conc(i)-x)/(K+conc(i)))-g(i))^2;
end
xdot = s;
```